Universidade de Aveiro Departamento de Biologia
2006

Sandra Isabel Moreira Pinto Vieira Guerra e Paz

O Tráfego subcelular da Proteína Precursora de Amilóide de Alzheimer (PPA) é dependente de Fosforilação

Phosphorylation-dependent Alzheimer's Amyloid Precursor Protein (APP) Targeting

Universidade de Aveiro Departamento de Biologia
2006

Sandra Isabel Moreira Pinto Vieira Guerra e Paz

O Tráfego subcelular da Proteína Precursora de Amilóide de Alzheimer (PPA) é dependente de Fosforilação

Phosphorylation-dependent Alzheimer's Amyloid Precursor Protein (APP) Targeting

dissertação apresentada à Universidade de Aveiro para cumprimento dos requisitos necessários à obtenção do grau de Doutor em Biologia, realizada sob a co-orientação científica da Doutora Odete A. B. da Cruz e Silva, Professora Auxiliar da Secção Autónoma das Ciências da Saúde da Universidade de Aveiro, e do Doutor Edgar F. da Cruz e Silva, Professor Associado do Departamento de Biologia da Universidade de Aveiro.

o júri

presidente

Prof. Dr. Armando da Costa Duarte
professor Catedrático do Departamento de Química da Universidade de Aveiro

Prof. Dr. med. Jens Wiltfang
full professor of the Psychiatry Department, Molecular Neurobiology, Klinik mit Poliklinik für Psychiatrie und Psychotherapie, Friedrich-Alexander University of Erlangen-Nürnberg, Erlangen, Germany

Prof. Dr. George Perry
full professor of the Biology Department, College of Sciences, University of Texas at San Antonio, San Antonio, United States of America

Prof. Dr. Francisco M. L. Amado
professor auxiliar do Departamento de Química da Universidade de Aveiro

Prof. Dr ª Odete A. B. da Cruz e Silva
professora auxiliar da Secção Autónoma das Ciências da Saúde da Universidade de Aveiro

Prof. Dr. Edgar F. da Cruz e Silva
professor associado do Departamento de Biologia da Universidade de Aveiro

agradecimentos

À Professora Doutora Odete A. B. da Cruz e Silva, minha co-orientadora, quero expressar o especial reconhecimento pelo apoio científico e acompanhamento permanente. O seu ensinamento, incentivo e apoio constantes tornaram-se decisivos para a realização de todo o trabalho científico apresentado nesta dissertação. Estou igualmente grata ao Prof. Doutor Edgar da Cruz e Silva pela sua preciosa co-orientação neste trabalho científico e pela disponibilidade e aconselhamento dispensados ao longo destes anos. A ambos uma outra gratidão, a que envolve o acompanhamento e participação num crescimento pessoal além do profissional.

Gostaria também de expressar um especial agradecimento a todos os meus colegas de laboratório, nomeadamente à Mestre Sandra Rebelo pela sua colaboração científica e pelo companheirismo demonstrado.

Ao Centro de Biologia Celular e ao Departamento de Biologia da Universidade de Aveiro agradeço o bom acolhimento que concederam ao desenvolvimento da minha dissertação de doutoramento.

Gostaria de exprimir o meu reconhecimento e agradecimento à minha família, em especial à minha mãe, não só pelo apoio e incentivo dados ao longo destes anos, mas especialmente por ter sido um verdadeiro porto de abrigo para a Maria e para mim.

Ao meu pai. Por conseguir ver a magia que há no mundo. Por me ensinar a pensar e a questionar.

O desenvolvimento do trabalho experimental e a participação em congressos internacionais foram possíveis graças ao apoio financeiro das seguintes instituições:

- FCT - Programa PRAXIS XXI (Bolsa PRAXIS XXI/BD/16218/98);
- FCT - Programa POCTI/BCI/34349/1999;
- V Framework Program of the European Union (Project DIADEM, QLK3-CT-2001/02362).
- Fundação Calouste Gulbenkian – Programa Gulbenkian de estímulo à Investigação 2003 (Área Cientifica: Biogénese da Neurodegenerescência e Neuroprotecção).
- Fundação Astrazeneca – Programa de Fundo de Apoio à Investigação 2004 (Área Cientifica: Sistema Nervoso Central).

resumo

A Doença de Alzheimer (DA) é uma das doenças neurodegenerativas mais comuns, e apresenta uma incidência mundial de 2-7% em indivíduos com mais de 65 anos e de cerca de 15% em indivíduos acima dos 85 anos de idade. Apesar da sua etiologia multifactorial, há uma correlação bem descrita entre esta patologia e um peptídeo neurotóxico denominado Abeta. Este peptídeo deriva fisiológica e proteoliticamente de uma glicoproteína transmembranar com características de receptor: a Proteína Percursora de Amilóide de Alzheimer (PPA). As possíveis funções fisiológicas da proteína PPA, o seu destino e vias de processamento celulares, conjuntamente com possíveis proteínas celulares que com ela interajam, são assim tópicos de interesse e objectos de investigação científica mundial. Neste contexto tem sido amplamente descrito o envolvimento do processo de fosforilação de proteínas, uma importante modificação pós-transducional que regula muitos e variados acontecimentos intracelulares, na regulação do processamento da PPA. Apesar do exposto, muito pouco é conhecido acerca da fosforilação directa da própria PPA. Esta proteína possui na sua estrutura primária sequências consenso para fosforilação, quer no seu ectodomínio quer no seu domínio intracelular, já descritas como sofrendo fosforilação "in vitro" e "in vivo". O resíduo Serina 655 pertence a um motivo funcional da APP, ^{653}YTSI^{656}, que forma um sinal de internalização e/ou de "sorting" basolateral. Este domínio é também o local de ligação para a APPBP2, uma proteína que interage com os microtubulos da célula. Embora ainda mal elucidados, os mecanismos pelos quais a fosforilação proteica regula o processamento da PPA parecem incluir uma alteração no tráfego desta proteína, sugerindo que o domínio fosforilável ^{653}YTSI^{656} desempenha um papel importante nesse processo.

Esta dissertação visou assim contribuir para elucidar o papel da fosforilação directa da molécula de APP, mais especificamente no seu resíduo Serina 655, na regulação do direcionamento e tráfego subcelular da proteína, e nas suas possíveis clivagens proteolíticas. De forma a respondermos a essas questões desenvolvemos um modelo experimental para seguir o tráfego intracelular, que usa uma combinação de biologia molecular, técnicas de microscopia de epifluorescência e técnicas de cultura celular. Os resultados obtidos implicam este resíduo como um sinal de direcionamento subcelular da proteína APP, e revelam como o redireccionamento desta proteína por fosforilação favorece um tipo de processamento não amiloidogénico desta. Adicionalmente, a fosforilação do resíduo Serina 655 parece possuir um papel regulador da actividade da PPA como molécula de transdução de sinais. As implicações destas observações na DA e em novas aplicações terapêuticas para a doença são subsequentemente discutidas.

abstract

Alzheimer's Disease (AD) is a common neurodegenerative disease affecting individuals worldwide with an incidence of 2-7% of post-65 and 15% of post-85 years old. This disease is multifactorial in its etiology but central to its pathology is a neurotoxic peptide termed Abeta. This peptide is physiologically derived by a proteolytic process on the transmembranar Alzheimer's Amyloid Precursor Protein (APP). Protein phosphorylation-dependent APP processing has been widely described and although the mechanisms involved remain far from clarified, alterations in APP trafficking seem to occur as part of the answer. Furthermore, the occurrence of consensus phosphorylation sites in the APP intracellular domain has been known for long, but little was known regarding the direct phosphorylation of APP. Efforts in unravelling the role of these domains are finally being successful in placing them as key control points in APP targeting and processing. Among these consensus sequences, the less studied ^{653}YTSI^{656} motif forms a characteristic internalisation and/or basolateral sorting signal sequence, and is known to be the binding site for a microtubule-interacting protein (APPBP2). Phosphorylation of this motif was thus suggested to be involved in APP targeting regulation, hitherto all attempts failed to confirm it or even to reveal substantial evidences.

In this project, the role of the ^{653}YTSI^{656} idomain, and in particular the phosphorylatable serine 655, in APP trafficking and proteolytic processing was studied. In order to address this question a new experimental methodology was developed, which coupled molecular biology, fluorescence imaging, and cell culture techniques. APP point mutants, mimicking serine 655 phosphorylated- and dephosphorylated-status, and tagged with the green-fluorescent protein, were used to study protein trafficking dynamics and processing. Results obtained place serine 655 phosphorylation as a key signal in APP sorting and targeting to specific subcellular locations. Also of high relevance was the observed implication of serine 655 phosphorylation as a regulatory mechanism that maybe involved in controlling APP function as a signal transducer. The implications of these observations in AD pathogenesis and therapeutic approaches are discussed.

INDEX

CHAPTER I

GENERAL INTRODUCTION

CHAPTER I – GENERAL INTRODUCTION

I. 1 – ALZHEIMER'S DISEASE

I. 1. 1 – CHARACTERIZATION OF THE DISEASE

Alzheimer's disease (AD) is a neurodegenerative disorder affecting a large percentage of the world's elderly population, being the most common form of senile dementia. The disease was first diagnosed by Alois Alzheimer in 1907, as a neuropathological syndrome characterized by progressive dementia and deterioration of cognitive function (Alzheimer, 1907). This German neurologist demonstrated for the first time a relationship between specific cognitive changes, neurological lesions revealed by autopsy and a clinical history of dementia. His patient (a 56-year-old woman) had her cognitive capacities and behaviour affected due to the direct physiological effects of her disease condition.

At the cerebral level, AD patients have a characteristic brain atrophy and mass loss, due to extensive neuronal damage and death (Fig. I.1). There is an overall shrinkage of brain tissue, with the most affected areas being the hippocampus and the cerebral cortex.

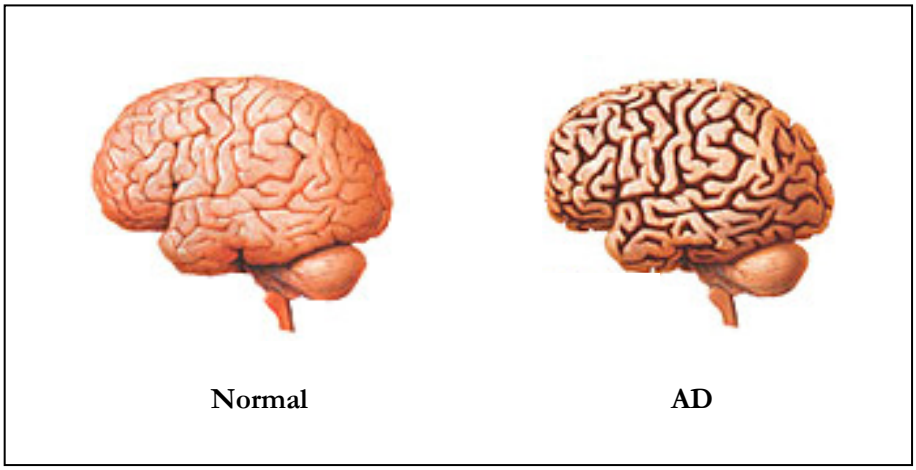

Figure I.1. AD patients exhibit shrinkage of the overall brain volume. Brains from a healthy person (left) and an Alzheimer's patient (right), showing AD-induced depthnening of brain sulci and loss of grey matter. From: http://www.life-enhancement.com/article_template.asp?ID=912.

The grooves or furrows in the brain, called sulci, are noticeably widened and there is shrinkage of the gyri, the well-developed folds of the brain's outer layer. In addition, the ventricles, or chambers within the brain that contain cerebrospinal fluid, are noticeably enlarged (Fig. I.2).

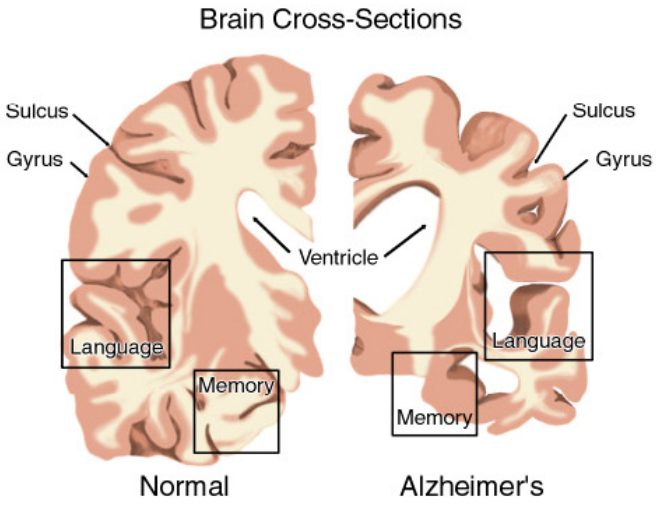

Figure I.2. Image representing a brain coronal section, as seen from the front. The left side represents a brain from a normal individual and the the right side represents a brain with Alzheimer's disease. From: http://www.ahaf.org/alzdis/about/BrainAlzheimer.htm.

As a dementia, clinical symptoms in AD are characterized by the development of multiple cognitive deficits, including memory impairment, and altered behaviour. Reduced overall activity is also observed (Fig. I.3). In the early stages of AD, short-term memory begins to decline when the cells in the hippocampus, which is part of the limbic system, degenerate. The ability to perform routine tasks also declines. As the cerebral cortex (the outer layer of the brain) becomes affected, judgment declines, emotional outbursts may occur, and language is impaired. Progression of the disease leads to the death of more nerve cells and subsequent behavioural changes, such as wandering and agitation. The ability to recognize faces and to communicate is completely lost in the final stages of the disease. Patients lose bowel and bladder control, and eventually need constant care. This stage of complete dependency may last for years before the patient dies. The average length of time from diagnosis to death is 4 to 8 years, although it can take 20 years or more for the disease to run its course.

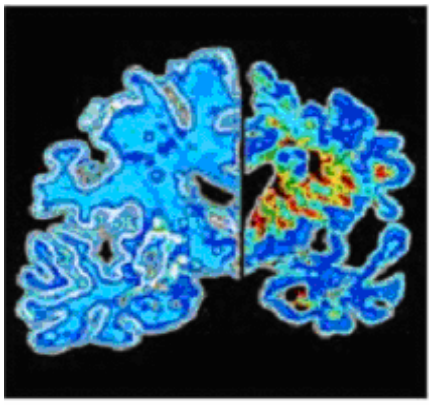

Figure I.3. Brain imaging (PET) scans of an Alzheimer disease brain showing brain shrinkage and reduced activity (right) and normal brain (left). From: http://www.pfizer.com/brain/etour5.html (photo credit - National Institute on Aging).

The extreme relevance of the scientific research involving AD ethiologies and the finding of therapeutic targets is well underlined in a transcript of the U.S. Pharmacist Continuing Education (ACPE Program No. 430-000-01-028-H01): "When Dr. Alzheimer first reported his cases, individuals over the age of 65 years represented only 3% of the U.S.A. population. The average life expectancy at that time was 47 years. It is estimated that by the year 2020, one fifth of the United States population, or more than 55 million people, will be 65 years old or older. Of these, about 10% will develop AD. Both the prevalence and incidence of AD increase with age, so it is estimated that by age 85, up to 50% of individuals will be affected". In the U.S., AD is the fourth-leading cause of death, and the third most expensive disease following heart disease and cancer. The total U.S. national cost of caring for AD patients is estimated to be over $90 billion annually." The importance of this disease is also highlighted by the projects on AD and associated disorders (ADAD) funded by the European Union in several € million (Sykes et al., 2001). For example, between 2000 and 2003 the V Framework Programme funded with € 2 million projects aiming to diagnose, prevent, delay the onset or treat AD (from: http://europa.eu.int/comm/research/ress/2000/pr2109-alz-en.html).

I. 1. 2 – AD HISTOPATHOLOGICAL CHARACTERISTICS

Post-mortem histological analysis of Dr. Alzheimer's patient's brain revealed dense bundles of unusual fibrils within nerve cells and numerous focal lesions within the cerebral cortex (Alzheimer, 1911). The dense fiber-like tangles were later called neurofibrillary tangles (NFTs) and the darkly staining focal lesions are now known as amyloid or senile plaques (AP) (Fig. I.4), as they had been previously observed in several other aged brain samples (reviewed in Brandt et al., 2005). The plaques may then occur in the absence of dementia, while the

tangles are seen in illnesses other than AD. The coexistence of both lesions, along with cerebral atrophy and neuronal degeneration, are the conclusive hallmarks of the disease.

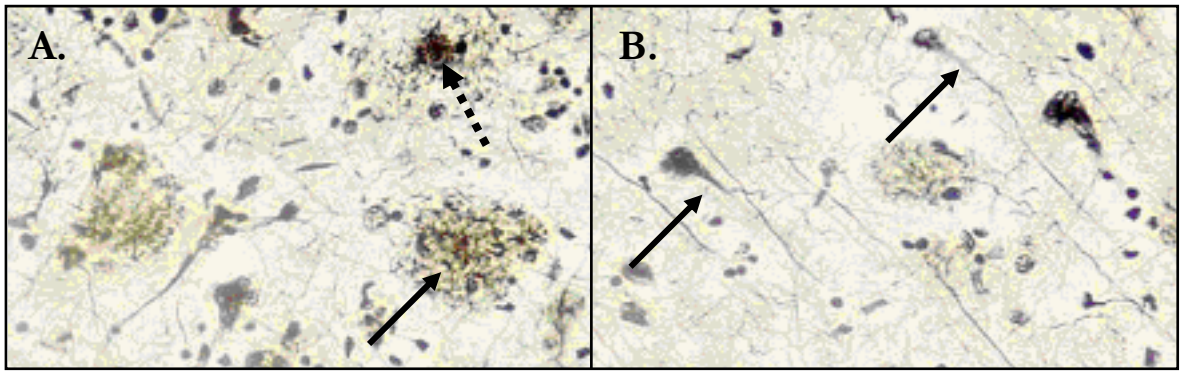

Figure I.4. Microphotographs of an AD patient sectioned brain tissue exhibiting high density of: **Panel A**: Amyloid plaques (full arrow) with the amyloid core (dashed arrow) indicated; **Panel B**: Neurofibrillary tangles. From: http://www.neuropat.dote.hu/alzheim.htm.

Neurofibrillary tangles are intraneuronal bundles of paired helical filaments (PHF) consisting predominantly of the protein Tau (Goedert et al., 1996), that occur at dystrophic neurites, and are mainly found in the pyramidal regions of the amygdala, hippocampus and neocortex (Williams, 2001). Tau protein is an axonal protein in neurons where it supports neurite outgrowth and stabilizes neuronal microtubules by acting on tubulin polymerization and stabilization (Smith, 1996). It was discovered that Tau can also function as a regulator of intracellular vesicles and organelle traffic (Drewes et al., 1998). Pathologically aggregated Tau is a hallmark of several dementias, in some cases caused by mutations in the *tau* gene (as in the frontotemporal dementia FTDP-17), but this not the case in AD (Poorkaj et al., 1998; Spillantini et al., 1998).

Amyloid plaques are extracellular lesions containing 7-10 nm thick intermixed amyloid fibrils of the 40 - 42 amino acid peptide Abeta (Allsop et al., 1983) and non-fibrillar forms of Abeta, though in its constitution more than 30 other proteins/peptides have also been found. The underlying protein component of these fibrils invariably adopts a predominant antiparallel β-pleated sheet configuration, from which the name Abeta (amyloid β) arose. Figure I.5 shows that the Abeta core of the AP consists of large numbers of closely-packed, radiating fibrils, similar in appearance to those seen in other forms of amyloidosis (Kidd, 1964; Terry et al., 1964). The amyloid plaques can be diffuse or neuritic (the latter containing dystrophic neurites with aggregated Tau), and are found diffusely throughout the brain, but notably in the cerebral cortex and hippocampus of AD patients (El Khoury et al., 1996; Dickson, 1997).

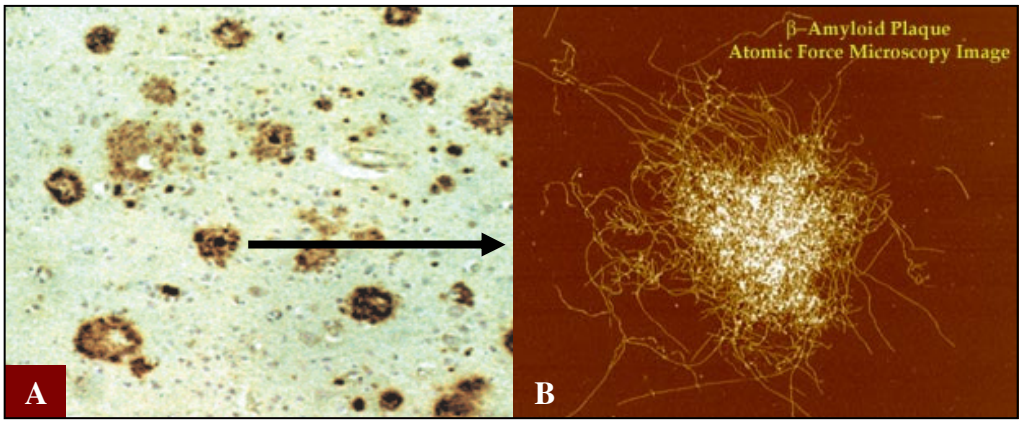

Figure I.5. Panel A: Microphotograph of an AD patient sectioned brain tissue (cerebral cortex) showing amyloid plaques (arrow) (from: http://w3.uokhsc.edu/pathology/deptlabs/Alzheimer/alzheimer_neuritic.htm). **Panel B:** Atomic force microscopy image of AP amyloid fibrils formed by Abeta "in vitro" aggregation (from: Harper et al., 1997).

The majority of Abeta peptides are 40 amino acids long (Abeta 1-40), soluble and apparently less neurotoxic, whereas the more hydrophobic peptides (less soluble) are 42 amino acids long (Abeta 1-42) and although they are less prevalent, overall they predominate in the protein core of plaques (Jarret and Lansbury, 1992; Jarret et al., 1993). Diffuse plaques, which are focal diffuse deposits of amyloid without accompanying dystrophic neurites, and that may represent an early stage of AD plaques, contain predominantly Abeta 1-42 and small levels of Abeta 1-43 rather than Abeta 1-40 (Gowing et al., 1994; Iwatsubo et al., 1994; Iizuka et al., 1995; Iwatsubo et al., 1995; Lemere et al., 1996).

Amyloid vs NFTs. Evidence points to amyloid deposition preceding and precipitating the formation of NFTs in some patients, with Abeta preceding Tau aggregation. In agreement with this, Tau deposition in transgenic mice is influenced by Abeta (Stalder et al., 1999; Lewis et al., 2001). In young Down's syndrome patients, Abeta deposits exist in the absence of NFTs, notably in areas of the brain most affected by AD (Iwatsubo et al., 1995; Leverenz and Raskind, 1998; Gouras et al., 2000). Typically, these two aggregates (APs and NFTs) constitute the neuropathologic criteria confirming AD. Post-mortem brain autopsy is still the most accurate and definitive mean of AD diagnosis (Crimson and Eggert, 1999), but the patient's death often occurs long after the onset of the dementia. Consequently, the relationship between the pathology and the actual mechanism of the disease remains unclear.

"In vivo" Diagnosis. Until recently, AD was diagnosed by ruling out other disorders known to cause similar symptoms ("diagnosis of exclusion"), such as cerebrovascular diseases, Parkinson disease, brain tumour, etc. (First, 1994). Nowadays physicians can use brain imaging

such as MRI (magnetic resonance imaging) techniques, alongside recently developed cognitive tests in order to identify and document specific changes in the brain as early as possible. Recently, an Alzheimer's-predicting FDG-PET scan has been developed where the metabolic activity in the hippocampus is measured to try to predict future AD development (Mosconi et al., 2005). In addition, a molecular-based diagnosis is presently the subject of particular interest. The aim is to identify alterations in molecular markers at an early stage of the disease, and to use these in the accurate clinical screening by means of recently developed microarray technology. Thus it is fundamental to understand the underlying molecular aspects of AD.

I. 1. 3 – AD RISK FACTORS AND GENETIC LINKAGE

Many theories exist as to the precise causes of AD, but the exact pathophysiological mechanisms remain unknown. It is a syndrome in which multiple molecular etiologies can trigger a varied but largely stereotyped pathogenic cascade. Whatever the causes that induce a variety of neurotoxic events they result in vast neuronal degeneration, which manifests as a progressive cognitive impairment with widespread neurological and neuropsychiatric disturbances (Emilien et al., 2000). From this perspective, AD resembles other common, multigenic degenerative pathologies of late life, such as atherosclerosis. Both AD prevalence and incidence estimates consistently follow an exponential pattern, both roughly doubling every 5 years after age of 65, when prevalence is about 5-10%. The prevalence of inherited forms of the disease ranges from 1% to 30%. A familial history of dementia is a risk factor in AD and several determinants may influence the development of the disease (Richard and Amouyel, 2001).

I. 1. 3. 1 – AD genetic risk factors

Late-onset AD. AD is typically a late-onset dementia, and in many cases sporadic in nature. The presence of the apolipoprotein E type 4 (Apoε4) allele on chromosome 19 is considered the major risk factor for the development of common late-onset AD. This risk factor is allelic dose-dependent, as the presence of one ε4 allele increases the risk of developing late-onset AD by 2-4 times, while a double allele increases that risk 4-8 times (Mayeux et al., 1998). Other genetic susceptibility factors have been proposed. Polymorphisms on genes encoding several proteins, including α2-macroglobulin, angiotensin I converting enzyme, Fe65 and Presenilin 1, are associated with the disease (Chapman et al., 1998; Alvarez et al., 1999; Rodriguez et al., 2000; Lambert et al., 2000). The situation may be further

complicated as some mitochondrial genetic polymorphisms have been recently proposed to be associated with AD (reviewed in Zhu et al., 2004).

Early-onset AD. Approximately 5-10% (Richard and Amouyel, 2001) of AD cases are inherited as a fully penetrant autossomal dominant trait, related to mutations on chromosomes 1, 14, and 21, and triggering early-onset AD (Schellenberg, 1995; Sandbrink et al., 1996b). These mutations contribute to the pathologic basis of the majority of AD Familial cases (FAD). Nonetheless, molecular and genetic studies of these forms have enormously increased our knowledge of the aetiology of the much more abundant sporadic form. The three genes identified with those chromosomal mutations code for the Amyloid Precursor Protein (APP) and for Presenilin 1 and 2 (PS1 and PS2) (Czech et al., 2000). Mutations in the *app* or *ps* genes are highly predictive for the disease, the prevalence of the AD phenotype being higher than 95% (St. George-Hyslop, 1999). The phenotype in the majority of FAD early-onset cases is indistinguishable from that in sporadic late-onset AD. These mutations lead to abnormal processing of the APP protein, resulting in increased accumulation of amyloidogenic peptides Abeta 1-40 and Abeta 1-42. This is a common theme in inherited forms of amyloidosis, where a mutant protein or peptide is particularly "amyloidogenic", i.e., it has an increased tendency to form antiparallel β-pleated sheet fibrillar structures.

APP as a risk factor. The Abeta peptide is part of a much larger precursor protein - the Alzheimer's amyloid precursor protein (Kang et al., 1987). The first of the 20 known mutations (Kowalska, 2004) to be discovered in the *app* gene (chromosome 21) was Glu^{22} to Gln ("Dutch" mutation) within the Abeta sequence (Hardy and Allsop, 1991). Subsequently, some families with early onset AD were found to have pathogenic mutations at APP Val^{642}, resulting in a change from Val^{642} to Ile, Gly or Phe (Chartier-Harlin et al., 1991; Goate et al., 1991; Murrell et al., 1991). All these mutations result in an increase in the relative amounts produced of the more amyloidogenic Abeta 1-42 compared with Abeta 1-40, i.e. a longer Abeta form with increased propensity to aggregate (Wisniewski et al., 1991; Burdick et al., 1992; Clements et al., 1993). The "Swedish" double mutation (Lys^{595}/Met^{596} to Asn/Leu, on the immediate Abeta N-terminus) results in secretion of larger amounts of total Abeta (Citron et al., 1992; Cai et al., 1993). The APP "Arctic" mutation (Glu^{693} to Gly) leads to decreased Abeta 1-40/1-42 levels in plasma and in cells conditioned media, but as a consequence of a higher Abeta tendency to aggregate. In fact, Abeta with the Arctic mutation forms protofibrils at a much higher rate and in larger quantities than wild-type Abeta (Nilsberth et al., 2001). Several APP mutations are listed in http://www.alzheimer-adna.com/Gb/APP/

APPsequence.html. Further, the levels of APP being expressed also appear to be highly significant. For example individuals who have Down's syndrome have at the same time an extra copy of chromosome 21 and a higher likelihood of developing AD by age of 50 (Esler and Wolfe, 2001).

Presenilins 1 and 2 as risk factors. The genes responsible for the majority of FAD cases were found to be *ps1* on chromosome 14 (Sherrington et al., 1995; Walter et al., 1996) and *ps2* on chromosome 1 (Scheuner et al., 1996), and not on *app* itself. Nonetheless, pathological mutations on either APP or Presenilins lead to a similar phenotype, diverting APP processing towards the production of long Abeta 1-42 compared to short Abeta 1-40 (Borchelt et al., 1996; Mehta et al., 1998). In fact, plasma and media samples from cultured skin fibroblast of subjects carrying these mutations exhibited a doubling in the levels of Abeta 1-42 when compared to controls (Scheuner et al., 1996). Additionally, PS1 mutant mice exhibit up-regulated intracellular calcium release from the endoplasmic reticulum (ER), which is being associated with greatly increased vulnerability to Abeta-induced apoptosis (Chan et al., 2002). There are at least 132 mutations reported to occur in Presenilins, with the majority being missense point mutations (for review see Kowalska, 2004).

I. 1. 3. 2 – AD non-genetic risk factors

Several environmental and non-genetic factors can contribute to the AD etiology. Some well-established risk factors for AD include age, female gender, low educational status, vascular changes, and decreased levels of acetylcholine (Amaducci et al., 1992; Rogers, 1998). More recently, head injury, elevated serum cholesterol, and high levels of aluminum in drinking water have been added to the list of potential risk factors (Guo et al., 2000; Rondeau et al., 2000; Wolozin et al., 2000). Cellular stresses, such as oxidative stress, have also been implicated as possible triggers for AD onset, along with their roles in its development, by interfering with signalling cascades (Farooqui et al., 2004; Maiese and Chong, 2004; Moreira et al., 2006). Moreover, a common phenotype observed in AD patients' brains is altered protein phosphorylation, which can potentially lead to altered cellular signalling (da Cruz e Silva et al., 2004a). The importance of this regulatory mechanism in AD and its possible implications on the disease onset will be further discussed and underlies the central theme of this thesis.

I. 1. 4 – THE "AMYLOID CASCADE" HYPOTHESIS OF AD ETIOLOGY

Advances in AD research, especially in molecular genetic analysis of early onset FAD, led to the formulation of the "Amyloid Cascade" hypothesis. This hypothesis states that overproduction of Abeta and its aggregation into amyloid plaques is the root cause of AD (Hardy and Allsop, 1991). Almost all cases of FAD are linked by highly penetrant mutations to genes that affect the release of Abeta from APP, leading to higher overall Abeta production or to higher formation of its amyloidogenic forms, namely Abeta 1-42. Genetic polymorphism in the ApoE gene, a molecular chaperone involved in Abeta aggregation, may contribute differently in the aggregation of the latter into amyloid fibrils (Folin et al., 2006). The "amyloid cascade hypothesis" (Fig. I.6) is now widely accepted, with Abeta having a central role in neurotoxicity and AD, and has been extensively reviewed (e.g. Selkoe, 1994; Iversen et al., 1995; Forloni, 1996; Mattson, 1997; Selkoe, 2001).

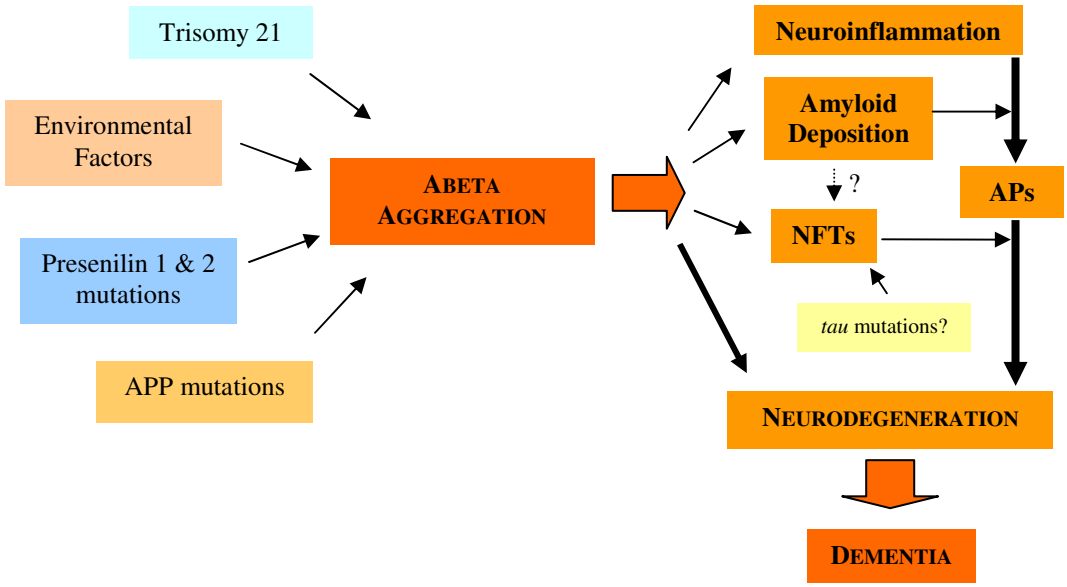

Figure I.6. "Amyloid cascade hypothesis" underlying the central role of Abeta aggregation.

At the molecular cascade level diffuse neurocentric amyloid deposits would evolve over time and eventually become neuritic APs. One hypothesis is that deposition of Abeta 1-42 may form a "precipitation core" to which soluble Abeta 1-40 could aggregate, in an AD-specific process. The "in vivo" aggregation of Abeta may precipitate a chronic and destructive inflammatory process in the brain, occurring in the immediate vicinity of APs in AD patient brains (Eikelenboom et al., 1994). Some of the proinflammatory molecules thereby produced

may be locally toxic to neuronal processes in the vicinity of AP, such as complement, cytokines, reactive oxygen and nitrogen intermediates. They also produce factors, such as Interleukin-1 (IL-1), which stimulate APP synthesis, leading to a vicious cycle of reciprocal activation and growth, which potentiates a local inflammatory cascade. These would culminate in the neurodegenerative process possibly via free radical production by microglia cells and/or complement lysis of neuronal membranes (Allsop, 2000). Although it is not clear if Abeta accumulation is a cause or effect in AD, its production nonetheless plays a central role.

I. 2 – THE ALZHEIMER'S AMYLOID PRECURSOR PROTEIN

I. 2. 1 – APP ISOFORMS AND GENE FAMILY

APP is a glycoprotein with a single transmembrane domain towards its carboxyl-terminus. The mammalian APP superfamily comprises three members: APP and APP-like proteins APLP1 and APLP2 (Sprecher et al., 1993; Wasco et al., 1993), of which APLP2 is the nearest relative (50% of homology). These three related proteins are well-conserved in evolution, functionally and structurally related, and share similar functions (Bayer et al., 1999; Coulson et al., 2000). The mammalian APP family members are type I integral membrane proteins that have relatively large extracellular domains and short intracellular domains. Of note is that APLP1 and APLP2 share homology at the amino acid sequence, domain structure and protein organization with APP, but lack the Abeta domain. Other known members of the APP superfamily are non-mammalian and include APPL in *Drosophila* (Rosen et al., 1989; Luo et al., 1992), APL-1 in *C. elegans* (Daigle and Li, 1993) and an APP homologue protein in *Xenopus* (Okado and Okamoto, 1992).

APP isoforms. The APP gene is located on human chromosome 21 (21q21.2-3) and contains 18 exons (GenBank A.N. D87675), with the Abeta sequence divided between exons 16 and 17 (Fig. I.7). The sequence of the Abeta peptide starts at residue 597 (except when otherwise indicated, numbering is according to the APP_{695} isoform) and spans the extracellular and membrane domains. At least eight isoforms of APP have been described, numbered according to their length in amino acids: L-677, 695, L-696, 714, L-733, 751, L-752, 770 (Kitaguchi et al., 1988; Ponte et al., 1988). These isoforms arise from alternative splicing of exons 7, 8 and 15 of the APP mRNA (Kosik, 1993) and differ in size extracellularly, but share the same cytoplasmic, transmembranar and Abeta peptide sequences.

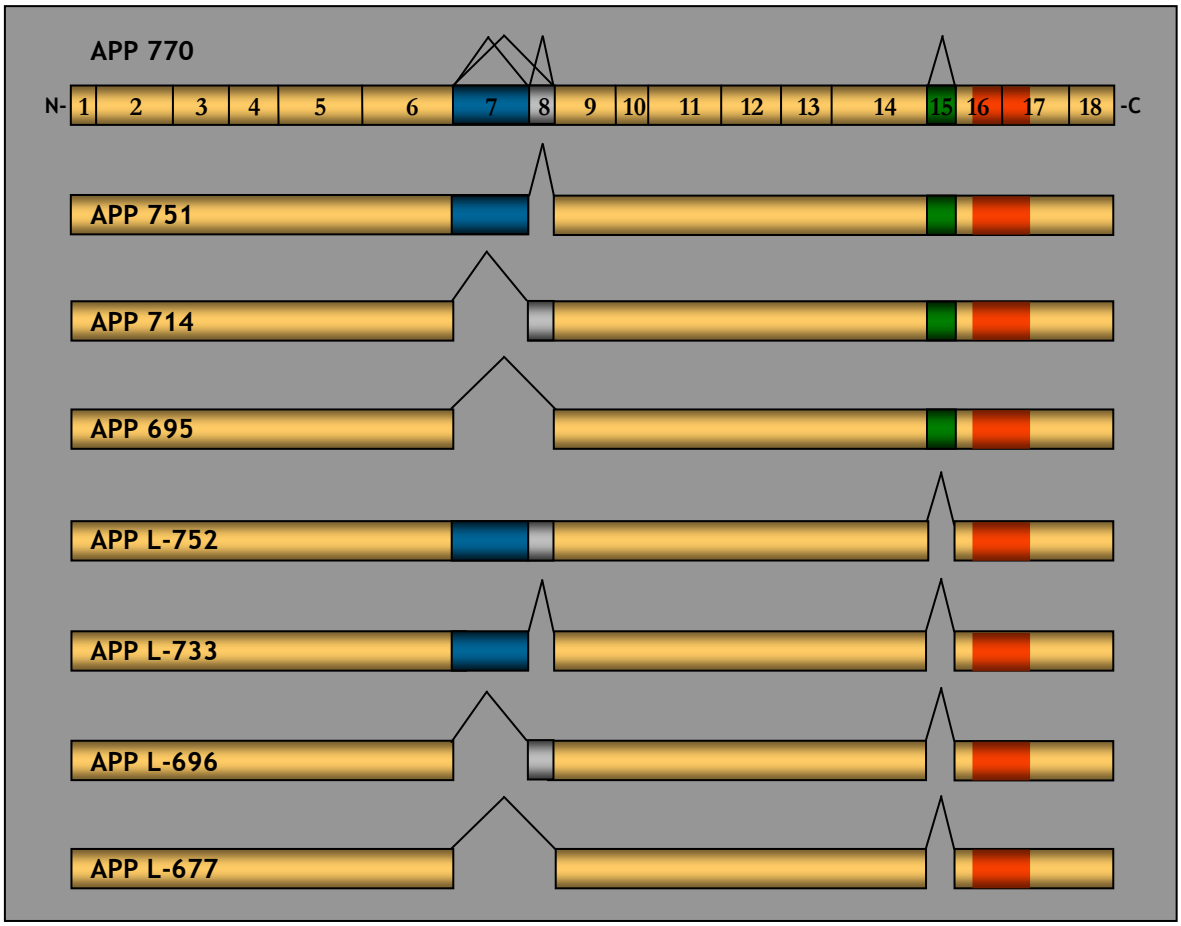

Figure I.7. Exon structure of the full length APP transcript and the final eight isoform products. The alternatively spliced exons are indicated in colour: *blue,* exon 7; *grey*, exon 8; *green*, exon 15. The Abeta sequence is indicated in red.

Analysis of APP mRNA expression levels revealed that APP can be detected in almost all tissues examined, as well as in cultured cells. It is ubiquitously expressed in mammalian cells (Tanzi et al 1987; Neve et al., 1988; Tanzi et al., 1988; Weidemann et al., 1989; Golde et al., 1990; Sisodia and Price, 1995) with a broad tissue distribution. The tissue-specific pattern of APP mRNA splicing was studied by RT-PCR analysis (Sandbrink et al., 1994a). The less abundant L-APP isoforms, lacking exon 15, are mainly expressed in leukocyte cells, such as T-lymphocytes, macrophages and microglial cells. They are also ubiquitously expressed in rat tissues, including brain, but not in neurons (Ohgami et al., 1993; Sandbrink et al., 1994a). The three major APP isoforms were found to be the 695, 751 and 770 (Fig. I.7). Of these, APP_{695} is the only one lacking exon 7. The exon 7-containing APP mRNA isoforms (751 and 770) are predominantly expressed in peripheral tissues. Brain tissue expresses little APP_{770} and, depending on the animal species and brain region analysed, low, intermediate or high levels of APP_{751} (Neve et al., 1988 ; König et al., 1989; Tanaka et al.,

1989; Kang and Muller-Hill, 1990). However, the exon 7-containing isoforms predominate in cultured astrocytes (Gray and Patel, 1993a,b; Rohan de Silva et al., 1997), with the 695:751:770 ratio being 1:4:2 (Gray and Patel, 1993a,b). A number of studies have indicated that alternative splicing of exons 7 and 8 changes in brain during aging and with AD, but results obtained are still inconsistent and controversial to consider altered alternative splicing as an AD risk factor (Sandbrink et al., 1994b; Rockenstein et al., 1995; Moir et al., 1998; Panegyres et al., 2000). Conversely to the 751 and 770 isoforms, the 695 is the APP isoform predominantly produced in the mammalian brain, with the 695:751:770 mRNA ratios being approximately 20:10:1 (Tanaka et al., 1989). Furthermore, APP_{695} is most highly expressed in neurons, representing 95% of total neuronal APP (Tanzi et al., 1987; Weidemann, 1989; LeBlanc et al., 1991), and is therefore often referred to as the "cerebral" or "neuronal" isoform. In conclusion, as APP_{695} is the isoform predominantly produced in the brain, and predominates within the CNS (Neve et al., 1988; Tanzi et al., 1993), this isoform has received the most attention in AD research.

I. 2. 2 – APP FUNCTIONAL DOMAINS

APP exon 7 encodes a 56-amino acid (aa) stretch with homologies to the Kunitz-type protease inhibitors (KPI) that inhibits proteases, such as trypsin or plasmin, and blood coagulation factors (Van Nostrand and Cunningham, 1987; Kitaguchi et al., 1988; Ponte et al., 1988; Wagner et al., 1992). Exon 8 encodes a 19-aa domain with homologies to the MRC OX-2 antigen found on the surface of neurons and certain immune cells such as thymocytes (Clark et al., 1985; Kitaguchi et al., 1988; Tanzi et al., 1988). In adition to KPI and OX-2, several other structural features have been identified within the APP ectodomain (Fig. I.8).

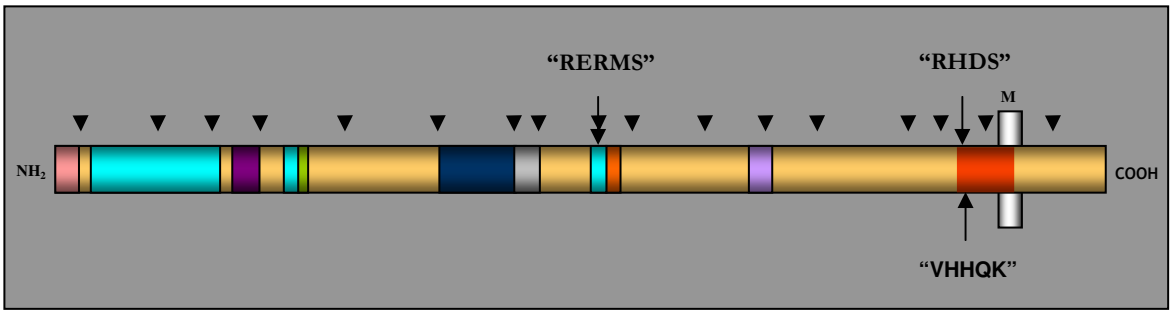

Figure I.8. APP functional subdomains (APP_{770} numbering). *Pink*, signal peptide (1-17); *light blue*, heparin-binding domains (28-123; 174-185; 391-412); *violet,* cupper-binding domain (135-155); *green*, zinc-binding domain (181-188); *dark blue,* KPI domain; *grey,* OX-2 domain; *"RERMS"*, putative growth-promoting motif (403-407); *orange*, gelateinase A (matrix metalloproteinase) inhibitor (407-417); *lavander*, collagen-binding site (523-540); *red,* Abeta; *"RHDS",* integrin-binding motif (aa 5-8 of Abeta); "VHHQK", heparin-binding motif (aa 12-16 of Abeta). APP exons boundaries are marked with arrowheads. **M**, cell membrane.

Two subdomains (328-332 and 444-612) were deduced to have a neuroprotective function, including the "RERMS" sequence with putative growth-promoting properties (Ninomiya et al., 1993). Several heparin-binding domains (Small et al., 1994), the stronger at 316-337 (exon 9 and beginning of 10), a collagen-binding site (Beher et al., 1993), an integrin-binding motif (amino acid sequence RHDS at residues 5-8 of Abeta) (Ghiso et al., 1992) and N-linked carbohydrate attachment sites (Weidemann et al., 1989) were also found in this region. Indeed, APP has been shown to bind laminin, collagen, and heparin sulphate proteoglycans (Breen et al., 1991; Kibbey et al., 1993). The ectodomain also contains two binding-sites for metals such as zinc (Bush et al., 1993; Bush et al., 1994) and copper (Hesse et al., 1994; Multhaup et al., 1996).

I. 2. 3 – PUTATIVE FUNCTION OF APP AND APP FRAGMENTS

Several putative roles have been postulated for APP, including participation in cell-cell and cell-matrix adhesion, heparin-binding, growth promoting activities, proteinase inhibition and receptor activity. Other suggestions include regulation of neurite outgrowth, promotion of cell survival, protection against a variety of neurotoxic insults, stimulation of synaptogenesis, modulation of synaptic plasticity, and involvement in learning and memory processes (for reviews: Mattson, 1997; De Strooper and Annaert, 2000; Dodart et al., 2000; Turner et al., 2003). The first clues to APP function derived from sequence analysis and studies that identified different functional APP subdomains on the extracellular portion of the molecule. Presently, many putative functions of APP result from studies on the APP subcellular protein binding partners (as discussed further on) or transgenic animal models (Higgins et al., 1994; Mucke et al., 1994; von Koch et al., 1997; Rassoulzadegan et al., 1998; Heber et al., 2000). Additionally, APP can be processed (section I.2.4) and various physiological functions have also been attributed to the resulting cleavage products.

Memory. There is evidence for a specific role of APP in long term memory (Doyle et al., 1990; Flood et al., 1991; Huber et al., 1993). APP knockout mice show impaired behavioral performance (Muller et al., 1994; Zheng et al., 1996). Additionally, blocking the extracellular domain of APP by intracerebral and intracerebroventricular administration of anti-APP antibodies targeted against various isoforms of APP differentially impairs behaviour and memory in rats (Doyle et al., 1990; Huber et al., 1993; Chan et al., 2002; Turner et al., 2003). Conversely, exposure of hippocampal slices to the secreted APP (sAPP) fragment αsAPP (see below section I.2.4) results in altered frequency of LTD and an increase in LTP (Ishida et al.,

1994), strengthening a role for APP in learning and memory processes. Indeed, infusion of αsAPP and the RERMS sequence enhances memory formation (Meziane et al., 1998) and prevent APP anti-sense-induced memory loss (Mileusnic et al., 2000).

Brain development. It has been suggested that the APP protein family has a role in the reelin signalling pathway, and may participate in neuronal migration and positioning during brain development (Ishida et al., 1994; Bothwell and Giniger, 2000). Supporting the hypothesis for APP involvement in cell differentiation and synaptogenesis, APP isoform levels were found to reach their maximum peak during the second postnatal week of the rat, the time of brain maturation and completion of synaptic connections (Loffler and Hubert, 1992). Also of note is the finding that APP can be regulated by cholinergic mechanisms (Bayer et al., 2001).

CAM- (cell adhesion molecule) and SAM- (substrate adhesion molecule) functions. CAM or SAM molecules are known to play important roles in synaptic remodeling in development and during regeneration of neurites after injury (Chan et al., 2002). All APP isoforms possess two heparin-binding domains responsible for APP binding to the glycan moieties of proteoglycans, such as glypican (Small et al., 1996; Williamson et al., 1996), heparin and heparin-based glycosaminoglycans, such as heparin sulphate, in a time-dependent and saturatable manner (Multhaup et al., 1994; Multhaup et al., 1995). Heparin is a well known extracellular matrix component, and the APP strong heparin-binding site was found to be conserved in human APP, APLP1 and APLP2, and to occurr at residues 316-337 of APP_{695} (Multhaup, 1994) (see above Fig. I.8). Other studies (Breen et al., 1991; Robakis et al., 1993; Coulson et al., 1997; Fossgreen et al., 1998; Storey et al., 1999; Soba et al., 2005) provided additional evidence for APP functioning as a CAM and SAM molecule. L-APP isoforms were observed to function as core proteins of the strong CAM apican proteoglycans (Pangalos et al., 1996). L-APP and L-APLP2 isoforms have an additional xylosylransferase recognition site for xylosylation (chondroitin-sulfate-glycosaminoglycans attachment) (Thinakaran et al., 1995; Gotting et al., 1998) (Fig. I.9). This post-translational modification confers more adhesiveness properties and less sensitivity to β-secretase cleavage (Sandbrink et al., 1996a). Fibroblasts from FAD patients that were observed to have down-regulated APP mRNA levels had at the same time decreased cellular adhesiveness (Ueda et al., 1989). Hep-1 cells expressing an APP FAD mutant cDNA also exhibited decreased comparative cell adhesion properties (Kusiak et al., 2001). Furthermore, down-regulation of APP using antisense oligonucleotides also reduced neuronal adhesion to specific substrata, and APP over-expression in the neuronal-like B103 cells led to more rapid cellular adhesion (Schubert and Behl, 1993).

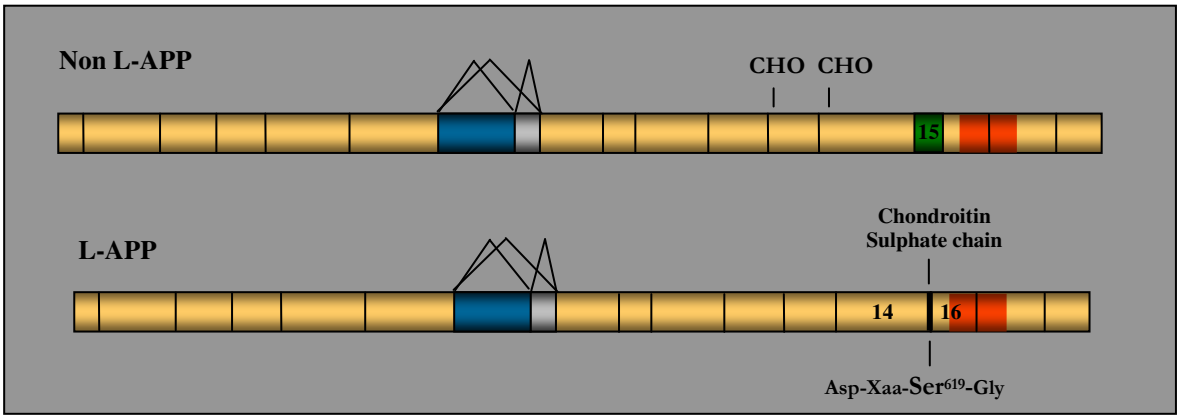

Figure I.9. Glycosylation relevant APP domains. CHO, chains of N-glycans linked at Asn residues 542 (exon 13) and 571 (exon 14) (APP_{770} numbering). L-APP isoforms lacking exon 15 possess a sequence for chondroitin sulphate chain attachment (at Ser^{619}). Abeta sequence is indicated in red.

Interstingly, cell surface APP has been recently reported to trans-interact with other APP (or APLP) molecules at the surface of adjacent cells, promoting trans-cellular adhesion "in vivo" (Soba et al., 2005).

Cell motility regulation. Reports show that interaction of APP with the APP-binding protein Fe65 (see section I.2.6) induced cell motility in wound healing assays (Guenette, 2002). At focal complexes, Fe65 binds to and recruits APP and additional proteins such as Mena (a cytoskeletal protein enriched in axonal growth cones) into a macromolecular complex that may be involved in microtubule assembly and promotes membrane extension and motility (Sabo et al., 2001).

Neurite outgrowth, synaptogenesis and synaptic plasticity. APP has also been allocated roles in neurite outgrowth, synaptogenesis and synaptic plasticity (for review e.g. Mattson, 1997). Cell surface APP-induction of neurite outgrowth stimulation was observed in hippocampal neurons (Qiu et al., 1995) and in B103 cells overexpressing APP (Schubert and Behl, 1993). Studies using recombinant αsAPP or antibodies against it have demonstrated its role in regulation of neurite outgrowth and cell survival in developing hippocampal neurons (Mattson et al., 1993; Matson, 1994). Roles in synaptic plasticity of mature hippocampal neurons were also attributed to αsAPP (Furukawa et al., 1996b; Ishida et al., 1997).

Growth-promoting and neuroprotective roles. Secreted APP containing the KPI insert was initially found by sequence analysis to be identical to protease nexin II (Van Nostrand et al., 1987). The latter is a growth regulatory molecule, produced by fibroblasts, that is an inhibitor of extracellular serine proteinases (Smith et al., 1990). A growth-promoting

effect of sAPP has been shown for fibroblasts and cultured neurons, and this activity has been claimed to reside in the amino acid sequence RERMS at residues 328-332 of APP_{695} (Ninomiya et al., 1993; Jin et al., 1994). Secreted APP has also been reported to be neuroprotective (Mattson, 1997) and sAPP is capable of protecting cells against Abeta or glutamate-mediated neuronal damage (Mattson et al., 1993; Goodman and Mattson, 1994). However, not all of the neurotrophic and neuroprotective activities of sAPP can be attributed to the RERMS pentapeptide region (Ohsawa et al., 1997). The alpha sAPP form is approximately 100-fold more potent than beta sAPP (see below section I.2.4) in protecting hippocampal neurons against excitoxicity or Abeta mediated toxicity. The former is also the sAPP species involved in developmental regulation and synaptic plasticity (Furakawa et al., 1996b), probably due to the VHHQK heparin-binding domain (residues 12-16 of Abeta), which is only present in the alpha sAPP form.

Cellular toxicity and apoptosis. The physiological properties of Abeta seem to be critically dependent on its state of aggregation (Howlett et al., 1995; Atwood et al., 2003), with its dimeric or oligomeric (protofibrillar) forms possessing cytotoxic properties (Roher et al., 1996; Mattson, 1997, Lambert et al., 1998). Hence, the endogenous APP derivatives are believed to oppositely modulate apoptosis through an autocrine loop. After KCl-induced apoptosis, incubation with antibodies against Abeta increased neuronal survival by 30% while antibodies against sAPP decreased it by 53% (Piccini et al., 2000). In primary neurons Abeta 1-40 maximally activated NF-κB (an immediate-early transcriptional regulator of numerous proinflammatory genes) (Kaltschmidt et al., 1997). Interestingly, the neurotoxic properties of injected Abeta on primate brains only appeared in aged but not in young animals, suggesting that aged brains may be more vulnerable to Abeta-mediated toxicity (Geula et al., 1998). However, further complexity is added to the system being that weak neurotrophic properties were also attributed to the Abeta soluble form (Tanimukai et al., 2002; Atwood et al., 2003).

Signalling cascades. αsAPP has been shown to induce alterations in various second messengers and effectors including cyclic GMP, protein kinase G (Barger et al., 1995; Furukawa and Mattson, 1998), phospholipase C, protein kinase C (Ishiguro et al., 1998), extracellular signal-regulated protein kinase (ERK) (Greenberg et al., 1994; Greenberg et al., 1995) and inositol trisphosphate (Ishiguro et al., 1998; Koizumi et al., 1998). Noticeably, αsAPP induces membrane hypolarization in neurons and decreased intracellular Ca^{2+} levels, leading to decreased glutamate-induced neuronal excitability. Its effects on ion fluxes and various signalling pathways might underlie its reported physiological roles (Mattson, 1997).

Evidence points to cyclic GMP as the second messenger mediating its role in synaptic plasticity, involving neuronal excitability and calcium homeostasis (Barger et al., 1995; Furukawa et al., 1996a).

Abeta may also play an important physiological role in the central nervous system at its physiological concentrations (picomolar to nanomolar), and in neurons the level of Abeta production is much higher than in non-neuronal cells (Simons et al., 1996). Physiological concentrations of Abeta were reported to increase tyrosine phosphorylation (Zhang et al., 1994; Luo et al., 1996a), phosphatidylinositol 3-kinase activity in cultured cortical neurons (Luo et al., 1996a), and to increase PC12 cells proliferation Luo et al., 1996b). Abeta 1-42 was further reported to activate hydrolysis of an acidic phospholipid by phospholipase A2 (PLA2) (Lehtonen et al., 1996).

APP Receptor-like activity. Being that APP resembles a type I integral membrane protein and binds to an heterotrimeric G protein (G_0), a major GTP-binding protein in brain (Nishimoto et al., 1993), it has been proposed that APP functions as a cell-surface receptor involved in signal transduction. The cytoplasmic APP sequence His^{657}-Lys^{676} shows a specific G_0-activating function and is necessary for the complex formation (Nishimoto et al., 1993; Yamatsuji et al., 1996). Furthermore, fibrillar forms of Abeta were reported to bind to cell-surface APP (Lorenzo et al., 2000), and cell surface APP_{751} forms complexes with protease nexin 2 ligands being subsequently internalized (Knauer et al., 1996).

I. 2. 4 – APP PROTEOLYTIC PROCESSING

APP metabolism is complex and can occur via several pathways (Nitsch et al., 1994; Checler, 1995; Buxbaum and Greengard, 1996; Selkoe et al., 1996), which have not all been fully elucidated. Three main proteolytic sites were first identified (Fig. I.10), with each cleavage being catalyzed by separate enzymes referred to as α-, β- or γ-secretases (Esler and Wolfe, 2001). These cleavage sites were therefore named α-, β- and γ-sites. In its simplest form, APP proteolytic processing was described as occurring via two distinct pathways, one being non-amyloidogenic and the other amyloidogenic. This classification arose as α- and β-cleavages appear to be mutually exclusive events, with one precluding and the other leading to Abeta production (Small and McLean, 1999; Nunan and Small, 2000).

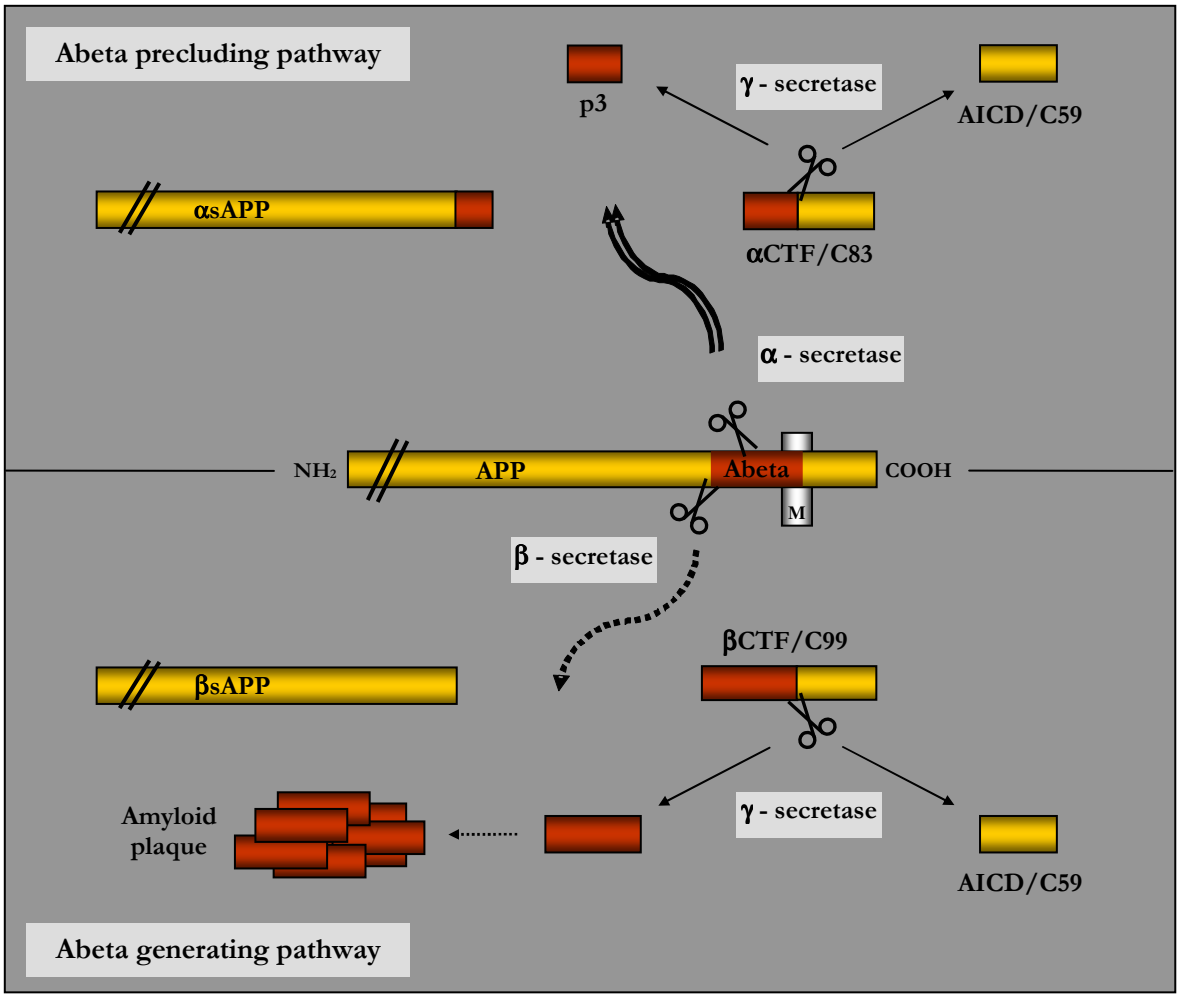

Figure I.10. Proteolytic processing pathways of APP. Top: "Non-amyloidogenic" pathway - α-secretase cleaves APP within the Abeta region precluding its formation and originating the fragments αsAPP and αCTF; **Bottom:** "Amyloidogenic" pathway - β-secretase cuts APP N-terminally to the Abeta region and gives rise to the fragments βsAPP and βCTF. The CTF fragments are further processed by γ-secretase to Abeta or p3 and the AICD fragments. The βCTF-derived Abeta product may potentially self-aggregate into amyloid fibrils.

Alpha and beta-secretases cleaving APP at the beginning or in the middle of the Abeta sequence liberate a large fragment (sAPP) from the extracellular domain of the protein, named αsAPP and βsAPP, respectively. These sAPP fragments differ in size by only 17 amino acids at their carboxy terminus (see Fig. I.10), which belong to the Abeta sequence and are present in αsAPP but absent in βsAPP. The remaining portion of APP is called the α-carboxy-terminal fragment (αCTF or C83), which is ~10 KDa, or the β- carboxy-terminal fragment (βCTF or C99), which is ~12 KDa. Subsequent to α- or β-cleavage, γ-secretase catalyzes two cleavages at the transmembrane (TM) sequence of the CTF product (Fig. I.11). One cleavage occurs in the middle of the TM (at the γ-site) and the other occurs at the end of the TM sequence (ε-site), near the cytoplasmic APP terminus (Fig. I.11). The former can occur at

several sites in close proximity, originating peptides of different lengths. βCTF is processed by γ-secretase (Younkin, 1998; Xu et al., 2002) to generate predominantly Abeta 1-40 (c.a. 90%) or 1-42 (c.a. 10%) fragments (Haass et al., 1992b; Seubert et al., 1992). Abeta species spanning from 1-39 to 1-43 amino acid long can also be produced, with fragments appearing to be more amyloidogenic with increasing length. Processing of αCTF by γ-secretase at the γ-site generates a short peptide termed p3 (3 KDa), which lacks the Abeta 17 N-terminal amino acids. Furthermore, using either α- or βCTF as a substrate, the additional product of the γ-secretase processing is a short 59/57 amino acid long C-terminal peptide, named the APP Intracellular Domain (AICD or AID) or CTF gamma (for review e.g. Koo, 2002). However, CTF gamma is very unstable "in vivo" and difficult to be detected both in brain or cell lysates (Pinnix et al., 2001; Zheng et al., 2003; Kimberly et al., 2005). In fact, the CTF gamma/C59 AICD is rapidly degraded (half-life of approximately 5 min) by a mechanism that is not inhibited by endosomal/lysosomal or proteasome inhibitors (Cupers et al., 2001). By sequence analysis of the AICD fragment, researchers have found that γ-secretase cleaves APP in an additional site (ε-site) (Sastre et al., 2001), a few amino acids downstream of the γ-site (Fig. I.11). Although both cleavages are independent of one another, they may occur nearly simultaneously (for review Selkoe and Kopan, 2003). This ε-site cleavage is thought to occur for better AICD membranar release, and as both cleavages rend a AICD peptide of 50 aa long, it was unknown which AICD peptide (C59/57 or C50) was physiologically functional (Selkoe and Kopan, 2003). Nonetheless, evidence points to the C50 AICD as the physiologically functional peptide (von Rotz et al., 2004).

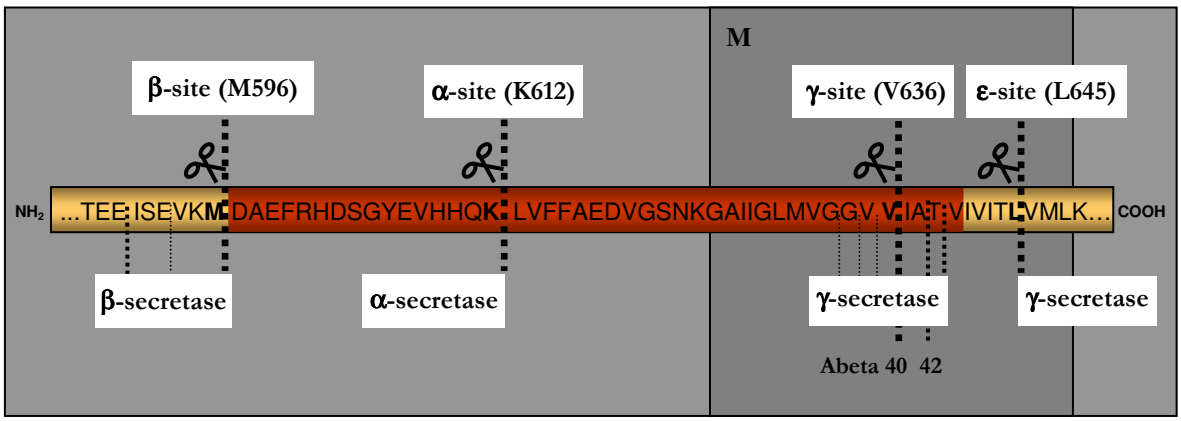

Figure I.11. APP cleavage by α-secretase precludes Abeta generation. In contrast, sequential cleavage of APP by β-secretase and γ-secretase results in the production of 40-43 amino acid long Abeta (in red) (depending on exactly where the γ-secretase cleavage occurs). The major cleavage sites of APP secretases are: Met^{596} for β-, and Lys^{612} for α-secretases, and Val^{636} (γ-site) and Leu^{645} (ε-site) for γ-secretase. **M,** cell membrane.

Additional reports have revealed that APP can also be proteolytic processed at it C-terminus by caspases, like caspase-3 (Gervais et al., 1999), caspase-6 and -8 (Pellegrini et al., 1999), or caspase-9 (Lu et al., 2000). The target residue for the caspase-directed APP cleavage is Asp^{664} (Gervais et al., 1999; Weidemann et al., 1999; Zambrano et al., 2004). The resultant C-terminus C31 peptide is a potent inducer of apoptosis, and this cleavage was shown to reduce APP internalization but to have varying effects on the secreted levels of Abeta (Pellegrini et al., 1999; Lu et al., 2000; Soriano et al., 2001).

α-Secretases. This protease cleaves APP within the Abeta fragment (Lys^{16}), close to the APP membrane-spanning domain (APP_{695} Lys^{612}-Leu^{613}). As mentioned above, cleavage at this site (the α-site, Fig. I.11) precludes Abeta generation and produces a soluble protein of 612 aa, αsAPP (Esch et al., 1990; Busciglio et al., 1993). This cleavage is constitutive and therefore depends on an enzyme that has an active pool at all times but that can be further activated by protein kinase C (PKC) activators and other second messenger cascades (Mills and Reiner, 1999). Metabotropic glutamate receptor agonists and carbachol, a M1 muscarinic acetylcholine receptor agonist, also upregulate α-secretase activity (Kirazov et al., 1997; Nitsch et al., 1997). Therefore, this pathway of APP processing has been referred to as constitutive and regulated. The search for the α-secretase identity led to an interest in zinc-dependent metalloproteases (Esler and Wolfe, 2001), and three potential candidates were identified (for review see Hooper and Turner, 2002). The first was the tumor necrosis factor alpha converting enzyme (TACE-α or ADAM 17), a disintegrin and metallopreotease (Black et al., 1997; Buxbaum et al., 1998) that releases tumor necrosis factor from its receptor form. It can also cleave a large number of other receptors including Notch (Brou et al., 2000) and TGF-α. Interestingly, TACE knockout mice showed deficiencies in αsAPP regulated but not constitutive secretion (Buxbaum et al., 1998; Merlos-Suarez et al., 1998), supporting the idea of more than one α-secretase cleavage activity. TACE ability to cleave APP constitutively was demonstrated in HEK293 cells, but it was one order of magnitude more sensitive to the inhibitor TAPI-1 than constitutive α-secretase (Slack et al., 2001). In addition, Checler et al. (2005) have observed that the majority (90-95%) of PKC-induced αsAPP production was due to TACE activity in fibroblasts, while this enzyme was only partially responsible for constitutive αsAPP production. Nitric oxide, a retrograde messenger in synaptic transmission, activates TACE "in vitro" and α-secretase "in vivo" (Zhang et al., 2000), and one can thus postulate that APP ectodomain shedding may be a crucial modulator of synaptic plasticity.

The second and third candidates are also members of the metalloproteases ADAM family: ADAM 10 and ADAM 9 (MDC9). Like TACE, they are initially expressed as inactive preproteins and their active forms can also affect αsAPP levels (Koike et al., 1999; Lammich et al., 1999). Co-transfection of APP with ADAM 10 or MDC9 results in increased (constitutive and regulated) sAPP secretion. ADAM 10 cleaves "in vitro" the Abeta peptide at the Lys^{16}-Leu^{17} bond, and the Flemish mutation Ala^{21}-Gly reduces this cleavage (Lammich et al., 1999). Of interest is the fact that the *Drosophila* Kuzbanian protein, an orthologue of ADAM 10, is involved in neurogenesis and axonal extension (Rooke et al., 1996).

β-Secretases. The site of β cleavage (β-site) occurs between residues 596 and 597 of APP_{695}, exactly at the N-terminus of Abeta (Fig. I.11), and releases βsAPP (595 aa long). The ubiquitous presence of constitutively secreted Abeta indicates that there is β-secretase activity in most cells (Haass et al., 1992b), but there is evidence that it is more active in brain than in peripheral tissues (Seubert et al., 1993). Furthermore, the levels and activity of β-secretases were found to be increased in AD (Fukumoto et al., 2002). The enzymes that cleave at the β-site have been identified as the aspartyl proteases β-site APP cleaving enzyme 1, BACE-1 (also termed Asp2 or memapsin2) (Vassar et al., 1999; Yan et al., 1999a; Vassar, 2004), and β-site APP cleaving enzyme 2 (BACE-2) (Farzan et al., 2000). They share 64% of sequence homology and are both membrane-anchored enzymes that are expressed in neural tissues, although BACE-2 expression is lower than BACE-1 (Bennett et al., 2000). Like all aspartic proteinases, BACE-1 and BACE-2 are generated as proenzymes, and while the BACE-2 activation by prodomain processing is autocatalytic, BACE-1 activation is mediated by furin or a furin-like enzyme (Bennett et al., 2000; Capell et al., 2000; Hussain et al., 2001). BACE-1 cleaves APP carrying the FAD Swedish double mutation ($K^{594}M^{595}$-NL) 10-fold more efficiently than wild-type APP (Yan et al., 1999a). This enzyme cleaves APP at Abeta positions 1 and 11, as cells over-expressing it had an increase in secreted levels of Abeta 1-40, 1-42, 11-40 and 11-42 (Vassar et al., 1999). Conversely, BACE-1 knockout mice showed a decrease in secreted Abeta, but the mice were phenotypically normal (Cai et al., 2001; Luo et al., 2001), suggesting that inhibition of the β-site cleavage is not toxic and could be of therapeutic value (Roberds et al., 2001). BACE-1 seems responsible for the cleavage of approximately 10% of the APP pool that is proteolytically processed in neuronal cells. Of these 10%, roughly 90% give rise to Abeta 1-40 and 10% to Abeta 1-42 (Haass et al., 1992b; Seubert et al., 1992). BACE-2 cleaves APP at Abeta position 1 but also and more efficiently at sites within Abeta

(Phe^{19} and Phe^{20}), after the alpha-site Lys^{16} (Farzan et al., 2000). Thus, BACE-2 can be distinguished from BACE-1 on the basis of autoprocessing of the prosegment and in APP processing specificity, with BACE-2 behaving more as an alpha-secretase-like APP enzyme (Yan et al., 2001). Cells overexpressing BACE-2 and APP with the Swedish mutation showed enhanced levels of the βCTF fragment. As BACE-2 maps to chromosome region 21q22.2-22.3, it is tempting to speculate that some of the FAD cases linked to chromosome 21 may also be related with BACE-2 polymorphisms or overexpression (Turner et al., 2003). The third β-secretase candidate to be identified was Carboxypeptidase B (Matsumoto et al., 2000), which in contrast to BACE enzymes lacks a transmembrane domain. It is a soluble enzyme located in the cytosol of various neurons and some microglial cells, especially in the hippocampus, which "in vitro" or when overexpressed in cells also leads to an increase in βCTF levels (Matsumoto et al., 2000).

γ-Secretases. βCTF and αCTF are cleaved, apparently intramembranously, by a multicomponent enzymatic complex called γ-secretase (reviewed in Wolfe and Haass, 2001; Selkoe and Kopan, 2003). This enzyme is also responsible for cleaving the Notch protein, a well known signal transducer, at its intramembranous sequence (Berezovska et al., 2001; Selkoe and Kopan, 2003). Similarly, both Notch and APP apparently need proteolytic trimming of their extracellular domain by TACE and α/β-secretase, respectively, to become a substrate for γ-secretase (De Strooper et al., 1998; Brou et al., 2000; Mumm et al., 2000; Struhl and Adachi, 2000). Several recent findings have broken down the γ-secretase complex into its constitutive parts. The two prime candidates for the γ-secretase catalytic region-containing protein are the previously mentioned **Presenilin 1** and **Presenilin 2**. They were initially identified by genetic linkage analysis of non-APP FAD mutations that increased Abeta 1-42 in humans, and mapped to chromosomes 14 and 1, respectively (Cruts et al., 1995; Duff et al., 1996; Hutton et al., 1996; Lemere et al., 1996). PS2 seems to be responsible for a smaller amount of CTF cleavage than PS1 (Herreman et al., 1999). PS1 knockout mice have markedly reduced γ-secretase activity (De Strooper et al., 1998), which is even more reduced in double knockout mice for PS1 and PS2 (Donoviel et al., 1999; Herreman et al., 1999). Nonetheless, there might be multiple γ-secretase enzymes with varying degrees of selectivity for producing Abeta 1-40 and Abeta 1-42 (Wolfe, 2001), as in PS1/PS2 double knockout mice there is a lack of Abeta 1-42 production in the early secretory pathway but not of Abeta 1-40 (Wilson et al., 2002). The PS1 and PS2 related genes encode integral membrane proteins with at least eight

transmembrane domains that are initially expressed as inactive preproteins (Thinakaran et al., 1996). Subsequent cleavage (named "PS maturation") between transmembranar domains 6 and 7 yields a C-terminal and an N-terminal fragments, which remain associated with each other in a multiprotein complex of high molecular weight (≥ 100 KDa) (Capell et al., 1998). PS1 maturation was observed to be necessary in order to obtain γ-secretase activity in primary neuronal cultures (Capell et al., 2005; Cupers et al., 2005). PS1 and PS2 are not found in the same complexes, but their tissue specific expression profiles can overlap (Saura et al., 1999).

The demonstrated physical interaction between APP and Presenilins N-terminus, first suggested that Presenilins could in fact be the elusive γ-secretase catalytic proteins (Pradier et al., 1999). This supports that Abeta 1-40 and Abeta 1-42 biogenesis may be the result of distinct enzymatic activities. However, the subcellular compartments of APP, CTF, PS and γ-secretase activity co-localizations argued against PS as the catalytic subunit (the "spatial paradox") of this enzymatic complex (further presented in section I.2.7). One of the strongest arguments in favour of PS as the catalytic subunit comes from the identification of a new, evolutionary conserved, Presenilin homologue gene family of GxGD aspartyl proteases with five members (Haass et al., 2002; Ponting et al., 2002). This gene family codes for proteins with extensive predicted transmembrane domains and two predicted catalytic aspartyl residues, similar to the PS domains 6 and 7. Another strong argument comes from the observation that several compounds that inhibit γ-secretase bind specifically to PS (Esler et al., 2000; Li et al., 2000; Seiffert et al., 2000).

Another component of γ-secretase is **Nicastrin**, which also affects the complex's enzymatic activity (Esler et al., 2000). Nicastrin is extensively glycosylated, has four conserved cysteine residues near its extracellular N-terminus (Leem et al., 2002) and possesses a single transmembrane domain (Yu et al., 2000). This protein interacts both with APP CTFs and PS1 and PS2 (Fig. I.12). Mutations of Nicastrin in residues within a conserved region lead to enhanced Abeta secretion, while deletion of the same region prevents Abeta secretion (Yu et al., 2000). Two other proteins identified as γ-secretase subunits are **APH-1** or **APH-2** (with APH-2 being only relevant in cerebral tissues γ-secretase activity) and **PEN-2** (Francis et al., 2002; Steiner et al., 2002; for review De Strooper, 2003). Recent reports provide evidence that γ-secretase is indeed an aspartyl protease complex composed of the four core components APH-1, nicastrin, Presenilin, and PEN-2 (De Strooper, 2003; Kimberly et al., 2003; Capell et al., 2005). It is now believed that an APH/immature Nicastrin complex is formed at the ER, and matured at the Golgi. Also at the Golgi, APH/Nicastrin first bind to PS, stabilizing the

unstable and readily degraded PS pool, and following the binding of PEN-2, PS endoproteolysis is triggered and the γ-secretase complex is thought to be finally active (Kim and Sisodia, 2005).

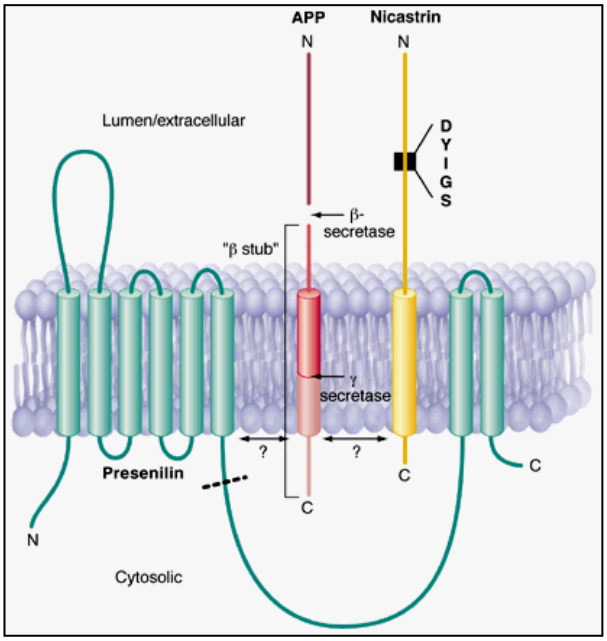

Figure I.12. Presenilin structure and APP interaction. Presenilin (at it C-terminus) associates with Nicastrin through the DYIGS motif in the extracellular domain, and after is cleaved (dashed line) into two molecules (from: Sisodia, 2000). The catalytic site is now believed to belong to Presenilin and not to Nicastrin.

I. 2. 5 – APP IS A RIP SIGNAL TRANSDUCTION MOLECULE

APP has a receptor-like architecture with a conserved cytoplasmic domain, and can be located at the cell surface, although no receptor function has been demonstrated for APP. Recently, it was reported that this type I membrane spanning molecule may function as a signal transducer by Class 1 Regulated Intramembrane Proteolysis (RIP) (Ebinu and Yankner, 2002; Koo, 2002). These molecules have a peptide sequence within their protein structure that is released after two subsequent protein cleavages (RIP proteolysis), and can be targeted to the nucleus, functioning as a gene transactivator. RIP proteolysis seems to occur at or near the plasma membrane and involves ADAMs and γ-secretase cleavages. The proteases involved in this process are thought to be under different regulation, with the activity of the first enzyme (responsible for the extramembranar substrate cleavage) being directly regulated. The activity of the second enzyme, responsible for the intramembranar substrate cleavage, seems to be directly regulated by substrate availability, which is dependent on the first and regulated cleavage. Several mammalian proteins are known to be processed by RIP to generate nuclear signalling, including APP, Notch-1, ErB-4, CD44, and $p75^{NTR}$ (Class 1 RIP), and SREBP-1

and ATF6 (Class 2 RIP) (reviewed in Ebinu and Yankner, 2002; Koo, 2002; Rawson, 2002; Pardossi-Piquard et al., 2005). Notch is a type I transmembrane receptor involved in cell fate decisions during embryogenesis and functions through cellular RIP. Upon ligand binding, Notch is proteolytically processed, initially by a TACE- (Brou et al., 2000) or an ADAM 10-dependent cleavage event (Hartmann et al., 2002), followed by γ-secretase intramembrane cleavage (De Strooper et al., 1999). In these respects APP and Notch processing may be similar (reviewed in Selkoe and Kopan, 2003). PS knockout mice are remarkably similar to the Notch knockout mice (Conlon et al., 1995), possibly due to the involvement of Presenilin in the intramembrane cleavage of Notch processing. In fact, APP and Notch were proved to be competitive substrates for PS1-dependent γ-secretase cleavage (Berezovska et al., 2001). In addition, γ-secretase cleaves the CTFgamma (CTF produced after APP cleavage at the γ-site) at a site (ε-site) corresponding to the S3 cleavage site of Notch (Sastre et al., 2001). Both the Notch Intracellular Domain (NICD) and the resultant APP AICD fragment may act as transcription factors (Schroeter et al., 1998; Cao and Sudhof, 2001; Cupers et al., 2001; Ebinu and Yankner, 2002; Kim et al., 2003; von Rotz et al., 2004).

The AICD fragment is very labile (Cupers et al., 2001), but the AICD-generating CTFs are very stable. This suggests that it may be necessary to further activate CTFs for the γ-secretase cleavage to occur, in contrast to the Notch signalling. The AICD fragment is extremely small when compared with the NICD and lacks motifs commonly found in transcriptional regulators, suggesting that it may function in signalling differently from NICD. In fact, to function as a transactivator the AICD forms a multimeric complex composed of the nucleocytoplasmic adaptor Fe65 and other proteins as the nuclear histone acetyltransferase Tip60 (Cao and Sudhof, 2001; Baek et al., 2002; Kim et al., 2003; von Rotz et al., 2004). NICD is known to be targeted to the nucleus, where it exerts its physiological function, and AICD translocation to the nucleus has already been observed (Kimberly et al., 2001; Kinoshita et al., 2002; von Rotz et al., 2004). Nonetheless, this model is controversial and Cao and Sudhof (2004) have proposed that the AICD itself is not necessarily nuclear targeted. The authors defend that the AICD role in the transsactivation process consists in activating Fe65, via conformational changes, for binding with Tip60 (Fig. I.13). Of note is that AICD half-life is not increased by binding Fe65 (Cupers et al., 2001). On the other hand, von Rotz and colleagues (2004) have observed in HEK293 and SH-5YSY differentiated cells the presence of AICD/Fe65/Tip60 complexes in multiple spherical nuclear coiled bodies, and JIP/AICD/Tip60 complexes in speckle-like structures.

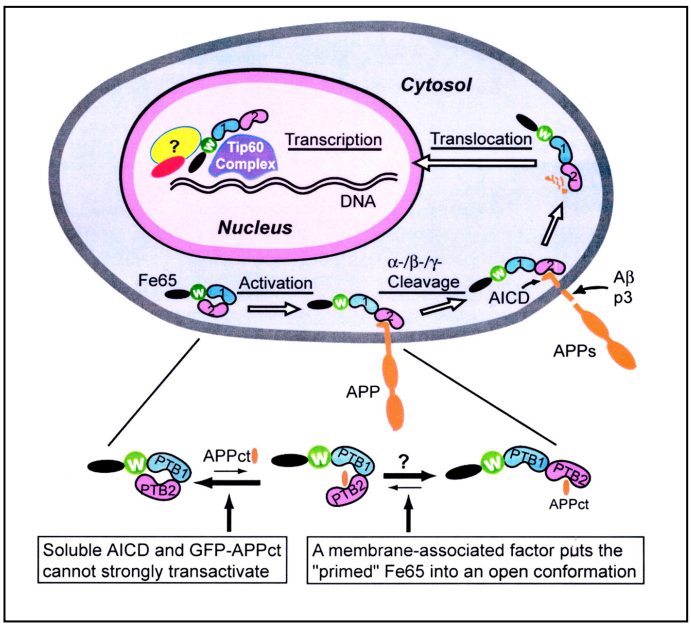

Figure I.13. A working model for the function of APP in transcriptional activation. AICD binding to Fe65 at its PTB2 domain would disrupt Fe65 PTB2-WW intradomain binding. This would in turn alter Fe65 initially closed conformation, and free the Fe65 WW domain for its transactivator role upon nuclear translocation. From: Cao and Sudhof (2004).

AICD/Fe65/Tip60 complexes were reported to transactivate the *kai1* gene, with the presence of the nucleasome assembly factor SET protein in the complex being necessary for maximal transactivation (Baek et al., 2002; Telese et al., 2005). KAI1 protein is involved in membrane receptor function regulation and in tumour cell proliferation inhibition (Baek et al., 2002). SET protein binds Fe65 (Telese et al., 2005) and was additionally shown to bind an APP C-terminal fragment and to mediate its apoptotic effects (Madeira et al., 2005). The AICD/Fe65/Tip60 complex was also recently reported to transactivate the Abeta degrading enzyme Neprilysin (Pardossi-Piquard et al., 2005), and to promote the gene expression of APP itself, in an autostimulatory loop (von Rotz et al., 2004). A different AICD-containing complex, with Fe65 and the ternary complex CP2/LSF/LBP1, was found to promote the expression of the glycogen synthase kinase-3β (GSK-3β) (Kim et al., 2003). This *gsk*-3β transativation appears to be inhibited by AICD complexes of another AICD-interacting adaptor protein named X11 (Lau et al., 2003).

Mature APP and Notch were observed to interact by two independent groups (Abraham et al., 2005; Fassa et al., 2005). Abraham and collaborators (2005) used a membrane-impermeable proteins crosslinker (DTSSP) in HEK293 and in primary neuronal cultures to detect this interaction. The group of S. Efthimiopoulos (Fassa et al., 2005) has further characterized this binding as Numb-independent, and observed that Notch overexpression did not significantly affect APP processing.

I. 2. 6 – APP C-TERMINUS DOMAINS AND APP-BINDING PROTEINS

Several proteins interact with APP, most of them possessing multiple protein-protein interacting domains, which in turn form complexes with other proteins, suggesting that these proteins function as adaptor proteins bridging APP to specific molecular pathways. The number of APP binding proteins thus far identified is quite vast and can be loosely divided into two overlapping categories: signal transduction and subcellular localization (da Cruz e Silva et al., 2004a). For both there is an emerging consensus that the APP C-terminus is critical in these interactions. Examples of APP binding proteins involved in signal transduction are: Abl, Disabled-1 protein (mDab-1), Fe65 and Fe65-like proteins, SET protein, X11 (or MINT-1) and X11-like proteins (or MINT-2 and 3), Numb, and G_0. APP binding-partners involved in APP targeting are fewer and include APPBP2 (or PAT1) and the X11 family proteins, important in microtubule association. X11 was also recently found to potentially function as an APP vesicle coat-protein (Hill et al., 2003). Recent findings on APP binding proteins have brought to light two other proteins putatively involved in APP traffic: the neuronal sorting receptor sorLA/LR11 (Andersen et al., 2005), and a novel sorting nexin (SNX30) (Lichtenthaler et al., 2005). The APP-G_0 binding (Nishimoto et al., 1993) may also have a role in APP targeting, as G_0 was found to be located at subcellular membrane domains specialized in the sorting of trafficking proteins (Qian et al., 2003). Other known APP binding proteins involved in trafficking are the Kinesin Light Chain (KLC) and JIP-1 [Jun N-terminal kinase (JNK) interacting protein 1]. Furthermore, examples exist where the binding to APP has not been clarified, as in the case of caveolin (Ikezu et al., 1998; Nishiyama et al., 1999).

The function of all the APP binding proteins has yet to be completely elucidated, but considerable contributions have already been made. For review on APP binding proteins involved in APP signal transduction see da Cruz e Silva et al. (2004a). Several other APP binding proteins have been described that appear to have very diverse roles such as in Abeta clearance and/or aggregation, as for example ApoE. Proteins which bind the N-terminus of APP have not been extensively documented, such as fibulin-1, whose binding blocks neural stem cells sAPP-mediated proliferation (Ohsawa et al., 2001), and F-spondin, which may mediate APP CAM and neurite outgrowth functions (Ho and Sudhof, 2004). In fact, almost all known APP binding proteins bind at its C-terminus, and specifically at one of two APP domains: ^{653}YTSI^{656} and ^{682}YENPTY^{687} (Fig. I.14 and Table I.1). A third domain (^{667}VTPEER^{672}) has not been implicated so far in any of the APP bindings, although it is included in the APP $G_0\alpha$- and Hsc73-binding sequences, but has a regulatory role that will be

discussed later (section I.3.3). These domains can be classified according to their attributed functions and are thought to be involved in regulating APP rate of secretion, endocytosis, and Abeta production (Ando et al., 1999; Iijima et al., 2000; Mueller et al., 2000; Ando et al., 2001; Sabo et al., 2001; Roncarati et al., 2002; da Cruz e Silva et al., 2004a).

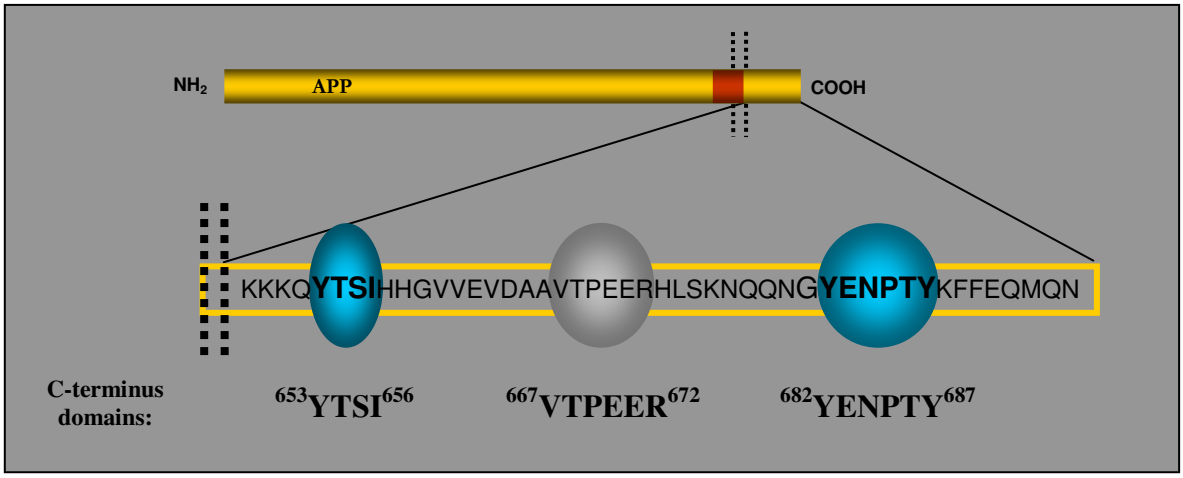

Figure I.14. APP C-terminal localization of the two sequence domains (YTSI and YENPTY) known to be the binding sites of several APP binding proteins. Adapted from: da Cruz e Silva et al., 2004a.

Table I.1. Numerous APP binding proteins bind to specific APP C-terminal domains. (ND –not defined).

Cytoplasmic APP-binding domain	APP binding protein	Putative Role	Subcellular localization and/or co-localization with APP	References
682YENPTY687 domain	UV-damaged DNA-bp	ND	. Cytosolic fraction (PC12 cells)	Watanabe et al., 1999
	Abl	. Abl active form phosphorylates APP at Y682 . Forms a trimeric complex with APP and Fe65 . Mediation of APP membrane internalization	. Cytoplasm and nucleus	Russo et al., 2001 Tarr et al., 2002
	mDabl	. Neuron migration (cell movement) . Links APP to signal transduction processes	. Co-localizes with APLP1 in membrane ruffles and vesicular structures	Homayouni et al., 1999
	Fe65 and Fe65L family	. Regulation of APP secretion . Regulation of cell movement (APP-Fe65 complex) . Promotion of gene transactivation (AICD/Fe65/ Tip60 complex)	. Cytoplasm and nucleus . In AD co-localizes with Tau protein in neurofibrillary tangles	Fiore et al. 1995 Bressler et al., 1996 Guenette et al., 1996 Kimberly et al., 2001 Sabo et al., 2001 Kinoshita et al., 2002

^{682}YENPTY^{687} domain (cont.)	X11 (or Mint-1) and X11L family	. APP trafficking (targeting) . APP coat vesicle protein . APP synaptic localization	. Cytosolic/Golgi adaptor protein . APP/Mint/Cask complexes are localized in neuronal processes and in the Golgi	Borg et al., 1996 McLoughlin and Miller, 1996 Sastre et al., 1998 Mueller et al., 2000 Hill et al., 2003
	JIP-1b	. Scaffolds APP with c-Jun Kinase (JNK) . Links APP to stress kinase signalling pathways . Involved in APP axonal trafficking	. APP and JIP-1b exhibit similar subcellular location: cytoplasmic significantly overlapped staining	Matsuda et al., 2001 Scheinfeld et al., 2002 Sisodia, 2002
^{653}YTSI^{656} domain	APPBP2 (or PAT1)	. Translocation of APP along microtubules toward the cell surface . Involved in nuclear gene transactivation/repression	. Nucleus and cytoplasm, also found membrane-associated. . Golgi and in filamentous cytoplasmic structures emanating from the Golgi, where it co-localizes with APP	Zheng et al., 1998 Gao and Pimplikar, 2001 Richards et al., 2003 Zhang et al., 2004
	KLC (?)	. Axonal transport of APP containing vesicles (anterograde and retrograde)	. Cellular cytoskeleton/ Microtubules	Kaether et al., 2000 Kamal et al., 2000; Kamal et al., 2001
	SET (?)	. Transactivation of the KAI1 gene (AICD/SET/Fe65/ Tip60 complex) . Mediation of APP C-terminal fragment-induced apoptosis	. Co-localizes with AICD at the nucleus (on the *kai1* gene promoter)	Madeira et al., 2005; Telese et al., 2005
^{657}H-K^{676} sequence	$G_0(\alpha)$	. APP cellular signalling . APP targeting	. Co-localizes with APP at neuronal growth cones . Co-localizes with APP at neuronal membrane microdomains	Strittmatter and Fishman, 1991 Nishimoto et al., 1993 Okamoto et al., 1995 Brouillet et al., 1999 Qian et al., 2003
^{658}H-D^{664} sequence	hARD1	ND	ND	Asaumi et al., 2005
^{649}K-S^{675} sequence	Hsc73	. APP/AICD traffic . APP/AICD proteasomal or lysosomal degradation	. Mainly cytosol, lysosomal membrabe, also in nucleus	Kouchi et al., 1999
ND	Numb and Numb-like proteins	. Link between APP and Notch signalling pathways	. Neurons cytoplasm, dendritic and axonal processes; excluded from nuclei	Roncarati et al., 2002
	AIDA-1a	. Modulator of APP processing	. Diffuse localization with some nuclear accumulation	Ghersi et al., 2004

The internalization signal YENPTY. The APP trafficking domain most widely studied has the amino acid sequence ^{682}YENPTY^{687} and is situated at the APP C-terminus. It contains an NPXY element, which is a typical internalization signal for membrane-associated receptor proteins (Chen et al., 1990; Koo and Squazzo, 1994; Lai et al., 1995), and has the structure of a type I β-turn (Ramelot et al., 2000). This motif is thought to function through interaction with various known APP binding proteins (Table I.1) via phosphotyrosine interaction domains of the latter.

The sorting signal YTSI. The amino acid sequence ^{653}YTSI^{656} forms a 4-residue tyrosine-based characteristic internalization and/or basolateral sorting signal (YXXI) (Hass et al., 1995; Lai et al., 1995; Zheng et al., 1998). When transplanted to the cytoplasmic domain of the transferrin receptor (TR), this sequence promoted the internalization of a TR-YTSI chimera in COS-1 cells and seemed to be partially responsible for its post-Golgi degradation (Lai et al., 1995). This domain has received less attention and until now only one protein (APPBP2) was shown to specifically bind to it. As the exact site of APP binding to the KLC protein is still unknown, the binding of KLC to the ^{653}YTSI^{656} domain is speculative and supported only by KLC homology to APPBP2. Nonetheless, this is a domain that could contribute to the targeting of APP to correct plasma membrane subdomains and be involved in APP signalling functions. In light of APP as a RIP receptor involved in signal transduction, which may underlie many of the physiological roles that have been attributed to it (e.g. neuroprotection, cell adhesion, cell growth stimulation and synaptic plasticity), this domain may have a potentially important regulatory function. The characteristics of both the putative and known ^{653}YTSI^{656} domain binding proteins are described below.

APPBP2 (or PAT1). APPBP2 is a microtubule-interacting protein that recognizes and binds full length APP and its C-terminus fragments at the ^{653}YTSI^{656} domain (Zheng et al., 1998; Gao and Pimplikar, 2001). It is a nucleocytoplasmic protein of 585 amino acids (65-70 KDa). In the cytosol it fractionates into a soluble and a membrane-associated pool, and has an apparent molecular weight of 160-180 KDa due to its binding to an unknown protein. APPBP2 is located throughout the cytoplasm in a punctuate or filamentous pattern, being more abundant in the perinuclear region of the cell (where microtubules are highly concentrated and where APP is also enriched). This protein seems to be involved in the translocation of APP along microtubules toward the cell surface and needs the tyrosine present in the YTSI sequence for efficient binding (Zheng et al., 1998). APPBP2 contains tandem-repeats also found in KLC (Zheng et al., 1998; Gao and Pimplikar, 2001), a protein

likewise known to complex with APP. Although still controversial, APPBP2 may also be involved in AICD traffic to the nucleus. AICD-nuclear exclusion was observed when AICD was co-transfected with an APPBP2 mutant carrying a deletion of its nuclear-localization signals (Gao and Pimplikar, 2001). Interestingly, AICD selectively caused cytoplasmic relocation of nuclear APPBP2 and its proteasomal degradation. APPBP2 has in its sequence DNA-binding and NR cyclin box-like motifs, the latter known to mediate the interaction of transactivators with their nuclear hormone receptors, including the retinoic acid receptor (Gao and Pimplikar, 2001). Also of note is that APPBP2 was found to interact with the androgen receptor and to inhibit its activity (Zhang et al., 2004).

Kinesin Light Chain. Co-immunoprecipitation, sucrose gradient, and direct "in vitro" binding demonstrated that APP forms a complex with kinesin-I by binding directly to the TPR (tetratricopeptide repeat) domain of the KLC subunit (Kamal et al., 2000). The identity of the APP domain involved in this binding is still elusive, but due to sequence homology between APPBP2 and KLC it may be postulated to be the ^{653}YTSI^{656} domain. Kinesin molecular motor proteins are responsible for many of the major microtubule-dependent transport pathways in neuronal and non-neuronal cells (Goldstein, 2001). The microtubule motor complex kinesin-I has two components: a kinesin heavy chain (KHC or KIF5B) that has ATP- and microtubule-binding motifs essential for vesicle transport, and a kinesin light chain (KLC). KLC associates with KHC and tethers membrane vesicles containing proteins to be transported axonally from the neuronal soma to nerve terminals (Hirokawa, 1998). APP is axonally transported in elongated tubules that move extremely fast and over long distances, and antisense treatment with oligonucleotides against KHC slows down that movement and increases the frequency of directional changes (Kaether et al., 2000). BACE-1 and PS were found in membrane vesicles transported along the axons of peripheral and central mouse neurons, with this transport being mediated by kinesin-1 and requiring APP (Kamal et al., 2001). The fast anterograde axonal transport of this compartment is mediated by APP and kinesin-I binding, and APP proteolysis liberates kinesin-I from the membrane (Kamal et al., 2001). Deletion of the *app-like* gene (*appl*) in *Drosophila* or overexpression of human APP or APLP2 C-terminal caused aberrant accumulation of transported vesicles within axons. This phenotype is observed in flies with mutations in kinesin or in dynein, a microtubule-activated ATPase that transport vesicles from neuronal dendrites back to the cell body. Deletion of its C terminus disrupted APP axonal transport and abolished the organelle axonal accumulation phenotype due to APP overexpression (Gunawardena and Goldstein, 2001). Taken together, these results suggest that one of the normal functions of APP may be

as a membrane cargo receptor for kinesin-I and that KLC is important for kinesin-I driven transport of APP into axons (Kamal et al., 2000; 2001). Interestingly, Tau protein was reported to inhibit the kinesin-dependent transport of Golgi-derived vesicles into neurites, and was also observed to exert inhibitory effects on APP transport into neurites, resulting in APP somatic accumulation (Stamer et al., 2002).

SET. The SET protein, also called template-activating factor (TAF1beta) or phosphatase 2A inhibitor 2 [I2(PP2A)], was found to bind an APP C-terminal fragment involved in neuronal apoptosis and cell death induction (Madeira et al., 2005). The exact sequence on APP to wich SET binds has not been elucidated. However, death induction by the APP C-terminal is mediated by SET and lost when APP Tyr^{653} is mutated to an aspartate. These suggest that SET binds to APP at the ^{653}YTSI^{656} domain or near by (Madeira et al., 2005). Interestingly, a complex including Fe65/AICD/Tip60/SET was found to be associated with the *kai1* gene promoter, and SET was shown to bind Fe65 at the WW transcativator domain and to be required for full levels of *kai1* gene transcription (Telese et al., 2005).

$G_{0}\alpha$. APP and the G_0 alpha subunit were first reported to interact in a GTP-dependent manner (after G_0-activation by GTP) by Nishimoto et al. (1993). The APP His^{657}-Lys^{676} sequence is necessary for this complex formation (Nishimoto et al., 1993; Okamoto et al., 1995; Yamatsuji et al., 1996). This sequence is predicted to have a stable structure starting with a hydrophobic pocket that can potentially be regulated by the immediately upstream ^{653}YTSI^{656} domain (Ramelot et al., 2000; Ramelot and Nicholson, 2001). G_0 is a membrane-associated heterotrimeric GTP-binding protein (G protein), and one of the major G proteins in brain (Rouot et al., 1987; Spiegel, 1987). G proteins share similar or identical beta and gamma subunits but different alpha subunits. The 39 KDa $G_0\alpha$ subunit is expressed at low levels in some peripheral tissues, but it is mainly cerebral (Rouot et al., 1987). These proteins are involved in many signal transduction pathways underlying systemic functions like learning and memory (Neves et al., 2002). G_0 is a member of the G protein family that links growth-promoting receptors and second messengers in hormone-induced cell growth (Post and Brown, 1996). G_0 is also the major non-cytoskeletal protein in the growth cone membrane, where it is thought to transduce signals not only from outside the cell but also from within (Strittmatter et al., 1990; Strittmatter and Fishman, 1991). APP was recently observed to be co-localized with Fe65 in growth cones, where they concentrate in actin-rich lamellipodia (Sabo et al., 2003). Neuronal growth cones are specialized transduction systems that lead the elongating axon towards appropriate synaptic targets by altering motility in response to a

variety of extracellular signals or independent intrinsic cues. APP-G_0 interaction in growth cones has not yet been reported but APP and $G_0\alpha$ were reported to interact in cholesterol and sphingoglycolipid-enriched microdomains (CSEM), a caveolae-like compartment specialized in signal transduction (Brouillet et al., 1999). Furthermore, in total neuronal membranes and in CSEM, APP binding to an antibody against APP ectodomain (22C11) led to the reduction of the high-affinity G_0 GTPase activity. This inhibition was specific for $G_0\alpha$ and was reproduced, in the absence of 22C11, by the addition of the APP C-terminus (Brouillet et al., 1999).

Two additional proteins were reported to bind APP at or near the ^{653}YTSI^{656} domain, although little is known about the physiological consequences of these interactions. Human hARD1 is an N-terminal acetylltransferase that was recently shown to bind APP at His^{658}-Asp^{664}, a sequence only lacking two amino acids of the APP hydrophobic pocket (Asaumi et al., 2005). The cytosolic chaperone Hsc73 appears to bind APP at an APP C-terminal sequence (K^{649}-S^{675}) that includes both the ^{653}YTSI^{656} domain and the hydrophobic pocket, and maybe involved in APP/CTFs proteasomal degradation (Kouchi et al., 1999).

I. 2. 7 – APP SUBCELLULAR TRAFFICKING

APP trafficking and maturation. In neuronal and non-neuronal cells, APP is known to be transported via the secretory pathway, a continuum of separate membrane-enclosed organelles leading to the cell surface. Newly synthesized proteins that are destined for secretion or cell-surface expression enter this pathway at the rough endoplasmic reticulum (RER). APP is known to undergo posttranslational modifications that include N- and O-linked glycosylation and tyrosine sulfation (Weidemann et al., 1989; Oltersdorf, 1990). APP N-glycosylation starts at the ER and the carbohydrate chains are further processed in the cis-Golgi, with immature N-glycated APP being found at both locations (Tomita et al., 1998). Two residues in the APP ectodomain (Asn^{467} and Asn^{496}) have consensus sequences for N-glycosylation, although only one appears to be N-glycosylated "in vivo" (Pahlsson and Spitalnik, 1996). APP maturation by O-glycosylation and tyrosyl-sulfation occurs while moving through the trans-Golgi network (TGN) (Weidemann et al., 1989). Maturation of all metabolic labelled APP cell-associated proteins reached maximum intensity after 30 min of chase (Peraus et al., 1997). O-glycosylation does not depend on correct APP N-glycosylation to precede it but, as it is performed at the TGN, is a subsequent process (Pahlsson and Spitalnik, 1996). Inhibition of APP O-glycosylation does not appear to affect APP biosynthesis or secretion (Pahlsson and Spitalnik, 1996). Nonetheless, the majority of APP

cleavage by secretases occurs after O-glycosylation, as shown by using HEK293 cells expressing mutant APP defective in O-glycosylation (Tomita et al., 1998). This mutant accumulated in subcellular reticular compartments and exhibited decreased cleavage to αCTFs or to Abeta 1-40/1-42. Mature APP (N-,O-glycated and sulfated) is therefore located in compartments from the trans-Golgi to the plasma membrane (Tomita et al., 1998). Moreover, most APP resides in the cell Golgi complex (Caporaso et al., 1994), but a small pool is carried into post-TGN secretory vesicles that carry it to the plasma membrane (Koo et al., 1996; Yamazaki et al., 1996; Peraus et al., 1997). In SH-SY5Y cells, the pool of TGN mature APP that is targeted to the plasma membrane takes 30 to 45 min to reach this cellular destination following APP translation (Cai et al., 2003). At the cell surface, APP can be cleaved or undergo re-internalization as a holoprotein via endocytosis, to be recycled back to the membrane, retrogradely delivered to the TGN or incorporated into secondary endosomes. Secondary endosomes target APP for complete degradation at the lysosomes or to be recycled back to the TGN/Golgi (Tagawa et al., 1993; Koo et al., 1996; Yamazaki et al., 1996). In central and peripheral neurons a pool of APP molecules is also transported from the cell body down axons by fast axonal transport (Koo et al., 1990; Ferreira et al., 1993; Kaether et al., 2000). Presynaptically targeted full-length APP (and APLP2) occurs in its mature form (syalated and N- and O-glycosylated) (Lyckman et al., 1998). APP was also detected in both pre- and post-synaptic sites, in the axoplasm of myelinated and unmyelinated nerve fibres, within vesicular structures in axonal, dendritic and synaptic compartments, as well as on the surface of axons and dendrites (Schubert et al., 1991; Ferreira et al., 1993; Allinquant et al., 1994; Caporaso et al., 1994; Simons et al., 1995). Of note is that APP was suggested to be up-regulated in synapses with increased membrane activity, e.g., in synapses subject to high transmission rates or during synaptogenesis (Schubert et al., 1991). Figure I.15 represents schematically APP neuronal trafficking pathways.

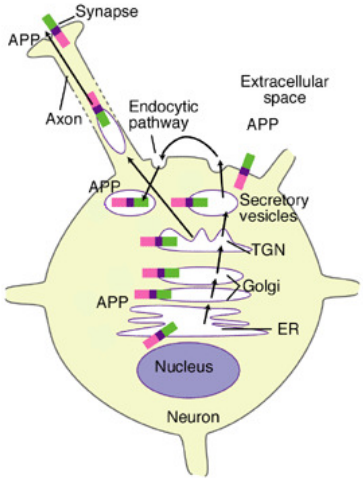

Figure I.15. APP trafficking through the cellular secretory and endocytic pathways. APP domains are indicated in colours: *pink,* cytoplasmic domain; *violet,* Abeta domain; *green,* ectodomain. From: Gouras, 2001.

In addition, pools of unprocessed synaptic APP are also transported retrogradely (transcytotic movement) from axonal synaptic compartments to neuronal cell bodies and dendrites (Simons et al., 1995; Yamazaki et al., 1995). In rat forebrain and PC12 cells, APP was observed in Rab5-containing endocytic organelles that derive from an endocytic pathway distinct from the one involved in synaptic vesicle recycling (Ikin et al., 1996; Marquez-Sterling et al., 1997). The latter further reported that cell-surface APP was initially internalized with membrane proteins of recycling synaptic vesicles, but subsequently sorted away from these vesicles and retrogradely transported to the soma.

APP processing and its intracellular trafficking. Through the use of radioactivity-based techniques, the half-life of total cellular APP was estimated to be of approximately 1 h (Weidemann et al., 1989; Koo et al., 1996). Nascent and immature (only N-glycosylated) APP can be degraded to a high extension by the proteasome, probably via the smooth ER (Yang et al., 1998; Kouchi et al., 1999). Additionally, immature APP may be cleaved by secretases at a low rate in the ER or the cis-Golgi but, as explained above, the majority of these cleavages occur after APP complete maturation. Mature APP is processed rapidly (turnover of 45 min) as it is transported to or from the cell surface via the secretory or endocytic pathways (Haass et al., 1992a; Sambamurti et al., 1992; Shoji et al., 1992; De Strooper et al., 1993; Kuentzel et al., 1993; Cook et al., 1997; Hartmann et al., 1997; Marambaud et al., 1997b). In several types of cultured cells a part of the TGN/Golgi APP pool was observed to be locally cleaved by the α-secretase. β-secretases can also cleave a fraction of Golgi APP but to a lesser extent. Additionally, a small percentage (1.5% in HeLa cells, Kuentzel et al., 1993) of full-length mature APP at the TGN is transported to the cell membrane. Approximately 30% of surface APP is cleaved to sAPP (Koo et al., 1996), with 20% being cleaved within 10 min (Lai et al., 1995). The remaining full-length APP and the cleavage products (CTFs) are re-internalized via coated pits and vesicles by receptor-mediated endocytosis (Yamazaki et al., 1996). The net result of cell surface APP proteolytic cleavage and endocytosis is the rapid removal of cell surface APP. Indeed, the estimated half-life for surface-expressed APP is less than 10 min (Koo et al., 1996). Consequently, only minor amounts of APP (as compared to the total cellular pool) are detected at the cell surface (Kuentzel et al., 1993). The half-life of internalized APP was calculated to be ~30 min (Koo et al., 1996), with a pool of endosomal APP being delivered into lysosomes. The remaining cell surface CTFs may be subsequentially cleaved by γ-secretase to AICD, at the cell surface or upon endocytosis in endosomes, or further degraded in lysosomes (Chen et al., 2000; Mathews et al., 2002; Kaether et al., 2006).

CTFs produced at the TGN/Golgi are thought to be cleaved locally or to be delivered to lysosomes for degradation (Chen et al., 2000). In neurons, sAPP may also be generated and released at the synaptic terminals via α-secretase cleavage (McLaughlin and Breen, 1999).

During the APP secretory pathway, the majority of Abeta fragments are thought to be generated in the late Golgi, from where these peptides are packaged into post-TGN vesicles destined for extracellular secretion (Gouras, 2001; Xia, 2001). This Abeta production seems to occur at the TGN and does not need post-TGN vesicles formation (Xu et al., 1997). At the TGN, the absolute levels of both Abeta 1-40 and Abeta 1-42 are high and the ratio Abeta 1-42 to total Abeta is 0.05-0.16 (Greenfield et al., 1999). A minority of Abeta peptides (1-40, 1-42 and x-42) is thought to be generated in the ER (Xia et al., 1998; Greenfield et al., 1999), but some authors defend that the γ-secretase complex is still not formed or active at the ER (Kaether et al., 2006). A major portion of Abeta peptides are also generated in the endocytic pathway, following internalization of APP from the plasma membrane. In fact, mutations of the APP ^{682}YENPTY^{687} domain that significantly impair APP endocytosis simultaneously inhibit Abeta levels (Perez et al., 1999). Recent findings locate β- and γ-secretases within the cholesterol-enriched plasma membrane lipid rafts, but Abeta production at the cellular membrane was reported to occur at lower amounts. APP was thus suggested to be potentially segregated from its proteases by the rafts lipid boundary (Kaether and Haass, 2004). Finally, Abeta production was also reported in axonal vesicular compartments (Kamal et al., 2001). The putative subcellular localization of APP proteolytic processing is shown in Figure I.16.

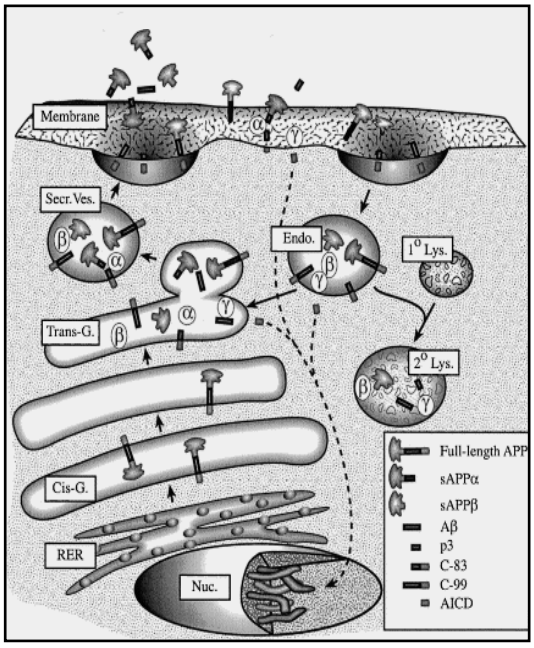

Figure I.16. Putative localization of APP processing in neurons. α-, β- and γ-secretase activities are represented by labelled balls, which are located at the putative subcellular compartments where the APP proteolytic cleavages occur. CTFs are cleaved to release the AICD, which may modulate gene transcription in the nucleus (dashed arrows). **Nuc.**, nucleus; **RER**, rough ER; **Cis-G.**, cis-Golgi; **Trans-G.**, trans-Golgi; **Secr. Ves.**, secretory vesicle; **Endo.**, endosome; **Lys.**, lysosome. From: Turner et al., 2003.

Intracellular Localization of Secretases. The α-, β- and γ-secretases are a heterogeneous group of enzymes located in various subcellular regions. The **α-secretase** was thought to reside in a late Golgi compartment (Sambamurti et al., 1992; De Strooper et al., 1993; Kuentzel et al., 1993) and at the plasma membrane, possibly in microdomains known as caveolae (Ikezu et al., 1998). Subsequent studies indicate that cleavage at the α-site can occur within the trans-Golgi apparatus or in post-TGN vesicles, and at the plasma membrane (Culvenor et al., 1995; Parvathy et al., 1999; Jolly-Tornetta and Wolf, 2000). The ratio between plasma membrane and intracellular cleavage appears to be cell-specific. There is reasonable consensus that it is primarily an APP intracellular source (probably at the TGN/Golgi) that is cleaved in the α-secretase regulated pathway (Jolly-Tornetta and Wolf, 2000; Hooper and Turner, 2002). Fahrenholz et al. (2004), when studying mice memory improvement upon α-secretase up-regulation, observed that the regulated α-secretase APP cleavage occured mainly during APP transport from the TGN to the plasma membrane. Intracellular APP α-secretase cleavage was first detected in studies using metabolic labelling approaches, where αCTFs products were detected intracellularly before the appearance of αsAPP in the medium (Sambamurti et al., 1992; De Strooper et al., 1993; Kuentzel et al., 1993). These results indicated that this APP cleavage also occurs during APP export through the secretory pathway. In fact, the majority of APP cleavage to αsAPP in N2a neuroblastoma cells (De Strooper et al., 1992; 1993), PC12 cells (Sambamurti et al., 1992), neuroblastoma H4 cells (Kuentzel et al., 1993), CHO cells (Jolly-Tornetta and Wolf, 2000), or even in an APP-expressing yeast system (Zhang et al., 1997) was shown to occur intracellularly at the TGN or in post-TGN vesicles, probably just after sulfate incorporation. In addition, the pool of APP that reaches the cell surface as full-length mature molecules may also undergo cleavage by α-secretase at that location. However, it is still not clear if this APP cleavage occurs at the plasma membrane or if it requires APP endocytosis and recycling (Sisodia, 1992; Nordstedt et al., 1993; Koo and Squazzo, 1994; Roberts et al., 1994; Parvathy et al., 1999).

The three putative α-secretases (TACE, ADAM 10 and MDC9) are synthesized as preproteins and cleavage of their inhibitory prodomain in late Golgi compartments (Lammich et al., 1999) turns them into active enzymes (Haniu et al., 2000; Schlondorff et al., 2000; Anders et al., 2001). These data are consistent with functional cleavage of APP normally occurring in the later stages of APP maturation and translocation to the cell membrane (Turner et al., 2003). The mature, proteolytically active form of TACE has been detected both

intracellularly and at the cell surface, but it is predominantly localized intracellularly in a perinuclear compartment (for review, see Hooper and Turner, 2002). Through the use of a TACE inhibitor, Jolly-Tornetta and Wolf (2000) have reported that TACE was the α-secretase involved in PKC-induced αsAPP secretion at the cell surface of CHO cells. They have also observed TACE involvement in the αsAPP PKC answer at TGN/Golgi, but only at a partial level, indicating the existence of another PKC-sensitive α-secretase at this location. ADAM 10 can occur at the cell surface but the majority is present in the Golgi apparatus and possibly in surface-destined transport vesicles (Lammich et al., 1999). Recently, this enzyme was discovered to be soluble and ready to be transported inside vesicles after its shedding maturation/activation by ADAM 9 (Tousseyn et al., 2005).

Early studies suggested that **β-cleavage** events occur in an endosomal compartment (Haass et al., 1992a,b; Shoji et al., 1992; Peraus et al., 1997). However, subsequent studies included the secretory compartments ER and Golgi complex (Cook et al., 1997; Hartmann et al., 1997; Tomita et al., 1998). BACE-1 is expressed initially as a pro-enzyme and it is cleaved after exiting the ER (Vassar et al., 1999). Consistent with observed regions of Abeta production, BACE-1 is located intracellularly at the Golgi, TGN, and secretory vesicles. Furthermore, BACE-1 also exhibits cell surface and endosomal localization, but does not co-localize with lysosomal markers (Huse et al., 2000). As noted above, BACE-1 was also found to localize at lipid rafts, which are membrane microdomains implicated in protein trafficking and proteolytic processing (Riddell et al., 2001). BACE-2 localizes in the ER, Golgi, TGN, endosomes, and plasma membrane, with its cellular localization patterns depending on the presence of its transmembrane domain. BACE-2 chimeras that increase localization of BACE-2 in the trans-Golgi network do not alter APP processing and cleavage fragment levels.

The resulting CTFs of APP α- or β-secretase cleavages are mainly delivered to lysosomes immediately after that cleavage (Kuentzel et al., 1993; Chan et al., 2002). Interestingly, Nicastrin has been identified as a major lysosomal membrane protein in a proteomic survey (Bagshaw et al., 2003). Furthermore, mature Nicastrin, PS1 and APP were found co-localized in the LAMP-1 positive endosomes membranes, where an acidic active **γ-secretase** was also present (Pasternak et al., 2003). The main subcellular γ-secretase activity locations are in fact the endosomes and the plasma membrane (Weidemann et al., 1997; Xia et al., 1997; Kaether et al., 2006). The finding that Presenilins predominate at the ER and early Golgi (Kovacs et al., 1996) was unexpected as only limited amounts of γ-secretase activity has

been detected at those compartments. This is the basis of the so-called "spatial paradox" (Annaert and De Strooper, 1999). Despite the high concentration of Presenilins in the ER, and its ER co-localization with Nicastrin (Yu et al., 2000), only very limited γ-secretase processing seems to occur there, and at least one component of the γ-secretase complex must originate from a post-ER compartment (Cupers et al., 2001; Cupers et al., 2005). Moreover, Nicastrin does not have an ER retention signal and seems to bind PS at the Golgi (Capell et al., 2005). APP and βCTF chimeras targeted to different subcellular compartments provided evidence that APP or βCTFs γ-secretase cleavage occurs in a post-ER compartment (Cupers et al., 2005). More recently, by blocking selective transport steps along the secretory pathway Kaether et al. (2006) demonstrated that the main subcellular locations of AICD generation are the plasma membrane and endocytic compartments. In synthesis, efficient γ-secretase cleavage of APP seems to occur in compartments that contain small amounts of PS1, while little γ-secretase activity is observed in compartments where abundant PS1 is residing (Cupers et al., 2005). In fact, PS1 may have an additional role in protein trafficking, as it was found to interact or to affect the activity of three Rab proteins (small GTPases involved in vesicular transport): Rab11 (Dumanchin et al., 1999), Rab8 (leading to altered βCTF transport, Kametani et al., 2004), and Rab6 (Scheper et al., 2004). Additionally, Nicastrin trafficking and post-translational processing (as glycosylation) were affected in PSs double knockout mice (Sisodia et al., 2001; Leem et al., 2002). PS-induced alterations in the levels and subcellular location of Rab proteins also suggest that Presenilins might be involved in APP vesicular routing (Dumanchin et al., 1999; Kametani et al., 2004; Scheper et al., 2004). At a specific neuronal level, APP, BACE-1 and PS1 were found to co-localize in an axonal vesicular compartment (Kamal et al., 2001) moving anterogradely in a kinesin-dependent manner.

I. 3 – PHOSPHORYLATION-DEPENDENT APP REGULATION

I. 3. 1 – PROTEIN PHOSPHORYLATION, PROTEIN KINASES AND PHOSPHATASES IN AD

Brain ageing is characterized by a progressive decline in cognitive functions and memory loss. It is becoming increasingly clear that protein phosphorylation is a fundamental process associated with memory and brain function, with prominent roles in the processing of neuronal signals and in the short-term and long-term modulation of synaptic transmission. In neurodegenerative disorders, such as AD and ALS (Amyotrophic Lateral Sclerosis), there is

evidence for abnormal regulation of protein phosphorylation, which appears to contribute to the pathogenesis of such diseases (Wagey and Krieger, 1998).

Reversible protein phosphorylation regulates most aspects of cellular processes. A key event in cell regulation, including signal transduction, is reversible protein phosphorylation. A protein kinase transfers a phosphate group from ATP to the protein, altering the conformation and function of the latter. A protein phosphatase removes the phosphate and the protein reverts to its original state (Figure I.17).

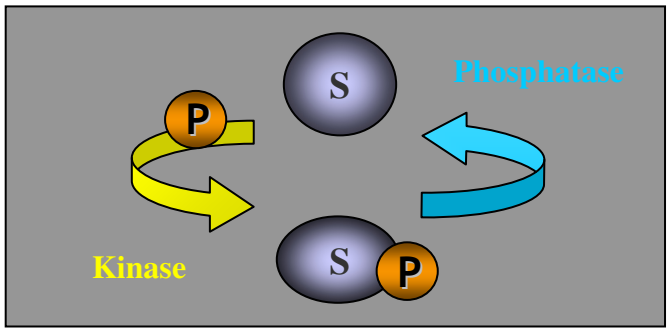

Figure I.17. Schematic diagram of kinase and phosphatase antagonic actions on a common substrate.

AD and phosphorylation. Of all mammalian tissues, the brain has the highest levels of protein kinases and phosphatases, suggesting that protein phosphorylation is particularly important in mammalian brain function. Impaired balance of cellular phosphorylation systems has been reported to occur in AD. These include abnormalities in both expression and activity levels of kinases, and/or phosphatases, thus leading to alterations in the processing of APP and Abeta production (Gandy and Greengard, 1994; da Cruz e Silva et al., 1995a; Tian and wang, 2002). For example, altered PKC activities and levels, decreased activity of protein phosphatases PP1 and PP2A, overexpression of calcineurin mRNA levels, protein Tau and Beta-tubulin hyperphosphorylated states (Gong et al., 1993; Matsushima et al., 1996; Bennecib et al., 2000; Hata et al., 2001; Vijayan et al., 2001) have all been associated with AD. Furthermore, many proteins that are relevant to the disease condition, including APP, Tau, PS1 and PS2, or BACE, are phosphorylated "in vivo" and can be regulated by phosphorylation. Alterations in the phosphorylation state of APP C-terminal fragments were reported in AD patients brains (Lee et al., 2003a). In the hippocampal pyramidal neurons of these brains phospho-APP was observed to accumulate inside large vesicular structures where it co-localized with endosome markers and BACE-1 (Lee et al., 2003a).

PKC levels and activity have been reported to be altered in AD brains (Cole et al., 1988), as well as in fibroblasts derived from patients with sporadic AD, familial AD, and Down's syndrome (Koo, 1997; Maasch et al., 2000). A significant decrease in PKC levels and PKC activity was observed in the membranous fraction of AD human cortex (Cole et al., 1988; Shimohama et al., 1993; Wang et al., 1994) and altered immunohistochemical distribution of some PKC isozymes in AD brain has also been reported (Masliah et al., 1990). Comparative studies of phosphatase activities in AD versus control brains (Gong et al., 1993) led to the findings that the activity of the Ser/Thr protein phosphatase PP1 and phosphotyrosyl-protein phosphatases in grey matter and of the Ser/Thr phosphatase PP2A in both grey and white matters were significantly lower in AD brains. In contrast, the mRNA of a PP2B catalytic subunit was found to be up-regulated in AD brain (Hata et al., 2001). The authors used cDNA microarray technology to study altered gene expression in an AD patient afflicted hippocampus. The most up-regulated gene in AD proved to be the β isoform of the catalytic subunit of calcineurin (PP2B Aβ). Indeed, in situ hybridization, histochemistry and RT-PCR analysis revealed that this PP2B Aβ was significantly up-regulated in the pyramidal neurons of AD hippocampus (Hata et al., 2001). Interestingly, work from Ermak et al. (2001) revealed that the mRNA levels of a calcineurin inhibitor (DSCR1) were also overexpressed in AD and Down's syndrome patients.

I. 3. 2 – PHOSPHORYLATION AND APP PROCESSING

Although the factors regulating APP processing and Abeta production have not been fully elucidated, it is now widely accepted that protein phosphorylation is involved. Processing of APP and Abeta production were shown to be regulated by phosphorylation and phosphorylation-dependent events (Gillespie et al., 1992; da Cruz e Silva et al., 1995a; Ando et al., 2001; da Cruz e Silva et al., 2003). As APP proteolytic processing is a necessary step in APP RIP cellular signalling and phosphorylation is involved in signal transduction pathways, further elucidation on the molecular mechanisms underlying phosphorylation-dependent regulation of APP processing is required.

Protein kinase C. Previous studies have revealed that APP levels and APP processing are under PKC regulation. Long-term exposure of a human glial cell line to PKC stimulating agents, such as the phorbol ester PMA (phorbol 12-myristate 13-acetate), increased APP mRNA levels and protein-binding activity to the APP promoter (Trejo et al., 1994; Lahiri and Nall, 1995). Short-term exposures to phorbol esters invariably results in a higher non-

amyloidogenic APP processing rate. Phorbol esters such as PMA or phorbol 12,13-dibutyrate (PDBu) enhance α-secretase cleavage of APP and αsAPP production in several cultured cell lines (Buxbaum et al., 1990; Caporaso et al., 1992b; Gillespie et al., 1992; da Cruz e Silva, 1993; Demaerschalck et al., 1993; Gabuzda et al., 1993; Slack et al., 1993; Dyrks et al., 1994; Marambaud et al., 1997a,b; Mills et al., 1997). The phorbol esters-induced APP processing is also evident in primary cultures of rat cortical neurons (Mills and Reiner, 1996), and specifically in rat cortical synaptosomes (McLaughlin and Breen, 1999). Furthermore, "in vivo" studies using rats expressing hyperactivated PKC demonstrated enhanced synaptosomal sAPP production and decreased levels of synaptosomal membrane-bound APP in selected brain regions (cortex and hippocampus) (Caputi et al., 1997). PKC-mediated stimulation of sAPP has been shown to be specific insofar as down-regulation of PKC blocked the phorbol ester-stimulated sAPP release (Buxbaum et al., 1994). Nonetheless, there is controversy in the effects of this α-secretase pathway induction and the consequential decrease in Abeta production, raising the question of competition between α- and β- secretases for substrate. In fact, PKC-activators or carbachol, which are known α-secretase pathway inducers, were reported to decrease Abeta secretion in cultured cells transfected with APP FAD mutant forms (Gabudza et al., 1993; Hung et al., 1993; Felsenstein et al., 1994). Constitutive overactivation of PKC in guinea pig brain also enhanced cortical α-secretory APP processing but without decreasing Abeta generation (Rossner et al., 2001a). The mechanisms of PKC-dependent induction of APP α-secretase cleavage are complex and still being unravelled. PKC is known to be involved in the process of post-TGN vesicle formation, through binding and activating the phospholipase involved in vesicles scission (Sabatini et al., 1996; Simon et al., 1996). Activation of endogenous PKC by phorbol esters or addition of purified PKC increases formation of APP-containing secretory vesicles from the trans-Golgi network (Xu et al., 1995), and drastically reduces the amount of APP at the cell surface (Koo, 1997). This can be explained by accelerated APP trafficking through the exocytotic pathway and accelerated α-secretase APP cleavage intracellularly and at the plasma membrane. The hypothesis that PKC phosphorylation of sites within the APP intracellular carboxy terminus may change the conformation of its extracellular domain and make it a better substrate for the cleaving enzyme was recently advanced (Turner et al., 2003). Nonetheless, da Cruz e Silva et al. (1993) showed that cleavage of APP tailless constructs (with a stop codon at the KKK sequence) to yield sAPP was still stimulated by phorbol esters. Hence, PKC-dependent sAPP-induction may occur as a sum of indirect and direct actions.

Ser/Thr Protein Phosphatase 1. Okadaic acid (OA), a Ser/Thr protein phosphatases type 1 (PP1) and type 2A (PP2A) inhibitor, was found to stimulate APP processing to sAPP in COS-1 cells (da Cruz e Silva et al., 1995a). APP processing and secretion modulation by OA was also observed in primary guinea pig neurons (Holzer et al., 2000). Da Cruz e Silva et al (1995a) were able to specifically implicate PP1 in this APP regulation through the use of OA and other inhibitors with different inhibitory potencies against PP1/PP2A. Interestingly, PP1 is known to be involved in long-term potentiation (LTP) and in long-term depression (LTD), thereby influencing learning and memory (Mulkey et al., 1994; Genoux et al., 2002; Waddell, 2003). Furthermore, PP1 and PP2B activities are interconnected in so far as PP2B is able to inhibit (dephosphorylate) DARPP-32, a potent PP1 inhibitor (Mulkey et al., 1994; Yan et al., 1999b), providing a further mechanism for PP2B modulation of APP processing. The mechanism by which PP1 down-regulates APP processing and/or sAPP secretion are not yet defined, but direct APP dephosphorylation remains a possibility (Oishi et al., 1997).

APP secretase phosphorylation. Another potential stage for phosphorylation-dependent regulation of APP proteolytic processing is through modulation of APP secretases. All three members of the ADAM family are synthesized as preproteins, so that their proteolytic function is regulated to prevent damage to other proteins, or the premature cleavage of their substrates, including APP (Turner et al., 2003). The TACE cytoplasmic domain contains potential phosphorylation sites, and the enzyme was reported to be phosphorylated at Ser^{819} after growth factor stimulation of the Erk/MAPK pathway or after PMA-induced PKC-activation (Black et al., 1997; Diaz-Rodriguez et al., 2002). PMA exposure did not alter TACE maturation or cellular distribution (Hooper and Turner, 2002), suggesting other still unknown roles for this phosphorylation that may involve its enzymatic kinetics of APP proteolysis (Fan et al., 2003). ADAM 10 is also stimulated after PKC activation (Etcheberrigaray et al., 2004). MDC9 was also phosphorylated after PMA activation of the PKC isozyme δ (Izumi et al., 1998; Roghani et al., 1999). The role of BACE-1 phosphorylation on a cytoplasmic serine residue is better known and involves regulation of BACE-1 subcellular traffic. When phosphorylated on serine residue Ser^{498}, this enzyme enters the recycling pathway of Golgi-retrieval after endocytosis (Walter et al., 2001). Phosphorylation at this serine, which is immediately upstream of the BACE-1 binding sequence for its vesicle coating protein GGA, was recently reported to enhance by three-fold the affinity of this binding (Shiba et al., 2004).

Phosphorylation may also affect γ-secretase activity. The PS2 protein can be highly phosphorylated, whereas little phosphorylation is observed for PS1 (Walter et al., 1996; 1998). Casein kinases 1 and 2 (CK1, CK2) phosphorylate PS2 at three serine residues in its N-terminus before PS2 maturational cleavage by caspases, and after this cleavage its C-terminus is also phosphorylated at three serine residues, putatively by the same casein kinases (Walter et al., 1999). After PS1 caspase cleavage, its C-terminal is also phosphorylated at two still unknown residues by protein kinases A and C (Walter et al., 1996; 1998).

I. 3. 3 – APP AS A PHOSPHOPROTEIN

Direct phosphorylation of the APP molecule is potentially an important mechanism for regulating APP binding, traffic and processing, and therefore worthwhile pursuing. APP is a phosphoprotein with putative phosphorylation sites on its extracellular and intracellular domains. Of particular note is the finding that AD patients' exhibit altered APP phosphorylation, with APP βCTFs carrying phosphorylated Thr^{688} being up-regulated in AD brains (Lee et al., 2003a). Furthermore, it was recently reported that phosphorylation of the APP CTFs appears to regulate the formation and/or stability of AICDs, probably by disrupting AICD complexes, leading to altered AICD-mediated signalling events (Zheng et al., 2003). A Thr^{668} phosphorylated APP C-terminal fragment, probably AICD, was shown to be present in the nucleus of CAD cells (a catecholaminergic cell line), where it localizes to subnuclear particles that define the splicing factor compartment (SFC) [e.g. the small nuclear ribonucleoprotein (snRNP), U2B, and serine/arginine-rich (SR) proteins], but is excluded from the coiled bodies and the gems (Muresan and Muresan, 2004). This distribution of phospho APP (pAPP) epitopes was found in CAD cells independent of their state of differentiation, as well as in primary cortical neurons, epithelial cells and fibroblasts. These authors further showed that exogenously expressed AICD becomes phosphorylated and distributes throughout the cell, with a fraction being translocated into the nucleus, where it co-localizes with endogenous pAPP epitopes and with Fe65 at intranuclear speckles. Hence, phosphorylation may be involved in the targeting of AICD to specific nuclear compartments. APP has seven potentially phosphorylatable residues, which have been shown to be phosphorylated "in vitro" and "in vivo" (Koo, 1997; Oishi et al., 1997; Iijima et al., 2000; Walter et al., 2000, Minopoli et al., 2001; Standen et al., 2001) (Fig. I.18). In Table I.2 a summary is given of these seven APP phosphorylation residues, with their putative kinases and functions.

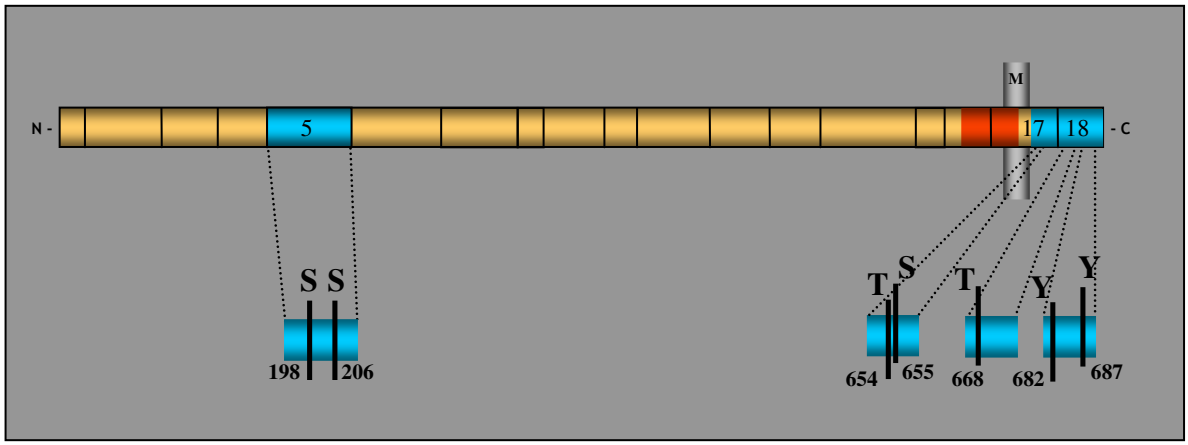

Figure I.18. Exon localization of APP phosphorylatable residues. Extracellular (NH2-terminal) APP domain has two phosphorylatable residues (Ser^{198} and Ser^{206}) and intracellular (COOH-terminal) APP domain presents five residues (Thr^{654}, Ser^{655}, Thr^{668}, Tyr^{682}, and Tyr^{687}). Adapted from: da Cruz e Silva et al., 2004.

Table I.2. APP phosphorylatable residues and kinases implicated.

APP Phospho Residue	Kinase	Putative Role of Phosphorylation	Reference
Ser^{198}	. CK2 . ecto-CK2	. Possible involvement in LTP in neurons and synaptogenesis	Hung and selkoe, 1994 Walter et al., 1997 Walter et al., 2000
Ser^{206}	. CK1 . ecto-CK1	. Possible involvement in LTP in neurons and synaptogenesis	Hung and selkoe, 1994 Walter et al., 1997 Walter et al., 2000
Thr^{654}	. CaMKII ("in vitro") . ND ("in vivo")	. Potential regulation of APP binding and APP secretory trafficking	Gandy et al., 1988 Oishi et al., 1997 Ramelot and Nicholson, 2001
Ser^{655}	. PKC ("in vitro" and "in vivo": cultured cells and rat brain) . CaMKII ("in vitro") . APP kinase I (rat brain)	. Potential regulation of APP binding and APP secretory trafficking . Involvement in PKC-regulated sAPP processing	Gandy et al., 1988 Suzuki et al., 1992 Oishi et al., 1997 Ramelot and Nicholson, 2001 Lee et al., 2003a
Thr^{668}	. Cdk5 . Cdc2 . MAPKs (GSK-3 and JNK-3)	. Potential regulation of APP binding to Fe65 and JIP-1 . Regulates neurite extension . Regulation of APP axonal trafficking . Attenuates APP cleavage by caspases . Down-regulates AICD-mediated nuclear signalling	Suzuki et al., 1994 Aplin et al., 1996 Oishi et al., 1997 Iijima et al., 2000 Ando et al., 2001 Ramelot and Nicolson, 2001 Standen et al., 2001 Sisodia, 2002 Taru et al., 2004 Kimberly et al., 2005

APP Phospho Residue	Kinase	Putative Role of Phosphorylation	Reference
Tyr^{682}	. Tyrosine kinase Abl (active form)	. Promotes the interaction with Shc proteins . May regulate the association of the cytoplasmic tail of APP with its binding partners	Haass et al., 1993 Koo and Squazzo, 1994 Zambrano et al., 2001 Tarr et al., 2002
Tyr^{687}	ND	. May regulate the association of the cytoplasmic tail of APP with its binding partners	Lee et al., 2003a

APP ectodomain phosphorylation. In its ectodomain APP was reported to be phosphorylated on serine residues (Ser^{198} and Ser^{206}). Phosphorylation of the two serine residues occurs in two distinct cellular locations: in a post-Golgi secretory compartment (most likely within secretory vesicles) and at the cell surface by ectoprotein kinases (Walter et al., 1997). The authors also found that "in vivo" sAPP was detected exclusively in the double phosphorylated form. Subsequently, it was shown that ectocasein kinases 1 and 2 were the kinases involved in the "in vivo" cell surface APP phosphorylation at residues Ser^{198} and Ser^{206}, respectively, in a process strongly inhibited by heparin (Walter et al., 2000).

APP cytoplasmic domain phosphorylation. The Ser/Thr and Tyr cytoplasmic phosphorylatable residues are located within three APP functional motifs, previously mentioned in section I.2.6 and shown in Figure I.14: ^{682}YENPTY^{687}, ^{667}VTPEER^{672}, and ^{653}YTSI^{656}. Other potentially phosphorylatable residues (Ser^{675}, Thr^{686}) were reported to undergo phosphorylation by Lee et al (2003a) but have received little attention.

In the internalization signal domain ^{682}YENPTY^{687}, Tyr^{682} phosphorylation is a consensual site and in contrast Tyr^{687} was initially reported not to undergo phosphorylation (Haass et al., 1993; Koo and Squazzo, 1994; Minopoli et al., 2001). More recently, however, "in vivo" phosphorylation of Tyr^{687} was reported (Lee et al., 2003a). APP is tyrosine-phosphorylated in cells expressing a constitutively active form of the Abl protooncogene, a non-receptor tyrosine kinase similar to c-Src, which can form a stable complex with APP and Fe65 (Zambrano et al., 2001). Abl-dependent Tyr^{682} phosphorylation appears to involve the nerve growth factor receptor TrkA, to mediate APP membrane internalization and to result in reduced γ-secretase APP processing (Koo and Squazzo, 1994; Lai et al., 1995; Tarr et al., 2002).

The Thr^{668} residue of the ^{667}VTPEER^{672} domain is found phosphorylated in rat brain and in several cell lines (Oishi et al., 1997). In PC12 cells immature APP is preferentially phosphorylated at this residue during the G2/M phase of the cell cycle (Suzuki et al., 1994; Oishi et al., 1997). At this phase total levels of holo APP do not change but the levels of secreted sAPP decrease and the levels of the CTFs increase (Suzuki et al., 1994). The known kinases involved are cyclin-dependent kinases in neurons (cdk5) and in PC12 or HeLa cells (cdc2) (Suzuki et al., 1994; Oishi et al., 1997; Iijima et al., 2000). GSK-3β and c-Jun protein kinase 3 (JNK-3) may also phosphorylate Thr^{668} "in vitro" (Aplin et al., 1996; Standen et al., 2001). Mature APP phospho Thr^{668} (pThr^{668}) only occurs in the brain (and not in non-neuronal tissues) (Ando et al., 1999; Iijima et al., 2000). In PC12 cells (Oishi et al., 1997) and neurons (Ando et al., 1999) pThr^{668} APP and pThr^{668} CTFs were selectively localized in neurites, mostly within the growth cones, while Thr^{668} dephosphorylated APP is found mostly in the cell body. Brain mature APP Thr^{668} phosphorylation occurs during and after neuronal differentiation, and in PC12 cells regulates neurite extension, correlating with the timing of neurite outgrowth in differentiating cells (Oishi et al., 1997). Furthermore, pThr^{668} was described to selectively target APP for axonal transport in APP/BACE-1/PS co-localizing vesicles (Amaratunga and Fine, 1995). Interestingly, enhanced levels of pThr^{668} CTFs were reported in AD brains, along with enhanced and extensive co-localization of an anti-pThr^{668} antibody with BACE-1 (Lee et al., 2003a). In addition, the authors have observed that βCTFs were found to be preferentially phosphorylated at this residue when compared with αCTFs. In fact, the ^{667}VTPEER^{672} domain has been the focus of intense research and Thr^{668} phosphorylation is now known to be involved in the regulation of APP protein binding at the ^{682}YENPTY^{687} domain (Ando et al., 2001). This is thought to occur through pThr^{668}-induced alterations of the APP C-terminus conformational structure (Ramelot et al., 2001). Specifically, pThr^{668} exerts differential regulation of APP binding to Fe65 (down-regulated) versus X11 or mDab1 (pThr^{668}-insensitive) (Ando et al., 2001). For example, Wasco et al. (1993) and Ando et al (1999) have reported that HEK293 cells overexpressing Fe65 show inhibited secretion of Abeta 1-40 and 1-42. This effect was further observed to be partially cancelled by a Thr^{668} mutation or by its kinases inhibitors (Lee et al., 2003a). In recent reports, Fe65 binding to APP was observed to enhance APP cleavage by caspases at Asn^{664} (Zambrano et al., 2004). In parallel, Thr^{668} phosphorylation was observed to attenuate this cleavage (Taru et al., 2004). Finally, pThr^{668}-induced decrease in AICD-Fe65 binding affinity appears to lead to down-regulation of the AICD-mediated gene transactivation (Kimberly et al., 2005).

Phosphorylation of the YTSI domain. The amino acid sequence ^{653}YTSI^{656} that functions as an APP sorting signal is not as well characterized as the other two domains and is the object of this thesis. Central to the domain are two consensus residues for phosphorylation, Thr^{654} and Ser^{655}, found to be phosphorylated "in vitro"and "in vivo" (see Table I.2 for references). The occurrence of full length APP phosphorylated at Thr^{654} or Ser^{655} has been reported in cultured cell lines and rat cortex (Gandy et al., 1988; Oishi et al., 1997). However, in human hippocampus of AD patients only phospho Ser^{655} CTFs, and not phospho Thr^{654}, was observed (Lee et al., 2003a).

Phosphorylation of APP at its Ser^{655} residue can be postulated to be involved in the PKC and PP1 APP mediated processing (section I.3.2). In PC12 cells, phosphorylation at Ser^{655} was found to be highest in mature rather than immature APP isoforms and was increased more than 10-fold by treatment with okadaic acid (Oishi et al., 1997). In addition, Ser^{655} is the only APP residue that undergoes "in vitro" and "in vivo" PKC-induced phosphorylation (Gandy et al., 1988; Suzuki et al., 1992; Isohara et al., 1999). PKC was demonstrated to rapidly phosphorylate this residue on an APP C-terminal synthetic peptide (Gandy et al., 1988). In a semi-intact PC12 cell system, APP holoprotein and APP CTFs were found to be specifically phosphorylated at Ser^{655}, after purified PKC addition or PMA incubation (Suzuki et al., 1992). Under these conditions, all the mature but not the immature major APP isoforms (695, 751 and 770) were found to be phosphorylated at Ser^{655}, and phosphorylation of threonine residues was not detectable by phosphoamino acid analysis even after longer exposures (Suzuki et al., 1992). A putative PKC-downstream APP kinase is APP kinase I, a Ca^{2+}-independent kinase of ~43 KDa that was found to phosphorylate Ser^{655} in rat brain (Isohara et al., 1999). APP kinase I was discovered by chromatographic analysis of soluble cytoplasmic fractions of rat brain homogenates. In these fractions, containing APP Ser^{655} Ca^{2+}-independent kinase activity, ~50% of the latter was due to APP kinase I and ~35% was due to a mixture of PKC and a fragment of PKC (Isohara et al., 1999).

At a molecular level, APP phosphorylation at Ser^{655} may regulate APP binding to other proteins, as it was reported to induce "in vitro" structural alterations to the APP C-terminus to a higher level than phosphorylation at Thr^{654}. While the latter affected mainly the structure of the threonine residue, phosphorylation at Ser^{655} induced significant structural alterations on Thr^{654}, Ser^{655}, and on the two downstream adjacent amino acids (I^{656} and H^{657}) (Ramelot and Nicholson, 2001). These are the first residues of the Ile^{656}-Val^{663} hydrophobic pocket, located immediately downstream to the ^{653}YTSI^{656} domain (Ramelot et al., 2000; Ramelot and

Nicholson, 2001). In fact, the chemical changes observed were up to six residues away from phosphorylated Ser^{655}, suggesting induced altered conformation of residues inside the pocket (Ramelot and Nicholson, 2001). Thus, the binding affinities of APP binding proteins for the ^{653}YTSI^{656} domain (e.g. APPBP2) or for the downstream sequence (e.g. $G_0\alpha$), may be significantly altered upon Ser^{655} phosphorylation. Further support for the existence of a linkage between the ^{653}YTSI^{656} domain and the hydrophobic pocket comes from comparison of APP sequences in various species. The YTSI and hydrophobic pocket domains were found to exist both in the same APP sequence or to be both absent. In several mammalian and fish species, and at least in chicken and frog, both the ^{653}YTSI^{656} and the Ile^{656}-Val^{663} hydrophobic pocket were found to be absolutely conserved. Contrarily, in *Drosophila* and *C. elegans* both motifs are degenerated (see Sabo and Ikin, 2002). Furthermore, Suzuki et al. (1997) demonstrated that APLP1 and APLP2, like APP, could both be phosphorylated "in vitro" by PKC. These authors highlighted the fact that Ser^{655} has "equivalent" serine residues in the amino acid sequences of APLP-1 and APLP-2 proteins (Suzuki et al., 1997). These proteins also have ^{653}YTSI^{656}-like domains and Ile^{656}-Val^{663} hydrophobic pocket-like sequences (Fig. I.19). Therefore, Ser^{655} is a pivotal residue whose phosphorylation may be potentially implicated in regulating APP interactions at these C-terminal motifs.

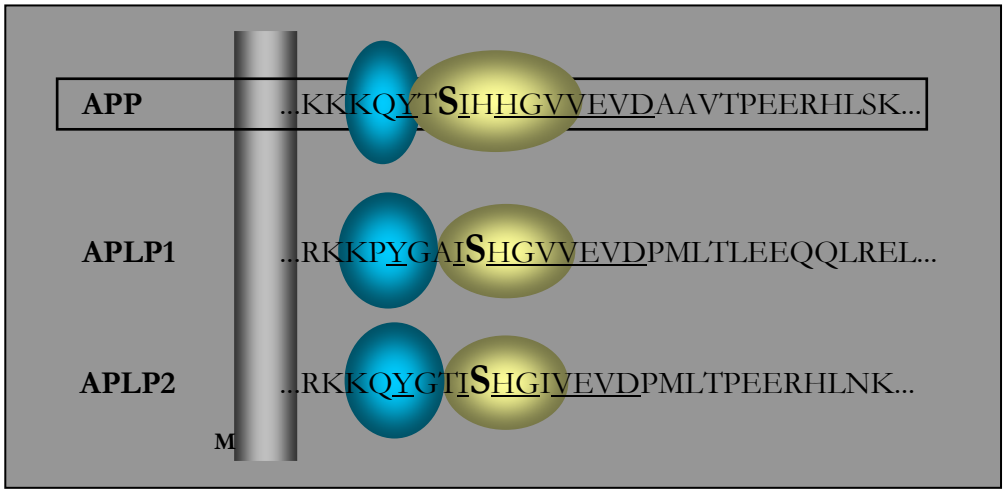

Figure I.19. Alignment of the Ser^{655} APP residue with other members of the APP mammalian superfamily. Sequence homology between APP and APLPs. C-termini demonstrating the existence of ^{653}YTSI^{656}-like YGXIS domains (*blue*) in APLPs and of a phosphorylatable serine residue within them (*bold*). The hydrophobic pocket (*yellow*) immediately downstream the YGXIS domain is also conserved. Conserved amino acid residues are underlined. **M,** cellular membrane.

I. 4 – AIMS OF THIS THESIS

The findings that APP cellular fate can be regulated by protein phosphorylation, a major mechanism regulating signal transduction pathways and protein-protein interactions, provide us with a strong hypothesis for APP as a signal transduction molecule. Phosphorylation-dependent events include APP traffic, cleavage, and protein-complex formation of APP and AICD, consequently affecting targeting to different intracellular molecular pathways. Thus, APP traffic targeting signals containing pivotal residues for regulatory phosphorylation mechanisms can be crucial in the disease process. APP direct phosphorylation studies that are now emerging focus on the phosphorylatable residues from the ^{667}VTPEER^{672} and ^{682}YENPTY^{687} motifs. The less well-studied APP ^{653}YTSI^{656} motif, a basolateral sorting signal in MDCK cells, seems to be involved in APP secretory trafficking and potentially in neuronal APP polarized sorting. PKC and PP1 are two phosphorylation effector proteins that are both involved in the regulated α-secretase APP cleavage into the neuroprotector and neurite outgrowth factor αsAPP. These effectors may function directly through APP phosphorylation, being that they are the best candidates for "in vivo" phosphorylation/dephosphorylation of the ^{653}YTSI^{656} serine 655 residue. Therefore, a possible mechanisms underlying APP α-secretase regulated cleavage may involve Ser^{655} phosphorylation-induced APP targeting to subcellular compartments or specialized domains. To date, data strongly suggests a putative involvement of ^{653}YTSI^{656} and Ser^{655} phosphorylation in the regulation of APP C-terminal fragment production, as well as in the regulation of APP/AICD traffic. Alterations of all these processes could have strong effects on APP cellular signalling and even Abeta production. Nonetheless, there is still no information about the physiological relevance of APP Ser^{655} phosphorylation including a potentially important role in APP signal transduction.

The aim of this thesis is to study the role of APP phosphorylation at the Ser^{655} residue and the consequential protein's cellular fate, both in terms of APP intracellular targeting and APP proteolytic processing. Understanding the underlying molecular mechanisms controlling APP trafficking and processing events, and their relevance to APP function as a signal transducer, should lead to new insights into the aetiology, pathogenesis and therapy of AD, shedding light onto the ongoing discussion.

CHAPTER II

SERINE 655 PHOSPHORYLATION-DEPENDENT APP_{695} TARGETING

CHAPTER II – SERINE 655 PHOSPHORYLATION-DEPENDENT APP_{695} TARGETING

II. 1 – INTRODUCTION

APP is a signal transduction transmembranar protein that is processed intracellularly via various pathways, including the secretory and endocytic pathways. Inside a cell, neuronal or non-neuronal, APP is generated in the ER (where it is N-glycosylated) and transported to the Golgi complex (where it matures through O-glycosylation and sulfation), where a pool can be carried into post-TGN secretory vesicles to the plasma membrane (see Chapter I). Regulation of APP trafficking and subcellular targeting, as well as consequential cleavages of subpopulations of APP, are not fully understood. APP secretases don't exist ubiquitously in the cell and their distribution seems to be restricted to specific cellular compartments. It is not yet clear if APP proteolytic cleavages are regulated by temporal APP substrate/enzyme co-distribution and/or by enzyme activation. Additionally, and when required, it is possible that more APP substrate may be "activated" and targeted to specific subcellular microdomains to be cleaved. Although the factors regulating APP trafficking/processing have not been fully elucidated, protein phosphorylation is thought to be involved. Activation of endogenous PKC increases formation of APP-containing secretory vesicles from the TGN (Xu et al., 1995), accelerating APP trafficking in the secretory pathway (Koo, 1997). In semi-intact cell systems APP Ser^{655} was the only phosphorylatable residue found to be phosphorylated by PKC or by a PKC downstream kinase (Suzuki et al., 1992). Furthermore, this residue belongs to the ^{653}YTSI^{656} basolateral sorting motif (Lai et al., 1995; Zheng et al., 1998) that is the binding site for APPBP2, a protein thought to be involved in regulating APP in the secretory pathway. Hence, all the evidence implicates ^{653}YTSI^{656} as a molecular targeting signal and place Ser^{655} at a pivotal regulatory position (Ando et al., 2001; Ramelot and Nicholson, 2001). APP Ser^{655} phosphorylation may be a key process regulating differential binding of APP scaffolding proteins to the ^{653}YTSI^{656} motif, with significant consequences for APP targeting. Nonetheless, and despite all the evidence pointing to the importance of this residue in the protein's cellular fate, very few studies have focused on this APP domain and even fewer on unravelling the possible functions of Ser^{655} phosphorylation.

In order to address this question, we first constructed a number of APP_{695} cDNA point mutations at Ser^{655} (from now on referred to as "S655"). This residue was mutated to

alanine (S655A) to mimic a constitutively dephosphorylated site, or to glutamate (S655E) to mimic a constitutively phosphorylated residue. These mutants, along with the parental wild-type APP cDNA, were used in a series of assays designed to study the putative S655 phosphorylation-dependent effects on APP trafficking and proteolytic processing.

II. 2 – AIMS OF THIS CHAPTER

The work presented in this chapter addressed the putative regulatory functions of APP phosphorylation at the ^{653}YTSI^{656} basolateral sorting signal. The main objectives of this chapter were:

1. To generate S655 APP phosphorylation mutants as GFP (Green Fluorescent Protein) fusion cDNAs in an appropriate mammalian expression vector.
2. To develop a model system to monitor wild-type (Wt) APP-GFP subcellular trafficking.
3. To apply the system developed to APP-GFP phosphorylation mutants and monitor intracellular protein trafficking.
4. To study whether any observed APP trafficking differences can be coupled to organelle specific targeting, in a S655 phosphorylation-dependent manner.

For Objective 1 APP cDNAs were engineered to be visible for epifluorescence microscopy when transfected into cells in culture. Hence, the APP_{695} S655A/E point mutants and parent Wt cDNAs were fused in frame with EGFP (Enhanced GFP, a fluorescent reporter) to render APP_{695}-GFP fusion constructs. The second objective involved the development of an experimental design to follow APP-GFP protein trafficking intracellularly. The method developed is based on inhibiting "de novo" protein synthesis and striving for low levels of protein expression, being first used and optimized to monitor Wt APP traffic (da Cruz e Silva et al., 2004b). Thus objectives 3 and 4 were subsequently addressed.

II. 3 – MATERIALS AND METHODS

A list of all solutions and protocols used, as well as other relevant information, is presented in Appendices I to III. All reagents were of cell culture grade or ultrapure.

II. 3. 1 – ANTIBODIES

The primary antibodies used in this study were the monoclonal antibody 22C11 (Chemicon) directed against the APP N-terminal aa 60-100, the monoclonal antibody JL-8 (BD Living Colours, Clontech) to detect the GFP moiety of APP-GFP proteins, polyclonal 369 (kind gift from Dr. S. Gandy) that recognizes the APP C-terminus (last 50 aa), and the monoclonal 6E10 (Sigma-Aldrich) to detect Abeta residues 1-17. For the co-localization studies the polyclonal anti-Calnexin (StressGen Biotechnologies) antibody was used as an ER marker, the monoclonal anti-Syntaxin 6 (BD Biosciences) antibody was used as a TGN/Golgi marker, and the monoclonal anti-Cathepsin D (Transduction Laboratories) antibody was used as a lysosomal marker. Additional antibodies used were anti-mouse and anti-rabbit IgGs Texas Red-conjugated secondary antibodies (Molecular Probes), for Immunocytochemistry procedures, and anti-mouse IgGs horseradish peroxidase-linked whole antibody (Amersham Pharmacia), for enhanced chemiluminescence (Amersham Pharmacia Biosciences) detection. Dilutions of the antibodies used in this and following chapters are given in Table II.1.

Table II.1. Antibodies, respective target proteins and specific dilutions used for the different techniques employed: IB., Immunoblot; ICC, Immunocytochemistry.

Target Protein/Epitope	Primary Antibody	Secondary Antibody
	Assay/Dilution	**Assay/Dilution**
APP N-terminal	**22C11** IB dilution: 1:250 ICC dilution: 1:50	Horseradish Peroxidase conjugated α-Mouse IgG IB dilution: 1:5000
		Texas Red-conjugated α-Mouse IgG ICC dilution: 1:300
APP Abeta 1-17	**6E10** IB dilution: 1:1000 ICC dilution: 1:200	Horseradish Peroxidase conjugated α-Mouse IgG IB dilution: 1:5000
		Texas Red-conjugated α-Mouse IgG ICC dilution: 1:300
APP C-terminal	**369** ICC dilution: 1:200	Texas Red-conjugated α-Rabbit IgG ICC dilution: 1:300
EGFP	**JL.8** IB dilution: 1:1000	Horseradish Peroxidase conjugated α-Mouse IgG IB dilution: 1:5000
Calnexin	**Calnexin** ICC dilution: 1:200	Texas Red-conjugated α-Rabbit IgG ICC dilution: 1:300

Target Protein/Epitope	Primary Antibody	Secondary Antibody
	Assay/Dilution	**Assay/Dilution**
Syntaxin 6	**Syntaxin 6** ICC dilution: 1:200	Texas Red-conjugated α-Mouse IgG ICC dilution: 1:300
Cathepsin D	**Cathepsin D** ICC dilution: 1:200	Texas Red-conjugated α-Mouse IgG ICC dilution: 1:300

II. 3. 2 – S655A AND S655E APP_{695} PHOSPHORYLATION cDNA CONSTRUCTS

Site-directed mutagenesis. The S655 human APP_{695} phosphorylation cDNA point mutants, produced by site directed mutagenesis, were already available in our laboratory (S655 to Alanine and S655 to Glutamate). Alanine is a non-phosphorylatable and non-polar residue, which blocks APP phosphorylation at that residue. Glutamate is a non-phosphorylatable but negatively charged residue that by its size and charge mimics to some extent the presence of a phosphate group at that position. The nucleotide sequences of the APP S655 point mutations were confirmed by DNA sequencing. APP_{695} was the isoform used given its relevance in AD neuropathology.

Vector preparation of APP-GFP fusion constructs. For the translational fusion of the APP cDNAs with a reporter gene coding for the GFP (Fig. II.1), the APP cDNAs were amplified by Polymerase Chain Reaction (PCR) using specific primers (NAPN and S1 primers, Appendix III). The PCR reaction was performed using Pfu DNA Polymerase (Promega) as indicated in Appendix II. PCR cDNA products were analysed by gel electrophoresis and digested with *Nru* I at 37 ºC and *Age* I at 25 ºC, for the subsequent subcloning into the GFP-encoding mammalian expression vector (pEGFP-N1; BD Living Colours, Clontech).

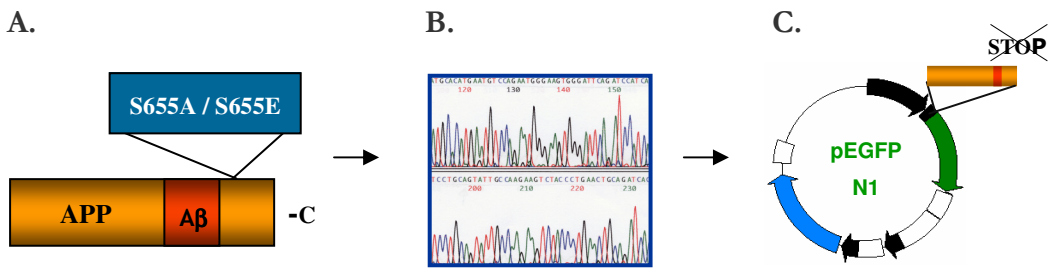

Figure II.1. Schematic representation of the APP-GFP fusion construct preparation. **A**: APP_{695} site-directed mutagenesis. **B**: Sequencing of mutated APP cDNAs. **C:** Subcloning of mutated APP cDNA into EGFP mammalian expression vector, upstream of the EGFP-encoding sequence.

The pEGFP-N1 mammalian expression vector was first digested with the restriction enzyme *Sma* I at 30 ºC, purified and further digested with *Age* I at 25 ºC, in appropriate buffers. The digestion products were electrophoretically resolved in 0.8% agarose gels and purified by means of a Gel Extraction kit (QIAgen), after which the vector was ready for ligation with the different APP inserts. Ligations were carried out overnight at 16 ºC using bacteriophage T4 DNA ligase (Promega). All subcloning procedures and DNA manipulation techniques used are extensively described in Appendix II, and the primers and vector description are presented in Appendix III.

Transformation, mini-amplification, and plasmid DNA extraction. APP-GFP fusion constructs were amplified in bacterial systems. *E. coli* XL1-blue competent cells were first transformed with an aliquot of each ligation reaction (see Appendix II). Bacterial cells were plated on LB agar plates containing the appropriate antibiotic (100 μg/ml kanamycin) to select transformants, and incubated at 37 ºC for 16 hours. Colonies were picked and left to grow overnight with agitation in liquid LB media supplemented with the appropriate antibiotic at 37 ºC. Plasmid cDNAs were extracted from these bacterial cultures.

APP-GFP cDNAs construct confirmation and mega-amplification. All putative APP-GFP fusion constructs-containing clones were first confirmed by plasmid DNA digestion with appropriate restriction enzymes (*Eco*R I and *Pst* I) and further analysed by gel electrophoresis. The nucleotide sequences and correct open reading frames fusions were confirmed by DNA sequencing. The confirmed S655A, S655E and Wt APP_{695}-GFP cDNAs subcloned into the pEGFP vector were subjected to mega-prep amplification in *E. coli* XL-1 Blue. A 400 μl aliquot of the resultant construct was purified by ethanol precipitation and used for transfection and expression in mammalian cells.

II. 3. 3 – CELL CULTURE AND TRANSIENT TRANSFECTIONS

Cell culture maintenance. A monkey kidney cell line (COS-7) was the model system in these studies given their low content in APP_{695}, easiness of transfection and the large number of previous studies in this cell line. For experimental procedures, cells were maintained in DMEM medium (Dulbecco's Modified Eagle's Medium, Sigma-Aldrich). Prior to experimental conditions medium was supplemented with 10% (v/v) foetal bovine serum (FBS; Gibco BRL, Invitrogen) and this is termed complete DMEM. Long term maintenance used complete DMEM supplemented with antibiotic/antimycotic solution (see Appendices I and II for detailed composition). Cultures were always maintained at 37 ºC and 5% CO_2.

Transient transfections. COS-7 cells were transfected with pEGFP-N1, Wt, S655A or S655E APP-GFP cDNAs using a cationic lipid reagent-mediated method (LipofectAMINE 2000 Reagent; Invitrogen Life Technologies. The day before transfection, cells were plated onto 100 mm cell culture plates with complete DMEM. Transfections were carried out according to the manufacter's instructions (see Appendix II), with cells at a density around 90%. Briefly, each cDNA and LipofectAMINE 2000 was separately diluted in DMEM medium (serum-free). Both solutions were mixed and left for 20 min at RT for DNA complex formation to occur. This mixture was then added to the medium of the respective plates of COS-7 cells. The plates were incubated at 37 ºC and 5% CO_2 for the times indicated. Table II.2 presents details on the transient transfections performed for each specific assay.

Table II.2. COS-7 cells transient transfection procedures adopted for each of the different assays. Recovery period: period for cell adherence and recovery upon removal of transfection medium.

Procedure	Transfected cDNAs	Quantity / Plate diameter	Transfection period	Recovery period
APP-GFP expression (Pilot experiment)	pEGFP Wt APP-GFP S655A APP-GFP S655E APP-GFP	2.0 μg / 35 mm	12 h	-
Time course of Wt APP-GFP levels	pEGFP Wt APP-GFP	8.0 μg / 100 mm	8 h	4 h
Intracellular APP-GFP tracking	Wt APP-GFP S655A APP-GFP S655E APP-GFP	8.0 μg / 100 mm	8 h	4 h
Nuclear targeting	Wt APP-GFP S655A APP-GFP S655E APP-GFP	4.0 μg / 60 mm	8 h	4 h
APP endocytosis assay	Wt APP-GFP S655A APP-GFP S655E APP-GFP	1.5 μg / 35 mm	8 h	4 h
Antibody uptake assay	Wt APP-GFP S655A APP-GFP S655E APP-GFP	4.0 μg / 60 mm	8 h	4 h
APP lysosomal targeting	Wt APP-GFP S655A APP-GFP S655E APP-GFP	1.5 μg / 35 mm	8 h	4 h

APP-GFP construct expression in COS-7 cells. For evaluating the expression of APP-GFP constructs in this mammalian cell line, COS-7 cells were grown in 35 mm six-well plates and transiently transfected with the APP-GFP cDNAs, along with the appropriate controls (non-transfected, MOCK, and pEGFP-N1 transfected cells). Cells were washed with PBS, harvested in 500 μl of 1% boiling SDS, and cells lysates were boiled for 10 min and sonicated for 30 sec. Samples aliquots were subjected to 7.5% SDS-polyacrylamide gel electrophoresis (SDS-PAGE), and electrophoretically transferred onto nitrocellulose membranes. Immunoblotting of the transferred proteins was performed as described in Appendix II, using the primary antibodies 22C11 (anti-APP) or JL-8 (anti-GFP) in overnight blots incubations (antibody dilutions are specified in Table II.1). Detection was achieved using horseradish peroxidase-linked secondary antibodies and an enhanced chemiluminescence detection system (ECL kit; Amersham Pharmacia Biosciences). For analysis of the intracellular APP-GFP localization, another subset of cells was treated as above but grown in six-well plates containing 100 μg/ml poly-L-ornithine (Sigma-Aldrich) pre-coated glass coverslips and fixed using a 4% paraformaldehyde solution (see Appendix II).

Time course of Wt APP-GFP levels in the presence of cycloheximide. The methodology here used for combined trafficking/processing studies (da Cruz e Silva et al., 2004b) makes use of a known protein synthesis inhibitor, cycloheximide (CHX, Sigma-Aldrich). CHX is a well known drug that reversible inhibits protein synthesis by blocking the mRNA translation at the level of polypeptide translocation. It has been used to study protein post-translational modifications and the role of protein synthesis in apoptosis, gene expression and steroidogenesis (Parat and Fox, 2001). In our experimental model, CHX is used to inhibit cellular "de novo" protein synthesis, enabling the isolation of APP-GFP protein populations, thus reducing the background of continuous protein synthesis and resulting in a more efficient tracking. The dose used (50 μg/ml) in the following assays was experimentally optimized (da Cruz e Silva et al., 2004b). Of note is that cells exposure to 100 μg/ml CHX for 5:30 hours was observed to have no effect on protein glycosylation processes (Brion et al., 1992), and still allowed for constitutive protein secretion from the Golgi. Hence, this reversible protein synthesis inhibitor enables monitoring of an APP cellular pool and the study of potential differences in the cDNA mutants as they are processed intracellularly.

For a comparison of the time courses of cellular endogenous APP and transfected Wt APP-GFP, COS-7 cells were transfected with pEGFP vector or Wt APP-GFP (Table II.2) and plated on six-well plates. Cells were incubated with DMEM medium supplemented with

50 μg/ml CHX, for the following time periods: 0:00, 1:00, 2:00, 3:00 and 5:00 h. At each specific time point, cells were harvested in boiling 1% SDS solution, samples boiled and sonicated, and their total protein content determined using the BCA kit (Pierce), according to the supplier's instructions. Mass-normalized aliquots were resolved by 6.5% SDS-PAGE and subjected to Immunoblot detection as described. Detection was carried out using an IgG horseradish peroxidase-linked secondary antibody and the ECL detection kit.

II. 3. 4 – APP-GFP TRAFFICKING ASSAYS

II. 3. 4. 1 – Intracellular APP-GFP tracking

Transiently transfected cells were harvested and replated onto six-well plates containing pre-coated glass coverslips. After a recovery period of 4 hours, cells were incubated in 1 ml of DMEM medium supplemented with 50 μg/ml CHX. For a time-course analysis the six-well plates were incubated for different periods of time - 1:00, 1:30, 2:00, 2:30, 3:00, 3:30 and 5:00 h - after which cells were fixed by means of the 4% paraformaldehyde fixation method. Coverslips with fixed cells were mounted with antifading reagent (FluoroGuard, Bio Rad) on microscope slides and analysed by epifluorescence microscopy. For co-localization studies of APP-GFP with specific organelles, a subset of the cells fixed at 0 h CHX was subject to Immunocytochemistry procedures (described below in section II.3.4.6). The anti-Calnexin (an ER marker) and anti-Syntaxin 6 (a TGN/Golgi marker) antibodies were used.

II. 3. 4. 2 – AICD nuclear targeting

Cells previously transfected with the APP-GFP constructs (Table II.2) were divided into six-well plates containing pre-treated and pre-coated coverslips and subject to the same procedures as described above in section II.3.4.1. Two sets of cells were immediately fixed after the recovery period. (0:00 h of CHX exposure) and a third was fixed upon 5:00 h of CHX exposure. Coverslips containing fixed cells were mounted with antifading reagent on microscope slides and subjected to Immunocytochemistry analysis.

II. 3. 4. 3 – APP endocytosis assay – APP/Transferrin co-localization

Endocytosis of Texas Red-conjugated Transferrin (Molecular Probes) was monitored in APP-GFP transiently transfected cells grown on poly-L-ornithine-coated glass coverslips. Cells were first exposed for 2:15 h to 50 μg/ml CHX, upon what were washed with complete DMEM. In order to eliminate endogenous transferrin cells were further incubated for 30 min at 37 ºC with DMEM medium supplemented with 20 mM HEPES and 50 μg/ml CHX.

Medium was exchanged for 500 µl fresh medium of equal composition but containing 1 mg/ml BSA and 100 nM Texas Red-conjugated transferrin, and cells incubated for a further 15 min at 37 ºC. The plates were immediately cooled to 4 ºC, washed twice with ice-cold PBS, and cells fixed on coverslips were processed for Immunofluorescence as previously described.

II. 3. 4. 4 – Uptake assay using an anti-APP N-terminal antibody

Cells grown in 60 mm plates were transiently transfected with Wt or the S655 phosphomutant APP-GFP cDNAs (Table II.2). After 8 hours of transfection cells from each plate were divided into 4 wells of six-well plates containing polyornithine-coated glass coverslips. Following a recovery period, each well was incubated with 2 ml of DMEM medium supplemented with 50 µg/ml CHX, for 2:30 hours. Cells were washed twice with ice-cold PBS and incubated for 20 min on ice with 150 µl of DMEM medium containing the anti-APP ectodomain (22C11) antibody. Cells were washed three times with ice-cold PBS and subsequently incubated at 37 ºC in 5 ml of complete DMEM with 50 µg/ml CHX, for the following time periods: 0, 15, 30 and 150 min. After two washes with PBS, cells were fixed with a 4% paraformaldehyde solution and processed for Immunocytochemistry with the Texas Red-conjugated α-mouse antibody.

II. 3. 4. 5 – APP-GFP constructs lysosomal targeting

COS-7 cells transfected and treated as described in Table II.2 were plated into six-well plates containing pre-treated coverslips. Cells were incubated with 50 µg/ml CHX for 3:00 h, fixed with 4% paraformaldehyde solution and processed for Immunocytochemistry with the anti-Cathepsin D antibody as described below.

II. 3. 4. 6 – Immunocytochemistry procedures

For co-localization procedures (Intracellular tracking, Nuclear targeting, Antibody uptake assays and Lysosomal targeting) Immunostaining was performed after cells fixation with 4% paraformaldehyde. For these procedures, cells were first permeabilized with methanol to allow for further incubations with specific antibodies. Briefly, after permeabilization cells were washed with PBS and incubated at 37 ºC with the appropriate primary antibodies. Except when otherwise specified, primary antibodies were incubated for 2 hours. Following three washes with PBS, 300 µl of Texas Red-conjugated secondary antibody were added to cells (for antibody dilutions see Table II.1). A further incubation was carried out in the dark for 2 h at 37 ºC to allow for labelling of antigen-primary antibody complexes.

Coverslips were further washed three times with PBS and mounted with the antifading reagent on microscope glass slides.

For the Intracellular tracking time-course assay, APP-GFP co-localization with two subcellular compartment markers was performed. At 0:00 h of CHX exposure, APP-GFP transfected cells grown on glass coverslips were fixed, permeabilized, and subjected to Immunocytochemistry using anti-Calnexin (an ER marker) or anti-Syntaxin 6 (a TGN/Golgi marker) primary antibodies. For the nuclear co-localization studies, transfected cells were fixed, permeabilized, and incubated with the antibodies 22C11 (anti-APP N-terminus; 4 h of incubation), 369 (anti-APP C-terminus), or 6E10 (anti-APP Abeta region; 4 h of incubation). For the Antibody Uptake assay, the Immunocytochemistry procedure was the same but the primary antibody incubation step was omitted. In addition, in a control experiment for non-endocytosed membranar APP-GFP analysis, cells were not permeabilized. For the APP-GFP lysosomal targeting assay, coverslips with fixed cells were incubated with the anti-Cathepsin D antibody.

II. 3. 4. 7 – Data analysis

Cells percentages (section II.4.3.1) and vesicles scored for fluorescence (sections II.4.3.4 and II.4.4) are expressed as mean ± SEM (standard error of the mean). Statistical significance analysis was conducted by one way analysis of variance (ANOVA) followed by the Tukey-Kramer test. Statistical significance symbols used were (*) for comparison of S655 phosphomutant and Wt data, and ($^{+}$) for S655A versus S655E data. Statistical significance levels are presented as (*/$^{+}$), $p < 0.05$; (**/$^{++}$), $p < 0.01$; and (***/$^{+++}$), $p < 0.001$.

II. 3. 5 – MICROSCOPY TECHNICAL DATA

Image acquisition. Cells mounted on coverslips were analysed using an Olympus IX-81 Motorized Inverted Epifluorescence microscope equipped with Olympus LCPlanFl 20x/0.40 and 60x/0.70 objective lenses. Photographs were taken at 18 ºC with a Digital CCD monochrome camera F-View II (Soft Imaging System) and processed with the AnalySIS software (Soft Imaging System).

Fluorophores and Epifluorescence Microscope filters. EGFP (Chroma 41020) and Texas Red (Chroma 41004) filter cubes were used for fluorophores visualization. Fluorescence excitation and emission spectra of the used fluorophores (EGFP, Texas Red), as well as the epifluorescence microscope filter cubes definitions, are presented in Appendix III.

II. 4 – RESULTS AND DISCUSSION

II. 4. 1 – CONSTRUCTION OF WT AND S655A/E APP_{695}-GFP CDNAS

PCR amplification of Wt and S655 phosphomutants APP fragments. APP_{695} Wt and S655A/E mutated cDNAs were amplified by PCR using specifically designed primers to remove the APP stop codon. Analysis of 1/10 of the PCR products was performed by electrophoresis in a 1.2% agarose gel. A single band per reaction of 2.1 Kb was observed, the expected molecular weight for the APP inserts. Figure II.2 shows representative agarose gels with the cDNA products (arrow) of the amplifications.

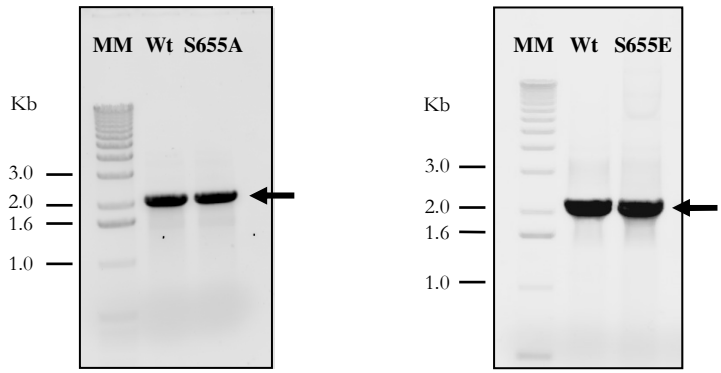

Figure II.2. APP products of PCR amplification. MM, molecular markers ("1Kb ladder", Invitrogen).

APP-GFP N-terminal fusion constructs. The remainder 9/10 of the PCR reaction products were subjected to sequential digestion with the endonucleases *Nru* I (that produces DNA blunt terminals) and *Age* I (cohesive DNA terminals). The vector pEGFP-N1 was also sequentially digested with the restriction enzymes *Sma* I (produces blunt terminals) and *Age* I. The pEGFP-N1 digestion product was resolved on a 0.8% agarose gel, extracted from the gel and purified by means of a Gel Extraction kit (QIAgen). The PCR APP resulting fragments, *Age* I/*Nru* I digested, were subcloned into the *Age* I/*Sma* I restriction sites of the pEGFP-N1 vector. Ligation products (2 and 5 μl) were used to transform *E. coli* competent cells. Transformation mixes were plated on LB agar plates with kanamycin, and randomly picked colonies were further grown overnight in LB/kanamycin liquid medium. Minipreps of these liquid cultures were performed to extract the plasmid DNAs for confirmation of the APP-GFP constructs. Extracted DNAs were digested with two endonucleases: *EcoR* I and *Pst* I. The strategy for a first confirmation of positive clones was based on the different number of

consensus sequences for *Eco*R I and *Pst* I enzymatic restriction of the pEGFP vector alone or the vector plus fusion construct. The restriction products were analysed by 1% agarose gel electrophoresis (Fig. II.3). The vector alone has only one site for *Eco*R I or *Pst* I restriction, and digestion yields one single band of 4.7 Kb (pEGFP expected size) corresponding to the linearized form of the vector. When APP is correctly inserted, the APP-GFP plasmid constructs have additional restriction sites for these two endonucleases: one for *Eco*R I and two for *Pst* I enzymatic cleavages. Hence, for these constructs, two *Eco*R I fragments of 5.1 Kb and 1.8 Kb, and three detectable *Pst* I fragments of 5.1 Kb, 0.9 Kb and 0.2 Kb were expected and obtained.

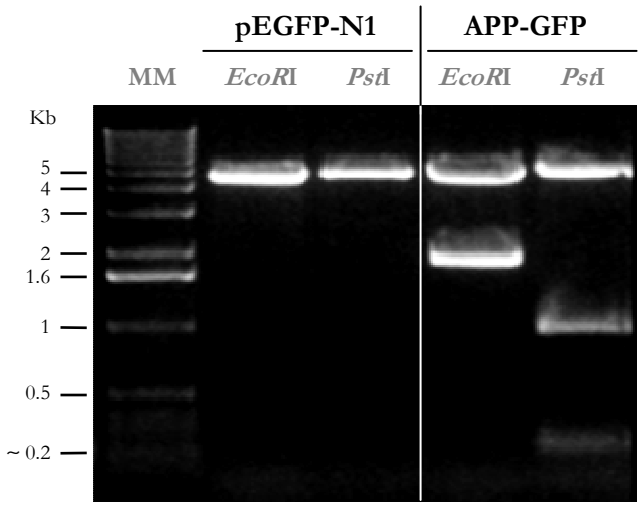

Figure II.3. Confirmation of APP_{695} -GFP fusions by endonuclease restriction. All APP-GFP constructs were confirmed by *Eco*RI and *Pst*I digestion. **MM,** molecular markers "1Kb ladder".

APP-GFP DNA fusions were confirmed by sequencing 0.1 ng of the plasmids. Sequencing was performed using six different primers and a personal Mastercycler Automated Sequencer (Eppendorf). The primers were designed to be complementary to different APP cDNA sequences spaced ~500 nucleotides apart: NAPN, APP500, APP1100, APP1500, APP1800 and APP2000 (sequences of primers in Appendix III). The resultant sequences confirmed not only the point mutations at the serine 655 residue but also the correct insertion of APP as an APP-GFP fusion, in frame with the GFP coding sequence. Part of the sequences obtained with the APP2000 primer, spanning the point mutations, are presented in Figure II.4.

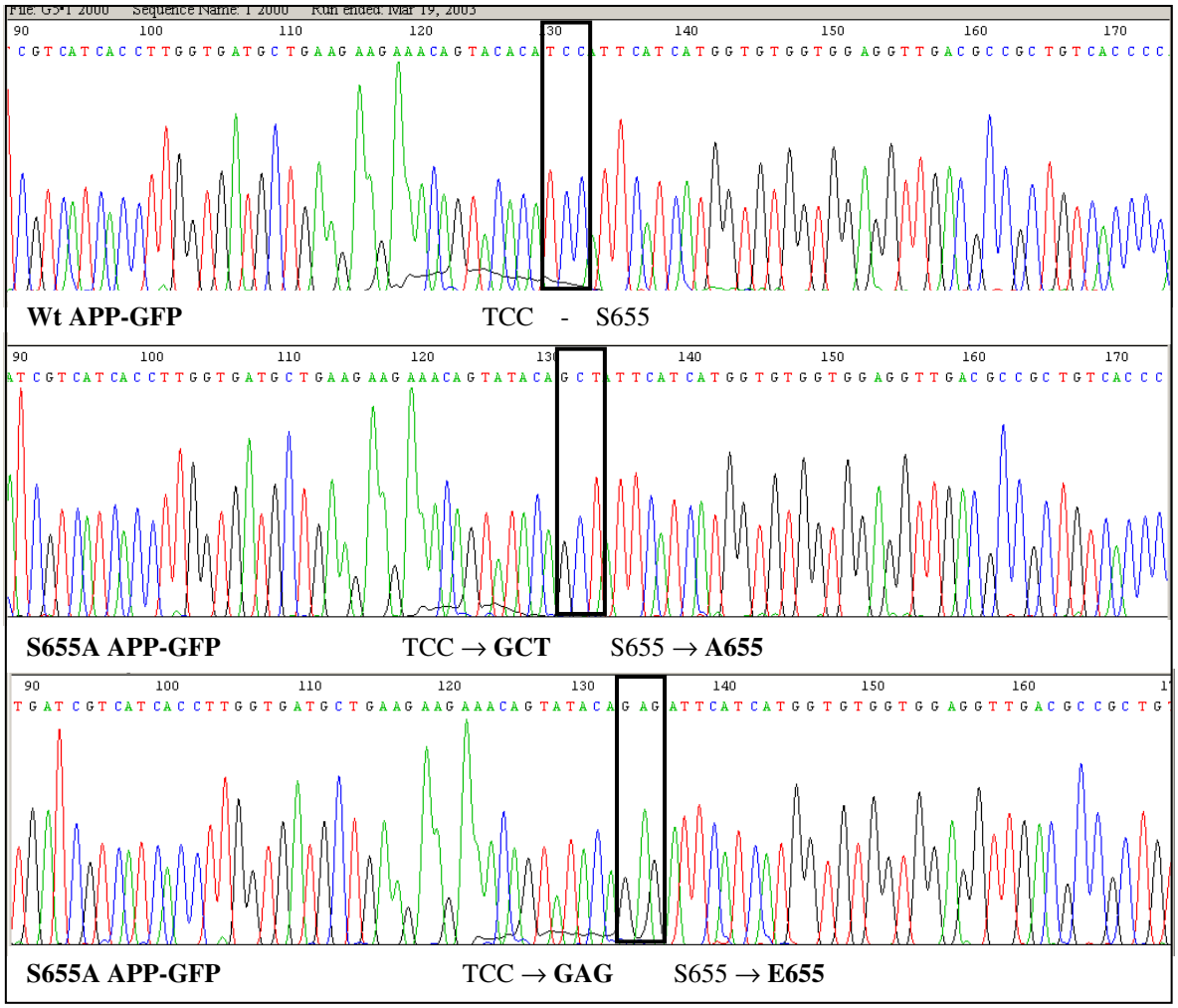

Figure II.4. Confirmation of APP_{695} -GFP mutations by DNA sequencing. APP-GFP constructs were sequenced using a series of appropriate primers. The sequences shown here were obtained using the "APP2000" primer, and display the specific point mutations at S655 (black rectangle). S655A and S655E have an additional but silent point mutation at Tyrosine 653 (TAC → TAT).

II. 4. 2 – APP-GFP EXPRESSION IN COS-7 CELLS

APP-GFP construct expression in COS-7 cells. The extracted and ethanol purified APP-GFP constructs were expressed in COS-7 cells using transient transfection methodology (described in section II.3.3). Cells lysates collected in 1% SDS were subject to SDS-PAGE, along with lysates of non-transfected, MOCK and pEGFP (vector only) transfected cells, used as controls. Gels were used to prepare Immunoblots and the latter were developed using the anti-APP 22C11 (Fig. II.5, A.I) and the anti-GFP JL-8 (Fig. II.5, A.II) antibodies. Another subset of pEGFP and APP-GFP transfected cells were fixed and analysed by epifluorescence microscopy (Fig. II.5, B).

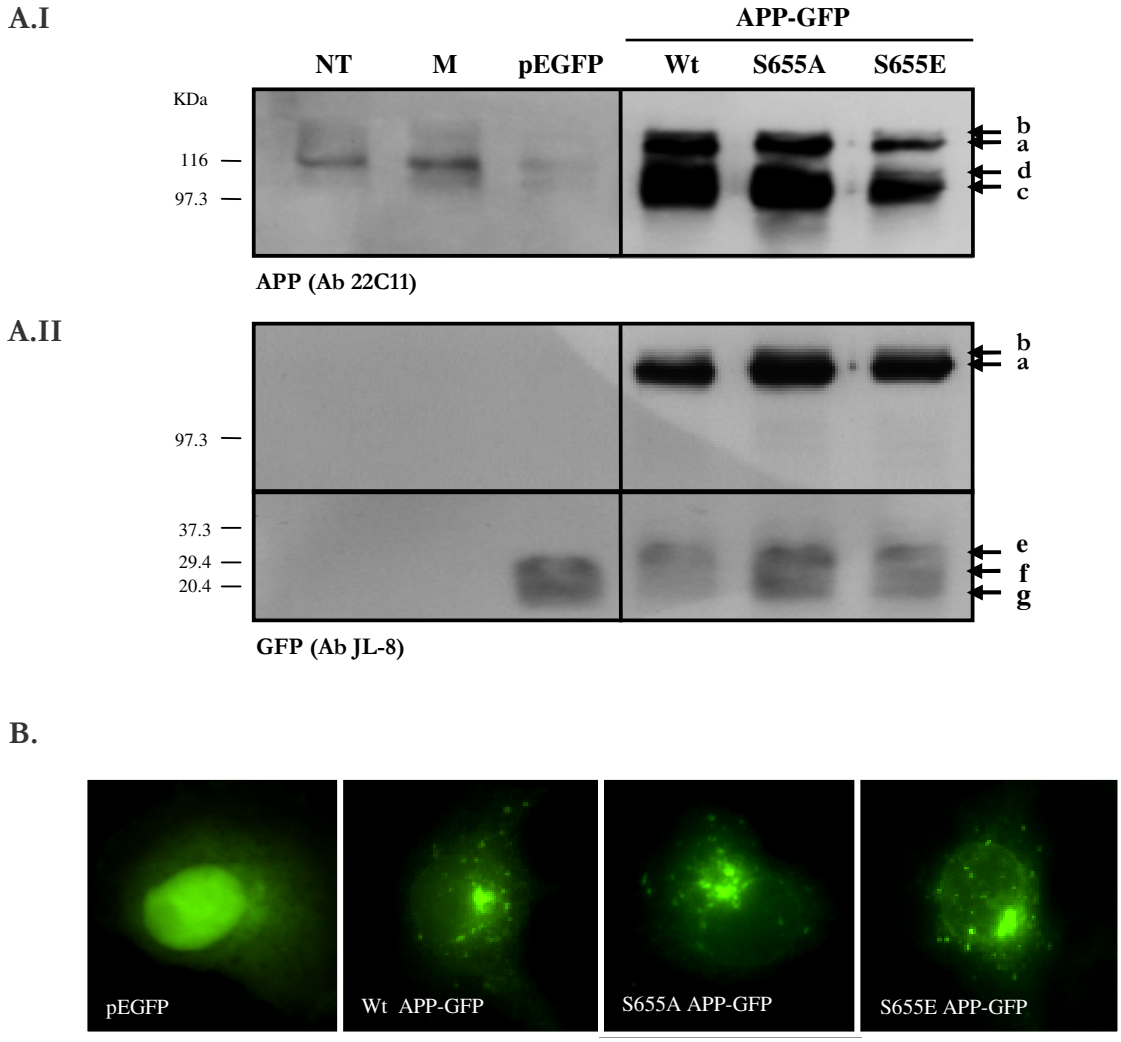

Figure II.5. APP-GFP expression in COS-7 cells. A: Immunoblot analysis of APP-GFP cell lysates. NT, non-transfected cells; **M**, mock transfected cells (no cDNA); Cells transfected with: **pEGFP**, EGFP-Vector; **Wt,** APP-GFP wild-type cDNA; **S655A**, APP-GFP S655A cDNA; **S655E**, APP-GFP S655E cDNA. **A.I** and **A.II:** Immunoblots of cellular lysates probed with the 22C11 (anti-APP N-terminus) and the JL-8 (anti-GFP) antibodies, respectively. **a** and **b** are the transfected APP-GFP forms, immature and mature, respectively. **c** and **d** are COS-7 endogenous APP forms; **e** corresponds to APP GFP-fused C-terminus fragments; **f** and **g** correspond to the GFP protein, with **g** appearing to derive from GFP cellular degradation. The relative position of protein molecular weight markers is indicated. **B: APP-GFP subcellular distribution** (epifluorescence microscopy analysis).

Detection with antibody 22C11 (Fig. II.5, A.I) revealed the COS-7 endogenous APP forms, immature APP_{695} (c, ~108 KDa) and immature $APP_{751/770}$ (d, ~115 KDa). These forms are not detected by the anti-GFP antibody (Fig. II.5, A.II) and their protein levels seem to suffer an up-regulation when cells are transfected with plasmids encoding exogenous APP ('APP-GFP' lanes, A.I blot). Two extra bands, migrating at ~136 (a) and ~145 (b) KDa,

appear only in the APP-GFP transfected cellular lysates and not in the controls. These correspond to the immature (a) and the mature (b) forms of the APP_{695}-GFP proteins, also positive with the anti-GFP antibody (A.II).

Additional bands of low molecular weight ("e", "f" and "g") appear when detection is performed with the anti-GFP antibody. The ~29 KDa band ("f") has the molecular weight expected for the GFP protein alone (27-30 KDa) and is stronger in the pEGFP lane (transfection with vector alone). The ~20 KDa band ("g") appears in all lanes corresponding to transfections of GFP alone or fusion constructs (pEGFP and APP-GFP lanes), and probably corresponds to a cellular degradation fragment(s). The "e" band migrating above at higher molecular weight (~34 KDa) appears only in APP-GFP transfected lysates. This band was further confirmed (data not shown) to contain APP-GFP derived C-terminal fragments (α- and βCTF-GFP).

Subcellular localization analysis of transiently expressed APP-GFP proteins (Fig. II., 5B) led to the observation that the three (Wt and S655 phosphomutant proteins) apparently had similar distribution patterns. Proteins were present mainly in the perinuclear region (ER and Golgi apparatus) and in cytoplasmic vesicles. Being that the ^{653}YTSI^{656} domain is thought to be involved in the regulation of APP trafficking, a time-dependent subcellular localization analysis was subsequently performed under mild conditions of inhibiting 'de novo' protein synthesis.

Time course of Wt APP-GFP levels in the presence of CHX. Preliminary studies with the wild-type APP-GFP and the pEGFP alone were carried out for comparative analysis of transfected and endogenously expressed APP turnover during CHX exposure. Procedures were as described in section II.3.3 and Table II.2, and the results obtained are shown in Figure II.6. The apparent molecular weights for the APP-GFP bands in these 6.5% gels were of 136.1 KDa (a) and 144.9 KDa (b), and are at the expected range since the GFP protein alone has a molecular weight between 27-30 KDa. The use of lower amounts of DNA for transfection resulted in more endogenous-like levels of expression of APP-GFP, with both - APP_{695}-GFP and endogenous APP - disappearing with time of CHX incubation. In fact, at 5 h of CHX incubation most of the transfected and endogenous APP species have disappeared (Fig. II.6, 5 h).

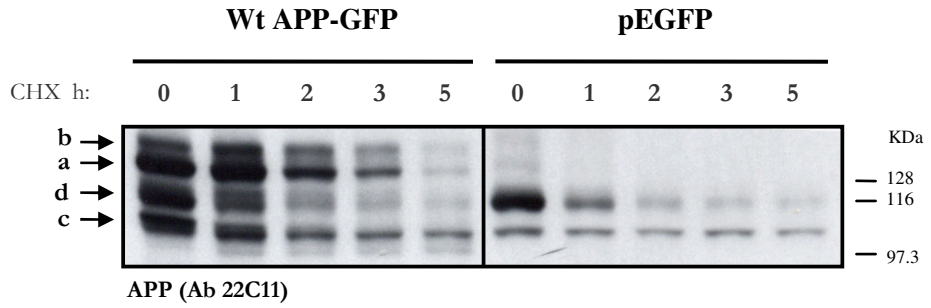

Figure II.6. Time-dependent effect of CHX exposure on intracellular APP levels (transfected and endogenous). APP expression levels were analysed by Immunoblotting with the 22C11 (anti-APP N-terminus) antibody. **CHX h**, period in hours of CHX exposure. **a** and **b** are the transfected APP_{695}-GFP immature and mature forms, respectively. **c** and **d** are endogenous immature APP forms, mainly 695 and 751/770, respectively. The relative position of protein molecular weight markers is indicated.

II. 4. 3 – INTRACELLULAR APP-GFP TRACKING

APP-GFP co-localization with ER and Trans-Golgi Network markers. Identification of the APP_{695}-GFP cellular distribution at ER and Golgi/TGN compartments was confirmed using specific organelle protein markers, visualized using Texas Red-linked secondary antibodies (Fig. II.7).

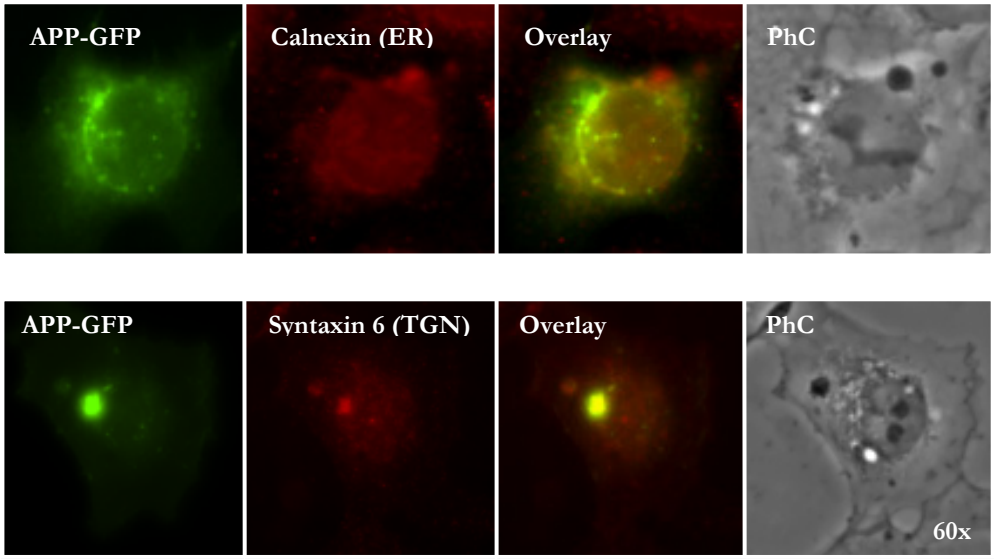

Figure II.7. Identification of APP-GFP localization in COS-7 cells by co-localization analysis of APP-GFP (green fluorescence) proteins with two subcellular compartment markers - Calnexin for the ER and Syntaxin 6 for the Trans-Golgi network (TGN). Detected by Immunocytochemistry with specific primary and Texas Red-linked secondary antibodies (red fluorescence). **PhC**, Phase Contrast.

The perinuclear distribution (ring-like) of green fluorescent APP-GFP protein was confirmed to co-localize extensively with the ER protein marker Calnexin (Fig. II.7, panel A, yellow/orange staining in the overlay image). The staining of the TGN/Golgi protein marker, Syntaxin 6 (Fig. II.7, panel B) was mainly visible in a nuclear juxtaposed structure, in accordance with the expected localization of Golgi complex. Subcellular APP-GFP co-localizes with, and is mainly concentrated at this Syntaxin 6-positive structure.

II. 4. 3. 1 – Subcellular localization of Wt and S655 phosphomutants in a time-dependent manner

The role of S655 APP phosphorylation in APP subcellular targeting and translocation was analysed. APP-GFP transiently transfected cells were exposed to CHX and fixed at different time points (see section II.3.4.1 and Table II.2). 60 cells per coverslip for each time point, in triplicate (three independent experiments), were scored by epifluorescence microscopy for the presence/absence of GFP fluorescence in specific subcellular compartments (ER, Golgi, cytoplasmic vesicles, nucleus and plasma membrane). This quantitative data (100% = 120 cells) is presented in Figure II.8. Further, the predominant pattern of APP_{695}-GFP subcellular distribution at each time point was also analysed. A representative cell for each time point is shown in Figure II.9.

From Figure II.8 it is evident that the trafficking of the Wt APP-GFP and S655 phosphomutants is somewhat different. For example, for the Wt APP-GFP (Fig. II.8, A) the percentages of cells with fluorescent ER decreased rapidly from 59.4 ± 13.7% (1:00 h) to 16.1 ± 3.9% at 2:00 h, and to < 10% by 2:30 h and only ~3% from 3:00 to 5:00 h. The ER fluorescence decrease for the S655A mutant was similar to the Wt (Fig. II.8, B). However, the S655E mutant had higher ER percentages at the early time points (1:00-2:30 h), although only significantly different from Wt at 2:30h (21.7 ± 1.7%, $p < 0.01$), pointing to a relatively delayed S655E ER exit (Fig. II.8, C).

Scoring Golgi fluorescence in a time-dependent manner revealed that for the Wt APP-GFP species, 97.2 ± 2.0% of the cells had fluorescent Golgi at 1:00 h, and this percentage decreased to 64.4 ± 2.8% by 2:00 h. At 2:30 h a small rise in the number of cells with Golgi fluorescence was observed (75.6 ± 5.2 %), and from that time point on it decreased to 58.3 ± 7.7% and 33.3 ± 5.3% (3:00 and 5:00 h, respectively) (Fig. II.8, A, "G").

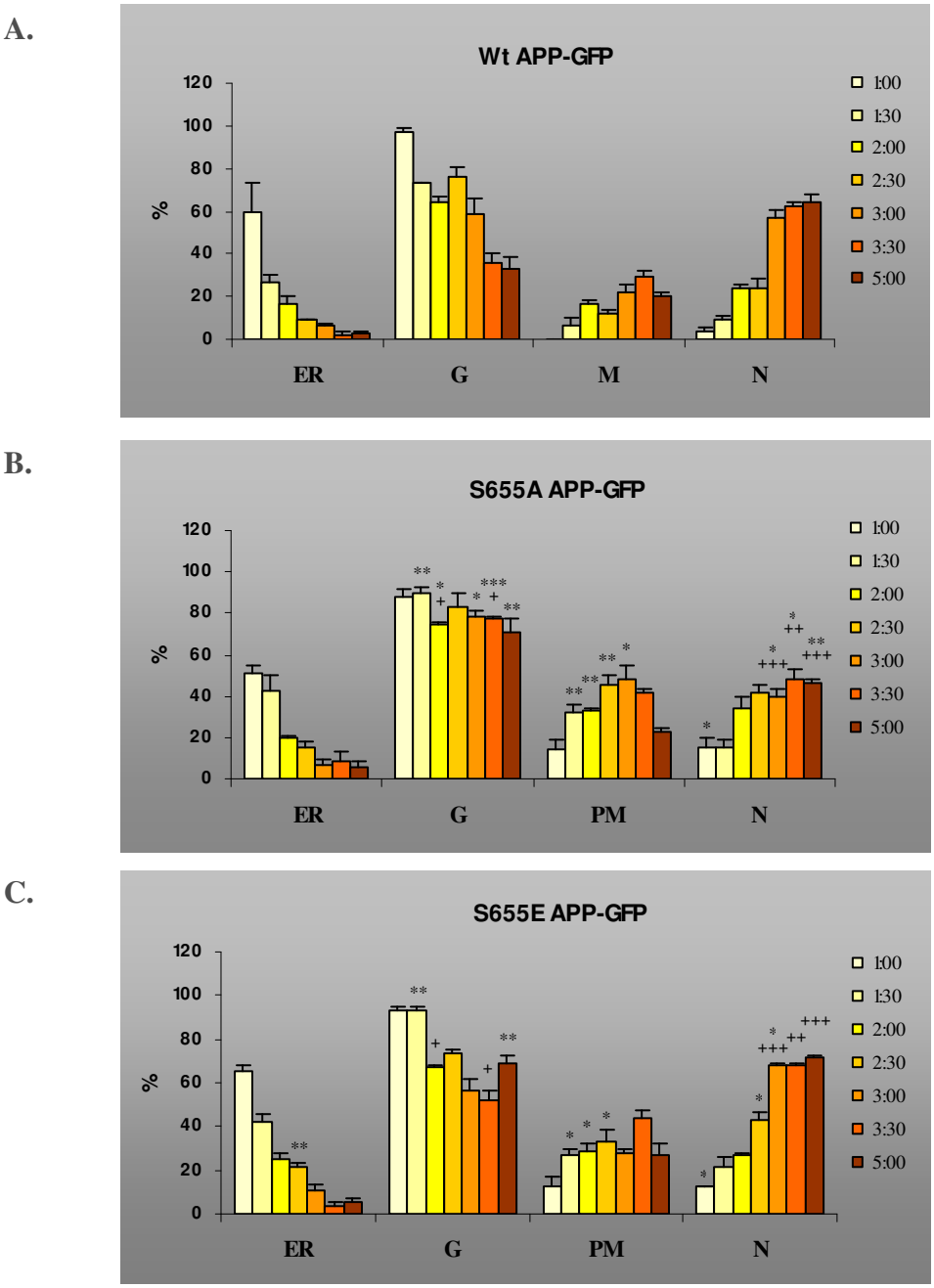

Figure II.8. Quantitative analysis of S655 phosphorylation state-dependent APP cellular trafficking. After fixing at the indicated time points of CHX exposure (1:00 - 5:00 h), COS-7 cells transfected with Wt **(A)** or S655 mutants **(B and C)** APP-GFP were analysed for the presence/absence of green fluorescence at different subcellular organelles. **ER**, endoplasmic reticulum; **G**, Golgi; **PM**, plasma membrane; **N**, nucleus. Tuckey test, and statistical significance levels are presented as (*/$^{+}$), $p < 0.05$; (**/$^{++}$), $p < 0.01$; and (***/$^{+++}$), $p < 0.001$; (*), S655 phosphomutants vs. Wt; ($^{+}$), S655A vs. S655E.

For the S655A mutant the percentage of Golgi-positive cells started at a slightly lower value (88.3 ± 3.5% at 1:00 h), but remained high and barely decreased in comparison to the Wt at subsequent time points (Fig. II.8, B, "G"). These values were 75.0 ± 1.0% at 2:00 h, 78.9 ± 2.4% (3:00 h), and 70.6 ± 6.5% at 5:00 h, all are significantly different from Wt. Hence, the

S655A mutant seemed to have impaired Golgi exit, which was pronouncedly delayed relative to Wt APP-GFP.

The percentages of S655E cells with APP-GFP fluorescent-positive Golgi were closer to the values obtained for the Wt (Fig. II.8, C, "G"). Values at 1:00 h and 2:00 h were almost equal to Wt (~93% and ~67%). Also, as for the Wt, from 2:00 to 2:30 h the "G" percentage increased to ~73%, and from 2:30 to 3:00 h decreased to ~56%. These results indicate a normal pattern of APP Golgi traffic at these time points. Nonetheless, from 3:30 to 5:00 h there was an increase in the number of Golgi fluorescing cells (52.2 ± 4.9% and 69.4 ± 3.1%, respectively, compared to 35.6 ± 4.8% and 33.3 ± 5.3% for the Wt). Additionally, at 1:30 h the percentage of "G" fluorescing cells was higher for S655E than for Wt (~93%, compared to 73%). This question will be further addressed in section II.4.3.4.

Plasma membrane (PM) fluorescence was also scored (Fig. II.8, "PM"), and both the S655A and S655E mutants exhibited significantly higher percentages of PM GFP-positive fluorescence than the Wt protein (e.g. ~32% and ~27% at 1:30 h, respectively, versus ~7% for the Wt). Furthermore, these percentages were overall higher for the S655A mutant when compared with the other two species (e.g. 45.6 ± 4.7% and 47.8 ± 7.1% at 2.30 and 3:00 h, compared to 33.3 ± 4.8% and 27.8 ± 1.5% for S655E, and 11.7 ± 1.9 and 21.7 ± 3.8% for Wt). In addition, the APP-GFP species nuclear time course distribution also presented differences, but this will be analysed in detail in section II.4.3.2.

Figure II.9 depicts a representative cell for each time point based on the quantitative data discussed above. For the Wt APP-GFP (panel A) we can observe that at 1:00 and 1:30 h the protein appears mainly in a typical ER "nuclear ring" distribution (arrow "ER"), with an intensely fluorescent Golgi complex, and in some cytoplasmic vesicles. The presence of green fluorescence at the plasma membrane only became significantly visible from 3:00 h on (arrow "PM"). The ER fluorescence almost completely disappeared for longer periods of CHX exposure, while Wt APP-GFP fluorescence was observed in cytoplasmic vesicles at all CHX incubation periods. Golgi fluorescence intensity, visibly decreased at 3:30 and 5:00 h (arrows "G"). In fact, upon 5:00 h of CHX exposure, fluorescence intensity was found to be drastically decreased overall. This faded fluorescence was distributed through the Golgi, cytoplasmic vesicles and PM, with the Golgi being the most intense. Of note is that due to the low fluorescence intensities, the CCD microphotograph camera exposure times had to be increased at 5.00 h.

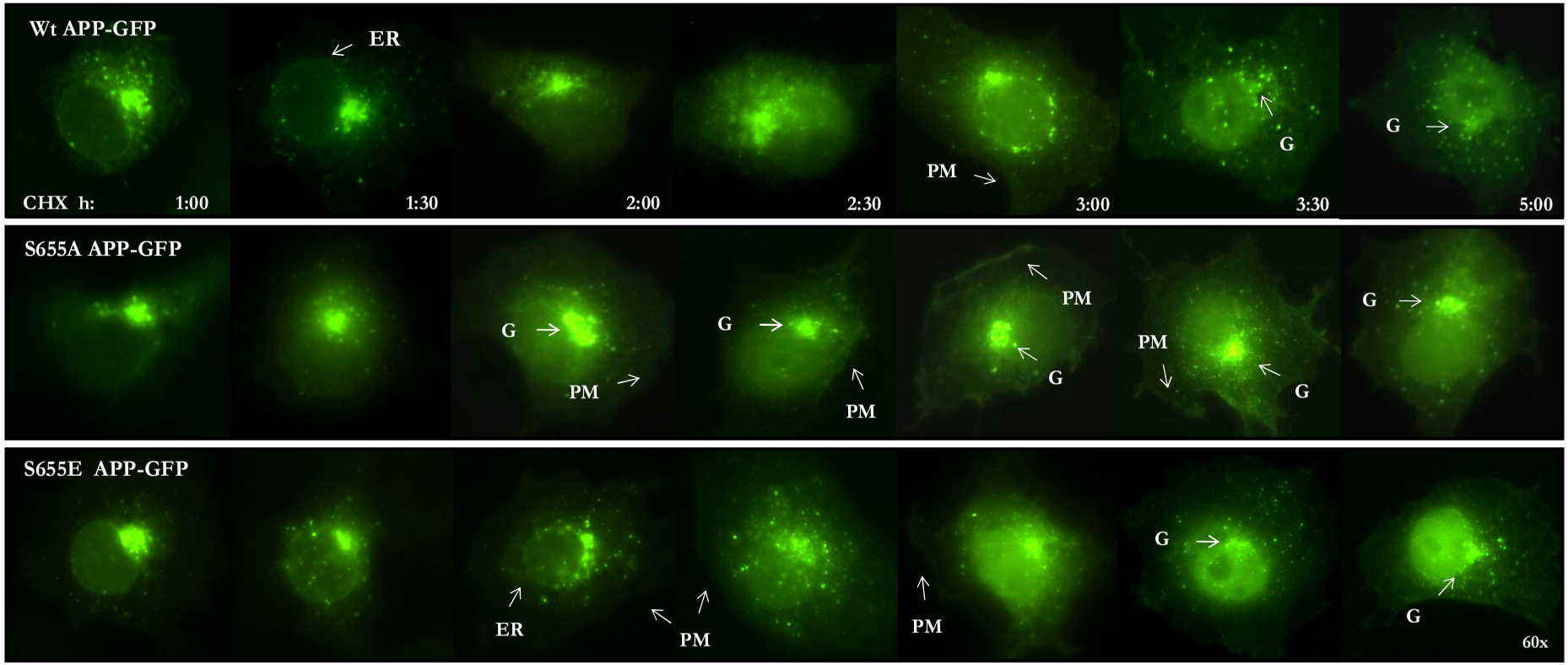

Figure II.9. Fluorescence microscopy monitoring (Qualitative analysis) of wild type (A), S655A (B) and S655E (C) APP-GFP fusion proteins. Microphotographs showing representative (from a score of 120 cells) APP-GFP subcellular fluorescence patterns, detected after the indicated hours of CHX exposure. Arrows indicate several subcellular structures that present relevant differences and are described in the text. **ER**, endoplasmic reticulum; **G**, Golgi; **PM**, plasma membrane.

Relatively to the Wt, and consistent with the quantitative data, the S655A mutant (Fig. II.9, B) presented a similar pattern of ER fluorescence staining, which decreased and almost disappeared by 1:00 to 2:00 h. More significantly for this mutant, and in agreement with the above mentioned findings (Fig. II.8, B), S655A has an almost non-decreasing Golgi fluorescence intensity. Additionally, for the first hours (1:00 to 3:00 h) this mutant was less visible in GFP-positive cytoplasmic vesicles, again suggesting an impairment in its Golgi exit. Also in agreement with the quantitative analysis, S655A-transfected cells showed plasma membrane fluorescence earlier than the Wt (2:30 versus 3:00 h for Wt). In fact, of the three APP-GFP species, S655A was the one presenting more intense fluorescence at the plasma membrane (arrows PM) at all time points.

The S655E APP mutant (Fig. II.9, C) had a slight delay in its ER exit, observed as ER fluorescence for up to 2:00 h, contrasting with 1:30 h for Wt (arrows ER). Consistent with the quantitative data (Fig. II.8), the time course and intensity of S655E Golgi fluorescence was very similar to the Wt, with the exception of the two last time points, where S655E was more intense (arrows G at 3:30 and 5:00 h). In addition, this mutant appeared to result in a similar or even higher number of fluorescent cytoplasmic vesicles when compared to the Wt species (2:00 and 2:30 h). The S655E phosphomutant also resulted in slightly increased PM fluorescence, but this was much weaker than for S655A (arrows PM from 2:00 to 3:30 h).

II. 4. 3. 2 – S655 APP_{695} phosphorylation alters AICD nuclear targeting

Of particular interest was the comparative fluorescence monitored in the nuclei for each of the species. The percentages of cells with GFP-positive nuclei and the overall nuclei fluorescence intensity increased with time of CHX exposure, although differences were observed. Two phases could be distinguished, in particular for the Wt and S655E species, a first accumulation ranging from 1:00 to 2:30 h and a second from 2:30 to 5:00 h (Fig. II.8, "N"). During the first phase both S655A and S655E transfected cells presented higher percentages of GFP-positive nuclei staining in comparison to the Wt. Percentages at 1:30 and 2:30 h were ~10 and ~24% for the Wt, ~16 and ~41% for the S655A, and ~22 and ~43% for the S655E mutant. For the second phase, where more cells in general had nuclear fluorescence, the percentages of S655E and Wt transfected cells with nuclear fluorescence increased at a similar rate, while an increase was not observed for the S655A mutant. For the last three time points, these percentages were of ~57/67/64% for the Wt, ~40/48/47% for the S655A mutant, and ~68/68/72% for the S655E mutant. Hence, the latter exhibited nuclear targeting kinetics similar to the Wt, but at all time points with slightly higher

population percentages. In addition, the intensity of nuclei staining was overall higher for the S655E protein and lower for the S655A (Fig. II.9 and Fig. II.10).

Given that nuclear fluorescence increased with time of CHX exposure, nuclear targeting of GFP-linked APP fragments seemed to be occurring. In order to determine whether nuclear GFP fluorescence was derived from the APP-GFP full-length species or from its proteolytic fragments, Immunocytochemistry studies were carried out with the 22C11 anti-APP N-terminus antibody (Fig. II.10) at 5:00 h of CHX exposure. As expected from the literature, no APP N-terminus nuclear presence (22C11 red fluorescence) was observed for any of the three species (arrows N), despite the presence of nuclear green-fluorescence.

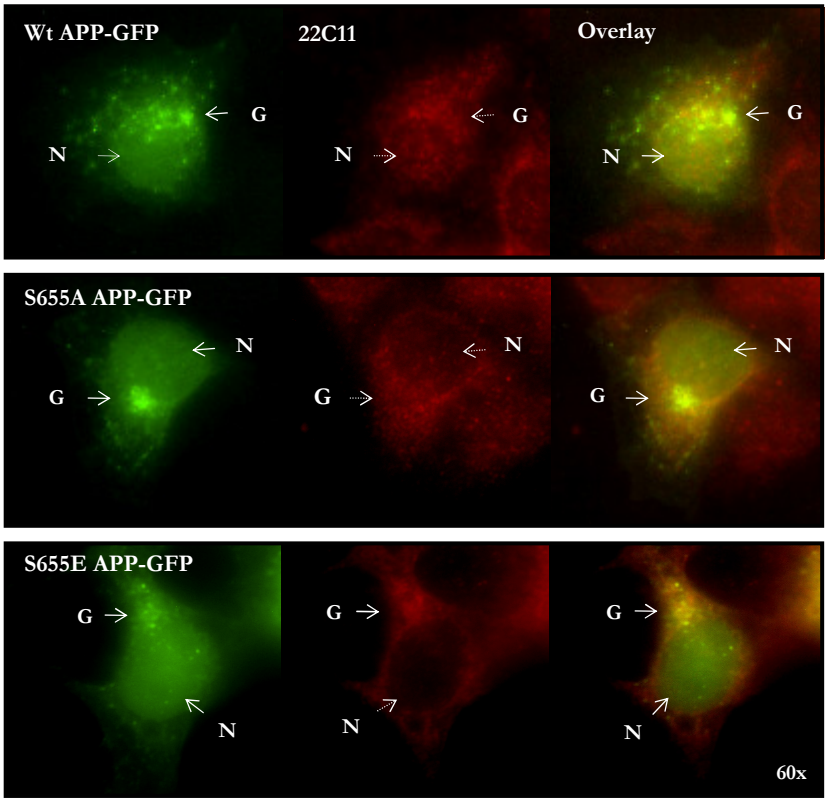

Figure II.10. Co-localization of APP-GFP and the anti-APP N-terminus 22C11 antibody (labelled with Texas Red-linked secondary antibody) at 5:00 h CHX. Arrows indicate: **G**, the Golgi region; **N,** the nucleus.

Golgi were also analysed for immunoreactivity with 22C11 (arrows G). For all the constructs tested the yellow/orange co-localization staining of GFP and 22C11 could always be observed, although to different degrees (Wt ~ S655A < S655E) and with the highest co-localization being observed for the S655E mutant. In fact, this construct could be singled out as the one with marked 22C11 Golgi staining. These results thus suggest that for the S655E mutant at 5:00 h there is a significant full-length APP-GFP population in the Golgi.

In order to determine whether nuclear GFP fluorescence was mainly due to AICD fragments proteolytically derived from each of the APP-GFP constructs (and not from CTFs or from GFP alone) further co-localization studies were carried out (Fig. II.11). Immunocytochemistry of APP-GFP transiently transfected COS-7 cells was performed with two antibodies, the 369 antibody (anti-APP C-terminus; panel A) and the 6E10 antibody (anti-Abeta 1-17; panel B), labelled with Texas Red-linked secondary antibodies. The 369 antibody recognizes full-length APP, both CTFs (α and β cleaved) and the AICD fragment; the 6E10 antibody recognizes full-length APP, the βCTF and Abeta fragments but not the αCTFs and AICDs. Wt and S655 phosphomutant APP-GFP fluorescence co-localized with the 369 and the 6E10 antibodies red fluorescence at the perinuclear region (ER, Golgi), cytoplasmic vesicles, and plasma membrane (Fig. II.11). Significantly, however, only the 369 antibody (panel A) but not the 6E10 (panel B) co-localized with APP-GFP at the nucleus (full arrows). Cells with less or non-visible nuclear green fluorescence (panel A, dashed arrows) had a concordant lower level of 369 staining. Hence, the nuclear green fluorescence scored in section II.4.3.1 is confirmed to be due to the presence of AICDs or αCTFs APP-GFP-derived fragments, and not βCTFs fragments or full-length APP-GFP. Furthermore a good correlation was observed between GFP nuclear fluorescence and APP C-terminus (369 antibody) red fluorescence (Fig. II.12, full arrows). Untransfected cells in the vicinity are indicated by dashed arrows, and these did not stain as intensely with the antibody 369. Consistantly all transfected cells had higher red nuclear fluorescence than non-transfected ones, confirming that APP-GFP-derived AICDs was being targeted to the nucleus.

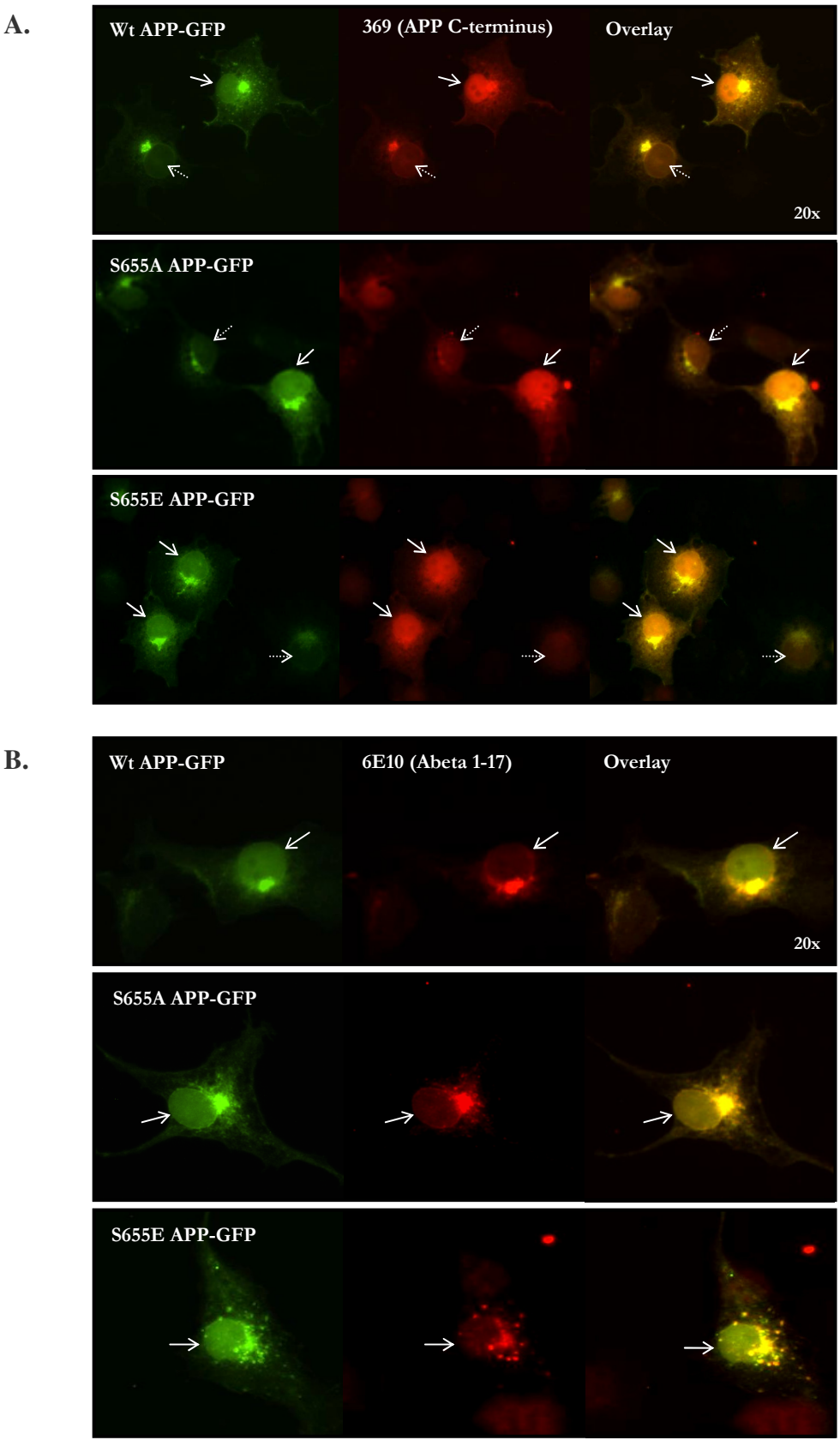

Figure II.11. Co-localization of APP-GFP with APP C-terminal fragments. APP C-terminal fragments were detected with the 369 (anti APP C-terminus) (**Panel A**) and the 6E10 (anti APP Abeta region) (**Panel B**) antibodies, labelled with Texas Red. Full arrows indicate cells with high nuclear green fluorescence; dashed arrows indicate cells with very faint nuclear green fluorescence.

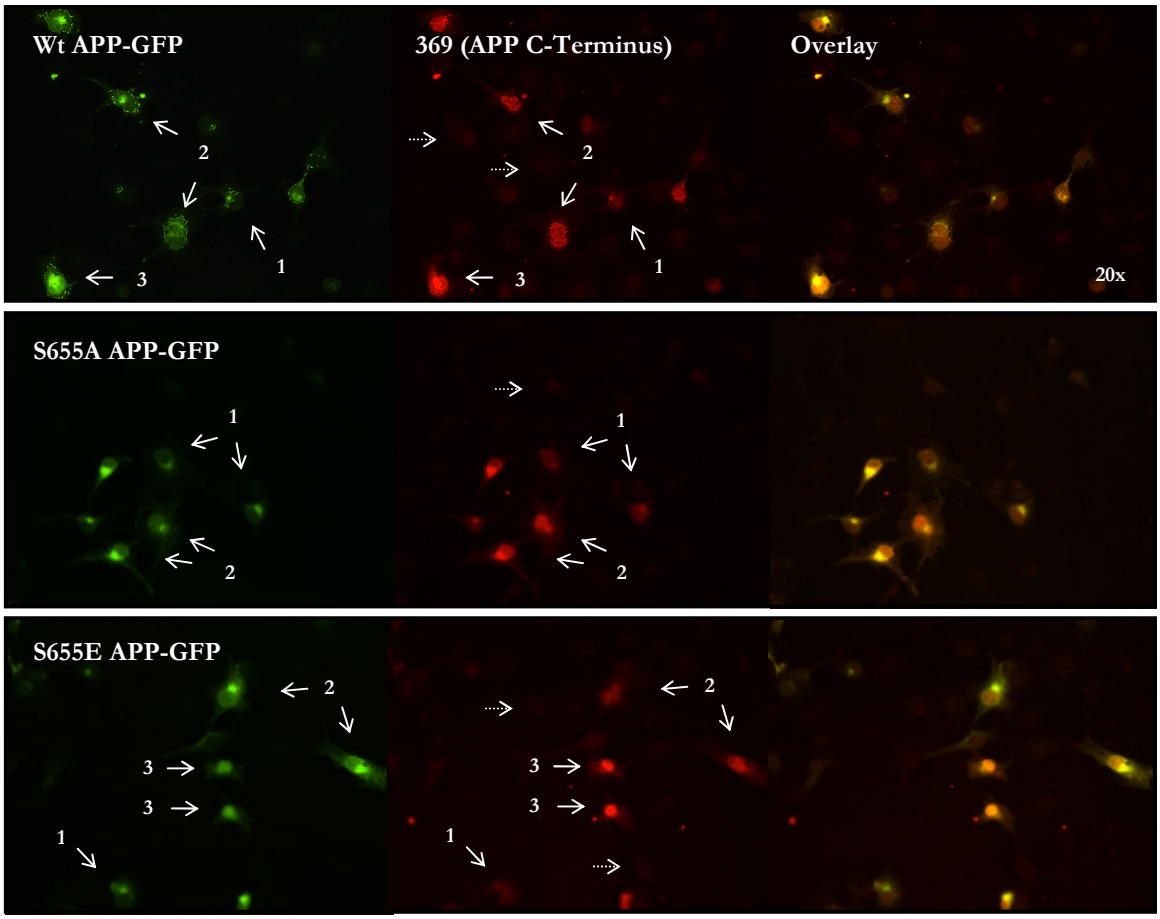

Figure II.12. Nuclear co-localization and correlation of APP-GFP and the 369 (anti-APP C-terminus) antibody. Dashed arrows indicate non-transfected cells. Full arrows indicate cells with green nuclear fluorescence; to increasing numbers correspond increasing intensities of green fluorescence at the nucleus.

In conclusion, increasing nuclear green fluorescence intensity always correlated with increasing 369 nuclear red fluorescence intensity. In addition, APP-GFP transfected cells with green fluorescence at their nuclei always presented increased red nuclear intensity when compared with the red nuclear staining of non-transfected cells. This supports the notion that the nuclear green fluorescence was not due to a nuclear targeting of GFP alone upon APP-GFP degradation. Furthermore, these results confirm that nuclear green fluorescence presence and intensity correlate well with the presence of AICD-GFP (or αCTF) at this compartment.

II. 4. 3. 3 – APP endocytosis assay

The higher S655A APP-GFP membranar levels observed in the trafficking studies could indicate some impairment in APP internalization by endocytosis. This, in turn, could indirectly influence α- and β-secretase APP substrate availability at the membrane and in the endosomes, as well as subsequent targeting of APP and specific APP fragments. To clarify this question a standard assay was used to monitor APP-GFP co-endocytosis with Texas Red-labelled transferrin molecules (Benmerah at al., 1998). The experimental procedure is described in section II.3.4.2 and in Table II. The CHX 2:45 - 3:00 h time period was chosen due to the high levels of Wt and phosphomutants APP-GFP present at the cellular membrane, and theoretically available for endocytosis. Results are presented in the panel below (Fig. II.13).

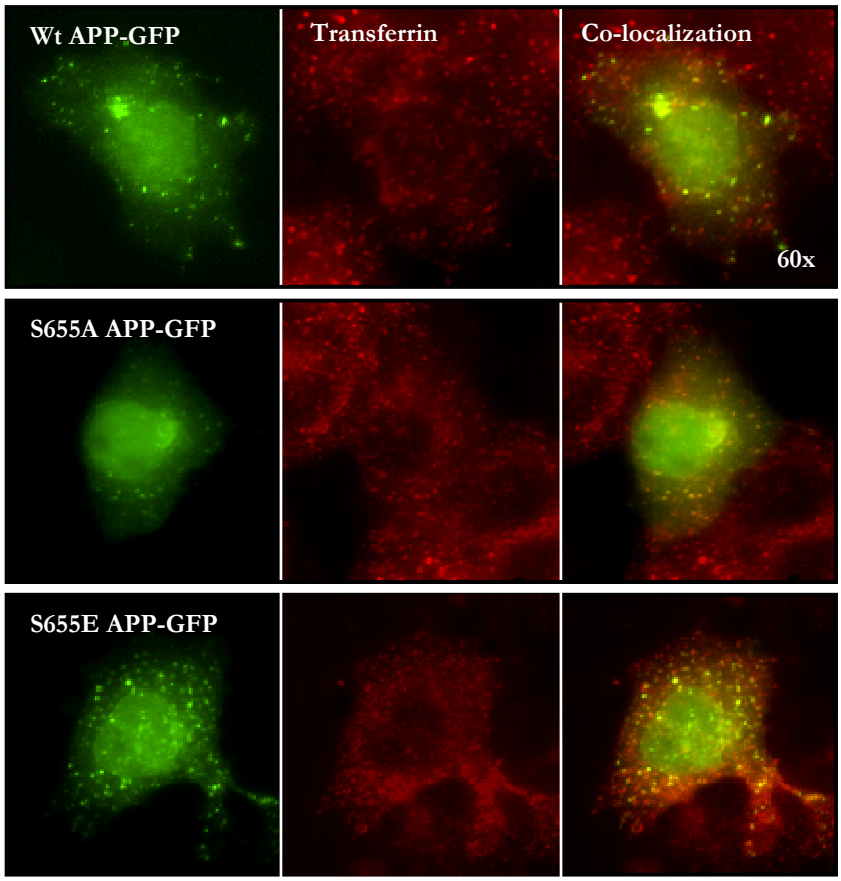

Figure II.13. Endocytosis studies of the APP-GFP constructs. Analysis of the co-localization of Texas Red-conjugated Transferrin (red endocytic vesicles), with the Wt or S655 phosphomutants-containing (green) cytoplasmic vesicles. Co-localizing vesicles in the "Overlay" panel have yellow/orange fluorescence.

All cells transfected with the different APP-GFP constructs exhibited a high number of APP-GFP/transferrin co-localizing endocytic vesicles per cell. As the transferrin staining appeared in a large number of vesicles, it was not possible to do a count of the co-localizing vesicles in order to identify possible differences in the ratio of co-localizing to transferrin-positive vesicles. Nonetheless, it appears that the S655E mutant has more APP-GFP incorporated into endocytic vesicles. In fact, the relative rate of intensity indicating GFP incorporation into vesicles appeared to be: S655E > Wt > S655A. Total membrane substrate availability could not account for these differences since, and as previously shown, S655A has the highest percentage of plasma membrane fluorescence and was at its highest value at this time point (Fig.s II.8 and II.9, "PM").

II. 4. 3. 4 – APP-GFP endocytosis and Golgi retrieval – Antibody uptake assay

As observed in the trafficking studies, there was an unexplained rise in the number of S655E APP-GFP transfected cells with Golgi fluorescence in the last CHX exposure periods. Additionally, from the transferrin assays it seemed that higher amounts of this mutant were undergoing endocytosis. Surface APP protein can undergo endocytosis and then be recycled back to the membrane, be delivered into lysosomes or retrieved to the TGN/Golgi apparatus (Yamazaki et al., 1996). The mechanisms regulating this sorting are not yet clear for APP, but the signal targeting endocytosed BACE to Golgi retrieval was found to be BACE phosphorylation at its cytoplasmic residue serine 498 (Walter et al., 2001). In order to investigate if serine 655 APP_{695} phosphorylation possesses a similar targeting role, COS-7 cells transiently expressing Wt, S655A or S655E APP-GFP proteins were subjected to antibody uptake assays. The experimental procedure is described in detail in section II.3.4.4 and in Table II. Briefly, after a 2:30 h CHX block, cells were incubated on ice with the anti-APP ectodomain 22C11antibody and further incubated at 37 ºC for 0, 15, and 30 minutes. Cells were monitored for the kinetics of APP-GFP endocytosis and retrieval to the Golgi, by time course analysis of co-localization between Texas Red fluorescence (22C11 labelling) and the transfected APP-GFP proteins (Fig. II.14). Control cells (non-transfected, NT) were also treated as APP-GFP transfected cells, and were observed to have almost undetectable 22C11 cell surface staining.

A.

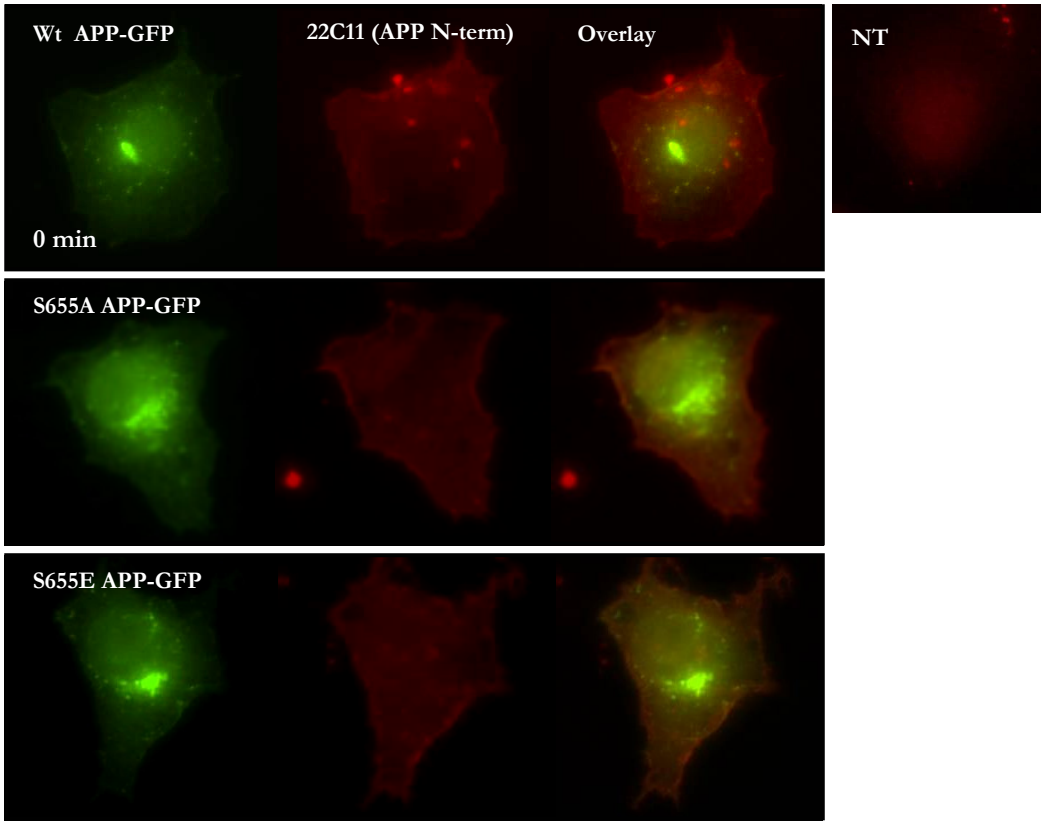
Wt APP-GFP
22C11 (APP N-term)
Overlay
NT
0 min
S655A APP-GFP
S655E APP-GFP

B.

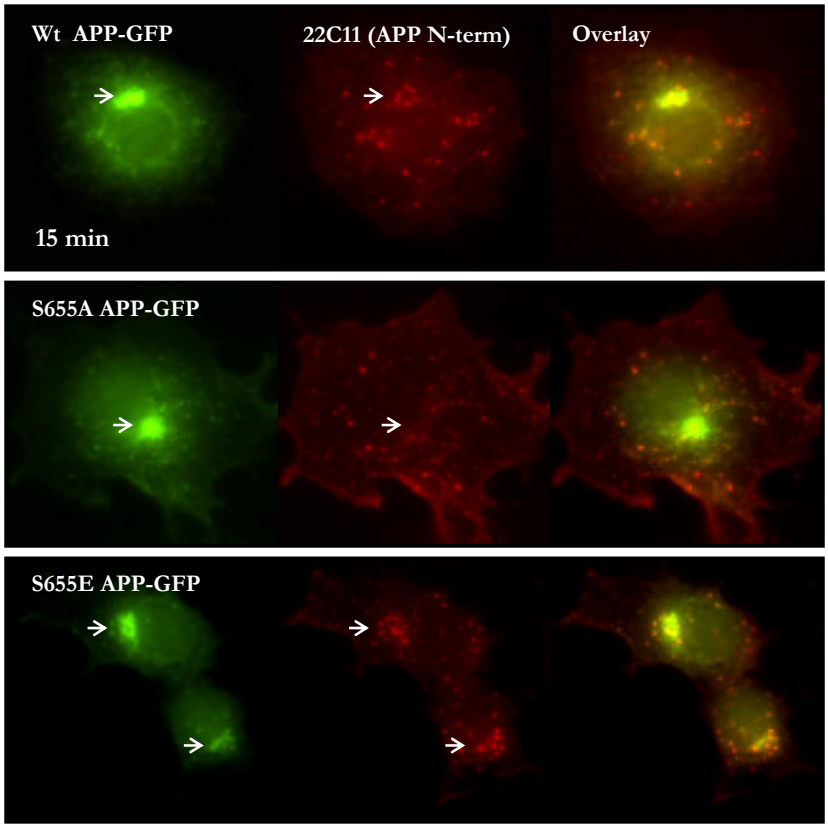
Wt APP-GFP
22C11 (APP N-term)
Overlay
15 min
S655A APP-GFP
S655E APP-GFP

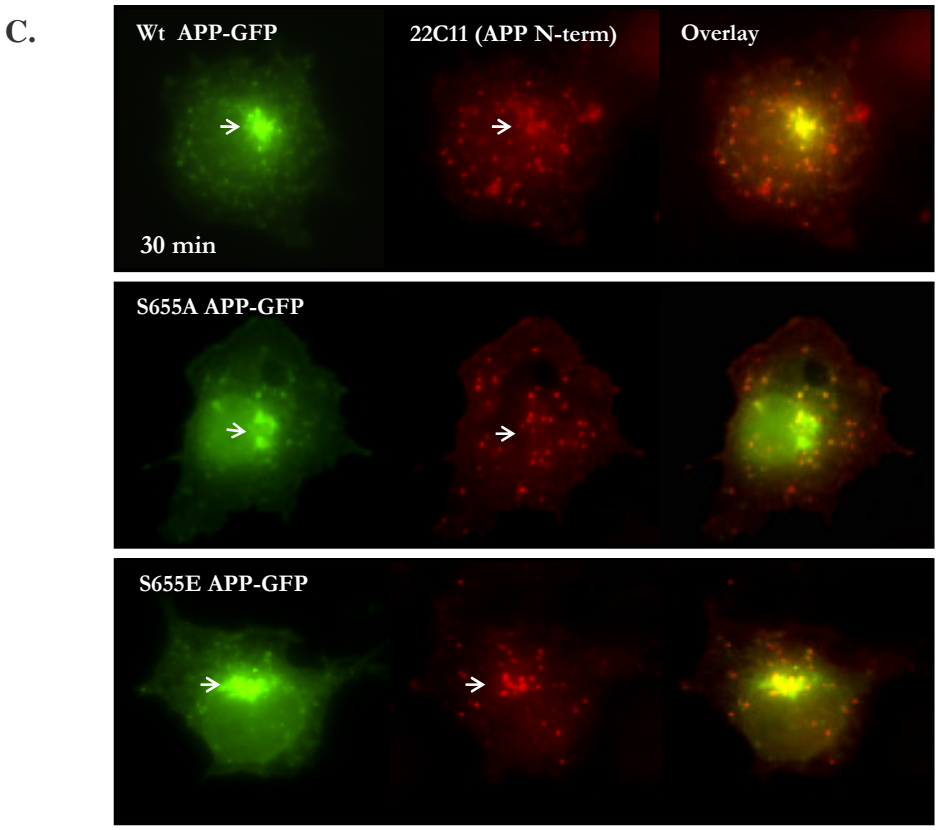

Figure II.14. Endocytosis and retrieval to Golgi of wild-type and S655 phosphomutant APP-GFP. Kinetic analysis of APP-GFP endocytic vesicles (red labelled with the N-terminal antibody 22C11) with time of endocytosis: 0 min (**panel A**), 15 min (**panel B**) and 30 min (**panel C**). Arrows indicate co-localizing vesicles near or at the TGN/Golgi area (yellow/orange in "Overlay"). **NT,** non-transfected cells.

APP-GFP endocytosis and Golgi retrieval. At 0 min (Fig. II.14, panel A) Wt, S655A or S655E transfected cells all have strong antibody red staining that co-localized with APP-GFP fluorescence at the cell surface. Upon incubating for 15 min at 37 ºC (Fig. II.14, panel B), a great number of vesicles where APP-GFP and 22C11 co-localized was observed for the three species. Part of these vesicles was found near or at the TGN/Golgi for the Wt and S655E proteins. However, this was much more marked for the S655E protein, as it could be detected in 50% of the population, compared to only 30% of the Wt APP-GFP cells. Contrarily, S655A showed very poor or none co-localization at TGN/Golgi at this time point. In fact, in 71% of the population expressing S655A, vesicles were randomly distributed throughout the cytoplasm and did not appear to be targeted to the Golgi.

At the 30 min time point, ~70% of S655E expressing cells had co-localizing APP-GFP endocytotic vesicles already fused to TGN/Golgi structures, compared with 50% for Wt and only 40% for S655A (Fig. II.14, panel C). Furthermore, the number of co-localizing vesicles

per cell also appears to be higher for S655E and lower for the S655A mutant. The increased number of Golgi co-localizing vesicles for the S655E mutant clearly supports that S655 phosphorylation can function as a targeting signal for APP PM-to-Golgi retrograde transport.

APP-GFP plasma membrane dynamics. To confirm that the vesicles monitored above resulted from endocytosis at the plasma membrane, cell surface APP was labelled for comparison, by omiting the cellular permeabilization step (Fig. II.15). Thus Texas Red-conjugated secondary antibody only labels the APP population at the plasma membrane, enabling us to monitor the APP surface population at the same time points.

The distribution patterns of the 22C11 red staining at 0 min of 37 ºC incubation (Fig. II.15, panel A) are identical to those previously observed in Figure II.14, panel A.. Upon 15 min of incubation, the intensity of 22C11 plasma membrane staining decreased for the three APP-GFP species (Fig. II.15, panel B), but particularly so for the Wt and the S655E mutant. Similarly, further decreases were observed after 30 min of 37 ºC incubation (Fig. II.15, panel C). These decreases in PM 22C11 staining did not result in increased co-localization of APP-GFP green/22C11 red fluorescence, confirming that the previously observed co-localizing vesicles (Fig. II.14) were indeed deriving from intracellular endocytosed APP-GFP molecules.

In addition, although APP-GFP PM populations decreased with time of incubation, this decrease was much less pronounced for the S655A mutant. These results strongly indicate a diminished rate of APP membranar internalization for this mutant, as already suggested in Figures II.8 and II.9.

A.

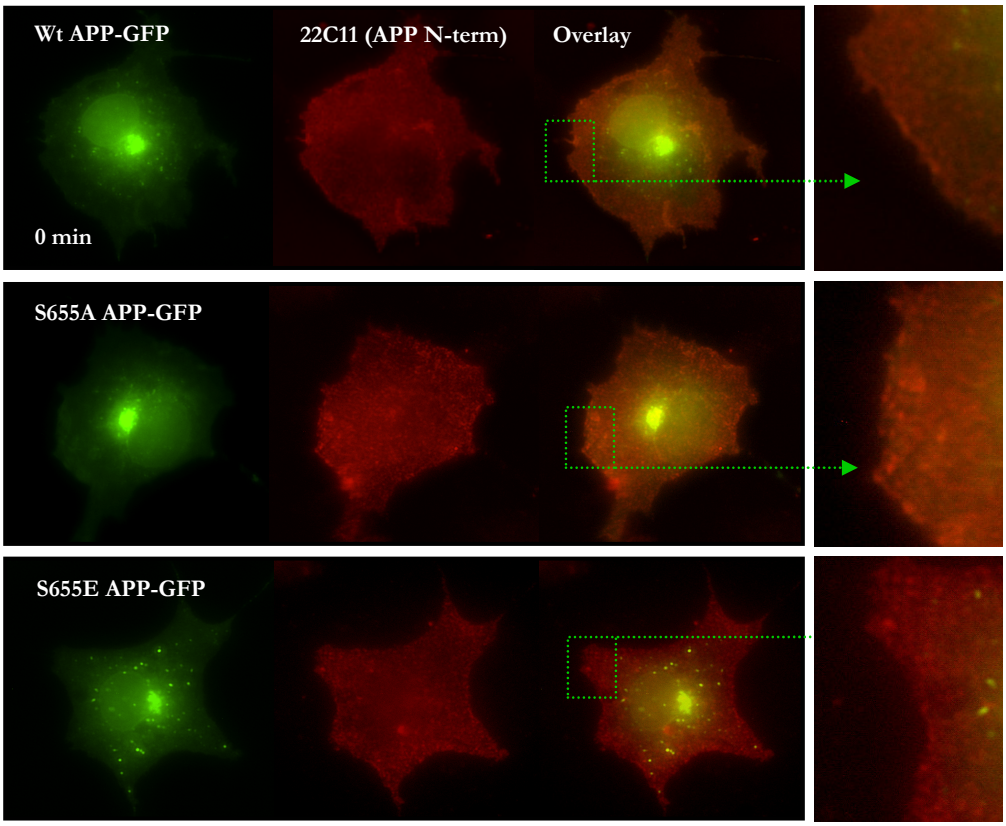
Wt APP-GFP
22C11 (APP N-term)
Overlay
0 min
S655A APP-GFP
S655E APP-GFP

B.

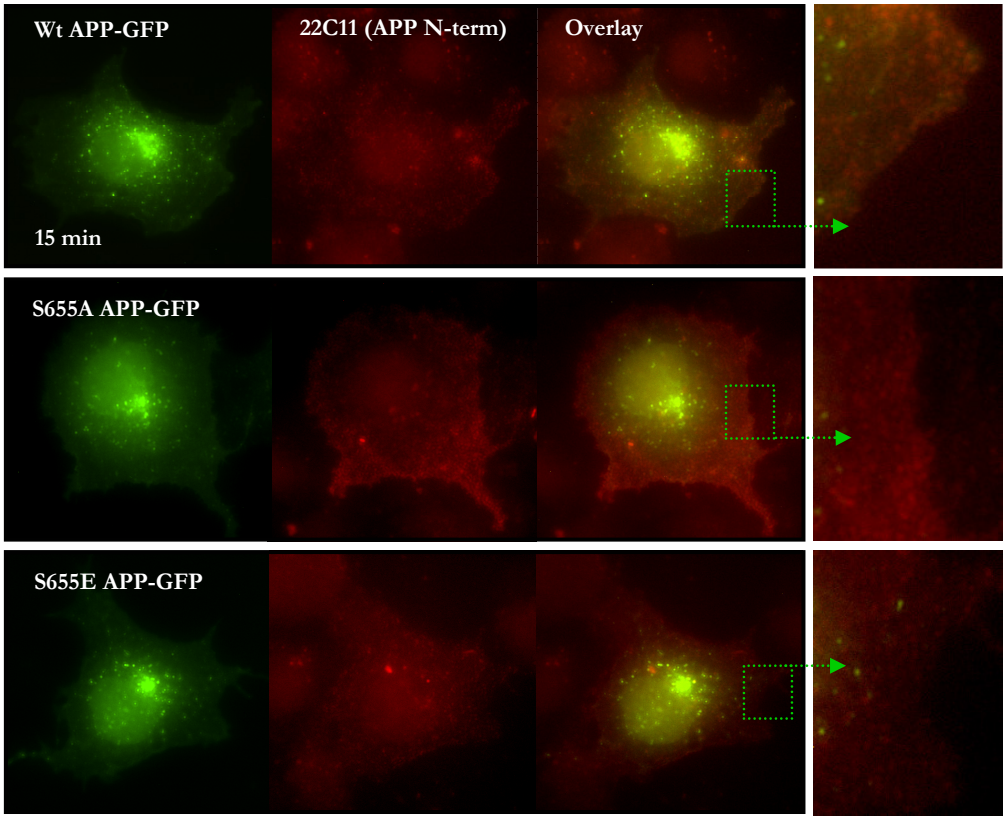
Wt APP-GFP
22C11 (APP N-term)
Overlay
15 min
S655A APP-GFP
S655E APP-GFP

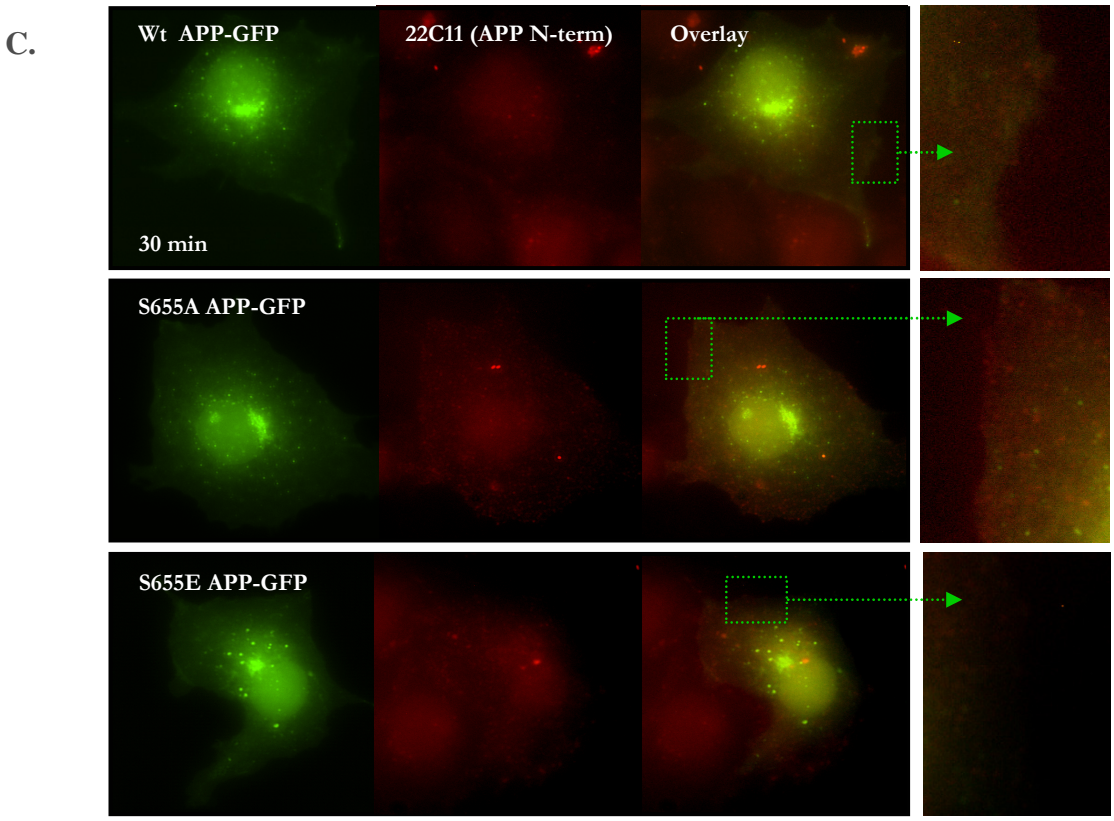

Figure II.15. Membranar APP-GFP dynamics. Membranar APP-GFP was labelled with the N-terminal antibody 22C11 and monitored with time of 37 ºC incubation: 0 min (**panel A**), 15 min (**panel B**) and 30 min (**panel C**). Microphotographs of panel B and especially of panel C required higher CCD exposure times, relatively to the same panels in Figure II.14.

APP-GFP S655A impaired endocytosis. From the experiments discussed above one is left with the suggestion that S655A does not incorporate into endocytic vesicles as well as S655E. Moreover, in the Antibody uptake assays (Fig. II.14) almost all 22C11-containing vesicles co-localized with S655E, but this was not so for the S655A mutant. In order to clarify whether S655 phosphorylation had an effect on APP endocytosis, 20 cells at the 15 min time point (as in Fig. II.14, B) were scored for red 22C11 endocytic vesicles alone and co-localizing yellow/orange vesicles (Fig. II.16). The percentage of non-colocalizing (red only) vesicles was thus calculated to be 3.4 ± 0.6% for Wt, 2.3 ± 0.4% for S655E and 9.8 ± 1.7% for S655A. These values for the S655A mutant were significantly different as determined by the Tukey test ($p < 0.01$ vs. Wt and $p < 0.001$ vs. S655E). Hence, the S655A mutant has indeed decreased endocytosis. Of note is that for all the APP-GFP species many of the cytoplasmic vesicles observed appeared to be endocytic in nature.

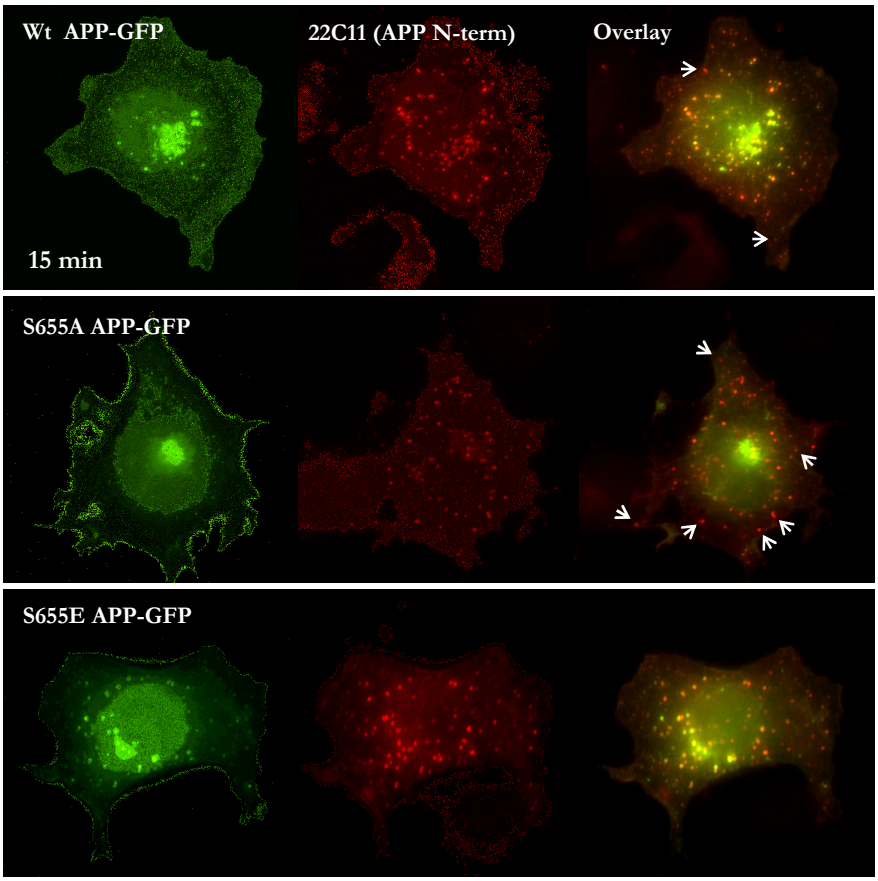

Figure II.16. Co-localization analysis of APP-GFP/22C11 endocytosed vesicles. Cells transiently transfected with the APP-GFP species and incubated for 2:30 h with CHX were surface labelled with the 22C11 antibody (red labelled). Upon 15 min of 37 ºC incubation cells were processed for immunofluorescence analysis of the number of green/red co-localizing and non-colocalizing cytoplasmic vesicles. Arrows indicate 22C11 red-positive vesicles that do *not* co-localize with APP-GFP.

II. 4. 4 – S655 PHOSPHORYLATION RESULTS IN LESS APP LYSOSOMAL TARGETING

Endocytosed APP can be recycled to the cell membrane, be sorted to TGN/Golgi or be targeted to lysosomes for complete degradation. As mimicking APP S655 constitutive phosphorylation-state resulted in slightly higher APP-GFP endocytosis and in its targeting at a higher rate to the TGN/Golgi, we analysed whether APP-GFP S655 phosphorylation could also affect targeting to lysosomes. APP-GFP constructs were co-localized with the enzyme Cathepsin D, a known lysosomal marker previously used in APP subcellular localization studies (Haass et al., 1992a). The experimental procedure is described in section II.3.4.5. The same end time point of CHX exposure used in the Antibody uptake assays (3:00 h) was used for a direct comparison. Results are presented in Figure II.17, the typical small dots of Cathepsin D subcellular distribution are stained with Texas Red-conjugated secondary antibody. This enzyme is reported to be mainly sorted directly from the TGN/Golgi to

lysosomes but can be targeted to the plasma membrane first and then directed to lysosomes via the endosomal pathway (Press et al., 1998).

Several cells were scored for the APP-GFP/Cathepsin D co-localization, in terms of percentage of red/green co-localizing vesicles relative to the total number of APP-GFP cytoplasmic vesicles (green). Of note is that the number of APP-GFP/Cathepsin D co-localizing vesicles was low, ranging from 5 to 20 per cell, when compared with the average number of ~100 APP-GFP endocytic vesicles per cell (Figure II.16). These results are in agreement with previous reports on APP lysosomal targeting, where APP could only be considerably detected in these structures when lysosomal proteolysis was inhibited with specific drugs (Hass et al., 1992a; Caporaso et al., 1994). Indeed, the percentage of Wt APP-GFP/Cathepsin D co-localizing vesicles was low, 5.0 ± 0.5%. The S655A mutant had a significantly higher lysosomal targeting than the Wt and S655E proteins, with a percentage of co-localizing vesicles around 9.6 ± 0.4% ($p < 0.001$ vs. Wt and S655E data). In contrast, the values obtained for the S655E protein were 3.1 ± 0.3% ($p < 0.01$ vs. Wt and $p < 0.001$ vs. S655A data) indicating a lower S655E targeting to lysosomes. Of note is that the majority of the Golgi area was not scored given the difficulty in distinguishing vesicular structures (see Fig. II.17 legend). However, the S655A mutant presented higher co-localization at that region, and S655E protein the lowest co-localization. Hence, the S655A mutant appears to be comparatively more targeted for lysosomal degradation, and S655 phosphorylation could represent a rescue mechanism. This will be addressed in the future.

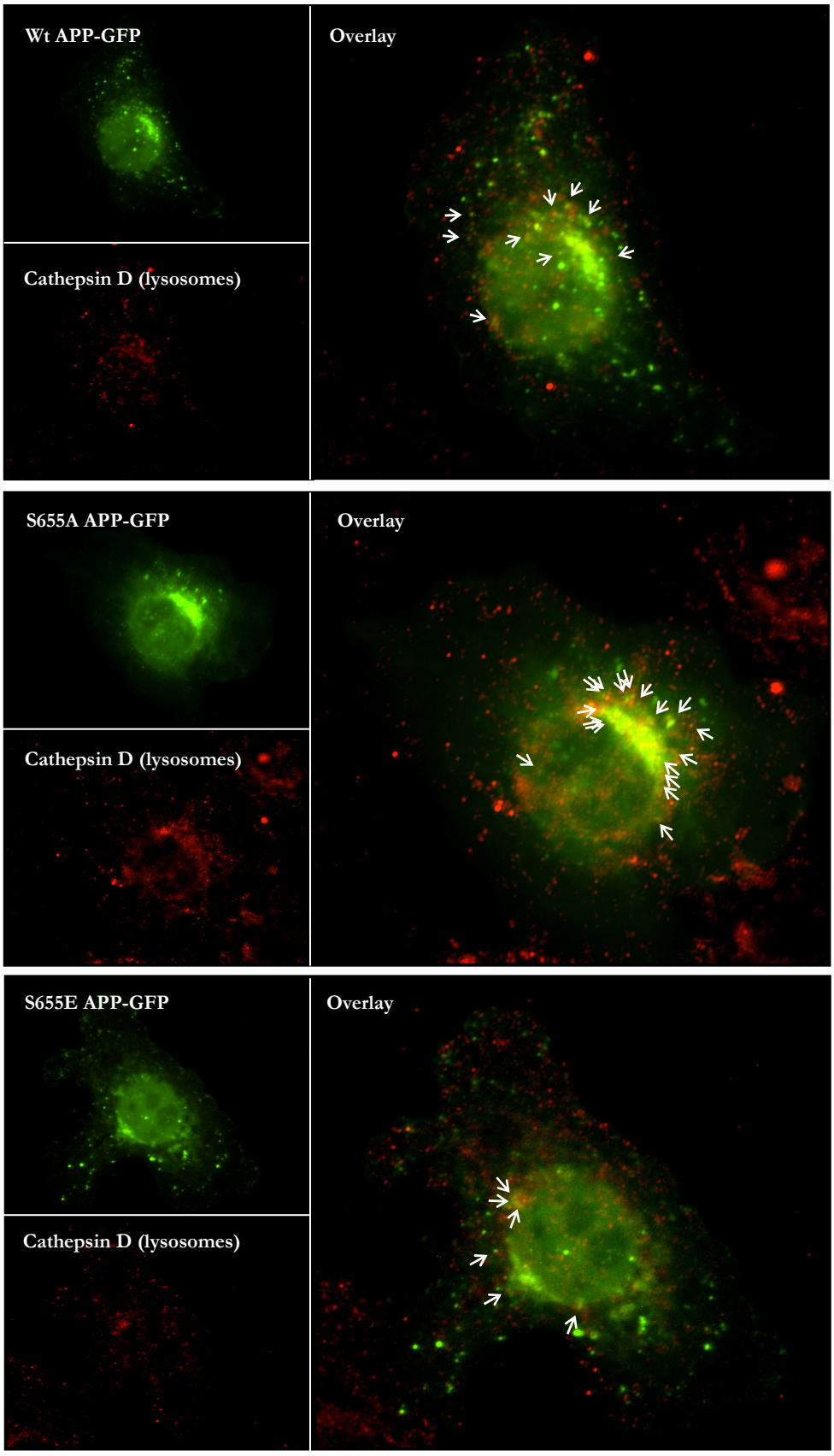

Figure II.17. Co-localization analysis of APP-GFP and the lysosomal marker Cathepsin D. Arrows indicate green (APP-GFP) and red (Cathepsin D) co-localizing vesicles. The majority of co-localizing vesicles observed at the TGN/Golgi area were not scored to not introduce errors due to the low resolution at that area.

II. 5 – CONCLUSIONS

APP S655 phosphomutant and APP-GFP fusion constructs were engineered and used together with cell culture and epifluorescence microscopy techniques, in order to determine the consequence of APP S655 phosphorylation on APP targeting and subcellular localization. The major observations from these studies were:

1. S655 phosphorylation-state determines the kinetics of APP traffic, with special relevance for the APP TGN/Golgi to PM anterograde and retrograde traffic.
2. APP TGN/Golgi exit is delayed for the S655A mutant. In addition, it seemed to be less efficiently incorporated into cytoplasmic vesicles.
3. In contrast, the S655E mutant, mimicking APP S655 constitutive phosphorylation, exited relatively better from the TGN/Golgi and seemed to be packaged into cytoplasmic vesicles more efficiently.
4. Both S655 phosphomutants had a higher number of cells with APP-GFP at the plasma membrane, with the S655A mutant showing the highest intensity. The higher PM staining for S655A appears to correlate with decreased endocytosis, this was shown not to be the case for S655E and will be addressed in Chapter III.
5. All APP-GFP proteins produced GFP-fused C-terminal fragments that were targeted to the cell nucleus. These fragments presented GFP intensities that correlated well with the intensities of nuclear 369 antibody-positive APP C-terminal fragments. Further, they were 22C11 and 6E10-negative, strongly suggesting that it is the APP AICD fragment that is nuclear targeted.
6. The nuclear targeting kinetics of APP-GFP-derived C-terminal fragments were observed to be very similar for the Wt and S655E proteins. Nonetheless, the S655E expressing cells exhibited a higher percentage of nuclei fluorescence and qualitatively these were more intense. Conversely, the nuclear targeting of a S655A-derived C-terminal fragment seemed to occur initially in a slightly faster manner but subsequently showed no further targeting, and overall exhibited relative lower nuclear staining intensity.
7. Cell membrane endocytosis is slightly increased for the mutant mimicking S655 phosphorylation and decreased for the S655A mutant. Moreover, the S655E and S655A endocytic vesicles were, respectively, more and less APP-GFP intense than

the Wt related ones. Hence, phosphorylated APP S655 seems to be preferentially endocytosed compared to the APP S655-dephosphorylated form.

8. Endocytosed S655E APP is retrieved faster and to a higher extent to the TGN/Golgi, while the S655A mutant is less likely to be recycled through the PM-to-Golgi retrograde pathway.

9. Part of the subcellular S655A population was observed to be preferentially delivered for lysosomal degradation, when compared with the other two APP-GFP proteins. This lysosomal targeting was two times higher for APP S655A, and slightly lower for APP S655E, relatively to Wt APP-GFP.

10. In conclusion S655E experiences faster anterograde and retrograde traffic and is preferentially targeted to the nucleus, being potentially rescued from the lysosomal pathway. S655A does not incorporate as well into vesicular like structures, is delayed at the Golgi and PM and is preferentially targeted to lysosomes.

CHAPTER III

SERINE 655 PHOSPHORYLATION-DEPENDENT APP_{695} PROCESSING

CHAPTER III – SERINE 655 PHOSPHORYLATION-DEPENDENT APP_{695} PROCESSING

III. 1 – INTRODUCTION

Proteolytic processing of APP to sAPP and Abeta, as well as AICD fragments, have been implicated to be regulated by phosphorylation and phosphorylation-dependent events (section I.3.2). Previous reports point to the phosphorylatable APP ^{653}YTSI^{656} domain as a molecular targeting signal, and place S655 at a pivotal regulatory position. In fact, the trafficking experiments performed with APP S655 phosphomutants described in Chapter II started to unravel that potential role. Under conditions of inhibiting "de novo" protein synthesis, the S655A phosphomutant, mimicking an APP S655 constitutive dephosphorylated state, was found to be more slowly sorted from the TGN/Golgi and packaged into cytoplasmic vesicles. Furthermore, under these conditions part of the S655A-GFP Golgi population failed to be exported and remained in the Golgi compartment. Conversely, the S655E mutant, mimicking a S655 constitutive phosphorylation, had no visible impairment in its Golgi-sorting, and upon integration at the cell membrane was endocytosed and rapidly recycled to the TGN compartment. In addition, the S655A mutant exhibited a down-regulation in its rate of endocytosis and an increased targeting to lysosomes. As altered APP protein trafficking may potentially lead to alterations in its cellular processing, the role of APP S655 phosphorylation on APP proteolytic cleavage was thus addressed and is described in this chapter.

III. 2 – AIMS OF THIS CHAPTER

The putative alterations on APP proteolytic processing due to the constitutive phosphorylated/dephosphorylated states of APP at serine 655 were addressed. The main objectives of this chapter were:

1. To monitor the levels of full-length (immature and mature forms) Wt and S655 phosphomutants APP-GFP proteins under CHX exposure (time course analysis).
2. To evaluate the rate of APP-GFP cellular catabolism in a S655 phosphorylation state-dependent manner.

3. To monitor the levels of medium sAPP secretion for each of the Wt and S655 phosphomutants APP-GFP under CHX exposure (time course analysis).
4. To assess, in a S655 phosphorylation state-dependent manner, sAPP secretion under basal conditions or upon blocking TGN/Golgi vesicles traffic.
5. To compare the efficiency of PMA to stimulate sAPP secretion from the Wt and S655 phosphomutant APP-GFP proteins.
6. To analyse APP S655 phosphorylation-dependent Abeta production.

Hence, the processes of APP maturation, catabolism, and proteolytic cleavage by the different APP secretases were evaluated in a time-dependent manner. Several parameters described above and relative to APP processing and metabolism were monitored, namely intracellular immature and mature APP, as well as sAPP and Abeta levels.

III. 3 – MATERIALS AND METHODS

A list of all solutions and protocols used, as well as other relevant information, is presented in the Appendix. All reagents were of cell culture grade or ultrapure.

III. 3. 1 – ANTIBODIES

The primary antibodies used in the following studies were the previously described monoclonal 22C11, to detect holo APP and all sAPP forms, and monoclonal 6E10 antibody, which cross-reacts with αsAPP. The anti-GFP JL-8 antibody was also used, for specific APP-GFP detection. An anti-β-Tubulin antibody (Zymed, Portugal) was used for control of specific cellular alterations. For Abeta immunoprecipitation and analysis the 1E8 monoclonal antibody was used (Nanotools, Germany). Anti-mouse and anti-rabbit IgGs horseradish peroxidase-linked whole antibodies were used as secondary antibodies for ECL detection.

III. 3. 2 – CELL CULTURE AND TRANSIENT TRANSFECTIONS

COS-7 cells were transfected with the APP-GFP constructs by means of the Lipofectamine reagent and as previously described in Chapter II. Further transfection details for each of the assays performed is outlined in Table III.1.

Table III.1. Transient transfection procedures adopted for the assays described in this chapter. Following removal of transfection medium and cell division into multi-well plates cells were allowed to recover for 4 -12 h.

General Procedure	Procedure	Transfected cDNAs	Quantity / Plate diameter	Transfection period
CHX Time Course Experiments	**APP-GFP and sAPP time course analysis**	Wt APP-GFP S655A APP-GFP S655E APP-GFP	8.0 μg / 100 mm	8 h
	Abeta secretion analysis (3:00 h CHX)	Wt APP-GFP S655A APP-GFP S655E APP-GFP	4.0 μg / 60 mm	8 h
Point Experiments	**APP and sAPP Inhibition upon severe CHX block**	Wt APP-GFP S655A APP-GFP S655E APP-GFP	4.0 μg / 60 mm	8 h
Point Experiments	**sAPP production at 20 ºC (basal and PMA-stimulated)**	Wt APP-GFP S655A APP-GFP S655E APP-GFP	4.0 μg / 60 mm	8 h

III. 3. 3. – ANALYSIS OF S655 PHOSPHORYLATION-DEPENDENT CELLULAR APP-GFP LEVELS

III. 3. 3. 1 – Time-course analysis of the cellular levels of immature and mature APP-GFP

COS-7 cells were transfected with the Wt and S655 phosphomutants APP_{695}-GFP cDNAs and treated as described above (Table III.1). Following a recovery period of cells which had been split into six-well plates, the media was substituted with DMEM supplemented with 50 μg/ml CHX. Incubation was allowed to proceed for extending time periods of time (0:00, 1:00, 2:00, 3:00 and 5:00 h), after which cells were harvested into 1% SDS. Cells lysates aliquots, mass normalized, were subject to Western blot analysis, as described below in section III.3.6, to detect their intracellular levels of full-length APP-GFP. As specified in Chapter II, complete DMEM without serum is here referred to as DMEM.

III. 3. 3. 2 – Comparative analysis of the Wt and S655 phosphomutants rate of cellular catabolism

The rate of cellular catabolism can be evaluated by analysing the different recovery capacities of the levels of full-length APP-GFP following a period where protein synthesis was severely inhibited. An assay based on protein secretion studies described in Brakch et al. (2002) was adopted, and COS-7 cells were transiently transfected with the three APP-GFP constructs as described in Table III.1. Cells were further incubated with fresh DMEM supplemented with CHX at 100 μg/ml ("CHX block"). After a 2:00 h incubation period the medium was withdrawn, cells were washed twice with PBS, and DMEM (CHX-free) medium was added. Cells were incubated at 37 ºC and 5% CO_2 for 3:00 h, after which cells and media were collected into 1% SDS. The cellular APP-GFP and medium sAPP contents were analyzed by Western blot.

III. 3. 4. – ANALYSIS OF S655 PHOSPHORYLATION-DEPENDENT SAPP PRODUCTION

III. 3. 4. 1 – APP-GFP-derived sAPP production in a CHX time-dependent manner

For the time course analysis of medium sAPP secretion in a S655 phosphorylation state-dependent manner, the conditioned media of cells treated as above (section III.3.3.1) were also collected into 1% SDS following CHX exposure for increasing periods: 1:00, 2:00, 3:00 and 5:00 h.

III. 3. 4. 2 – Temperature- and PMA-dependent sAPP production

COS-7 cells were transfected with the APP-GFP cDNAs as described in Table III.1, and pre-incubated for 15 min at 20 ºC, a temperature known to block APP/sAPP vesicle secretion from the TGN/Golgi (Kuentzel et al., 1993; Xu et al., 1995; Sabatini et al., 1996, Walter et al., 1997). Subsequently, APP-GFP proteins were monitored by epifluorescence microscopy at the following time points of further incubation at 20 ºC: 0 min, 15 min, 30 min, 1 h, 2 h, and 4 h. For the sAPP production assays at 20 ºC, APP-GFP transfected cells were pre-incubated at 20 ºC for 15 min, cells medium was substituted for equal fresh medium, and cells further incubated for 2 h at 20 ºC. A control set of APP-GFP transfected cells was incubated for 2 h at 37 ºC. The 2 h cells incubation was performed with 0.5 ml DMEM (basal conditions) or with 0.5 ml DMEM supplemented with the phorbol ester PMA (phorbol 12-myristate 13-acetate) (Calbiochem) at 0.5 μM (PMA-stimulation conditions). Conditioned media and cells were collected into a final boiling 1% SDS solution, and APP-GFP and sAPP levels were evaluated by Immunoblotting using the 22C11 antibody.

III. 3. 5. – ABETA SECRETION ANALYSIS

The levels of different secreted Abeta fragments were analyzed for the three APP-GFP constructs. APP-GFP transfected cells were treated as described in Table III.1 and incubated for 3:00 h with 50 μg/ml CHX as for the cellular APP-GFP assays (section III.3.3.1). This time point was chosen, as by 3.00 h differences were already evident between the three APP-GFP constructs and APP depletion had not become significant. After the incubation period, cells and conditioned medium were collected, the latter centrifuged at 310 x *g* for 5 min, and the resultant supernatants immediately frozen in dry ice. Cell lysates in 1% SDS were resolved by SDS-PAGE and subjected to immunoblot detection of APP-GFP proteins. The Abeta detection analysis of the conditioned media was performed in collaboration with Dr. Hermann Esselmann and Prof. Jens Wiltfang (Neurobiology Lab, University of Goettingen, Germany). Briefly, immunoprecipitation of medium secreted Abeta fragments was accomplished using 25 μl dynabeads (Dynal, Germany) coated with the anti-Abeta 1E8 antibody. Immunoprecipitated samples were resolved on 12% Bicine/Tris gels containing 8 M urea (Lewczuk et al., 2004) and different Abeta peptide forms were revealed by immunoblotting using the 1E8 antibody. Synthetic Abeta peptides were run in parallel for the identification of the different Abeta peptide species.

III. 3. 6 – SAMPLE PREPARATION AND PROTEIN ANALYSIS

At the specified time points, cells and conditioned medium were harvested into 1% SDS final solutions, and samples were boiled for 10 min with cell lysates being further sonicated for 30 sec. Total protein content was determined by the BCA kit method (Pierce), according to the supplier's instructions (see Appendix II). Mass-normalized aliquots were subjected to 6.5% (cellular holo APP-GFP) or 7.5% (medium sAPP) SDS-PAGE in Tris-Glycine buffer. The proteins and protein fragments resolved by SDS-PAGE were electrophoretically transferred onto nitrocellulose membranes. Immunoblotting of the transferred proteins was performed with the above described antibodies (section III.3.1) and detection was achieved using an enhanced chemiluminescence detection system (as in Chapter II).

Protein band quantification and statistical analysis.

Immunoblots autoradiographic film exposures were scanned in a GS-710 calibrated imaging densitometer (Bio-Rad), and protein bands quantified using the Quantity One densitometry software (Bio-Rad). Data are expressed as mean ± SEM (standard error of the mean) of triplicate determinations from at least three independent experiments. Statistical significance analysis was conducted by one way analysis of variance (ANOVA) followed by the Tukey-Kramer test. Statistical significance symbols used were (*) for comparison of S655 phosphomutant and Wt data, and ($^{+}$) for S655A versus S655E data. Statistical significance levels are presented as (*/$^{+}$), for $p < 0.05$; (**/$^{++}$), for $p < 0.01$; and (***/$^{+++}$), for $p < 0.001$.

III. 4 – RESULTS AND DISCUSSION

III. 4. 1 – TIME-COURSE ANALYSIS OF FULL-LENGTH APP-GFP CELLULAR LEVELS

In order to determine APP_{695} cellular processing in a S655 phosphorylation-state dependent manner, Immunoblot time course analyses of APP-GFP and derived sAPP were performed in parallel with the time course traffic assays of section II.3.4.1. COS-7 cells were transiently transfected at low levels with the fusion APP-GFP cDNAs and treated as described in section III.3.3.1. Mass normalized cells lysates were resolved by SDS-PAGE and analyzed by Immunoblotting with the anti-APP N-terminal antibody 22C11 (Fig. III.1, A). Relevant bands (a and b), which correspond to the transfected APP-GFP proteins, were quantified by densitometry and the data (Table III.2) plotted as percentages of their respective OD at 0:00 h. Data obtained for the levels of immature APP-GFP (band a) with time, and the levels of mature APP-GFP (band b), are plotted in Fig. III.1, B. The latter reflects the rate of cellular catabolism of mature APP-GFP, such as proteolytic cleavages and degradation.

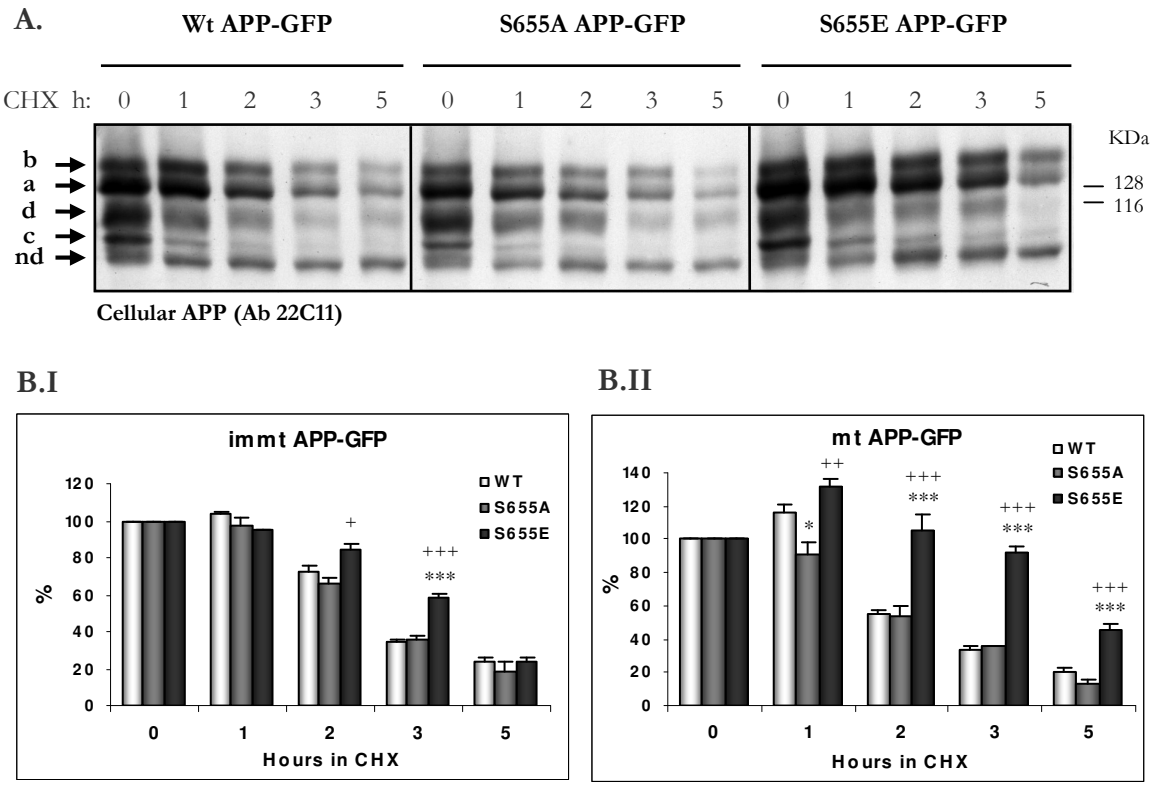

Figure III.1. Cellular processing of the Wt and S655 APP-GFP phosphorylation mutants. A: Immunoblot detection of Wt and S655 mutants (S655A and S655E) in cells lysates with time (hours) of CHX incubation. **a** and **b** are the transfected immature and mature APP_{695}-GFP forms, respectively. **c and d**, endogenous APP forms, **nd**, non-determined band (further discussed in section III.4.3). **B:** Plotted data for the levels of APP-GFP immature ("immt") (**B.I**) and mature ("mt") (**B.II**) forms with time.

Table III.2. Comparison between immature and mature APP-GFP intracellular levels with time of CHX exposure, expressed as percentages of the respective initial 0:00 h level. (n), number of independent experiments.

		APP-GFP Percentage		
APP-GFP	**Hours in CHX**	**Wt** (n=6)	**S655A** (n=6)	**S655E** (n=6)
Immature	0:00	100.0 ± 0.0	100.0 ± 0.0	100.0 ± 0.0
	1:00	104.2 ± 0.7	97.5 ± 4.2	94.7 ± 0.3
	2:00	72.7 ± 3.3	65.4 ± 3.5	83.9 ± 4.1
	3:00	34.6 ± 1.4	36.0 ± 2.1	58.1 ± 2.2
	5:00	23.6 ± 2.2	18.6 ± 4.7	24.1 ± 2.3
Mature	0:00	100.0 ± 0.0	100.0 ± 0.0	100.0 ± 0.0
	1:00	115.5 ± 5.5	90.4 ± 8.2	131.6 ± 5.3
	2:00	55.0 ± 2.7	53.3 ± 6.8	105.2 ± 9.2
	3:00	33.2 ± 2.2	35.6 ± 0.6	92.2 ± 3.4
	5:00	20.0 ± 2.7	12.9 ± 2.1	45.0 ± 4.3

The depletion patterns of the immature APP-GFP forms, which are related to the rates of APP maturation and its degradation, were very similar for Wt and S655A APP-GFP. These depletions decrease to 35% by 3:00 h of CHX incubation, and stabilize to around 20-25% thereafter (Graph III.1, B.I). However, the pattern of immature S655E depletion with time was slightly slower, dropping only to 58% by 3:00 h of CHX exposure, although reaching the same final ~20% level at 5:00 h (Table III.2).

From Graph B.II we can observe that the mature forms of the three APP-GFP species exhibited differences in their processing patterns. During the time monitored, the mature forms of Wt and S655A species decreased to 10-20% of their initial levels, while the S655E mutant only decreased to ~45% (Fig. III.1, B.II, 5:00 h). The half-lifes of the three APP-GFP mature forms were calculated to be 2.46 ± 0.16 h for the Wt, 2.12 ± 0.08 h for the S655A, and 5.56 ± 0.41 h ($p < 0.001$ vs Wt and S655A data) for the S655E mutant. Hence, S655 constitutive phosphorylation greatly increases mature APP-GFP half-life. Interestingly, the mature Wt APP-GFP time course has a pattern that is similar to the S655E one initially

(0:00-1:00 h), from which it deviates between 1:00 to 2:00 h towards the S655A pattern. Indeed, from 2:00 h on, the mature Wt and S655A patterns are more alike. Graph III.1 B.II, shows that the levels of Wt mature APP-GFP suffered an initial increase (0:00-1:00 h), and although mature S655A catabolism was similar to Wt, it lacked the Wt 1:00 initial peak. This suggests an availability of this mutant for a faster and immediate cellular processing/degradation. As previously observed in Chapter II, the slightly higher S655A lysosomal targeting (Fig. II.17) may be one of the factors contributing to this result. As with the Wt, the pattern of mature S655E disappearance exhibited an initial increase although higher, but the mature S655E levels decreased below 100% only between 2:00-3:00 h. Thus one is left to conclude that the S655E mature form has a lower rate of degradation, resulting in a doubled half-life (5.56 h), when compared to the other two APP-GFP proteins (2.46 and 2.12 h, Wt and S655A, respectively). Of note is that the level of APP-GFP maturation, calculated as the percentage of the mature form relatively to total APP-GFP levels, was found to be equal for the three proteins. These were calculated using the APP-GFP data in the 0:00 h CHX lysates, and were of 36.0 ± 3.3% for the Wt, 32.8 ± 2.7% for the S655A, and 34.0 ± 4.0% for the S655E species.

III. 4. 2 – COMPARATIVE RATES OF WT AND S655A/E APP-GFP CELLULAR CATABOLISM

Further evidences of the differential fates of the S655 mutants may be obtained by addressing their rate of cellular catabolism. This was evaluated by analysing the different recovery capacities of cellular APP-GFP levels following APP-GFP depletion (severe protein synthesis inhibition conditions). The correspondent medium sAPP levels were also analysed for comparison. For this purpose, COS-7 cells transfected with the APP-GFP cDNAs, and treated as described in section III.3.3.2, were first incubated for 2:00 h with a high CHX dose (100 μg/ml) ("CHX block" period). This CHX treatment allows for the clearance of newly synthesized proteins (Brion et al., 1992; Brakch et al., 2002; da Cruz e Silva et al., 2004b). The medium was substituted with fresh CHX-free DMEM, and cells were allowed to recover for 3:00 h, upon which cells and conditioned medium were collected. Medium samples were subjected to SDS-PAGE, and Immunoblotted with the 22C11 antibody (Fig. III.2, A). The inhibitory effects of CHX on APP-GFP and $sAPP_{695}$ levels were evaluated by densitometry analysis of APP-GFP and sAPP bands, and data were expressed as percentages of control (CHX-free) levels (Fig. III.2, B and C).

A.

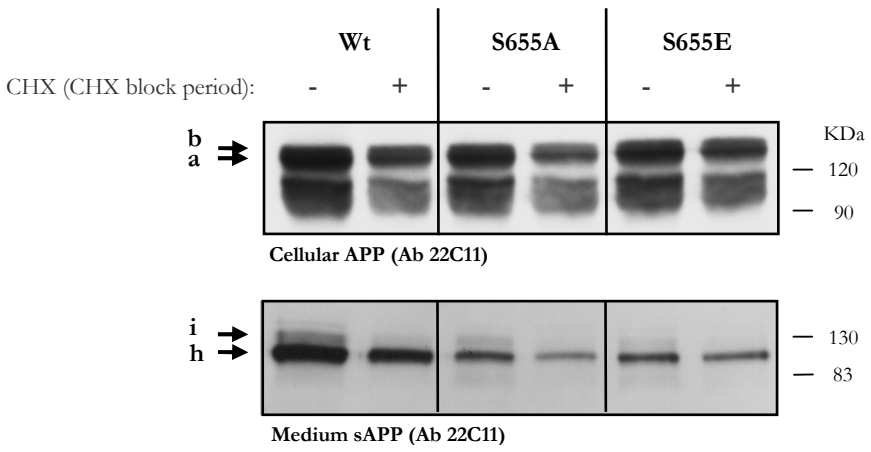

B.

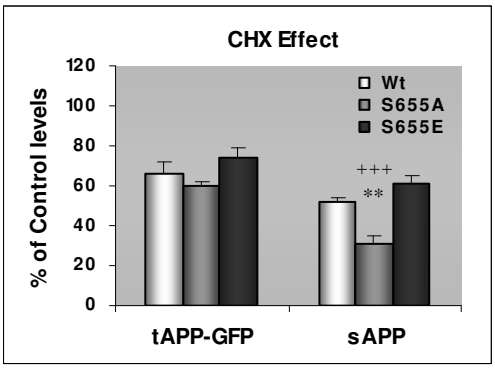

C.

APP-GFP Species	% of Control Levels	
	tAPP-GFP (n=4)	**sAPP$_{695}$** (n=4)
Wt	65.7 ± 6.0	52.5 ± 1.5
S655A	59.9 ± 2.3	31.1 ± 4.4
S655E	73.8 ± 4.8	60.6 ± 4.6

Figure III.2. CHX inhibitory effects on Wt and S655 phosphomutants APP-GFP and sAPP levels. A: APP Immunoblots of cells subject to a CHX pre-treatment ("CHX block") and collected following a CHX-free recovery period. Medium was also collected at the end of that period and medium sAPP detected. **a** and **b**, immature and mature APP-GFP forms; **h,** medium sAPP$_{695}$. **i,** endogenous sAPP$_{751/770}$. **B and C:** Graph and table with the CHX-induced levels of total cellular APP-GFP (**tAPP-GFP**, immature plus mature forms) and derived medium secreted sAPP$_{695}$ (**sAPP**).

When comparing both S655 phosphomutants, we can see differences in the CHX-induced decrease of their cellular APP-GFP levels. CHX induced a greater decrease in the cellular content of the S655A mutant (~40%) when compared to the S655E mutant (~25%) (Fig. III.2, B and C). These values are statistically significantly different by the Student's two-tail t test. An intermediate down-regulation by ~34% was observed for the wild-type APP-GFP. Thus, after cellular depletion of APP-GFP proteins, the S655A protein was the most affected in terms of decreased APP-GFP levels. Conversely, the levels of the APP-GFP S655E protein were the less affected by this treatment. This differential inhibition is also observed when medium sAPP levels are evaluated upon the CHX block. Of note is that, as already observed, COS-7 cells have low levels of endogenous APP 695 isoform, and so the

majority of the $sAPP_{695}$ observed (Fig. III.2, A, band h) derives proteolytically from the transfected full-length APP_{695}-GFP. Under basal conditions the relative levels of medium secreted sAPP were found to be very similar for the three APP-GFP species: 91.0 ± 5.8 % for S655A and 96.0 ± 5.8 % for S655E, in comparison with Wt levels (taken as 100%). After the CHX exposure period (Fig. III.2, B and C), the S655A mutant showed the highest decrease in sAPP production (~70% decrease). The S655E-derived sAPP levels were not so affected (~40% decreased), and were more similar to Wt ones (~50% decreased). The levels of inhibition of medium sAPP for the three species vary accordingly to the levels of inhibition of intracellular full-length APP-GFP, although more pronouncedly.

In conclusion, upon protein synthesis inhibition, the S655A cellular pool is depleted at higher extent and/or is more difficulty replaced. Conversely, the S655E cellular pool is more easily maintained or recovered in these conditions. These results point to a higher rate of cellular catabolism for the S655A mutant, and a lower rate for the S655E mutant.

III. 4. 3 – TIME-COURSE ANALYSIS OF TOTAL AND αsAPP$_{695}$ PRODUCTION

The influence of S655 phosphorylation on the cleavage of APP-GFP to total sAPP and αsAPP was further analyzed in detail. The pattern of sAPP production with time of CHX exposure was evaluated for the Wt and mutant proteins. Conditioned media, collected at the same time points as the cellular lysates of the previous section III.4.1, were subjected to Western blot analysis. Two antibodies, 22C11, for total sAPP detection (derived from alpha and beta-secretase cleavages) (Fig. III.3, A and B.I), and 6E10 for specific detection of αsAPP (Fig. III.3, A and B.II), were used. The sAPP band deriving from APP-GFP cleavage (band h) was quantified by densitometry analysis for Wt and mutants, and the data plotted graphically as fold-increase over sAPP production at 1:00 h (Graphs III.3, B). A table with the sAPP fold-increases is presented, to allow for a better comparison of the results (Fig. III.3, C).

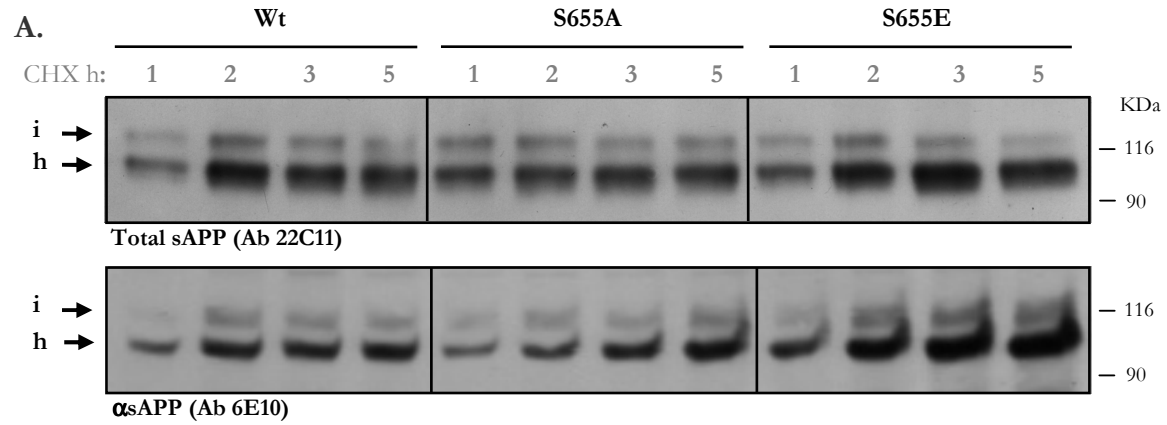

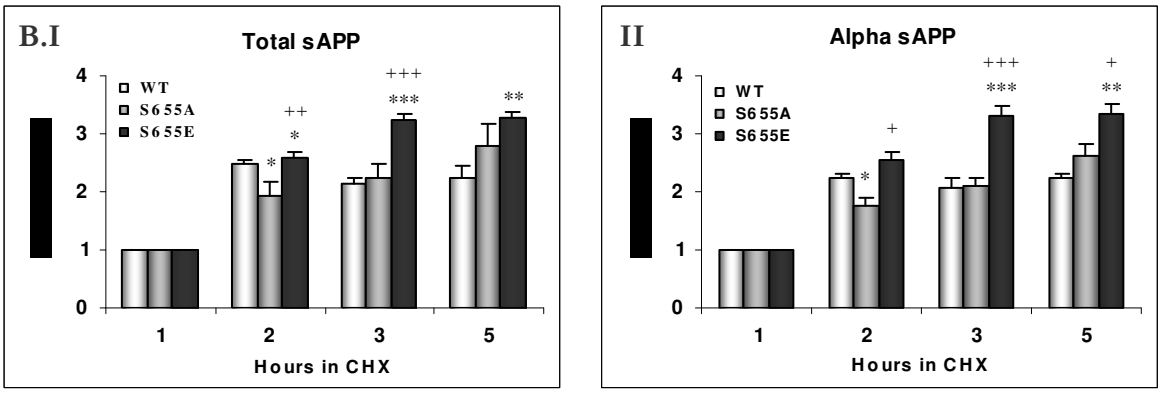

C.

APP-GFP	Hours in CHX	Fold-Increase: Total $sAPP_{695}$ (n=4)	Fold-Increase: Alpha $sAPP_{695}$ (n=4)
Wt	1:00	1.00 ± 0.00	1.00 ± 0.00
	2:00	2.49 ± 0.07	2.25 ± 0.07
	3:00	2.12 ± 0.10	2.07 ± 0.17
	5:00	2.25 ± 0.18	2.23 ± 0.09
S655A	1:00	1.00 ± 0.00	1.00 ± 0.00
	2:00	1.92 ± 0.26	1.79 ± 0.18
	3:00	2.24 ± 0.23	2.11 ± 0.27
	5:00	2.80 ± 0.35	2.61 ± 0.21
S655E	1:00	1.00 ± 0.00	1.00 ± 0.00
	2:00	2.59 ± 0.09	2.53 ± 0.17
	3:00	3.24 ± 0.11	3.29 ± 0.18
	5:00	3.28 ± 0.10	3.36 ± 0.14

Figure III.3. S655 Phosphorylation state-dependent APP processing to secreted total sAPP and αsAPP. **A:** Immunoblot analysis of total $sAPP_{695}$ (upper blot) and $\alpha sAPP_{695}$ (lower blot) secreted and accumulated into conditioned medium with time of CHX exposure (hours in CHX). **h**, $sAPP_{695}$; **i**, $sAPP_{751/770}$. **B:** Graphs with time courses of total sAPP (**B.I**) and $\alpha sAPP_{695}$ (**B.II**) levels, expressed as fold-increases over 1:00 h sAPP level. **C:** Table with the data of the APP-GFP derived total (α+β) and αsAPP secretions.

Comparison of Figures III.3 B.I and B.II reveals that the patterns of total (α+β) sAPP and αsAPP secretion are similar for each of the APP-GFP species. Thus, the majority of the total $sAPP_{695}$ produced consists, as expected, of the $\alpha sAPP_{695}$ form. The analysis of both types of graphs (Fig. III.3, B.I and B.II) indicates that the time-course pattern of Wt sAPP fold-increase is similar to the S655E pattern until 2:00 h, but at 3:00 h and 5:00 h it approaches the S655A pattern. Wild-type sAPP levels seemed to reach a maximum at 2:00 h (fold-increase of 2.49 ± 0.07), to have a small decrease until 3:00 h, followed by a small increase to 5:00 h. This 2:00 h peak does not seem to happen or is 'masked' in the case of the phosphomutants. The S655A mutant has a more linear and slower increase in its sAPP levels, which reaches its peak (2.80 ± 0.35) only at 5:00 h. Hence, S655A sAPP production and/or secretion are initially comparatively delayed, relative to the Wt. The S655E species presented the faster and higher total and αsAPP fold-increases, which peaked at 3:00 h (fold-increases ~3.3) (Fig. III.3, B and C). Hence, a hypothesis previously formulated of S655E having an enhanced half-life due to being less cleaved by secretases was discarded. Taken together, the cellular APP-GFP and sAPP results strongly support a lower targeting of the S655E mutant to degradation pathways. Results also support the previous Chapter II findings of a higher rate of S655E trafficking between the two main subcellular sites of α-secretase cleavage: the TGN and the plasma membrane. The S655A pattern of delayed sAPP secretion is also consistent with this mutant having a delayed Golgi exit and less PM retrieval to the Golgi (Fig.s II.8 and II.9). It is possible that in COS-7 cells the main site of α-secretase cleavage is the TGN/Golgi. In several cell lines such as H4 neuroglioma cells, CHO cells or the kidney-derived HEK cells (Kuentzel et al., 1993; Marambaud et al., 1997; Walter et al., 1997), sAPP was observed to be mainly produced intracellularly at the TGN/Golgi and possibly at secretory vesicles. Of note is that the previously observed undefined band (band nd, ~105 KDa) in cells lysates (Fig. III.1, A) could potentially correspond to intracellularly produced $sAPP_{695}$. This band was observed to be only present at the APP-GFP transfected cells and was found to be immunonegative with the APP C-terminal 369 antibody (data not shown). For the Wt and S655E species, the patterns of variation of band "nd" with time of CHX exposure (Fig. III.1, A) were very similar to the medium sAPP patterns of Fig. III.3, B. For the S655A mutant, however, the pattern of band "nd" variation is similar to the Wt pattern and not to S655A medium sAPP (Fig. III.3, B). A potential explanation may reside in S655A being cleaved intracellularly to a similar extent as the Wt species but having a delayed TGN sAPP secretion, consistent with the observed slower increase in the S655A medium sAPP levels (Fig. III.3, B and C).

III. 4. 4 – S655 PHOSPHORYLATION-DEPENDENT APP CLEAVAGE AT THE SECRETORY PATHWAY

The previous results may indicate that intracellular APP and sAPP secretions are more delayed for the S655A species and occurs faster for the S655E mutant. One of the major pathways of sAPP production and secretion is the secretory pathway, specifically the TGN, secretory post-TGN vesicles and PM (Khvotchev and Sudhof, 2004). The traffic analyses of Chapter II strongly suggest that S655E is more incorporated into vesicles and that the S655A mutant is less targeted for vesicle incorporation. This could result in differential rates of intracellular sAPP production and secretion, along with differential amounts of APP delivered to the PM and subsequentially cleaved to sAPP. In order to further clarify this question, the APP-GFP species sAPP production was evaluated at 20 ºC. Incubating cells at 20 ºC causes a block in post-TGN vesicles secretion (Sabatini et al., 1996), but does not inhibit ER-to-Golgi traffic or cellular endocytosis (Kuismanen and Saraste, 1989; Ellinger et al., 2002). This low-temperature block also allows for the APP cleavage to sAPP within the TGN, after sulphation (Kuentzel et al., 1993).

APP-GFP expressing cells were first pre-incubated for 15 min at 20 ºC, to allow temperature lowering and stabilization. Cells were further incubated for 4 h at 20 ºC and APP-GFP traffic monitored at specific time points of 20 ºC incubation: 0 min, 15 min, 30 min, 1 h, 2 h, and 4 h. Figure III.4 shows that cells incubation at 20 ºC severely reduced APP-GFP-positive vesicles, with the few cytoplasmic vesicles still observed at 4 h most probably resulting from endocytosis. In addition, a gradual higher condensation of the Golgi APP-GFP fluorescence could also be observed. These alterations occurred in a time-dependent manner, and are in agreement with a block in post-TGN vesicle release and even formation at the later periods (Fig. III.4, 2:00 and 4:00 h). The same effects could be observed for the three APP-GFP species, but they started at different times of 20 ºC incubation. The S655A mutant is apparently faster to disappear from cytoplasmic vesicles, including vesicles near or at the TGN/Golgi area, than the other two APP-GFP proteins. A significant decrease in the number of S655A-containing vesicles is already visible by 1 h of 20 ºC incubation, with this effect being visible for the Wt and S655E only after 2 h at 20 ºC. In fact, at 2 h the S655E protein is still present in a large number of cytoplasmic vesicles at the TGN/Golgi, while fewer TGN vesicles are observed for the Wt. In addition, the fluorescing Golgi condensation effect also starts sooner for the S655A mutant (1 h), followed by the Wt (2 h) and the S655E species (2-4 h). These observations are in agreement with higher and lower targeting to post-TGN vesicles for the S655E and S655A mutants, respectively, and relatively to the Wt protein.

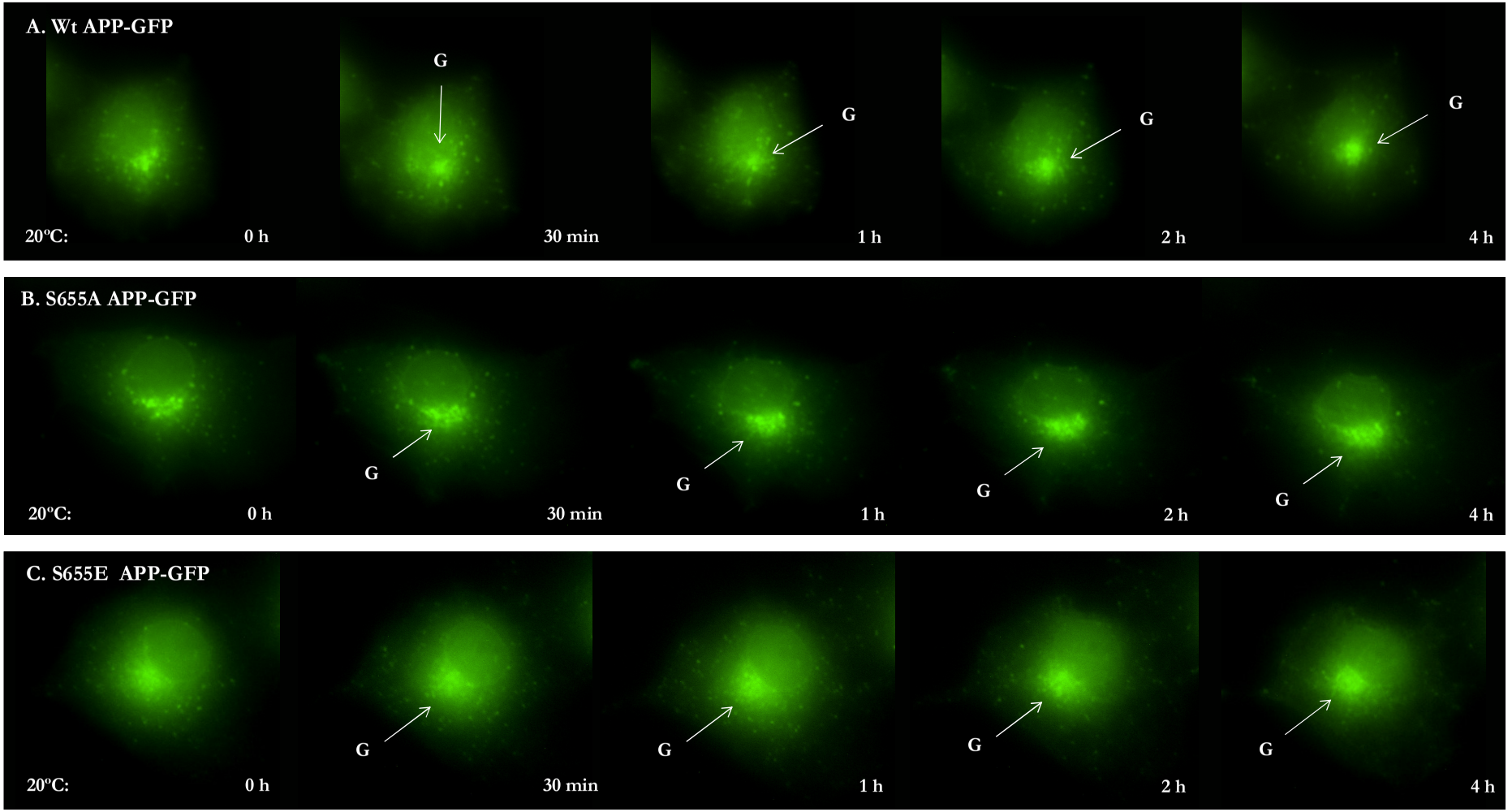

Figure III.4. APP-GFP protein traffic upon several time points of cells incubation at 20 ºC. The subcellular traffic of **A:** Wt APP-GFP; **B:** S655A APP-GFP; and **C:** S655E APP-GFP proteins were monitored in single cells by epifluorescence microscopy. Arrows indicate the Golgi (**G**) region.

Further evaluation addressed the proteolytic processing of the APP-GFP species under the 20 ºC temperature block. The 2 h time point was chosen due to the fact that the block on post-TGN vesicles release was already visible for the three APP-GFP species (Fig. III.4). Moreover, although at 4 h this block was more severe, sAPP was reported no longer to be detectable upon 4 h of cells incubation at 20 ºC (Kuentzel et al., 1993; Walter et al., 1997). Hence, a subset of cells expressing the APP-GFP constructs were incubated for 2 h at 37 ºC, and another subset was first pre-incubated for 15 min at 20 ºC for temperature stabilization, cells conditioned medium was exchanged, and cells were further incubated for 2 h at 20 ºC. After the 2 h incubation period, cells and conditioned media were collected. Cellular and medium samples were subject to Immunoblot analysis with the 22C11 antibody (Fig. III.5, A), and the relevant bands quantified by densitometry analysis. The cellular APP and medium secreted sAPP levels are tabulated and represented graphically in Figure III.5, B. Cellular tubulin was also detected and used as control.

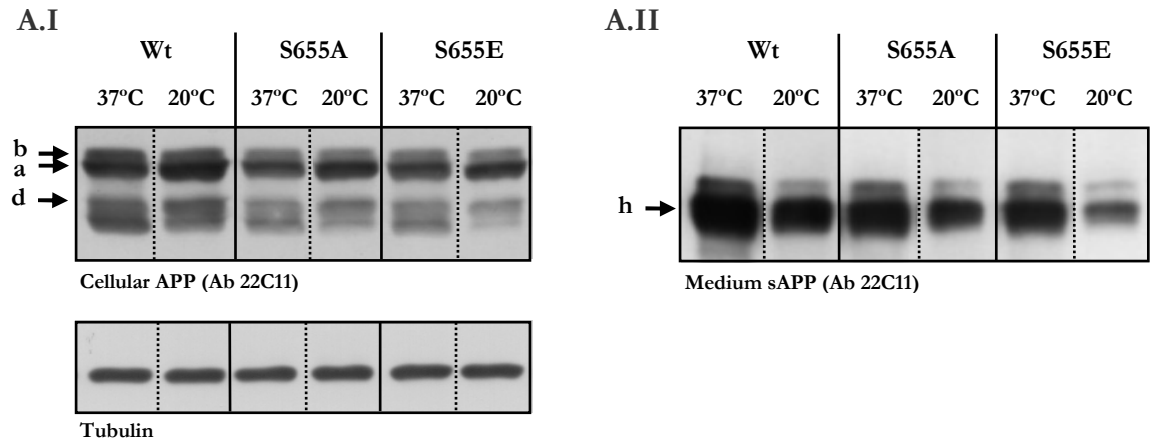

B.I

APP-GFP Species	Temperature Effect on sAPP (n=3)
Wt	41.4 ± 3.9%
S655A	40.7 ± 4.8%
S655E	26.1 ± 3.6%

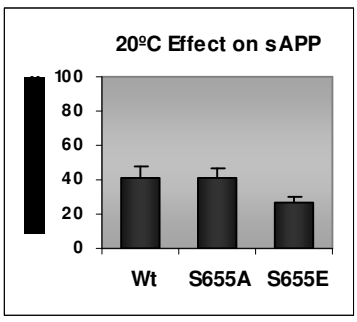

Figure III.5. 20 ºC temperature effects on the APP-GFP proteins processing to sAPP. A: Immunoblot analysis of APP-GFP in cellular lysates (**A.I**) and medium secreted sAPP (sAPP) (**A.II**) upon 2 h of cells incubation at 37 ºC or 20 ºC. Cells lysates were also probed for tubulin as a control (**A.I**). **a** and **b**, immature and mature APP-GFP, respectively; **d**, endogenous APP; **h**, medium secreted $sAPP_{695}$. **B.I** and **B.II:** Table and Graphic analysis, respectively, of the percentage of sAPP levels at 20 ºC relatively to the respective 37 ºC control levels.

Figures III.5, A.II and B, show that lowering the temperature from 37 ºC to 20 ºC results in lower levels of medium secreted sAPP derived from the three APP-GFP proteins or endogenous APP. Additionally, for all APP-GFP constructs, as for endogenous APP, the levels of the cellular forms increase upon incubation at 20 ºC (Fig. III.5, A.I), correlating with a lower cleavage of APP to sAPP. This has already been reported for H4 and HEK 293 cells (Kuentzel et al., 1993; Walter et al., 1997). The decrease in sAPP secretion is thought to result from a blockage in post-TGN vesicles and most probably also from lowering the temperature below the APP secretases temperature optima, which results in less efficient APP cleavage.

Interestingly, while the 20 ºC-induced inhibitions on Wt and S655A sAPP secretions are similar, the S655E-derived medium sAPP seems much more sensitive to the temperature block (Fig. III.5, B). Upon 2 h of 20 ºC incubation around 40% of Wt and S655A sAPP were still detected in medium, while medium secretion of S655E sAPP fell to 25% of control levels (incubation at 37 ºC). In fact, when sAPP data at 20 ºC is corrected for the relative APP-GFP transfection rates, the medium S655E sAPP level is half (56.8 ± 12.0%) of Wt levels, while the S655A secretes the same (97.3 ± 7.1%) as the Wt. Hence, at 20 ºC part of Wt and S655A cellular populations are still able to be cleaved to sAPP and secreted while S655E is less able to produce and/or secrete sAPP. In the 20 ºC APP-GFP traffic assay (Fig. III.4, 0 - 2 h) the S655E protein was observed to be apparently more trapped inside post-TGN vesicles, while the Wt and S655A proteins were more blocked at the TGN/Golgi apparatus. Taken these results in consideration, it appears that S655E is mainly cleaved at post-TGN vesicles and/or at the plasma membrane. These are the subcellular locations where, during 2 h of 20 ºC incubation, S655E APP-GFP is trapped (post-TGN vesicles) or has difficulties to reach (plasma membrane).

III. 4. 5 – PMA-INDUCED STIMULATION OF SAPP PRODUCTION

In order to evaluate the PMA stimulatory effects on the APP-GFP proteins processing to sAPP, cells expressing the APP-GFP constructs were treated as described in the previous section (III.4.4), and incubated for 2 h with 0.5 μM PMA at 37 ºC or 20 ºC. Detailed procedures are described in section III.3.4.2 and Table III.1. The 2 h cells and conditioned media were collected, and analyzed by Western blot using the 22C11 antibody (Fig. III.6, A.I and A.II, respectively). The fold-increases in medium secreted sAPP levels, after PMA exposure, are tabulated in Figure III.6, B.I, and represented graphically (Fig. III.6, B.II). Cellular tubulin was also detected in the cells lysates and used as control.

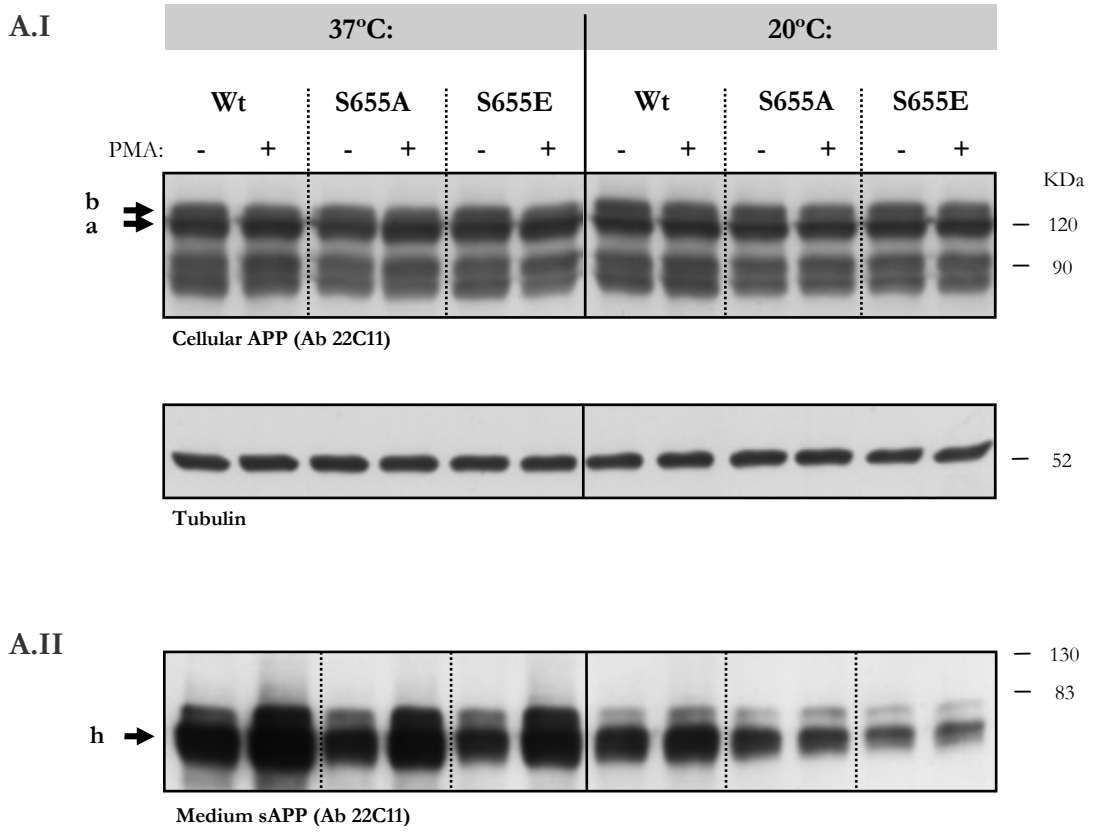

B.I

APP-GFP Species	PMA Effect on sAPP Secretion	
	37 ºC (n=6)	20 ºC (n=3)
Wt	3.15 ± 0.40	1.91 ± 0.07
S655A	2.49 ± 0.17	1.32 ± 0.20
S655E	2.88 ± 0.24	1.43 ± 0.21

B.II

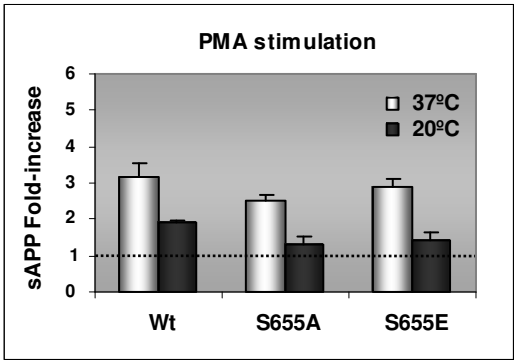

Figure III.6. Temperature-dependent PMA-induced stimulation of APP-GFP cleavage to sAPP. A: Immunoblot analysis of cellular (**A.I**) and medium secreted (**A.II**) sAPP upon cells incubation at 37 ºC or at 20 ºC, in the presence (PMA +) or absence (PMA -) of PMA. Cells lysates were also probed for tubulin as a control (**A.I**). **a** and **b**, immature and mature APP-GFP, respectively; **h**, medium secreted $sAPP_{695}$. **B.I** and **B.II:** Table and Graphic analysis, respectively, of the PMA-induced medium secreted sAPP fold-increases for each of the APP-GFP constructs at 37 ºC and 20 ºC.

Results show that the ability of PMA to stimulate medium sAPP levels is not statistically significantly different for the three APP-GFP constructs. This agrees with previous reported work (Da Cruz e Silva, 1993; Hung and Selkoe, 1994). Nonetheless, both S655A phosphomutants appeared to be less sensible to the PMA-induced stimulus than the Wt protein, in terms of sAPP increased secretion (Fig. III.6, A.II). At 37 ºC, PMA was able to induce a ~3 fold-increase in medium secreted sAPP, but this stimulation decreased markedly at 20 ºC (Fig. III.6, B and C). Hence, part of the cellular mechanism by which PMA stimulates sAPP levels seems to be blocked at 20 ºC. Of note is that, in several cultured lines, a major via of phorbol esters-induction of sAPP levels occurs by activation of TGN intracellular sAPP production and secretion (Kuentzel et al., 1993; Marambaud et al., 1997; Jolly-Tornetta et al Wolf, 2000). Thus, it is possible that formation and/or release of APP and sAPP-containing post-TGN vesicles is part of the PMA stimulatory mechanism, as it is blocked upon 2 h of 20 ºC incubation. This will be further addressed in the following Chapter.

III. 4. 6 – COMPARATIVE ANALYSIS OF ABETA SECRETION

The different times of retention at the TGN/Golgi for the two S655 APP-GFP mutants may result in different extensions of cleavage in the β-secretase pathway. Thus, the following studies addressed the β-secretase processing of the three APP-GFP species, which was evaluated directly by monitoring Abeta production. For this purpose, COS-7 cells expressing the APP-GFP cDNAs (Table III.1 and section III.3.3.3) were incubated for 3 h in the absence or presence of CHX. This time point was chosen, as by 3 h differences were already evident between the three APP-GFP constructs and APP depletion had not become significant. Conditioned media were collected for analysis of Abeta fragments, by means of Immunoprecipitation and separation by urea gel electrophoresis. The respective Immunoblots were probed with an antibody against the Abeta sequence, and the various Abeta forms were quantified by densitometric analysis (Fig. III.7). Experiment A (Fig. III.7, A) was performed in the presence of CHX and experiment B shows the results of three independent experiments performed in the absence of CHX (Fig. III.7, B).

A. Abeta Secretion 3 h with CHX

A.I

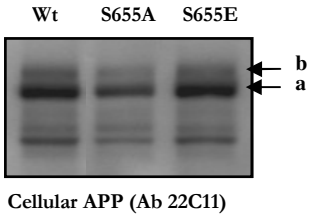

A.II

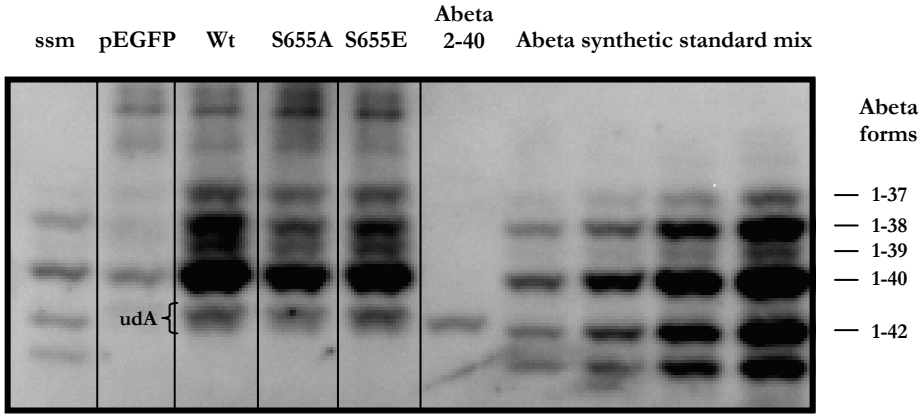

A.III

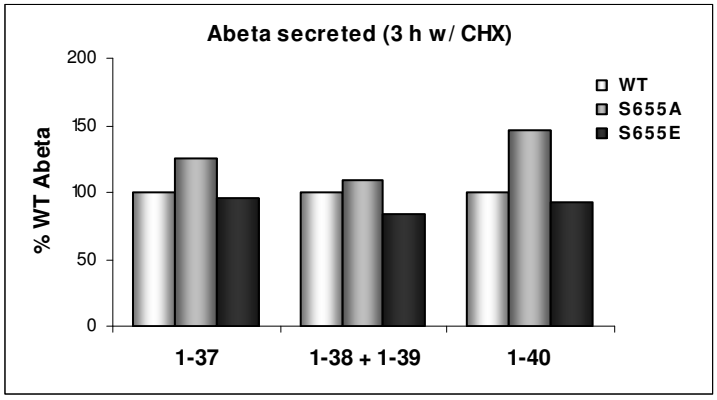

A.IV

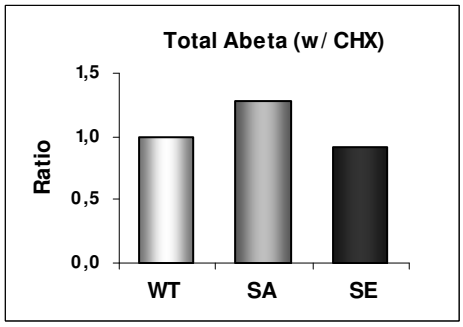

B. Abeta Secretion 3 h without CHX

B.I

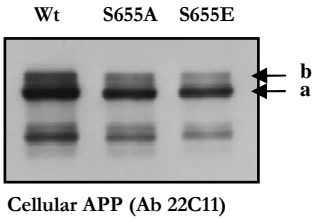

B.II

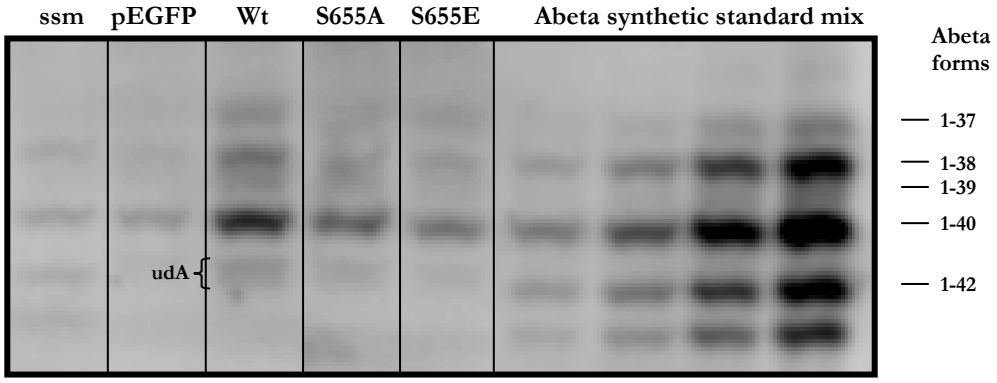

B.III

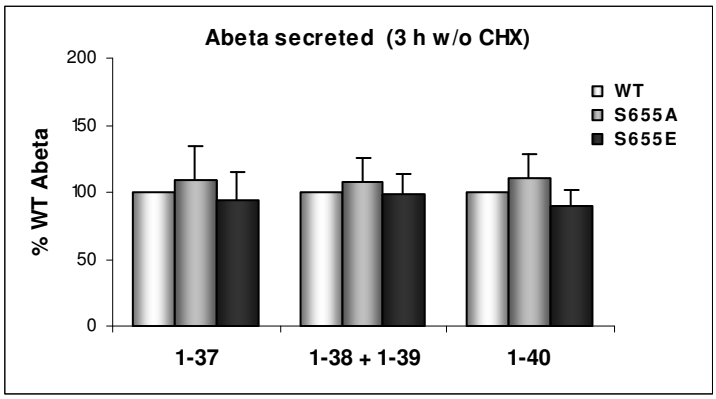

B.IV

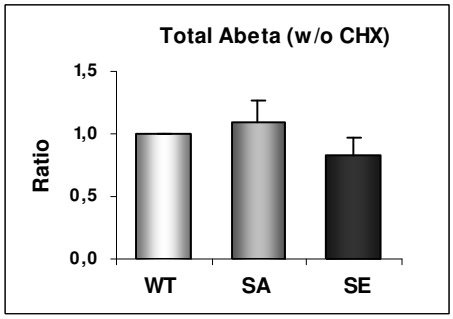

Figure III.7. Abeta secretion. Conditioned medium was collected for 3 h in the presence (**A)** or absence (**B**) of CHX. **I:** Expression of cellular APP-GFP at 0 h; **II:** Immunoblots of media samples detected with Abeta specific antibodies; **ssm,** synthetic standard mix; **udA**, undefined Abeta forms, running between the 1-40 and 1-42 forms. **III and IV:** Graphs plotted with data obtained from the Immunoblots, where Abeta OD values are expressed as a ratio of the Wt OD levels: for each known Abeta form (**III**), or total Abeta forms (**IV**).

The Immunoblots were analysed by densitometry and the S655 mutants O.D. data are plotted as percentages or fold-increases over Wt O.D. data. Figure III.7 A.III and B.III show the relative levels of each of the detected and determined Abeta species as percentages of the respective Wt O.D. value (taken as 100%). Figure III.7 A.IV and B.IV shows the data on total Abeta species (the sum of each individual species), presented as fold-increases of the Wt O.D. sum value (taken as 1). These O.D. data were initially corrected for the relative cellular APP-GFP expression levels (Fig. III.7, A.I and B.I). Of note is the presence of two bands (udA bands) in the Immunoblots, migrating ahead the 1-40 but before the 1-42 Abeta forms, which seem not to correspond to the 2-40 and are still undefined.

Upon CHX exposure (Fig.s III.7, A) both mutants exhibited differences in total Abeta levels, as well as individual Abeta species. Total S655A Abeta production was 1.28 fold higher than Wt, and total S655E Abeta was 0.91 of Wt production. Under these conditions, the S655E Abeta fragments that decreased most were the 1-38 and 1-39 species. For the S655A mutant, the Abeta species which increased more was the 1-40 (fold-increase of 1.50). Unfortunately, only one experiment under CHX exposure was successful, as under these conditions the levels of Abeta produced are low and difficult to measure. Nonetheless, a tendency for S655A to result in higher and S655E in lower Abeta productions could be observed in the absence of CHX (experiment B). In fact, the comparative levels of Abeta secretion for the APP-GFP proteins followed similar patterns, whether monitoring each Abeta species separately (Graph III.7, B.III) or total Abeta (Graph III.7, B.IV). The S655E mutant presented a small decrease of total Abeta production (0.83 $\pm$ 0.13 of Wt values), and a small increase (1.10 $\pm$ 0.17) was observed for the S655A mutant. Although not high, these small differences in the levels of Abeta secreted into the medium for 3 h may be physiologically relevant, bearing in mind that AD is a slow progressive disease.

III. 5 – CONCLUSIONS

In this chapter the cellular fate of the Wt and S655 phosphomutant APP-GFP proteins was analyzed in terms of the APP catabolic pathways, such as restricted cleavages to sAPP and Abeta (directly) and other degradation pathways (indirectly). The major observations taken from these studies were:

1. Mature Wt and S655A proteins are intracellularly catabolized to the same extent, although the S655A mutant presents a slightly shorter half-life. In turn, the S655E mutant presented a longer (doubled) half-life and its catabolism was reduced.

2. The S655E species has a higher and faster rate of αsAPP increase, while the S655A mutant has a slowest rate of αsAPP production and/or secretion.

3. Under CHX exposure, the mature S655E APP-GFP form is catabolized to a lower extent although being highly cleaved by the α-secretase. Hence, S655E seems to be preferentially targeted to the α-secretase pathway.

4. Interestingly, both the time course patterns of cellular Wt mature APP-GFP and Wt medium (total and α) sAPP are initially similar to those obtained for S655E. However, the Wt APP-GFP processing becomes more similar to the S655A processing at the later time points. This strongly suggests that cycles of S655 phosphorylation and dephosphorylation - which can only occur for the Wt APP-GFP protein - are involved in these pathways of APP cellular processing.

5. From the 20 ºC assays, we could observe that the S655E phosphomutant is more committed to be intracellularly packaged into post-TGN vesicles. In parallel, the S655E sAPP production is more severely inhibited at this temperature than for the other two APP-GFP proteins. These results suggest that majority of the S655E proteolytic cleavage to sAPP occurs in subcellular structures involved in the secretory traffic, most probably at post-TGN vesicles or at the plasma membrane.

6. The S655A mutant is apparently less targeted to post-TGN vesicles packaging, as observed from its faster depletion of cytoplasmic vesicles at the TGN/Golgi region upon the 20 ºC temperature block.

7. All the three APP-GFP species were able to respond to the phorbol ester PMA, in terms of enhanced sAPP secretion, with no statistically significantly differences

being observed in the PMA-induced sAPP fold-increases, either at 37 ºC or at 20 ºC. Hence, at least one of the major mechanisms of PMA-induced sAPP stimulation is S655-phosphorylation state independent. Nonetheless, both S655 phosphomutants had a tendency for being less stimulated by PMA to produce sAPP.

8. Additionally to their differential rates of α-secretase processing, the S655 mutants showed a tendency to be differentially cleaved by the β-secretase pathway. Although no statistically significantly differences were observed for 3 h of Abeta medium secretion, during this period the S655A mutant was cleaved at a slight higher extent to Abeta, while the S655E mutant produced slightly less Abeta fragments.

CHAPTER IV

PKC-DEPENDENT APP PROCESSING

CHAPTER IV – PKC-DEPENDENT APP PROCESSING

IV. 1 – INTRODUCTION

Direct and indirect approaches indicate that protein kinase C and protein phosphatases 1 (PP1) are enzymes putatively involved in the "in vivo" phosphorylation/dephosphorylation of the APP S655 residue. Interestingly, these proteins have been also implicated in the regulation of APP proteolytic processing and in the production of the neuroprotective αsAPP fragment, both in cultured cells and in cortical neurons. To date, the intracellular mechanisms of S655 phosphorylation and the protein kinases and phosphatases involved have not been widely studied. Previously, in section III.4.5 (and as reported in da Cruz e Silva et al., 1993), we observed that the αsAPP-stimulation induced by phorbol esters (PE) did not seem altered for the S655 phosphorylation site mutants. Nonetheless, the results do not rule out a physiological relevant association between APP S655 phosphorylation and PE-induced sAPP production.

Several isoforms of PKC are known, some of which have been differentially implicated in AD or in APP proteolytic processing. APP processing by α-secretase can be stimulated by PEs and by intracellular diacylglycerol (DAG) generation. At the same time, classical (Ca^{2+}-dependent) and novel (Ca^{2+}-independent) PKC isozymes, which are both activated by DAG and PEs, have been described to regulate APP processing. For example, specific overexpression of PKCα or PKCε in 3Y1 fibroblast cells led to enhanced levels of αsAPP production (Kinouchi et al., 1995). PKC isoforms are involved in specific intracellular functions, but the different isoforms display little substrate specificity "in vitro". Selective PKC isoform spatial and temporal targeting to subcellular compartments appears to be a mechanism to achieve localization-dependent specificity (Maasch et al., 2000). Translocation of specific PKC isoforms to subcellular membranes allows for activation of the enzyme, as well as for positioning of the enzyme close to its substrate. PE-dependent PKC-activation functions through PKC targeting, in a mechanism both isoform-specific and cell type-dependent (Pascale et al., 1996; Cedazo-Minguez, 1999). PKCα and β1 isoforms were reported to be regulators of α-secretase APP processing in the neocortex with constitutive overactivated PKC (Rossner et al., 2001b). In this model system, both isoforms translocated from the cytosol to the cell membrane, both were responsible for PE-driven enhanced PKC

activity, and for the concomitant αsAPP increased production. Recent findings (Lanni et al., 2004) implicate PKCα and also PKCε in the regulated secretion of αsAPP in SH-SY5Y neuroblastoma cells. PKCα-deficient cells exhibited impaired αsAPP stimulation by PEs, but still responded significantly to carbachol stimulation. For PKCε-deficient cells, the PE response was even more severely impaired, in terms of increased αsAPP levels, and the carbachol-induction of αsAPP secretion was completely blocked (Lanni et al., 2004). In fact, blockade of PKCε activation attenuates the PE-induced αsAPP increase (Yeon et al., 2001; Zhu et al., 2001). Interestingly, the PKCα and PKCε isoforms rapidly translocated to different intracellular compartments in response to PE treatment: PKCα to the plasma membrane and PKCε to the PM and Golgi-like structures (Lanni et al., 2004). These are the two subcellular locations implicated in the APP α-secretase cleavage and αsAPP production. In fact, PKCα and δ but not ε are known to regulate the release of TGN secretory vesicles by inducing vesicle membrane scission from the TGN membrane (Sabatini et al., 1996). PKC was already reported to be involved in the budding and release of post-TGN APP-containing vesicles in a semi-intact PC12 cell system (Xu et al., 1995). More contradictory is the question if PE-induced PKC activation induces higher APP cell surface expression, with reports demonstrating opposite results (e.g., Bullido et al., 1996; Jolly-Tornetta and Wolf, 2000). Nonetheless, in these studies the PKC isozyme(s) involved were not addressed.

The only candidate protein to dephosphorylate S655 is the Ser/Thr protein phosphatase 1, PP1. This protein belongs to the family of the Ser/Thr phosphatases PP1/PP2 (A and B). Three genes encode the ~37 KDa PP1 catalytic subunits (PP1α, β/δ, and γ). The catalytic subunits of Ser/Thr phosphatases share high amino acid sequence homology but exhibit little substrate specificity "in vitro". These enzymes were found to be targeted to their specific "in vivo" substrates by regulatory subunits that are highly specific (for review see e.g. Wera and Hemmings, 1995). The potential use of Ser/Thr PP1 regulatory proteins in AD and other neurodegenerative disorders has been discussed in Tian and Wang (2002) and in da Cruz e Silva et al. (2004a). The PP1/PP2A inhibitor okadaic acid was observed to induce APP cell surface expression in lymphocytes (Bullido et al., 1996). In fact, PP1 was observed to be directly involved in a mechanism of regulation of sAPP production and/or secretion (da Cruz e Silva et al., 1995a). Interestingly, okadaic acid exposure resulted in a 10 fold-increase in S655 phosphorylation levels (Oishi et al., 1997). Therefore, PP1 is of research interest when considering S655 dephosphorylation and its effects on APP processing. A role in APP

processing and Abeta generation was also attributed to another Ser/Thr protein phosphatase: PP2B (or calcineurin). Specific inhibitors of PP2B induce an inhibitory effect on Abeta production similar to PKC activators (Desdouits et al., 1996). PP2B and PKC were suggested to have opposite regulatory effects on a Rab protein (Rab6), which is involved in Golgi exit and Golgi/endosomes intertraffic (Scheper et al., 2004). Interestingly, modulation of Rab6-mediated transport has been shown to affect APP processing (see Scheper et al., 2004). Moreover, PP2B is known to inhibit "in vivo" the PP1 inhibitor DARPP-32 (Mulkey et al., 1994; Yan et al., 1999b), thus potentially leading to PP1 activation. Hence, PP2B is also of interest, being that PP1 and PP2B activities are interconnected.

IV. 2 – AIMS OF THIS CHAPTER

The Ser/Thr kinases and phosphatases involved in APP S655 phosphorylation/dephosphorylation are still elusive, thus the main objectives of this chapter were:

1. To evaluate the subcellular localization of various PKC isozymes and Ser/Thr phosphatases in COS-7 cells, and compare it with APP subcellular distribution.
2. To differentially down-regulate PKCα and PKCε, in order to evaluate the effects on endogenous APP and sAPP levels.
3. To evaluate and compare the degree of co-localization between PKCα and PKCε and the APP-GFP (Wt and S655 phosphomutant) proteins.
4. To evaluate the effect of PKCα and PKCε down-regulation on the subcellular distribution and processing of the APP-GFP proteins.
5. To analyse the relative abundance of PKC isozymes and Ser/Thr phosphatases in rat cortex lysates.

The mechanism(s) by which signal transduction via protein phosphorylation can regulate APP metabolism may include substrate/enzyme co-distribution and phosphorylation-dependent subcellular targeting. Thus, COS-7 cells were first characterized in terms of the presence and subcellular distribution of different PKC isozymes and Ser/Thr phosphatases.

Furthermore, PKCα and PKCε were specifically investigated. These isozymes have been implicated in the regulation of α-secretase APP processing as well as being candidate proteins involved in regulating TGN/Golgi and endocytic functions. In Chapter II we showed that APP TGN and endocytic traffic could be affected by S655 phosphorylation. Hence, COS-7 cells were subject to PDBu long-term exposures for differential PKCα/PKCε down-regulation and APP cellular processing was evaluated under these conditions. Co-localization, subcellular localization, and subcellular processing to sAPP were also evaluated for the APP-GFP species. The cerebral relevance of the enzymes putatively involved in APP S655 phosphorylation/dephosphorylation was also addressed, with the relative abundance of APP, PKC and Ser/Thr phosphatases being evaluated in rat cortex lysates.

IV. 3 – MATERIALS AND METHODS

A list of all solutions and protocols used, as well as other relevant information, is presented in the Appendix. All reagents were of cell culture grade or ultrapure.

IV. 3. 1 – ANTIBODIES

Besides the previously described anti-APP 22C11 and the anti-Syntaxin 6, other primary antibodies used in this study were rabbit polyclonal antibodies against PKC isozymes α, β, γ, δ, ε and ζ (Gibco, BRL), and polyclonal antibodies against the catalytic subunits of PP1α, PP1γ and PP2B (da Cruz e Silva, 1995b). Anti-β-Tubulin (Zymed, Portugal) and anti-APP KPI domain (Chemicon, PG-Hitec) primary antibodies were also used. Secondary antibodies used were horseradish peroxidase-conjugated anti-mouse and anti-rabbit IgGs, and alkaline phosphatase-conjugated anti-rabbit IgGs (Sigma-Aldrich) for colorimetric NBT/BCIP detection (Promega). Texas Red- (Molecular Probes, BD Biosciences) and Fluorescein-conjugated (Calbiochem, VWR International) anti-mouse and anti-rabbit IgGs secondary antibodies were also used for Immunocytochemistry. Antibody dilutions and applications are presented in Table IV.1.

Table IV.1. Antibodies, respective target proteins and specific dilutions used for the different techniques employed: IB., immunoblot; ICC, immunocytochemistry.

Target Protein/Epitope	Primary Antibody	Secondary Antibody
	Assay/Dilution	**Assay/Dilution**
APP N-terminal	**22C11** IB dilution: 1:250 ICC dilution: 1:50	Horseradish Peroxidase-conjugated α-Mouse IgG IB dilution: 1:5000
		Fluorescein-conjugated α-Mouse IgG ICC dilution: 1:50
		Texas Red-conjugated α-Mouse IgG ICC dilution: 1:300
PKC isozymes	**Anti-PKC *x*** IB dilution: 1:2000 ICC dilution: 1:200	Horseradish Peroxidase-conjugated α-Rabbit IgG IB dilution: 1:5000
		Fluorescein-conjugated α-Rabbit IgG ICC dilution: 1:50
		Texas Red-conjugated α-Rabbit IgG ICC dilution: 1:300

Target Protein/Epitope	Primary Antibody Assay/Dilution	Secondary Antibody Assay/Dilution
PP1α	**Anti-PP1α** IB dilution: 1:2500 ICC dilution: 1:50	Horseradish Peroxidase-conjugated α-Rabbit IgG IB dilution: 1:5000
		Fluorescein-conjugated α-Rabbit IgG ICC dilution: 1:50
		Texas Red-conjugated α-Rabbit IgG ICC dilution: 1:300
PP1γ	**Anti-PP1γ** IB dilution: 1:2500 ICC dilution: 1:50	Horseradish Peroxidase-conjugated α-Rabbit IgG IB dilution: 1:5000
		Fluorescein-conjugated α-Rabbit IgG ICC dilution: 1:50
		Texas Red-conjugated α-Rabbit IgG ICC dilution: 1:300
PP2B	**Anti-PP2B** IB dilution: 1:2500 ICC dilution: 1:50	Horseradish Peroxidase-conjugated α-Rabbit IgG IB dilution: 1:5000
		Fluorescein-conjugated α-Rabbit IgG ICC dilution: 1:50
		Texas Red-conjugated α-Rabbit IgG ICC dilution: 1:300

IV. 3. 2 – SUBCELLULAR DISTRIBUTION OF APP, PROTEIN KINASE C ISOFORMS AND SER/THR PROTEIN PHOSPHATASES IN COS-7 CELLS

COS-7 cells were cultured in 100 mm cell culture plates with complete DMEM at 37 ºC and 5% CO_2. For Immunocytochemistry procedures using anti-APP, PKC, or PPs antibodies, cells were further divided into six-well plates containing polyornithine pre-coated glass coverslips, and incubated until ~ 80% confluence was reached. Cells on coverslips were fixed, subject to Immunocytochemistry studies as described in section II.3.4.6, and analysed by epifluorescence microscopy. For the co-localization studies of APP with PKCα, PKCε, PP1α and PP2B, the Wt APP-GFP construct was used. Wt APP-GFP cDNA was transfected into COS-7 cells, as described previously in section II.3.3 and Table II.2.

IV. 3. 3 – APP PROCESSING UPON PKCα AND PKCε DOWN-REGULATION

Monolayers of COS-7 cells approximately 90% confluent were incubated with 1 μM of the phorbol ester phorbol-dibutyrate (PDBu) in DMEM (serum-free) or complete DMEM

(with serum). Cells and conditioned media were collected every two hours for ten hours, into 1% SDS solutions. Samples were further analysed by Immunobloting using the anti-PKC isozyme antibodies, and the 22C11 and 6E10 antibodies.

IV. 3. 4 – APP SUBCELLULAR LOCALIZATION UPON MODULATION OF PKCα AND PKCε LEVELS

The wild-type APP_{695}-GFP construct was transfected into COS-7 cells, as described above (section IV.3.2). Cells were divided into six-well plates containing pre-treated coverslips, and treated with 1 μM PDBu for 8 hours. This was performed in the absence or presence of serum, in order to down-regulate PKCα alone or both PKCα and PKCε, respectively. After this period, cells were fixed, processed for Immunocytochemistry with the anti-Syntaxin 6 antibody (as in section II.4.3), and analysed by epifluorescence microscopy.

IV. 3. 5 – S655 PHOSPHORYLATION-DEPENDENT APP SUBCELLULAR LOCALIZATION AND PROCESSING UPON MODULATION OF PKCα AND PKCε LEVELS

Co-localization of the S655 phosphomutant APP-GFP proteins with PKCα and PKCε under basal conditions was first analysed using the same approach described above for the Wt construct (section IV.3.2). Further analysis focused on S655A and S655E APP-GFP subcellular distribution following 8 h of PKCα down-regulation, or PKCα plus PKCε down-regulation. The same methodology as for the Wt APP-GFP was used (section IV.3.4).

In parallel, the subcellular processing of the APP-GFP constructs was assayed under these conditions. COS-7 cells transfected with the APP-GFP constructs (as in section IV.3.2) were divided into six-well plates and incubated with 1 μM of PDBu under the presence or absence of serum. Conditioned media was first collected at 2 h of PDBu exposure and substituted by equal PDBu-containing fresh media. Upon a total of 8 h of exposure to PDBu, cells and conditioned media were collected into 1% SDS solutions. Samples were further analysed by Immunobloting using the 22C11 antibody.

IV. 3. 6 – APP, PKCS AND PPS EXPRESSSION IN RAT CORTICAL LYSATES

To evaluate APP, PKC isozymes and PP1/PP2B expression in rat cortex, 1% SDS lysates from young adult male rats were comparatively analysed with mass-normalized COS

cells lysates by Immunoblotting. The anti-PKCs and anti-PPs primary antibodies were used in addition to the anti-APP N-terminal and anti-APP KPI domain antibodies.

IV. 3. 7 – SDS-PAGE, IMMUNODETECTION AND DATA ANALYSIS

Total protein concentration was determined as described previously (section III.3.6). Mass-normalized aliquots were subjected to 7.5% (APP and sAPP detection) or 12% (PKCs and PPs detection) SDS-PAGE, and to Immunoblot procedures using the primary antibodies specified above (described in Appendix II). Immunodetection was accomplished using horseradish peroxidase-conjugated secondary antibodies and the ECL detection system. For Tubulin detection, alkaline phosphatase-conjugated antibodies and a colorimetric system (NBT-BCIP) were used. Protein band quantification was performed as described previously in section III.3.6. Data are expressed as mean ± SEM (Standard Error of the Mean) of triplicate determinations from at least three independent experiments. Statistical significance analysis was conducted by ANOVA followed by the two-tail Student's t test (endogenous APP assays) or the Tuckey test (APP-GFP proteins assays). Statistical significance symbols used were (*) for statistically significant differences against control determinations or against Wt APP-GFP data, and ($^{+}$) for statistically significant differences between the two S655 APP-GFP phosphomutants data. Statistical significance levels are presented as ($*/^{+}$), for $p < 0.05$; ($**/^{++}$), for $p < 0.01$; and ($***/^{+++}$), for $p < 0.001$.

IV. 4 – RESULTS AND DISCUSSION

IV. 4. 1 – SUBCELLULAR DISTRIBUTION OF APP, PROTEIN KINASE C ISOFORMS AND SER/THR PROTEIN PHOSPHATASES IN COS-7 CELLS

The subcellular distributions of PKC isozymes and Ser/Thr protein phosphatases putatively involved in APP S655 "in vivo" phosphorylation were analysed in COS-7 cells and compared with endogenous APP distribution (Fig. IV.1). Cells were subject to Immunocytochemistry procedures using the 22C11 antibody against APP or specific antibodies against six different PKC isozymes [conventional (α, β, γ); novel (δ, ε); and atipical (ζ)], and three Ser/Thr protein phosphatases (PP1α, PP1γ and PP2B).

The subcellular distribution of endogenous APP (Fig. IV.1, A) revealed to be similar to the previously observed Wt APP-GFP distribution (Chapter II), and as reported for other cultured cell lines (e.g. Peraus et al., 1997; Kouchi et al., 1998). APP is therefore present mainly at perinuclear structures, namely the Golgi (G) and the ER, and throughout the cytoplasm in small vesicles and in smooth ER-like tubular structures. Faded localization at the plasma membrane is observed only in some cells.

For PKC isozymes, PKCα and PKCε isozymes were the most easily detected PKC isoforms in COS-7 cells (Fig. IV.I, B). The β and ζ isozymes were detected but at low levels, and the γ and δ were not detectable (Fig. IV.I, C) with these immunocytochemistry procedures. Of note is that these γ and δ isozymes have not been particularly associated with APP processing. Figure IV.I B, reveals that the PKC isozymes have isoform-specific distributions, but are all nuclear enriched. The PKCα and PKCε isoforms are found speckled in the nucleus (N), but excluded from the nucleolus (Nu), in cytoplasmic vesicular structures (CVS) and at the plasma membrane (PM). The β and ζ isoforms are mainly found at the nucleus, being concentrated at nucleolar (Nu)-like structures.

The three Ser/Thr protein phosphatases studied are all nucleus-enriched, with PP1γ being the only one present at the nucleolus (Fig. IV.I, D). Of note is that PP1α and PP2B nuclear staining is speckled. Additionally, PPs are also found at cytoplasmic locations, with PP1α and PP2B being found in cytoplasmic vesicular structures. Of note is that PP2B is the phosphatase tested that is found in a higher number of cytoplasmic vesicles, and that it is also distinctly visible at cells plasma membrane.

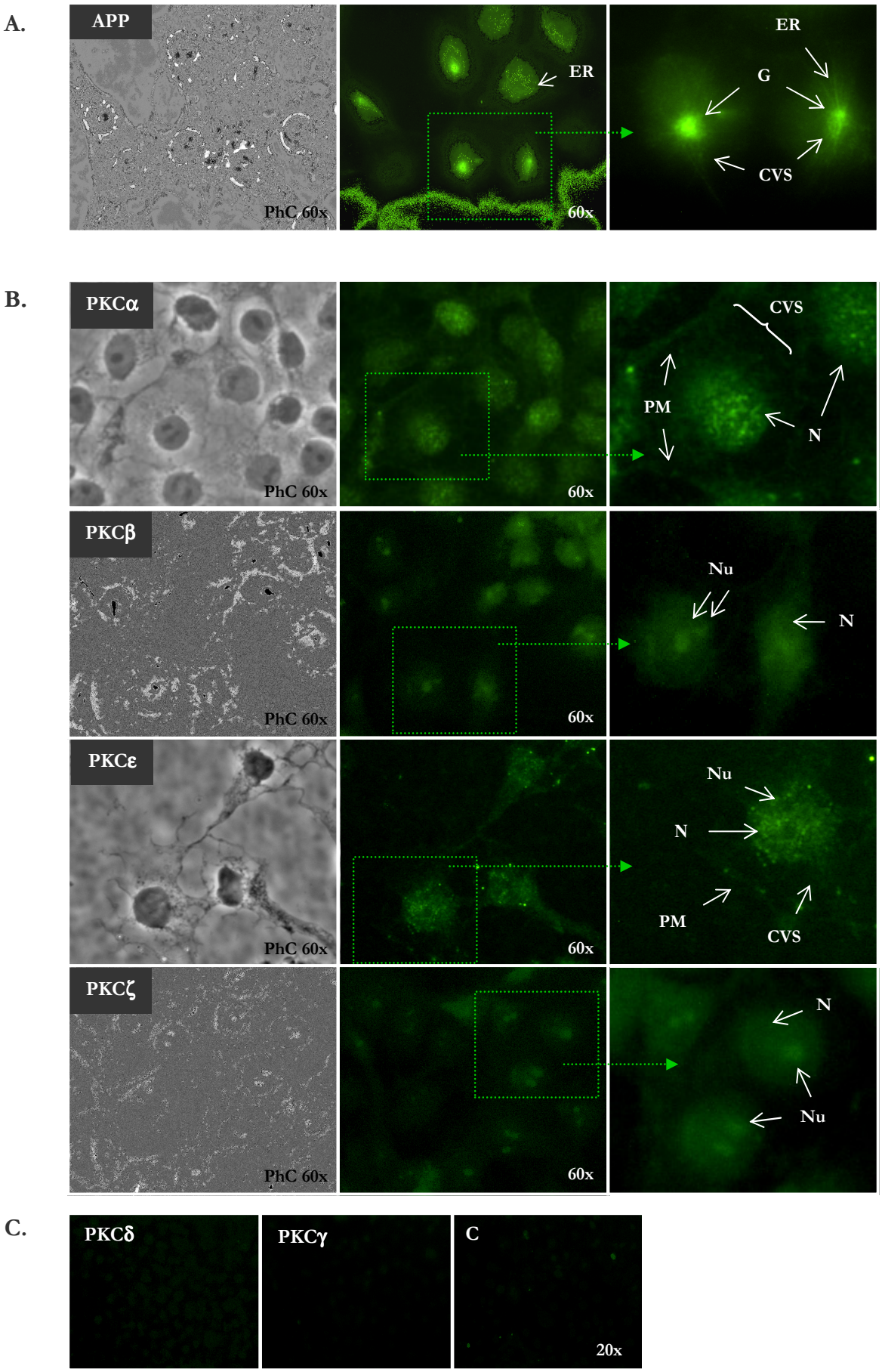
A.
APP
PhC 60x
ER
60x
ER
G
CVS
B.
PKCα
PhC 60x
60x
CVS
PM
N
PKCβ
PhC 60x
60x
Nu
N
PKCε
PhC 60x
60x
Nu
N
PM
CVS
PKCζ
PhC 60x
60x
N
Nu
C.
PKCδ
PKCγ
C
20x

D.

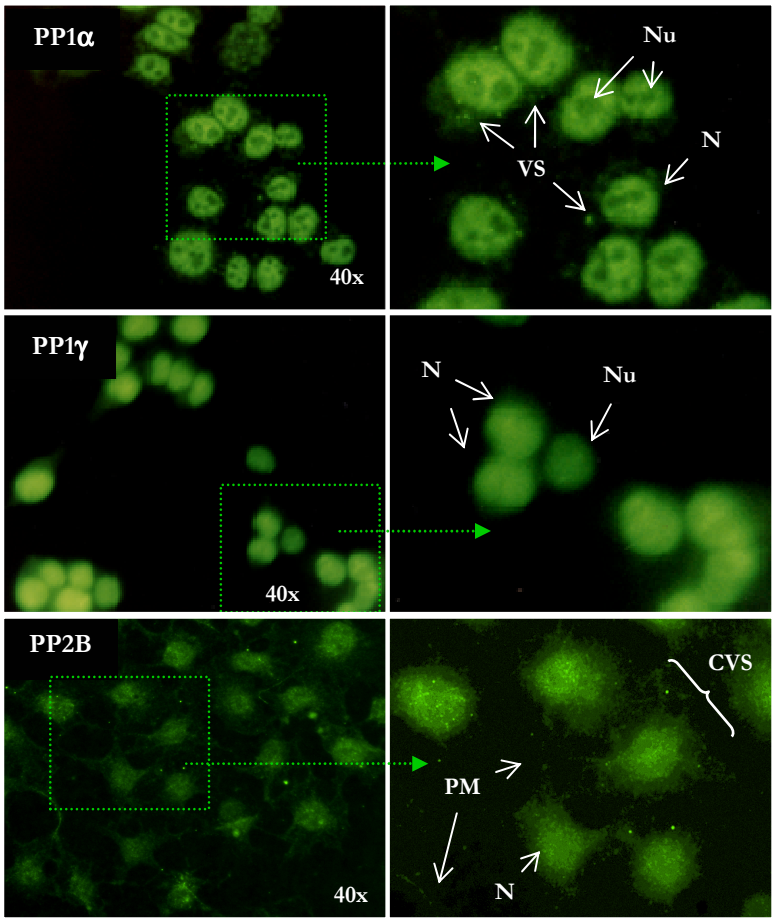

Figure IV.1. Immunocytochemistry analysis of COS-7 cells endogenous subcellular distribution of A: APP; B: Four PKC isozymes (α, β, ε, and ζ; detectable) C: Two PKC isozymes (γ and δ; absent); D: Three Ser/Thr phosphatases. G, Golgi region; **ER,** endoplasmic reticulum; **PM,** plasma membrane; **N,** nucleus; **Nu,** nucleolus; **CVS,** cytoplasmic vesicular structures. **C,** control cells subject to Immnunocytochemistry procedures with secondary antibody only. **PhC**, Phase constrast.

Further analysis focused on the putative co-localization of Wt APP-GFP with PKCα, PKCε, PP1α and PP2B (Fig. IV.2). These were the PKC and phosphatase proteins that were both easily detected in COS-7 cells and found to be distributed at known sites of APP processing: cytoplasmic vesicles and PM (Fig. IV.1). Wt APP-GFP seems to have some co-localization (arrows in the overlay panel) with PKCα at the Golgi region and at very few cytoplasmic vesicles (Fig. IV.2, A). PKCε immunoreactivity was mainly observed in nuclear speckles, but also in small cytoplasmic vesicles, in this case concentrated at or near the Golgi area (Fig. IV.2, B). Wt APP-GFP and PKCε were found to co-localize in some of these Golgi vesicles. Figure IV.2 C shows that PP1α and Wt APP-GFP apparently only co-localize in some punctate structures at the PM. In addition, very few cytoplasmic vesicles were found to

be both positive for Wt APP-GFP and PP2B, and although some of these were found near the PM (Fig. IV.2, D), PP2B does not seem to co-localize with Wt APP-GFP specifically at the PM.

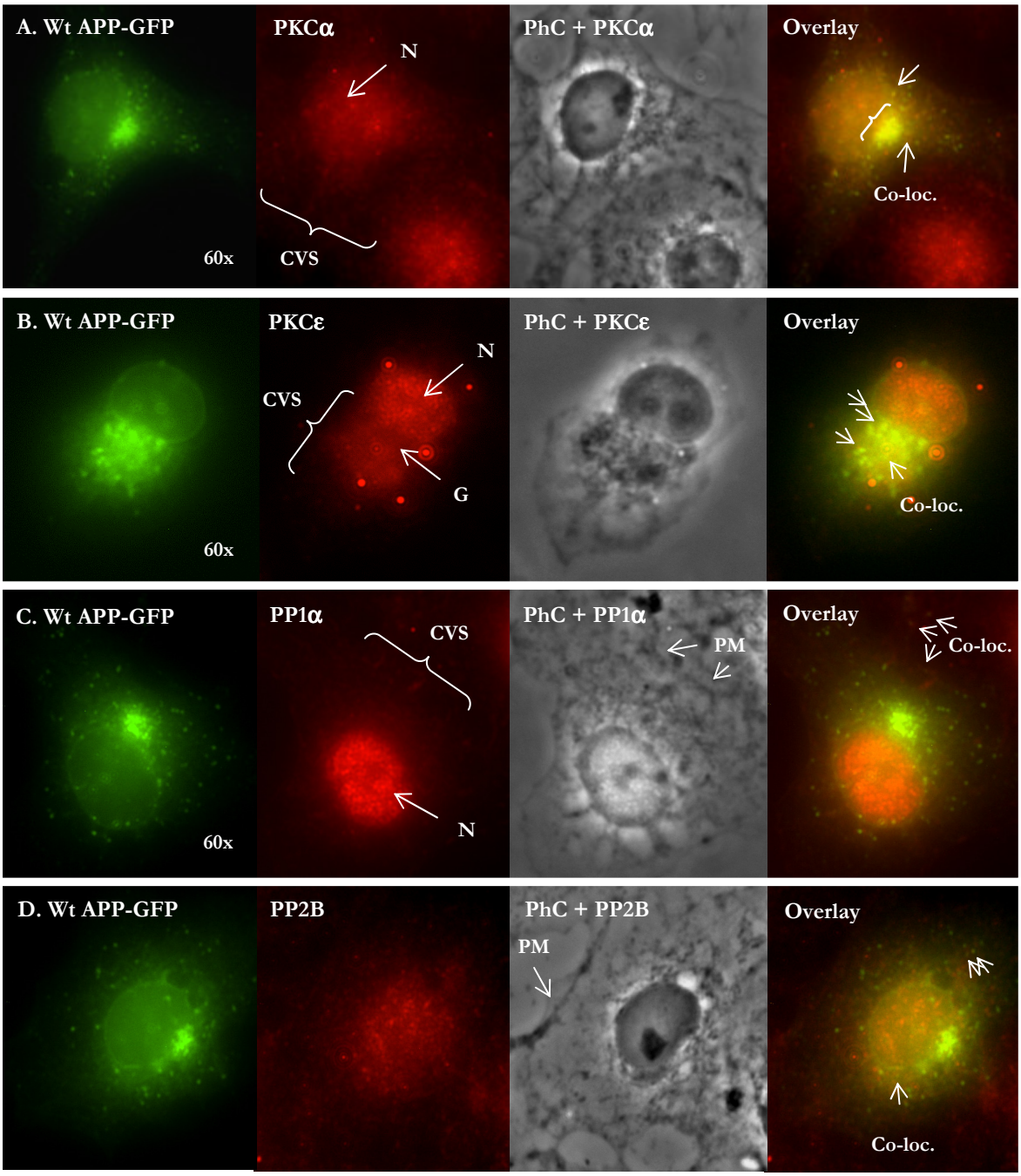

Figure IV.2. Co-localization of Wt APP-GFP with PKCα (A), PKCε (B), PP1α (C) and PP2B (D). COS-7 cells transfected with the Wt APP-GFP construct were subject to immunocytochemistry procedures using Texas Red-conjugated secondary antibody for PKCs and phosphatases detection. **CVS,** cytoplasmic vesicular structures; **G,** Golgi area; **PM,** plasma membrane; **N,** nucleus.

IV. 4. 2 – PKCα AND PKCε DIFFERENTIAL DOWN-REGULATION, AND THE EFFECT ON CELLULAR APP

Previous observations from our group and others (e.g. Bourgoin et al., 1996) indicate that expression of different PKC isozymes, namely PKCα and PKCε, can be differentially modulated upon exposure to phorbol esters, such as PMA or PDBu. Thus, this approach was used to evaluate PKCα and PKCε involvement in APP cellular processing (see section IV.3.3 for details). First, the expression levels of four PKC isozymes (α, β, ε and ζ) were monitored upon COS-7 cells treatment with 1μM PDBu, in a time-dependent manner, and both in the absence or presence of serum (Fig. IV.3). Cellular Tubulin levels were used as control.

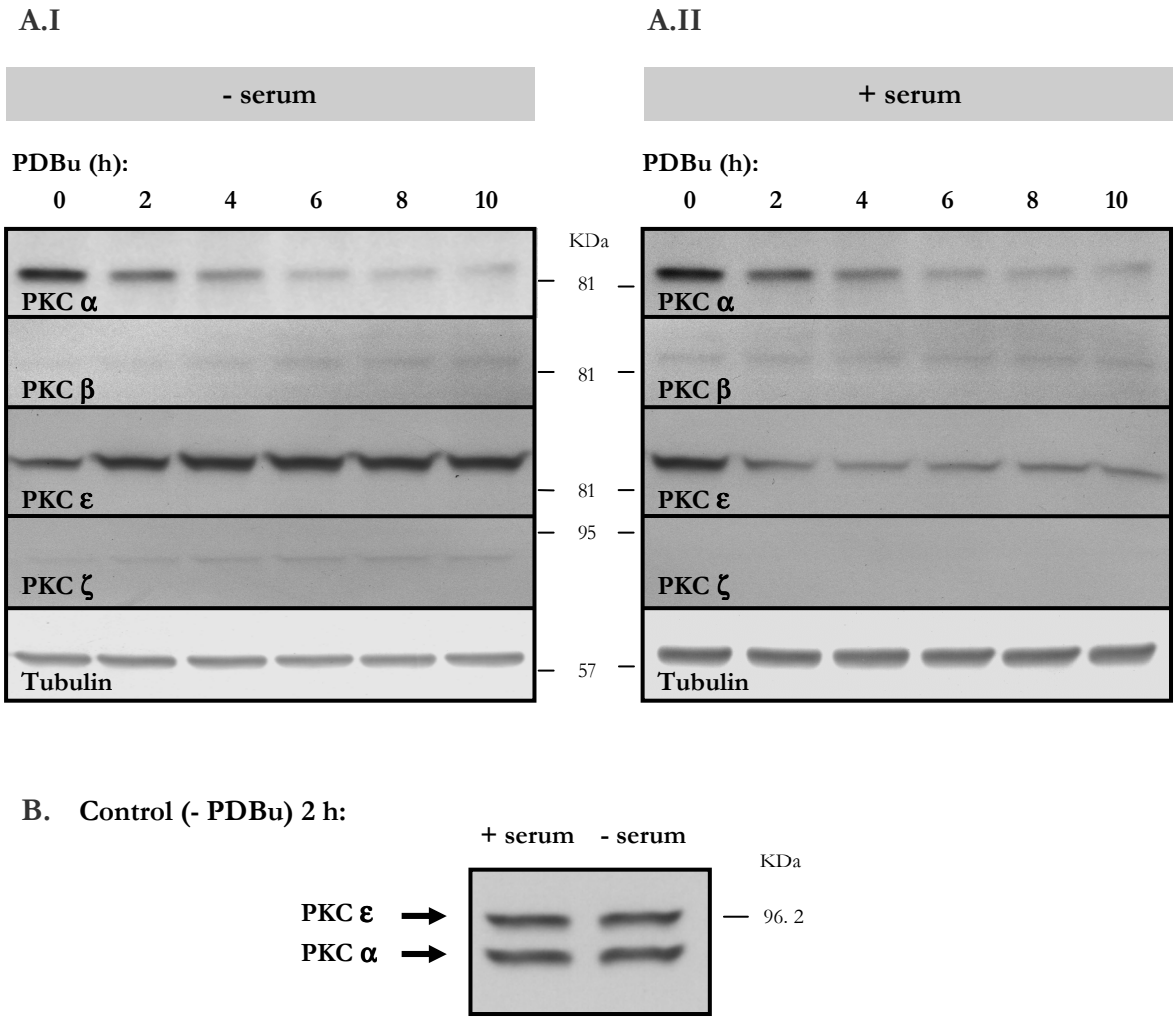

Figure IV.3. PKC isozyme protein expression levels upon exposure to PDBu. Immunoblot analysis of experiments carried out in DMEM, without serum (**A.I**) or in complete DMEM (**A.II**). Tubulin expression levels were monitored as a control. **B:** The cellular levels of PKCα and PKCε were analysed in COS-7 cells lysates maintained in DMEM with or without serum for 2 hours.

During PDBu exposure in the absence of serum the only isozyme found to be down-regulated was PKCα, the levels of the β and ζ isozymes increased slightly, and PKCε was up-regulated (Fig. IV.3, A.I). In contrast, PDBu addition in the presence of serum, both the PKCα and ε isozymes were down-regulated (Fig. IV.3, A.II). The levels of the β isozyme were found to be unaffected with time, and the ζ isozyme was barely detected. The main differences in the PKCα and ε isozymes levels were found immediately upon 2 hours of PDBu exposure. In minus serum conditions PKCα decreased to less than half of its initial levels and PKCε increased by 70%, while in plus serum conditions both isozymes decreased to 60 and 30%, respectively. These effects were PDBu specific as the withdrawal of serum alone did not result in PKC levels alterations (Fig. IV.4, B). Subsequently, the effects of these PKCα and PKC(α+ε) down-regulation on holo APP levels (Fig. IV.4) were analysed.

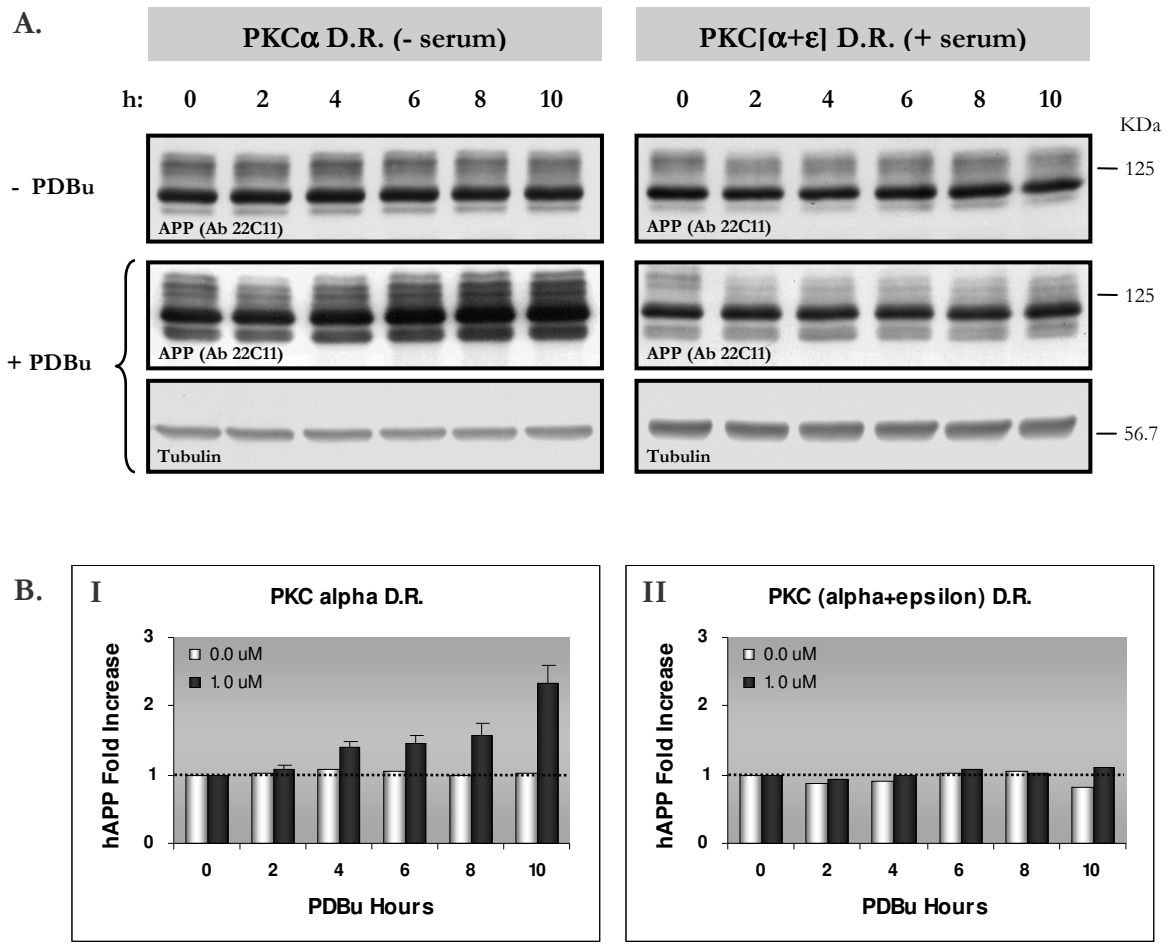

Figure IV.4. Effect of PDBu mediated PKC alpha and epsilon down-regulation (D.R.) on intracellular levels of holo APP. A: Immunoblots of endogenous holo APP with time, in the absence (left panel, n=3) or presence (right panel, n=2) of serum in the medium. **B:** Graphic representation of the PDBu-dependent fold-increase in holo APP levels, over the respective level at 0:00 h, in the absence (**I**) or presence (**II**) of serum.

With increasing periods of exposure to PDBu there was a significant increase in the intracellular levels of endogenous APP (Fig. IV.4, A - left panel - and B.I), but only in the absence of serum. This effect was dependent on the period of exposure and also on the concentration of PDBu (data not shown) with maximal levels of expression (2.33 ± 0.33 fold-increase) for 1 μM PDBu and 10 h of exposure (Fig. IV.4, B.I). In the presence of serum, intracellular holo APP levels are unaffected with time, either in the absence or presence of PDBu (Fig. IV.4, B.II). Being that in the presence of serum PKCε levels are additionally down-regulated, these suggest that PKCε is implicated in the holo APP increase. Friedman et al (1997) have also observed a PMA dose-dependent up-regulation of APP levels in PC12 cells, which appeared related to differential down-regulation of PKC isozymes. Up-regulation of the *app* gene may account for this up-regulation effect, as PDBu is documented to affect the AP-1 promoter resulting in increased APP mRNA levels (Trejo et al., 1994). In fact, both PKCα and PKCε have been reported to regulate transactivation of the AP-1 promoter, but with prevalence for the epsilon isozyme (Uberall et al., 1994; Soh et al., 2003). Hence, in the light of the results, PKCε may be involved in the APP mRNA up-regulation. In addition, PKCε may also be involved in APP recycling pathways and enhance APP half-life by potentially "rescuing" it from degradation. In fact, a possible route of endosomes-to-TGN retrieval is Rab6-dependent (Mallard et al., 2002) and, interestingly, Rab6-mediated transport is up-regulated by PKC and affects APP processing (Scheper et al., 2004). Furthermore, PKCε has been specifically implicated in the regulation of endocytic and Golgi-related processes (Lehel et al., 1995; Hoy et al., 2003).

IV. 4. 3 – PKCα AND PKCε IN APP REGULATED CLEAVAGE TO sAPP

Further analysis addressed the processing of endogenous APP to medium secreted sAPP under the conditions of differential PKC alpha and epsilon down-regulation, by means of Immunoblotting procedures. The accumulative secretion of sAPP under PDBu exposure was analysed in a time-dependent manner and compared with control secretion (Fig. IV.5).

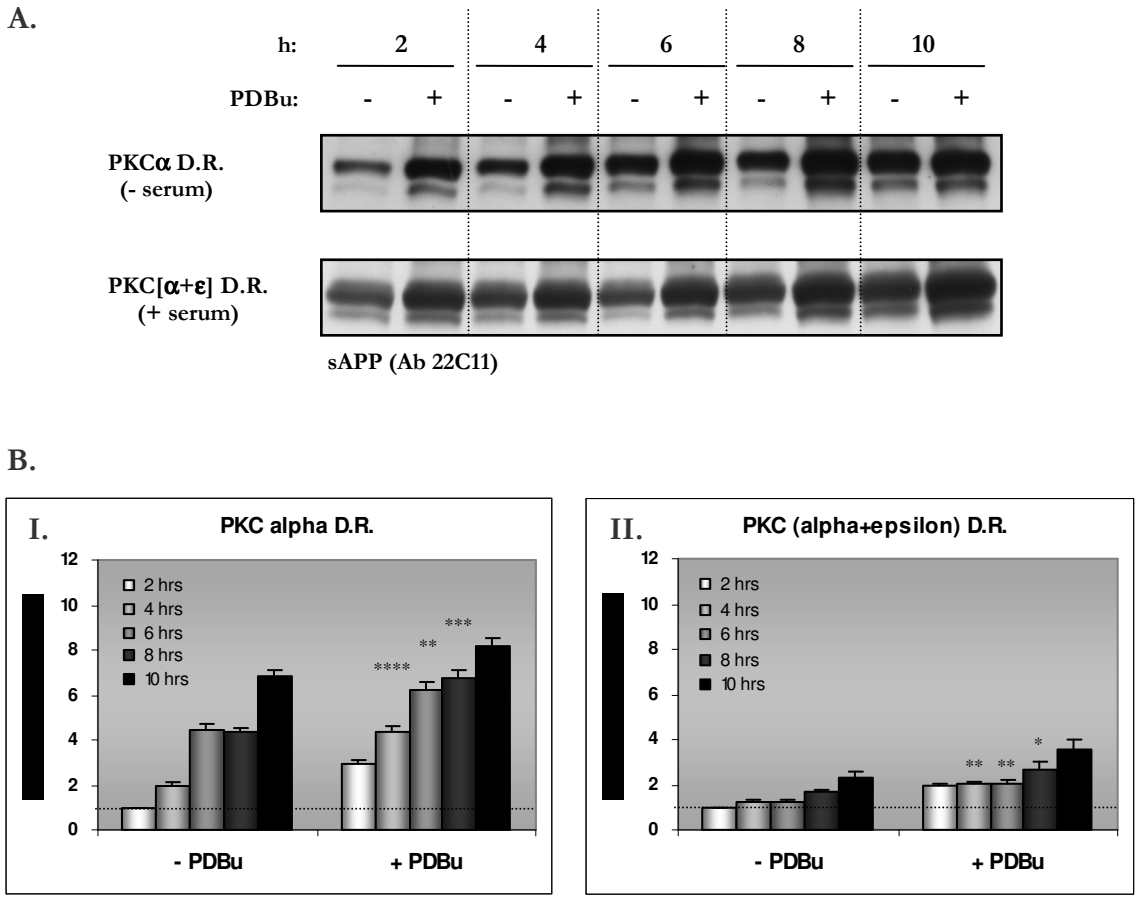

Figure IV.5. Effects of PKC down-regulation (D.R.) on sAPP production in a time-dependent manner. A: Immunoblots of sAPP cumulative secretion in the absence or presence of PDBu and serum. **B.I and II:** Quantitative analysis of the sAPP levels with time and in the absence or presence of serum, respectively. Data are presented in terms of fold-increase, where control (- PDBu) sAPP levels at 2:00 h are taken as 1.

Following exposure of cells to PDBu, the levels of medium secreted sAPP are increased at all time points of drug exposure, both in the absence or presence of serum (Fig. IV.5, A and B). These increases were confirmed to be mainly due to the αsAPP fragment, as observed by Immunoblot analysis with the 6E10 antibody (data not shown). For a quantitative analysis, O.D. data from the sAPP bands densitometric analysis were plotted in Figures IV.5 BI and B.II, as fold-increases over the initial control sAPP levels at 2:00 h. Results following 2 hours of PDBu exposure show that while in serum-free conditions PDBu is able to increase sAPP levels by three-fold (2.91 ± 0.24), when serum is present the increase is less and about two-fold (2.15 ± 0.15) (Fig. IV.5, B.I and B.II). Of note is that the presence of serum alone has an up-regulating effect on sAPP secretion (compare control 2 h sAPP levels at Fig. IV.5, A). Following the 2 h initial period, the PDBu-induced fold-increase in sAPP secretion (over control levels at the same time point) appears to slowly decrease with time of PDBu exposure.

In fact, at 10 hours of PDBu exposure the accumulative sAPP levels are no longer statistically significantly different from control levels, for both serum conditions. These results suggest that there is a lost of the ability of PDBu to stimulate sAPP production/secretion with time. Work from our lab revealed that after cells exposure to PDBu for the above time points, posterior additions of PDBu have gradually decreasing stimulatory effects on sAPP (da Cruz e Silva et al., in preparation). This study was only performed in the absence of serum. Hence, there is a gradual loss of further PDBu stimulation ("acute" stimulation following prolonged PDBu exposure) that correlates well with the decrease in PKCα levels (Fig. IV.3, A.I). PKCα may be involved in part of the stimulatory mechanism of PE action on sAPP levels, with this question being further addressed below in section IV.4.5.3.

IV. 4. 4 – Effect of Modulating PKCα and PKCε on APP Subcellular Localization

Along with the observed consequences that down-regulating PKCα alone or PKCα and PKCε had on APP cellular processing, further analysis focused on the effects that these down-regulations may have on APP subcellular localization. Transfection with the Wt APP_{695}-GFP was thus used (method described in section IV.3.4), and its subcellular localization monitored following 8:00 h exposure to PDBu in the absence or presence of serum (Fig. IV.6).

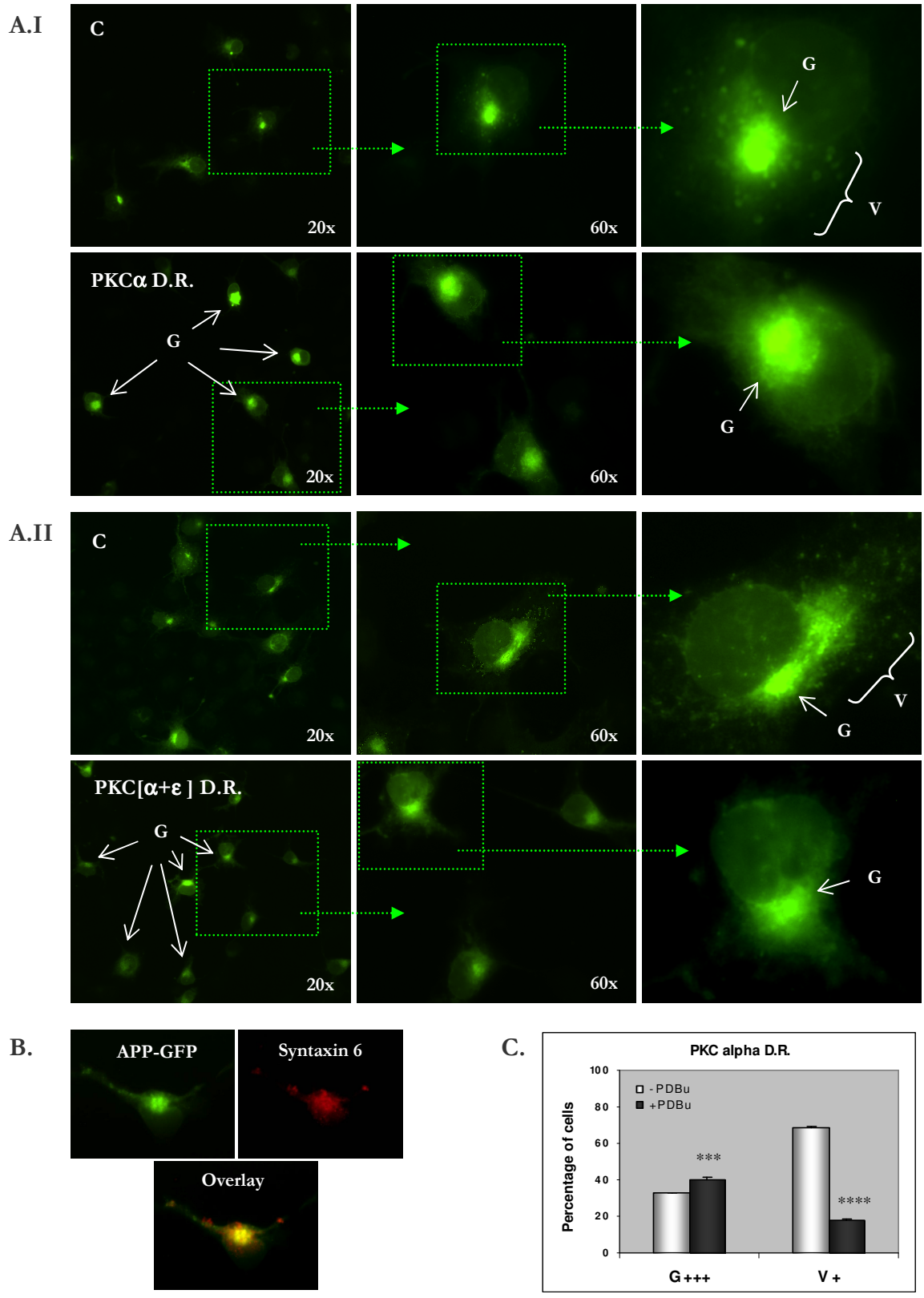

Figure IV.6. Effect of PKC alpha down-regulation and PKC epsilon up- or down-regulation (D.R.) in the subcellular localization of Wt APP-GFP in COS-7 cells. A: in the absence (C) or presence of PDBu (PDBu) for 8 hours, and in the absence of serum (**A.I**) or in the presence of serum (**A.II**). **G,** Golgi apparatus; **V,** cytoplasmic vesicles. **B:** Co-localization of Wt APP-GFP with the TGN/Golgi marker Syntaxin 6. **C:** The percentages of cells with high green fluorescence intensity at the Golgi (G+++) or presenting green fluorescent cytoplasmic vesicles (V+) were scored in serum-free conditions (PKC alpha D.R.).

In the absence of serum and upon 8:00 h of exposure to PDBu, the number of cytoplasmic vesicles per cell decreased dramatically (Fig. IV.6, A.I). In fact, there was a drop in the number of cells with a significant number of fluorescent cytoplasmic vesicles from 70% to 18% (Fig. IV.6, C). PDBu treatment also caused the number of cells with high fluorescing Golgi to increase marginally, and more significantly the fluorescence in the Golgi became more intense, rather suggesting swelling of this structure (Fig.s IV.6, A.I and C). Co-localization of this subcellular structure with Syntaxin 6 confirmed its identity as the TGN/Golgi (Fig. IV.6, B). Thus, decreased APP trafficking via vesicle formation upon PDBu exposure and down-regulation of PKCα is evident. When this assay was performed in the presence of serum (Fig. IV.6, A.II), the resulting PDBu-induced phenotype was very similar in terms of a high decrease in the number of cytoplasmic fluorescent vesicles. Nonetheless, in serum-plus conditions the number of cells with intense Golgi did not appear to increase as much, and this structure did not swell dramatically as in the absence of serum. In fact, scoring the number of cells with swelled Golgi structures resulted in 67.4 ± 1.5% for the serum-free condition but only 22.2 ± 3.5% ($p < 0.0001$) for the serum-plus condition. The absence of Golgi swelling and the lower increase in fluorescence intensity indicates that less APP is trapped in this organelle.

These results suggest the involvement of PKCα in APP TGN/Golgi exit, with its down-regulation leading to inhibition of APP packaging and/or export into post-TGN secretory vesicles. This is in agreement with previous findings indicating a central role for PKC in the control of constitutive and regulated APP Golgi exit (Xu et al., 1995), and a role for PKCα, but not ε, in the formation and budding of post-TGN vesicles (Bourgoin et al., 1996; Sabatini et al., 1996, Singer et al., 1996). The decrease in APP cytoplasmic vesicles, induced by PKCα down-regulation, seems therefore to be the cause of the previously observed gradual loss of acute PDBu-induced sAPP stimulation with time of PDBu exposure. Thus, a mechanism by which phorbol esters induce sAPP levels includes stimulation of the budding of TGN APP-containing vesicles, in a PKCα-dependent manner.

Additionally, the observed absence of Golgi swelling and lower Golgi intensity when serum and PDBu are both present (and both PKC isozymes are down-regulated), indicates a lower APP Golgi population under these conditions. Previously we have observed that the PKCε isozyme seems to be implicated in APP up-regulation (Fig. IV.4), and under conditions of PKCε D.R. (serum-plus) the APP levels are lower than under PKCε U.R. (serum-free) conditions. Furthermore, the PKCε isozyme has been implicated in positive regulation of the

endocytic processing and is putatively involved in PM-to-TGN retrograde traffic (as previously observed in section IV.4.2). Supporting this hypothesis are the findings that upon phorbol ester exposure, PKCε is rapidly activated and up-regulates endocytosis, while PKCα is activated later and inhibits the initial PKCε effect on endocytosis (Song et al., 2002). Further, in response to phorbol ester treatment, PKCα was reported to translocate to the plasma membrane and PKCε to Golgi-like structures (Lanni et al., 2004).

IV. 4. 5 – S655 PHOSPHORYLATION-DEPENDENT APP CELLULAR FATE UPON MODULATION OF PKCα AND PKCε LEVELS

Further work focused on the putative involvement of S655 phosphorylation in PKC-dependent APP cellular traffic and processing. For that, the subcellular localization and proteolytic processing of the S655 phosphomutants and Wt APP-GFP proteins were comparatively analysed under normal conditions or under conditions of PKCα specific or PKCα and PKCε down-regulation (see section IV.3.5 for procedure details).

IV. 4. 5. 1 – S655 phosphomutants subcellular co-localization with PKCα and PKCε

The subcellular co-localization of the three APP-GFP species with both PKCα and PKCε proteins, under normal conditions, was first addressed. For that, COS-7 cells transfected with the APP-GFP constructs were grown on coverslips and subject to Immunocytochemistry procedures using specific antibodies for PKCα and PKCε isozymes and Texas Red labelling (Fig. IV.7).

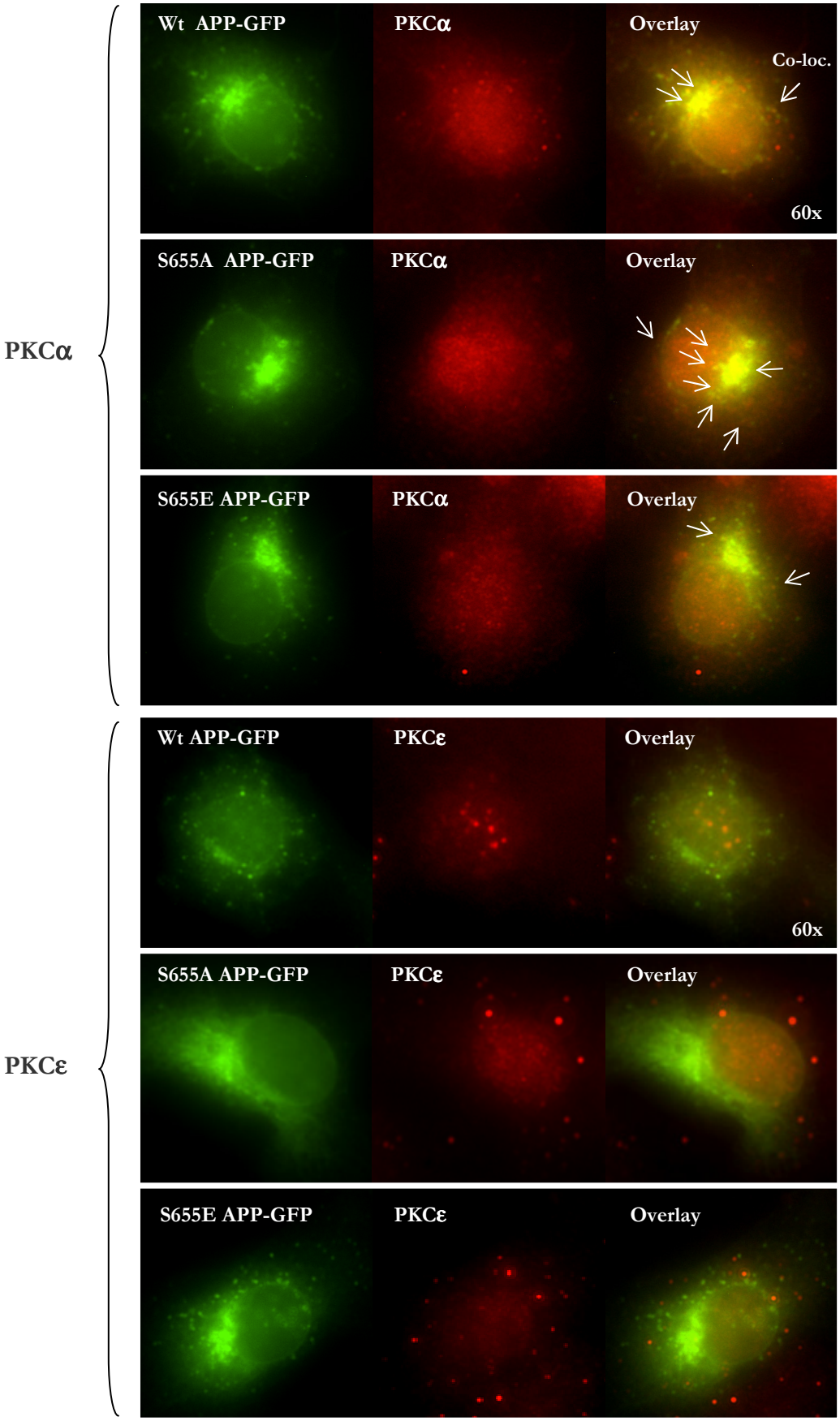

Figure IV.7. Wt and S655 phosphomutants APP-GFP subcellular co-localization with PKCα and PKCε (red labelled). Arrows in overlay microphotographs indicate vesicular structures with co-localization.

Immunocytochemistry results show that APP-GFP green and PKCα red fluorescence (Fig. IV.7, upper panel) seem to co-localize in few small cytoplasmic vesicles per cell, near the Golgi region (white arrows). Analysis of the co-localization leads to the suggestion that the S655A mutant might present a higher co-localization degree with this isozyme. The S655E protein, however, has an apparent lower degree of co-localization and is similar to the Wt APP-GFP. In contrast, the three APP-GFP proteins appear not to co-localize with nuclear PKCε speckles, and other PKCε-positive structures are difficult to visualize (Fig. IV.7, lower panel). As the cytoplasmic vesicles of both these PKC isozymes are very small, further co-localization studies will be forthcoming using confocal microscopy procedures.

IV. 4. 5. 2 – S655 phosphomutant subcellular distribution upon PKCα and PKCε D.R.

The subcellular distribution of the S655 phosphomutants upon modulation of PKCα levels alone, or PKCα and PKCε down-regulation was also addressed. Briefly, cells expressing the APP-GFP constructs were exposed for 8 h to 1 μM PDBu, in the absence or presence of serum. Cells were subsequently subjected to Immunocytochemistry analysis using the anti-APP 22C11 antibody, which allows for APP-GFP and endogenous APP detection (Fig. IV.8).

Epifluorescence analysis revealed that for the three APP-GFP species there is a sharp decrease in the number of APP cytoplasmic vesicles after 8 h of PDBu exposure, similar to that previously observed for the Wt (Fig. IV.6). In serum-free conditions (upper panel) higher Golgi fluorescence intensity and Golgi swelling is observed for the three APP-GFP species. In serum-plus conditions (Fig. IV.8, lower panel), these Golgi PDBu-induced features appear less severe for the Wt and S655A species, although this is not so evident for the S655E mutant. Immunocytochemistry analysis (Fig. IV.8, 22C11 microphotographs) revealed an almost completely overlap between the subcellular distributions of endogenous APP and APP-GFP, although the red fluorescence was more intense. These confirmed holo APP-GFP species and endogenous APP Golgi retention under conditions where PKCα levels are highly decreased (Fig. IV.3). PKCα seems therefore to be involved in APP incorporation into TGN vesicles in an S655-phosphorylation independent manner. The low levels of APP-GFP and PKCα co-localization (Fig. IV.7, overlay panel) further suggest that the mechanism of action of PKCα is fast and transient. Of note is that the S655A mutant has an apparent higher co-localization with PKCα at cytoplasmic vesicles near the Golgi, consistent with S655A impaired and delayed Golgi exit, and with more time spent on S655A incorporation into post-TGN vesicles.

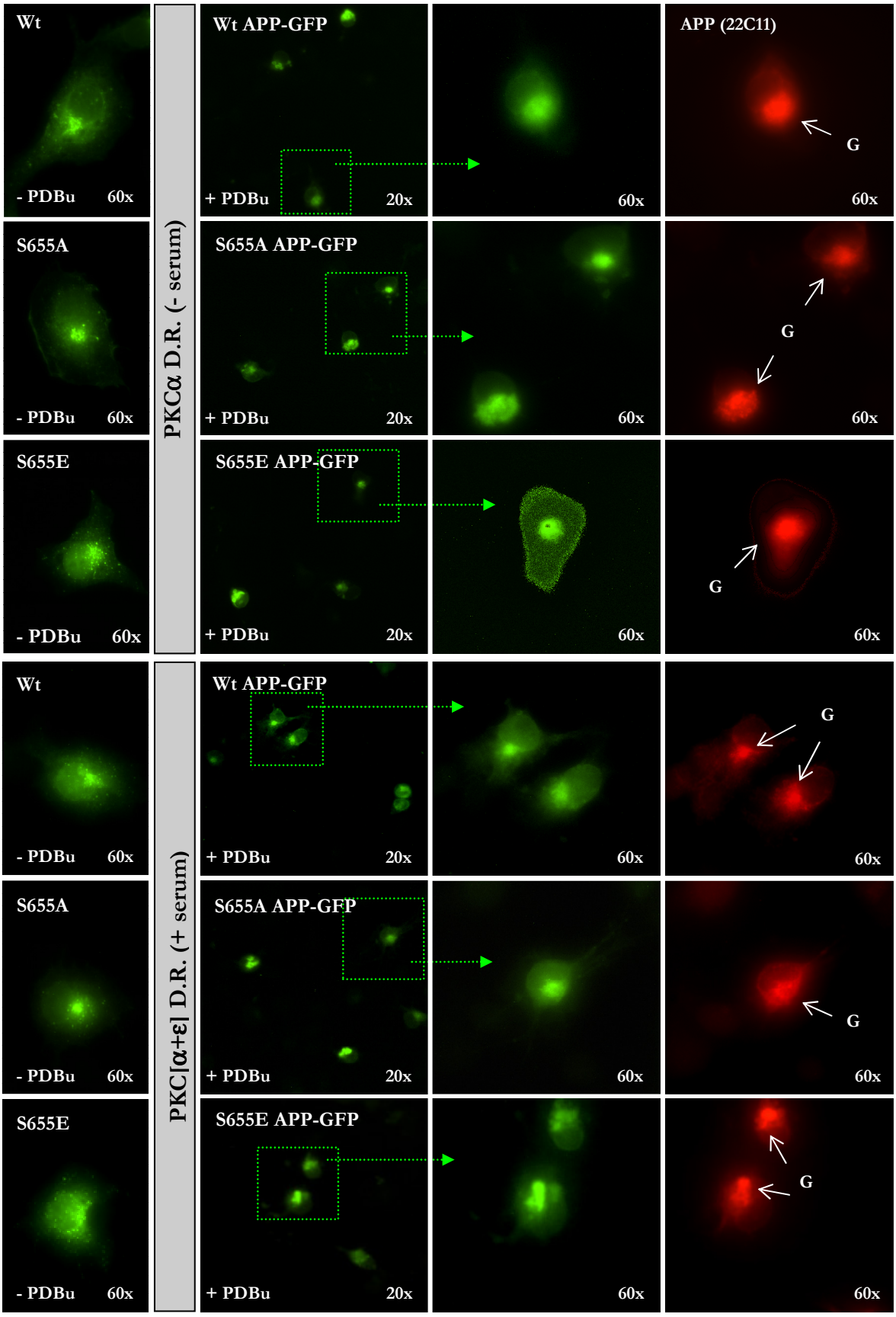

Figure IV.8. Wt and S655 phosphomutants APP-GFP (green) and total cellular APP (22C11, red) subcellular localization upon 8 h of PDBu exposure (+ PDBu), in the absence or presence of serum. Control, non-PDBu exposed cells **G,** Golgi region.

A putative involvement of PKCε in APP PM-to-TGN retrograde transport still remains to be further elucidated, as well as if APP S655 phosphorylation may constitute part of the PKCε mechanism of sAPP induction. It is tempting to speculate that the S655E mutant may retain more the Golgi swelling and intensity in conditions of PKCε down-regulation due to its higher Golgi retrograde transport. Future work may focus, for example, S655 phosphorylation state-dependent APP-GFP localization at the TGN/Golgi during the first 2 h of PDBu exposure. This is a period where PKCε already suffers a major D.R. (Fig. IV.3), and where subcellular distribution differences may be more distinctly visible for the three APP-GFP species.

IV. 4. 5. 3 – Wt and S655 phosphomutant processing with PKCα and PKCε D.R.

In parallel with the subcellular assays, the processing of APP-GFP species to sAPP was evaluated under conditions of specific PKC isozymes down-regulation. APP-GFP expressing cells were exposed to PDBu for 8 h in the presence or absence of serum. Media samples were collected upon 2 h of PDBu exposure, media substituted for equal PDBu-containing medium, and media was further collected upon a total of 8 h of PDBu exposure (Fig. IV.9).

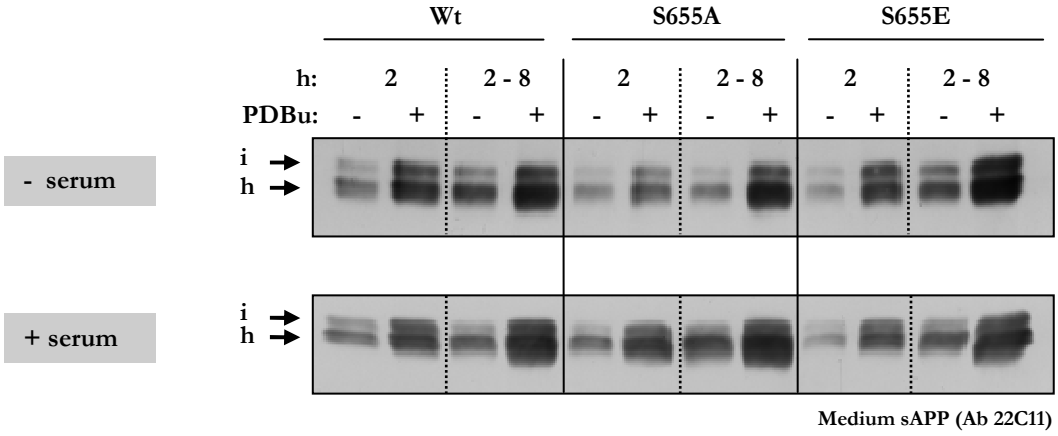

Figure IV.9. PDBu effect on APP-GFP Wt and S655 phosphomutants processing. Immunoblot analysis of sAPP in media collected upon 2 h and 2-8 h of PDBu exposure. Both serum-free and serum-plus conditions were assayed. **h** and **i**, medium secreted $sAPP_{695}$ and $sAPP_{751/770}$, respectively.

Figure IV.9 shows that not only at the initial 2 h period of exposure to PDBu, but also in the following 6 h ("2-8 h"), the levels of sAPP are higher in the PDBu exposed cells relative to control determinations. This was true for the three APP-GFP species (band "h") and for

endogenous sAPP secretion (band "i"), under both serum conditions. Of note is that upon 2 h of PDBu exposure, Wt sAPP levels suffered a 3.5 fold-increase in serum-free conditions and only a 2.5 fold-increase in serum-plus conditions, similarly to endogenous APP (section IV.4.3). In the subsequent exposure period (2-8 h) a robust PDBu-induced sAPP increase could still be observed for all species. In synthesis, enhancement of sAPP and APP-GFP levels seem to occur independently of the APP phosphorylation state at the S655 residue, as previously observed in the PMA assays (see Fig. III.7), and occur under both serum-plus and serum-minus conditions.

Taken together with the observed effects of PKC isozymes D.R. in APP-GFP subcellular distribution (Fig. IV.8), PDBu appears to exert its long-term sAPP stimulatory effects in an APP population that is trapped at the TGN/Golgi and available for intracellular cleavage. Nonetheless, concentrating APP at the TGN/Golgi region in the absence of post-TGN vesicles seems not, per se, a condition that leads to an enhancement in sAPP production (previous results of 20 ºC assays, Fig.s III.4 and III.5). Hence, it is probable that an additional step, as e.g. PDBu-induced PKC-activation of TGN α-secretase (Skovronsky et al., 2000), may be required and occurring. The S655 phosphomutations are therefore not sufficient to override the PKC isozymes down-regulation in terms of APP TGN vesicular exit. This points to more than one point of phosphorylation control, i.e., more than one event that is regulated by phosphorylation.

IV. 4. 6 – APP AND PKCS/PPS EXPRESSION IN RAT CORTEX

As APP S655 has been reported to occur "in vivo" in mammalian brains (Oishi et al., 1997; Lee et al, 2003a), a neuronal system was also characterized in terms of the co-distribution of APP and its putative S655 phosphorylation/dephosphorylation enzymes. The relative expression of APP, PKC isozymes and Ser/Thr phosphatases, were thus determined in rat cortex lysates and COS cells (Fig. IV.10).

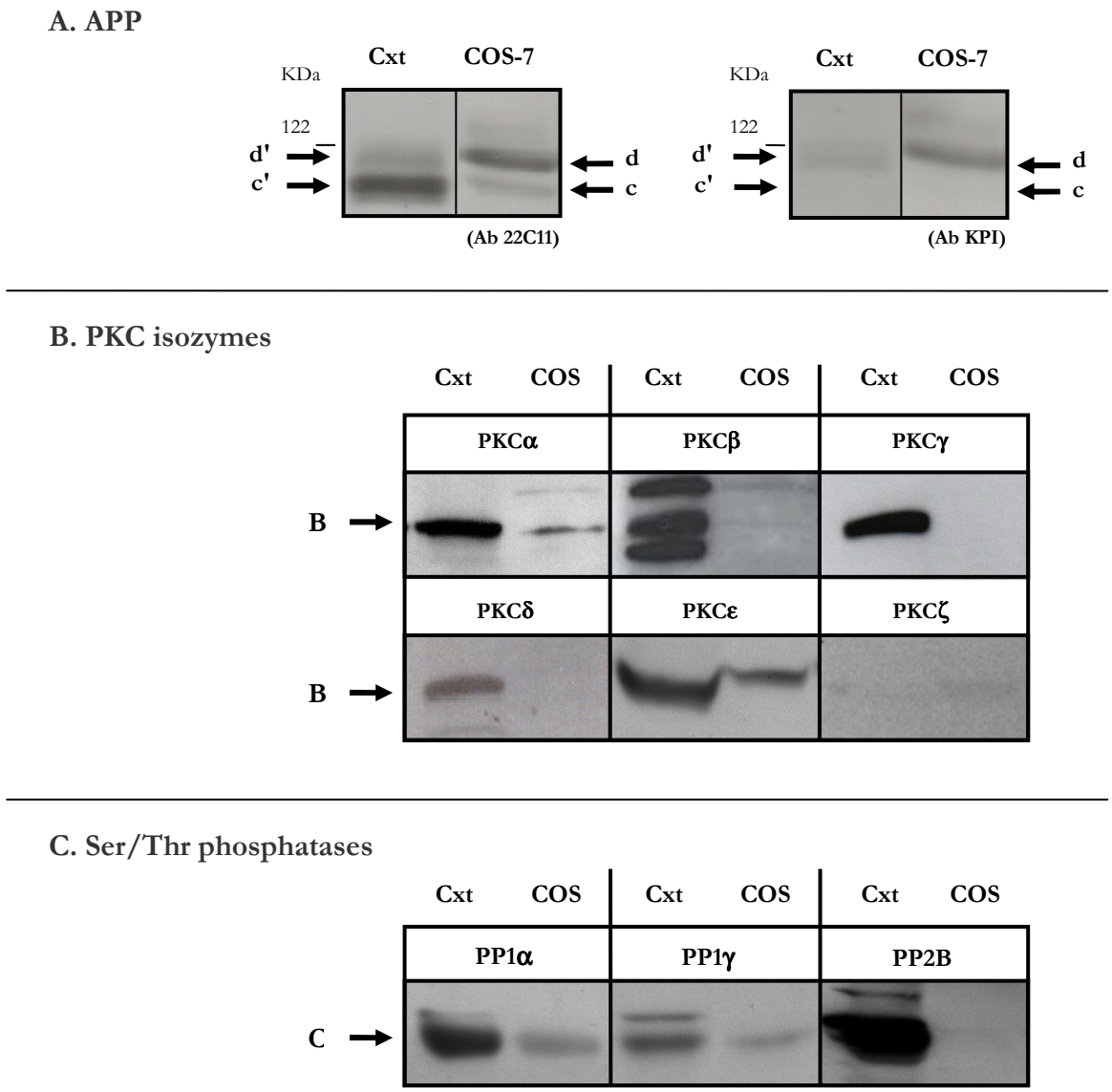

Figure IV.10. Comparison of COS cells and rat cortex (Ctx) expression levels of APP (A), PKC isozymes (B) and Ser/Thr protein phosphatases (C). c, COS immature APP isoform 695; **d**, COS immature APP isoforms 751/770; **c',** rat cortical immature APP isoform 695; **d',** rat cortical immature APP isoform 751/770. Arrows B and C indicate the PKCs/PPs specific bands.

As previously observed, COS cells present almost only KPI-positive APP isoforms (751 and 770, band d), and much less APP_{695} (Fig. IV.10, A). This was expected, as COS cells are derived from peripheral (kidney) cells. The rat cortical samples are in contrast enriched in the immature APP 695 isoform (band c').

In agreement with the Immunoblot analysis (Fig. IV.3), COS-7 cells have mainly PKCα and PKCε isozymes, with PKCβ and ζ being barely detected and PKCγ and δ undetected (Fig. IV.10, B). Comparatively, rat cortex presents high expression of all PKC isozymes with exception of the ζ (Fig. IV.10, B). Relative to the Ser/Thr phosphatases protein expression (Fig. IV.10, C), COS-7 cells have significant amounts of both PP1 isoforms tested, but very low amounts of PP2B. In rat cortex tissue, PP1α and PP2B are highly enriched, especially PP2B, while PP1γ was present at considerable although lower amounts. Finally, with the exception of the PKCζ, both type of enzymes (PKC isozymes and Ser/Thr phosphatases) are more abundant in the cortical lysates than in COS cells samples.

IV. 5 – CONCLUSIONS

The putative system of APP S655 cellular kinases and phosphatases was addressed in terms of their co-localization with APP. The roles of PKCα and PKCε in APP cellular fate were also analysed. The main conclusions of these studies were:

1. In COS-7 cells the PKC isozymes which are more abundant and apparently present at subcellular sites of α-secretase processing (plasma membrane and cytoplasmic vesicles) are PKCα and PKCε.

2. While the Ser/Thr phosphatase PP1γ is mainly nuclear, PP1α and PP2B were observed at the plasma membrane and cytoplasmic vesicles. Some co-localization with Wt APP-GFP was observed at the plasma membrane (PP1α) and at cytoplasmic vesicles (PP2B).

3. In conditions of long-term exposure to PDBu in serum-free medium, which leads to PKCα down- and PKCε up-regulation, the levels of cellular APP suffer an up-regulation (~2 fold-increase). This increase seems PKCε-dependent as demonstrated by its absence when both PKC isozymes are down-regulated.

4. PKCα seems to contribute more for the phorbol ester sAPP stimulation than PKCε. In a simplistic way we could say that the first seems to contribute for 2/3 and the latter for 1/3 of the PDBu-induced sAPP stimulation.

5. PKCα down-regulation leads to a loss of APP-containing cytoplasmic vesicles, indicating a role for this PKC isozyme in APP TGN/Golgi secretion, specifically in the post-TGN vesicle formation.

6. This PKCα-dependent mechanism is independent of the APP S655 phosphorylation state. Nonetheless, results do not eliminate that S655 phosphorylation up-regulates sAPP vesicle incorporation at the TGN. In fact, an apparent higher degree of S655A and PKCα co-localization supports this mutant being slowly packaged into post-TGN vesicles.

7. Under prolonged PKCα down-regulation, PKCε up-regulation seems to lead to a higher APP Golgi retention. A working hypothesis comprehends the involvement

of PKCε in the up-regulation of APP endocytosis and consequently APP PM-to-Golgi retrograde transport.

8. Long-term exposure to PDBu results in the inhibition of APP-containing post-TGN vesicles formation and higher APP Golgi retention. This is accompanied with higher sAPP production. Hence, the induction of APP cleavage to sAPP under long-term PDBu exposure appears to correlate with the amounts of APP available at the Golgi.

CHAPTER V

SERINE 655 PHOSPHORYLATION-DEPENDENT APP_{695} NEURONAL TARGETING

CHAPTER V – S655 PHOSPHORYLATION-DEPENDENT APP_{695} NEURONAL TARGETING

V. 1 – INTRODUCTION

The physiological role of APP in normal brains and in AD is the focus of considerable research. Full-length APP and its longer proteolytic product sAPP (soluble APP) have neuroprotective, neuritogenic and synaptogenic properties (Furukawa et al., 1996a,b; Ando et al., 1999; Torroja et al., 1999b, Cai et al., 2006). Several other functions have been attributed to APP that include roles in substrate-cell and cell-cell adhesion (Kusiak et al., 2001*,* Soba et al., 2005), as a gene expression transactivator by RIP signalling (Cao and Sudhof, 2001; Baek et al., 2002; Koo, 2002; Cao and Sudhof, 2004), and in vesicular traffic through neuronal terminals (Torroja et al., 1999a; Kamal et al., 2001; Muller and Kins, 2002; Sisodia, 2002; Satpute-Krishnan et al., 2003; Cottrell et al., 2005; Cai et al., 2006). Missorting of APP and accumulation of APP in neurons may contribute to some forms of AD and correlates with mild neuronal damage and impairment of axonal transport (L'Hernault and Arduengo, 1992; Tomimoto et al., 1995; Ahlgren et al., 1996; Praprotnik et al., 1996; Tienari et al., 1996a; Torroja et al., 1999a; Kamal et al., 2001; Muller and Kins, 2002; Pigino et al., 2003). In fact, APP binds the axonal motor protein kinesin, putatively via binding to KLC (Kamal et al., 2000; 2001), and during its axonal transport APP may generate Abeta peptides (Amaratunga and Fine, 1995; Kamal et al., 2001; Muller and Kins, 2002; Yoon et al., 2006).

Neurons have a highly polarized structure that includes specialized terminals, and APP undergoes neuronal sorting and polarized transport. While intraneuronal APP is localized both at the axonal and somatodendritic domains, plasma membranar APP is almost exclusively found at the soma and axonal surfaces (Simons et al., 1995; Yamazaki et al., 1995). Furthermore, the intraneuronal APP pool is also subjected to polarized transport (Allinquant et al., 1994). Intracellular APP is described to first travel from the Golgi towards the axon terminal by fast anterograde transport (Koo et al., 1990; Ferreira et al., 1993*;* Simons et al., 1995; Yamazaki et al, 1995; Lyckman et al., 1998; Kaether et al., 2000). Consequently, axonal full-length APP can be transcitotically transported back to the neuronal cell body (the "soma") and from there to dendrites (retrograde transport) (Simons et al., 1995; Yamazaki et al., 1995; Kaether et al., 2000). APP can also be cleaved during its subcellular transport, where it can generate Abeta peptides, but APP proteolytic cleavages appear to be highly regulated in neurons (Hung et al., 1992).

In hippocampal neurons in culture the Abeta sequence and APP N-glycosylation, in this order of importance, were found to participate in intraneuronal APP sorting to the axon (Tienari et al., 1996b). Furthermore, the use of C-terminus deletion mutants prevented APP from being directed to the axon, indicating the existence of axonal targeting domains in the APP cytoplasmic tail (Tienari et al., 1996b). In the polarized Madin-Darby canine kidney (MDCK) cells, APP is sorted basolaterally in a process involving two distinct sorting signals. These are the APP ^{653}YTSI^{656} cytoplasmic signal and an undetermined signal in its ectodomain near the Abeta sequence (De Strooper et al., 1993; Haass et al., 1995). Hence, phosphorylation at the APP sorting domain ^{653}YTSI^{656} has a potential role in regulating APP neuronal traffic. Furthermore, the fact that the ^{653}YTSI^{656} motif is the binding sequence to the KLC-homologous APPBP2 protein (Lai et al., 1995; Zheng et al., 1998) also suggests a putative role for ^{653}YTSI^{656} in APP traffic to and through neurites, the neuronal processes. This hypothesis is also attractive as APP phosphorylation at other cytoplasmic residue, Thr^{668}, enhances its localization within neuronal growth cones and neurites (Ando et al., 1999; Iijima et al., 2000; Muresan and Muresan, 2005). Thr^{668} phosphorylation also appears to enhance APP interaction with axonal KLC (Inomata et al., 2003; Muresan and Muresan, 2005), and to lead to higher Abeta production (Ando et al., 1999). The previously observed S655 phosphorylation state-dependent effects in APP subcellular traffic (non-neuronal COS-7 cells, Chapters II and III) also suggest a possible role for S655 phosphorylation in APP neuronal traffic. Additionally, S655 was found to be phosphorylated in adult rat brain (Suzuki et al., 1992; Oishi et al., 1997; Isohara et al., 1999), and in human AD brains (Lee et al., 2003a). Hence, this chapter focuses on putative S655 phosphorylation state-dependent APP neuronal targeting.

V. 2 – AIMS OF THIS CHAPTER

This chapter focussed on APP phosphorylation dependent targeting using primary neuronal cultures as a model system, in order to analyse the "in vivo" relevance of APP phosphorylation. The main objectives of this chapter were:

1. To compare APP distribution during neuronal "in vitro" development, in a S655 phosphorylation state-dependent manner.
2. To analyse the effect of APP S655 phosphorylation on the APP distribution in axonal and dendritic neurites of mature neurons.

3. To distinguish whether APP phosphorylation state affects APP targeting and/or neuritic outgrowth upon 24 h period of APP-GFP expression.
4. To address if APP phosphorylation can affect the nuclear targeting of APP-GFP derived C-terminal fragments in neuronal cultures.
5. To analyse possible effects of S655 phosphorylation on the intracellular level of the pre-synaptic protein GAP-43.

For Objective 1 rat cortical primary neurons were prepared and transfected with the APP-GFP Wt and S655 phosphomutants cDNAs at several days "in vitro" (DIV). APP-GFP distribution at the soma and dendrites were further analysed by epifluorescence microscopy. For an evaluation of the neuritic (axonal and dendrites) extension of APP-GFP distribution two parameters were used: distal versus proximal categories, and comparison with the MAP-2 (microtubule-associated protein 2) dendritic staining. The presence, intensity and identity of GFP nuclear fluorescence was also addressed in a phospho state-dependent manner. Subsequently, the putative APP S655 phosphorylation-dependent effects on the protein level of the axonal protein GAP-43 were addressed.

V. 3 – MATERIALS AND METHODS

A list of all solutions and protocols used, as well as other relevant information, is presented in Appendices I to III. All reagents were of cell culture grade or ultrapure.

V. 3. 1 – ANTIBODIES

The primary antibodies used in this study were the previously described anti-APP N-terminus monoclonal antibody 22C11, the anti-GFP monoclonal antibody JL-8, and the anti-APP C-terminus polyclonal 369 and anti-APP Abeta region monoclonal 6E10 antibodies. For the co-localization studies the monoclonal anti-microtubule associated protein 2 (MAP-2) antibody (Calbiochem, VWR International) was used. For the protein expression studies the polyclonal anti-growth associated protein-43 (GAP-43) antibody (Chemicon, PG-Hitec) was used. Additional antibodies used were anti-mouse and anti-rabbit IgGs Texas Red-conjugated secondary antibodies (Molecular Probes), and anti-mouse IgGs Alexa 350-conjugated secondary antibody (Molecular Probes) for Immunocytochemistry procedures, and anti-mouse and anti-rabbit IgGs horseradish peroxidase-linked whole antibody (Amersham Pharmacia), for enhanced chemiluminescence (Amersham Pharmacia Biosciences) detection. Dilutions of the antibodies used in this Chapter are given in Table V.1.

Table V.1. Antibodies, respective target proteins and specific dilutions used for the different techniques employed: IB., Immunoblot; ICC, Immunocytochemistry.

Target Protein/Epitope	Primary Antibody	Secondary Antibody
	Assay/Dilution	**Assay/Dilution**
APP N-terminal	**22C11** IB dilution: 1:250	Horseradish Peroxidase conjugated α-Mouse IgG IB dilution: 1:5000
APP C-terminal	**369** ICC dilution: 1:200	Texas Red-conjugated α-Rabbit IgG ICC dilution: 1:300
APP Abeta 1-17	**6E10** ICC dilution: 1:200	Alexa 350-conjugated α-Mouse IgG ICC dilution: 1:100
EGFP	**JL.8** IB dilution: 1:1000	Horseradish Peroxidase conjugated α-Mouse IgG IB dilution: 1:5000
MAP-2	**anti-MAP-2** ICC dilution: 1:1000	Texas Red-conjugated α-Mouse IgG ICC dilution: 1:300
GAP-43	**anti-GAP-43** IB dilution: 1:1000	Horseradish Peroxidase conjugated α- Rabbit IgG ICC dilution: 1:5000

V. 3. 2 – PRIMARY NEURONAL CULTURE AND TRANSIENT TRANSFECTIONS

Rat cortical primary neuronal culture. Cortical neuronal cultures were prepared from cortex of Wistar Hannover 18 days rat embryos as described in detail in Appendix II. Neuronal cultures were plated on 0.1 mg/ml poly-D-lysine (Sigma Aldrich, Portugal) pre-coated glass coverslips (epifluorescence microscopy) or plates (Immunoblot analysis) at 9.0 x 10^4 cells/cm^2. Cells were maintained in complete Neurobasal medium (composition in Appendix I) in a humidified incubator at 37 ºC, 5% CO_2. Cells conditioned medium was partially substituted with fresh equivalent medium when required.

Transient transfections. Transient transfections with the APP-GFP constructs were performed at 0, 3, 10 and 13 DIV using LipofectAMINE 2000 (Invitrogen Life Technologies) and as described in the literature (Dalby et al., 2004; see Appendix II). Upon 24 h of transfection, cells were collected into 1% SDS boiling solutions (Immunoblotting analysis), or fixed with the 4% paraformaldehyde fixative solution for Immunocytochemistry and epifluorescence microscopy analyses.

APP-GFP and GAP-43 protein expression in neuronal cells. For evaluating the expression of APP-GFP constructs in neuronal cells at 14 DIV, cells lysates were prepared as described in Chapter III (section III.3.6). Briefly, cells transfected at 13 DIV with the APP-GFP constructs were harvested in 1% SDS solution. Mass-normalized aliquots were subject to Immunoblot analysis in 6.5% SDS-PAGE gels followed by APP-GFP immunodetection using the 22C11 (APP) and JL-8 (GFP) antibodies. The relative expression level of the growth-associated protein GAP-43 was also assessed in these cellular lysates.

V. 3. 3 – APP-GFP NEURONAL TRAFFICKING

Intraneuronal APP-GFP trafficking with time of "in vitro" culture. Cells processed as described above were fixed and mounted with FluoroGuard antifading reagent (BioRad) on microscope slides (Immunocytochemistry procedures are described in section II.3.4.6 and Appendix II). The APP-GFP intraneuronal distribution was further analysed by epifluorescence microscopy at 1, 4, 11, and 14 DIV. 11 and 14 DIV APP-GFP transfected neurons were monitored in more detail in terms of their number of APP-GFP-positive neurites and neuritic terminals. Neurites were scored as "proximal" and "distal" (Hill et al., 1994; Silverman et al., 2001). Proximal neurites were considered to have lengths equal or inferior to two neuronal soma diameters (17.1 ± 0.4 μm in average), and distal neurites had lengths superior to two soma diameters.

MAP-2 co-localization studies in 14 DIV APP-GFP expressing neurons. Fixed neuronal cells, transfected with the APP-GFP constructs for 24 h at 13 DIV, were processed for Immunocytochemistry with the anti-MAP-2 antibody, a dendritic marker. Cells were first incubated for 2 h with MAP-2 antibody diluted 1:1000 in PBS with 3% BSA, washed three times with PBS, and anti-mouse IgG Texas Red-conjugated antibody was added to cells. A further incubation was carried out in the dark for 2 hours to allow for labelling of antigen-primary antibody complexes. Coverslips were further washed with PBS and mounted with the antifading reagent on microscope slides. Fixed cells were analysed by epifluorescence microscopy for the presence of APP-GFP in dendrites (MAP-2-positive) and axon (MAP-2-negative) and for the number of APP-GFP growth cones. Additionally, the length of APP-GFP dendritic distribution was compared with the one of MAP-2. The presence and intensity of APP-GFP-derived C-terminal fragments at neurons nuclei was also qualitatively addressed.

Identification of the nuclear targeted S655E APP-GFP-derived C-terminal fragment. Fixed neuronal cells, transfected with the S655E APP-GFP construct at 13 DIV and expressing the APP-GFP protein for 24 h, were processed for Immunocytochemistry with the anti-APP C-terminus 369 antibody and the anti-APP Abeta domain 6E10 antibody. Cells were first incubated with these two antibodies for 2 h upon permeabilization with methanol, washed with PBS, and further incubated for 2 h with the anti-rabbit IgG Texas Red-conjugated antibody and the anti-mouse IgG Alexa 350-conjugated antibody. Coverslips were further washed with PBS and mounted with the antifading reagent on microscope slides. Cells were analysed by epifluorescence microscopy for nuclear co-localization.

V. 3. 4 – DATA ANALYSIS

Immunoblots autoradiographic film exposures were scanned in densitometer and protein bands quantified by densitometry. Data on neuritic APP-GFP targeting, and protein expression levels, are expressed as mean ± SEM (standard error of the mean). Statistical significance analysis was conducted by ANOVA, with a level of statistical significance being considered $p < 0.05$, followed by the Tukey-Kramer test. Statistical significance symbols used were (*) for comparison between the S655 phosphomutants and the Wt data, and ($^{+}$) for S655A versus S655E data. Statistical significance levels are presented as ($*/^{+}$), $p < 0.05$; ($**/^{++}$), $p < 0.01$; and ($***/^{+++}$), $p < 0.001$.

V. 4 – RESULTS AND DISCUSSION

V. 4. 1 – APP-GFP NEURONAL TRAFFICKING WITH TIME OF "IN VITRO" CULTURE

APP targeting in immature neurons. In order to address the role of APP S655-phosphorylation in neuronal APP targeting, rat primary cortical neurons were transfected with the APP_{695}-GFP Wt and S655 phosphomutants as described above (sections V.3.2 and V.3.3). Cells were fixed and analysed at several stages of neuronal "in vitro" development and maturation (Dotti et al., 1988; Goslin and Banker, 1989). Figure V.1 shows that at 1 DIV the somatic body was the only structure clearly visible with GFP fluorescence, reflecting an initial stage of neuronal development before neurites protruding. A speckled pattern of APP-GFP somatic fluorescence could be observed for the three APP-GFP constructs (Fig. V.1, A). With time in culture, neurons start to develop neurites and to become polarized. 4 DIV neurons presented several short neurites and an obviously more developed neurite (Fig. V.1, B). At this stage the latter has been reported to be the cell axon, which grows at a faster rate than dendrites (Dotti et al., 1988; Goslin and Banker, 1989). By epifluorescence microscopy analysis, the presence of Wt APP-GFP fluorescence was observed at 4 DIV in neuronal locations where endogenous APP has been described. Wt APP-GFP was found both at the small somatic body and at the long neuritic processes, being enriched in the neuronal soma at the perinuclear region (Fig. V.1, B). Both type of neuritic processes, axons and dendrites, presented a discontinuous pattern of green fluorescence. In the cells expressing the S655 phosphomutants the soma did not suffer any visible alteration in terms of fluorescence distribution or intensity. This is similar to COS-7 cells when "de novo" protein synthesis is not inhibited (Chapter II, Fig. II.5). APP-GFP fluorescent cells were further monitored for the characteristics of the GFP-positive neurites, such as the branching and fluorescence intensity of the axon. For all constructs, ~80% of the APP-GFP expressing cells had a more elongated and ramified neuritic process that should correspond to the axon (arrows), and smaller neuritic processes corresponding to dendrites (Fig. V.1, B). The majority of dendrites were small, and cells mainly presented a long putative axon with ~3 terminals, arriving from axonal branching. In fact, the ramification of the putative GFP-positive axon was found to be equal between cells expressing the S655 APP-GFP phosphomutants: 3.5 ± 0.6 for S655A and 3.4 ± 0.6 for the S655E mutant. Furthermore, in terms of fluorescence intensity or GFP-visible length, no detectable differences were observed in "axonal" staining for the three APP-GFP species.

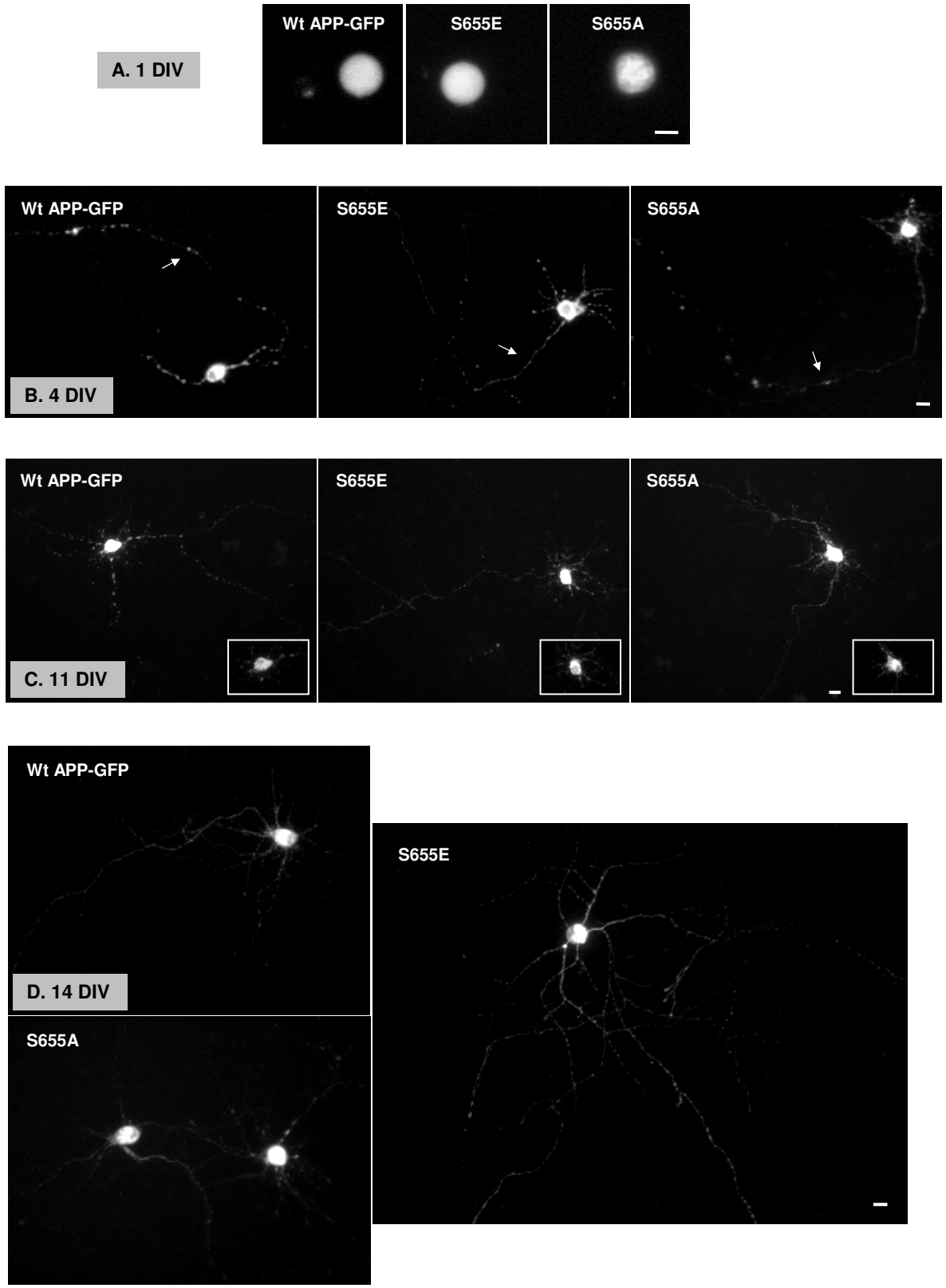

Figure V.1. Neuronal APP S655 phosphomutants distribution. The subcellular localization of APP Wt, S655A or S655E GFP-labelled fusion proteins was analysed by epifluorescence microscopy at 1, 4, 11 and 14-d-old rat cortical neurons. Arrows at 4 DIV indicate putative axons as the longest neurite. At all days in culture the pattern of APP-GFP labelling at the cells soma was virtually identical for the three APP-GFP species. However, differences were found in the APP-GFP neuritic distribution at 14 DIV, a time when the S655E mutant was observed in more distal neurites than the Wt or S655A APP-GFP proteins. DIV, days "in vitro". Bar, 10μm.

S655-dependent APP distribution in polarized maturing neurons. APP-GFP proteins localization was further monitored at 11 DIV, as dendrites are reported to continue to develop with time in culture, and at 11 DIV the process of establishment of polarization is almost or totally completed (Dotti et al., 1988; Goslin and Banker, 1989). At this stage the pattern of APP-GFP somatic staining was maintained as for immature neurons, and no differences were observed between the three constructs (Fig. V.1, C). In a large number of cells the axon could still be distinguished and, when comparing with 4 DIV neurons, appeared to be slightly more branched. Furthermore, and as expected from the literature, some (up to two) fluorescing dendrites were longer than at 4 DIV (Fig. V.1, B and C).

Fluorescing neurites of 11 DIV transfected neurons were scored as proximal or distal (depending on their length, see section V.3.3) and scored. Hence, distal neurites include both axon and long dendrites. Other parameters monitored included the level of GFP-visible neuritic ramification (Table V.2). The number of proximal neurites and proximal terminals was similar for the three APP-GFP proteins at 11 DIV, but the level of proximal neurites ramification was lower for S655A (1.6, $p < 0.05$) than for the Wt or S655E proteins (1.9). Axonal ramifications were also scored when possible and found to be equal between the Wt and S655 phosphomutants (4.3 - 4.5). Overall, at 11 DIV all APP species behave similarly although the S655E mutant seemed to be slightly more targeted to distal neurites and the opposite could be occurring for the S655A protein. In line with this observation, the ratio between distal terminals and visible protruding processes (GFP-positive processes that protrude from the neuronal soma) was slightly lower for the S655A protein (1.0), and the ratio between distal and proximal neurites was slightly higher for the S655E mutant (1.2).

S655 phosphorylation increases APP targeting to mature neurites. Upon two weeks of "in vitro" culture, neurons are reported to be fully mature and the majority of their synapses fully functional (Dotti et al., 1988; Goslin and Banker, 1989). Microphotographs of APP-GFP 14 DIV expressing cells (Fig. V.1, D) show no visible alterations in APP-GFP intracellular somatic staining for the three proteins. This was as discussed above for 1, 4 and 11 DIV. In terms of neurites fluorescing pattern, at 14 DIV the number of protruding processes (~7) and the number of proximal (~6) and distal (~3) neurites were found to be equal for the three proteins (Table V.2). Strikingly, at 14 DIV, S655E was found more abundant in distal terminals when compared to the other two APP-GFP proteins, with the number of these terminals being almost the double than for S655A (13.4 ± 0.9 vs. 7.0 ± 0.6, respectively). These numbers were more similar between the S655A and Wt proteins, with the

latter exhibiting 8.9 ± 0.6 distal terminals per cell. Visually, the S655A APP-GFP-containing distal neurites were in general shorter and/or less ramified and, in contrast, S655E expressing cells visually appear with longer and/or more branched distal neurites (Fig. V.1, D). In fact, in this neuronal culture the S655E mutant presented the highest level of fluorescent neuritic ramification (Table V.2), either distal [(S655E) 4.2 > (Wt) 3.0 > (S655A) 2.4)] or proximal [(S655E) 2.1 > (Wt) 1.8 > (S655A) 1.7)]. This had consequences in the total number of APP-GFP-positive terminals: S655E (25.7 ± 1.1; $p < 0.01$ vs. Wt, and $p < 0.001$ vs. S655A) > Wt (20.9 ± 1.1) > S655A (16.1 ± 0.8; $p < 0.05$ vs. Wt, and $p < 0.001$ vs. S655E).

Table V.2. Characteristics of APP-GFP distribution in the neurites of 11 and 14 DIV cortical neurons. (n), number of cells scored.

		11 DIV			14 DIV		
Scores and Ratios		**Wt** (n=50)	**S655E** (n=45)	**S655A** (n=67)	**Wt** (n=60)	**S655E** (n=85)	**S655A** (n=40)
Neurites per cell	PP[1]	7.3 ± 0.3	5.6 ± 0.3***	6.4 ± 0.3	7..3 ± 0.4	7.6 ± 0.2	6.9 ± 0.4
	Proximal[2]	5.7 ± 0.3	4.7 ± 0.4	5.3 ± 0.3	6.4 ± 0.4	5.9 ± 0.3	5.3 ± 0.4
	Distal[3]	2.7 ± 0.5	2.0 ± 0.2**	1.8 ± 0.1***	3.1 ± 0.2	3.4 ± 0.2	3.1 ± 0.3
Neuritic Terminals per cell	Proximal	11.0 ± 0.8	9.1 ± 0.9	8.8 ± 0.6	11.6 ± 0.9	12.3 ± 0.7+	9.1 ± 0.7
	Distal	8.2 ± 0.6	6.4 ± 0.6*	6.1 ± 0.5*	8.9 ± 0.6	13.4 ± 0.9***/+++	7.0 ± 0.6
Neuritic Ramification	Proximal	1.9 ± 0.1	1.9 ± 0.1+	1.6 ± 0.1*/+	1.8 ± 0.1	2.1 ± 0.1+	1.7 ± 0.1+
	Distal	3.2 ± 0.2	3.4 ± 0.2	3.4 ± 0.2	3.0 ± 0.2	4.2 ± 0.3**/+++	2.4 ± 0.2+++
Ratio Distal terminals /	/ PP	1.2 ± 0.1	1.2 ± 0.1	1.0 ± 0.1	1.3 ± 0.1	2.0 ± 0.1**/+++	1.0 ± 0.1+++
	/ Proximal terminals	0.9 ± 0.1	1.2 ± 0.2	0.9 ± 0.1	1.2 ± 0.1	2.2 ± 0.4*/+	0.9 ± 0.1+

[1] Protruding processes from the soma. Some of these processes show immediate ramification by bifurcation, but were considered just one process coming out of the somatic body.
[2, 3] Processes with terminal tips distant from the neuronal soma by ≤ 2 and > 2 somatic diameters, respectively.

Potentially, it appears that S655E has a higher transport into distal processes and this is also reflected in the ratio between distal terminals and the number of GFP-visible protruding processes: S655E (2.0 ± 0.1; $p < 0.01$ and $p < 0.001$ vs. Wt and S655A, respectively) > Wt (1.3 ± 0.1) ≥ S655A (1.0 ± 0.1). In addition, the ratio between distal terminals and the number of proximal terminals showed the same relationship: S655E (2.2 ± 0.4; $p < 0.05$ vs. Wt or S655A) > Wt (1.2 ± 0.1) ≥ S655A (0.9 ± 0.1; $p < 0.05$ vs. S655E).

To analyse whether the neuritic traffic differences may be due to varying expression levels of the APP-GFP constructs, these were evaluated in a subset of 14 DIV neurons by Immunoblot analysis (see section V.3.2). Figure V.2 shows that in the cells lysates three bands appeared when probing with the anti-APP 22C11 antibody (Fig. V.2, left panel). Of these, two bands (bands b and c) were not visible with the anti-GFP antibody (Fig. V.2, right panel), and had similar apparent molecular weights as COS-7 cells endogenous APP forms. This is as expected for neuronal endogenous APP proteins (Selkoe et al., 1988). The APP-GFP band "a", the only band visible either with the anti-GFP or the 22C11 antibody, migrated at ~133 KDa. This is a molecular weight expected for the immature form of the APP_{695}-GFP fusion protein, when compared with band "a" obtained in COS-7 cells transfections (Fig. II.5). Bands analysis revealed that the Wt and S655E APP-GFP proteins were expressed at similar levels, while the S655A mutant was expressed at slightly higher levels (1.3 fold higher). Hence, the higher S655E neuritic targeting its not an artefact of a higher S655E APP-GFP expression.

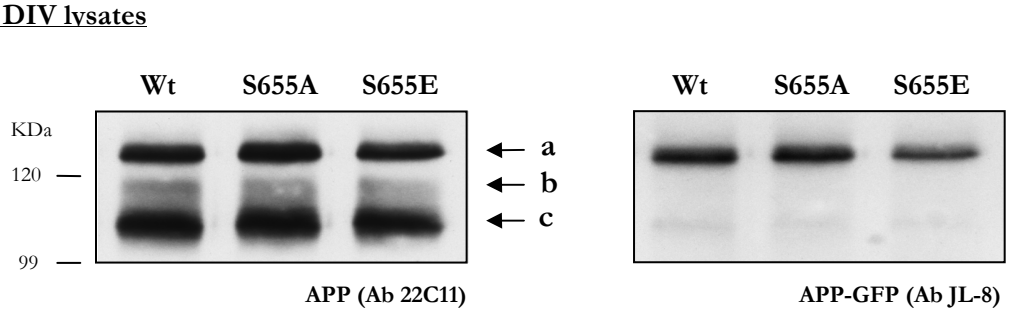

Figure V.2. APP-GFP expression in 14 DIV neuronal cells. Immunoblot analysis of APP-GFP expressing 14 DIV neuronal lysates, using antibodies against APP N-terminus (22C11) and against GFP (JL-8) for APP-GFP detection. **a**, APP_{695}-GFP, probably immature; **c'** and **d',** endogenous neuronal APP proteins.

V. 4. 2 – APP-GFP NEURITIC TARGETING – CO-LOCALIZATION WITH MAP-2

APP-GFP distribution in axons and dendrites of 14 DIV neurons. In order to characterize the nature of the APP-GFP positive neurites and neuritic terminals at 14 DIV, co-localization studies of the APP-GFP proteins and the dendritic marker MAP-2 were performed (Fig. V.3). The latter is a protein that, at this developmental stage, is widely reported to be restricted to the cell soma and dendrites, being absent from axonal processes or only present at their "basis" (most proximal portion) (Caceres et al., 1986).

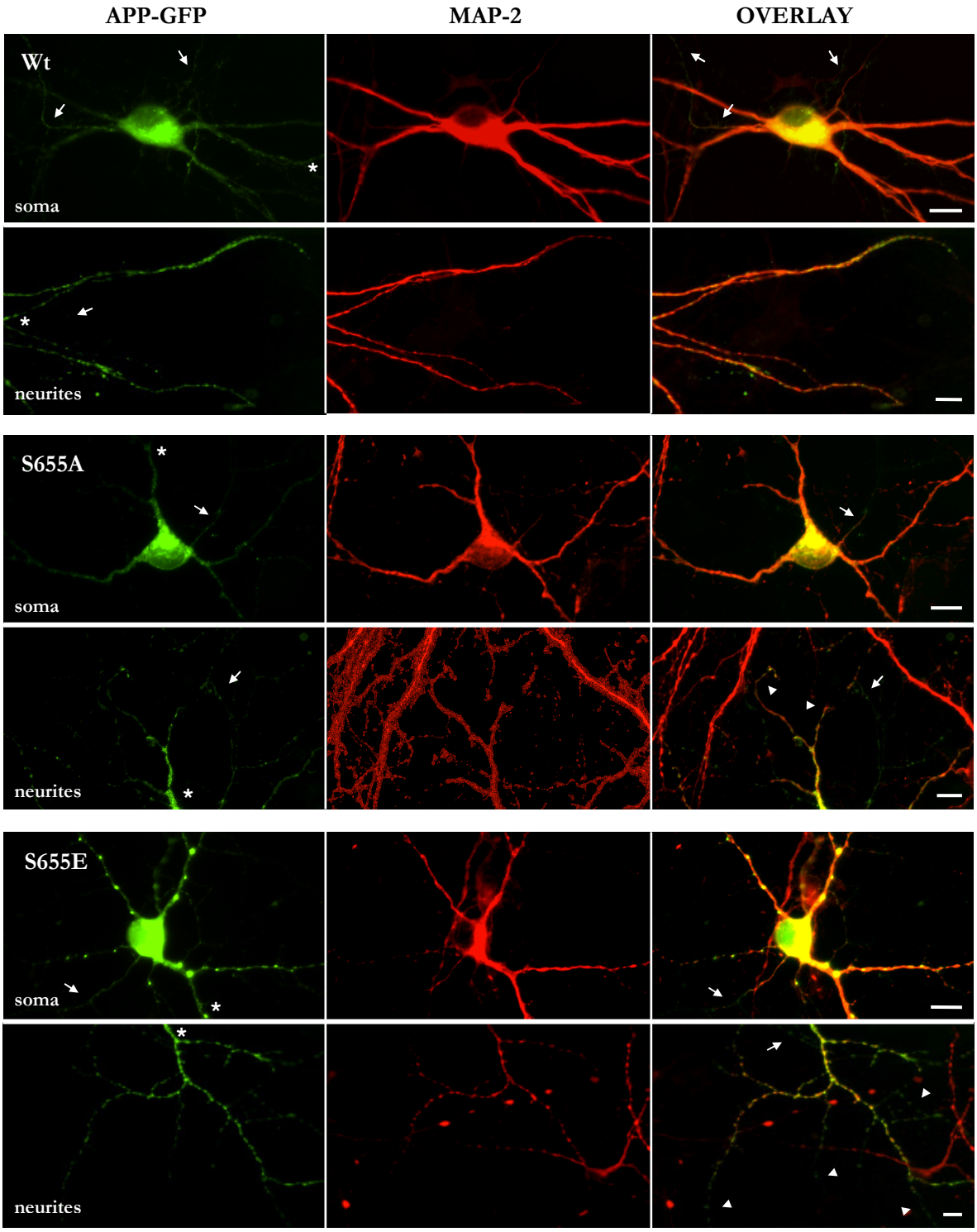

Figure V.3. Dendritic and axonal distribution of Wt and S655 phosphomutants in 14 DIV cortical neurons. Co-localization analysis of neuronal APP-GFP and the dendritic marker MAP-2 (Texas-red). **Soma:** The majority of APP-GFP-positive neurites were observed to be dendrites, where MAP-2 and APP-GFP co-localize (yellow labelling in the overlay). Arrows indicate the cells axon, as defined by the almost absence of MAP-2 labelling, which exhibit a much fainter APP-GFP fluorescence than dendrites. **Neurites:** Cells dendritic trees (asterisk) were monitored for the extent of APP-GFP and MAP-2 staining. At the dendritic terminals (arrowheads), Wt and S655A APP-GFP green fluorescence were observed to mainly match in length the red MAP-2 immunostaining. Conversely, the S655E dendritic green fluorescence usually surpassed MAP-2 labelling. Distal portions or terminals of the APP-GFP-positive axon could also be observed (arrows); in the S655A photo the axon makes a contact with a dendritic terminal of an adjacent non-transfected neuron. Bar, 10μm.

As can be observed in the "soma" panels of Fig. V.3, axonal processes are APP-GFP-positive (arrows) for all APP species, but did not stain for MAP-2 (red fluorescence), thus facilitating their identification. The axonal GFP fluorescence intensity is fainter than in dendrites, with the axon being more difficult to identify and to follow. Nonetheless, and correlating with an increased S655E axonal transport, the axon had generally a higher intensity and was more easily detected in the S655E expressing neurons. Co-localization analysis showed that the S655E-positive neurites and neuritic terminals corresponded both to axonal and dendritic branches. Again, the S655E mutant was found more abundantly in longer neuritic processes, both when axonal or dendritic in origin, and these were typically more intense than for the other two APP-GFP proteins. The S655A fluorescence generally decreased with increasing neuritic length, while S655E fluorescence intensity was maintained with distance from the soma. In some neuritic terminals, APP-GFP could be observed to be concentrated at growth cones, which when of dendritic nature had also a concentration of MAP-2. This has already been described for APP (Ando et al., 1999; Sabo et al., 2003). GFP-visible dendritic and axonal growth cones were additionally scored in 20 cells per APP-GFP protein type. The S655E protein was present in a higher number of growth cones (GC) of both kinds - axonal (Ax) and dendritic (Dt). Average values obtained were of: 4 Dt GC and 3 Ax GC for S655E > 1.7 Dt GC and 0.7 Ax GC for Wt ≥ 2 Dt GC and 0.4 Ax GC for S655A.

S655 phosphorylation increases APP targeting to mature neurites. Visually, the S655E APP-GFP also appeared to be more distally transported in neurites (as in Fig. V.1). In order to confirm the existence of a S655 phosphorylation-dependent APP neuritic trafficking, these 14 DIV neurons were monitor using two independent parameters. The first was the proximal/distal parameter used above in section V.4.1, and a small set of APP-GFP expressing cells (around 15) was scored. Noteworthy is the fact that this data was collected blind. The second evaluation made use of the length of MAP-2 staining as an internal control of the APP-GFP length of transport.

Using the distal/proximal parameters, the S655E protein was found in 26 ± 3 distal neuritic terminals, a number significantly higher than the Wt and S655A values (18 ± 2; $p < 0.05$). Of note is that these neurons (Fig. V.3) had longer neurites than the previous 14 DIV neurons of section V.4.1. In fact, there was a decreased number of proximal neurites and a higher number of distal neurites. The same parameter (two-soma diameters) was used, and values still confirmed an increased S655E distal transport, with the number of S655E distal terminals being ~1.5 fold higher than of S655A.

The lengths of APP-GFP and MAP-2 dendritic staining were also compared. In the majority of Wt and S655A-positive dendrites, the extension of APP-GFP green and MAP-2 red dendritic fluorescences matched in length (Fig. V.3, Wt and S655A "neurites"). This was true for 56% of Wt cells and 76% of S655A cells. For the S655E protein, the APP-GFP green fluorescence went beyond the red MAP-2 staining. This is clear in Fig. V.3 S655E microphotographs (arrowheads in the "neurites" panel), where the green APP-GFP fluorescence was distally maintained in dendritic terminals that were no longer positive for MAP-2. Indeed, S655E staining at neuritic terminals was observed to largely surpass in length the MAP-2 staining in the majority of the dendrites of all (100%) cells monitored. Again, this confirms an increased S655E neuritic terminal targeting.

APP-GFP expression has no apparent effect on MAP-2 length of staining. The length of the MAP-2-positive dendritic portions was also addressed in the 14 DIV neurons expressing the APP-GFP constructs. This study aimed to clarify whether APP S655 phosphorylation was affecting both the APP neuritic traffic dynamics and the MAP-2-positive dendritic length. For that, the length of MAP-2 staining was measured on the three longer dendrites of 20 APP-GFP expressing cells. In addition, control determinations were taken by measuring MAP-2 dendritic length in various non-transfected cells in the vicinity of APP-GFP expressing neurons (Table V.3). No alterations in this parameter could be observed for any of the APP-GFP species, with MAP-2 length of staining being in average of 150μm per dendrite, either in APP-GFP transfected or non-transfected neurons.

Table V.3. MAP-2 dendritic staining in APP-GFP transfected (n=60 dendrites) and control (neighbour non-transfected) cells (n=30 dendrites).

	MAP-2 staining (μm)		
	Wt	**S655A**	**S655E**
APP-GFP cells	154 ± 6	147 ± 6	149 ± 5
Control cells	155 ± 9	142 ± 7	149 ± 7

V. 4. 3 – NUCLEAR TARGETING OF APP-GFP-DERIVED C-TERMINAL FRAGMENTS

When performing the above described co-localization studies of APP-GFP proteins with MAP-2, differences were detected in terms of the presence and intensity of green fluorescence at cells nuclei. The nuclear targeting of APP-GFP derived C-terminal fragments

in 14 DIV APP-GFP expressing neurons was particularly addressed. Hence, 20-35 cells per APP-GFP construct were monitored for the presence or absence of GFP green fluorescence in their nuclei. Additionally, when the green nuclear fluorescence was detected, its intensity was further characterized as "medium" or "intense" (Fig. V.4). This evaluation was performed not only by analysis of APP-GFP nuclear labelling, but also by comparison with the MAP-2 immunostaining, which was used as a negative control as MAP-2 is a nuclear excluded protein.

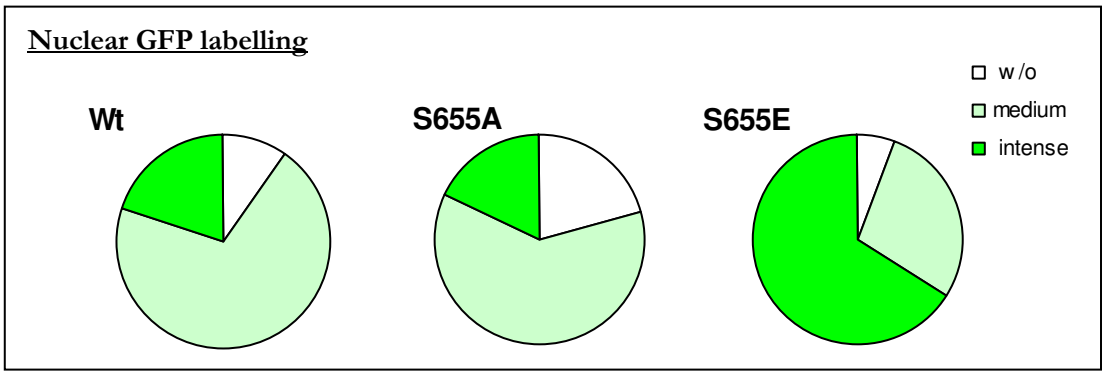

Figure V.4. Characterization of Wt and S655 phosphomutants APP-GFP-derived nuclear green fluorescence in 14 DIV neurons. The absence (**w/o**) or presence of green fluorescence at the nuclei of APP-GFP 14 DIV cortical neurons was scored, with green fluorescence intensity being divided into **medium** or **intense.** Data is presented as percentage of the number of cells evaluated (Wt: 20; S655A: 33; S655E: 35).

In Wt APP-GFP expressing neurons, only 10% of the cells did not have visible nuclear green fluorescence (Fig. V.4). Moreover, the majority of cells presented nuclear green fluorescence of medium intensity (70% of cells). For the S655A mutant, although the majority of the population (~60%) presented green nuclear fluorescence of medium intensity, there was a higher number of cells where nuclear labelling was absent (~20%, double than for Wt). The S655E mutant however, presented nuclear GFP staining in virtually all neurons (~94%) and this staining was more intense than for the other two APP-GFP species. In fact, two thirds of the population (~66%) had intense nuclear green fluorescence, and this can be denoted from the S655E "soma" panel of Fig. V.3. Noteworthy is that a higher nuclear GFP labelling in S655E expressing cells was also previously observed for COS-7 cells (Chapter II, section II.4.3.2). These suggest a higher targeting of APP-GFP-derived C-terminal fragments bearing the S655E phosphomimicking mutation. Hence, in an independent experiment, the co-localization of nuclear S655E APP-GFP fluorescence with the anti-APP 369 (APP C-terminus) and 6E10 (APP Abeta region) antibodies was performed (details in section V.3.3).

As in Chapter II (Fig. II.11), this aimed to further characterize the APP-GFP fragments nuclear targeted. Cells were analysed by epifluorescence microscopy for the nuclear presence of the GFP and the antibodies specific fluorescences, and their nuclear co-localization (Fig. V.5, arrows).

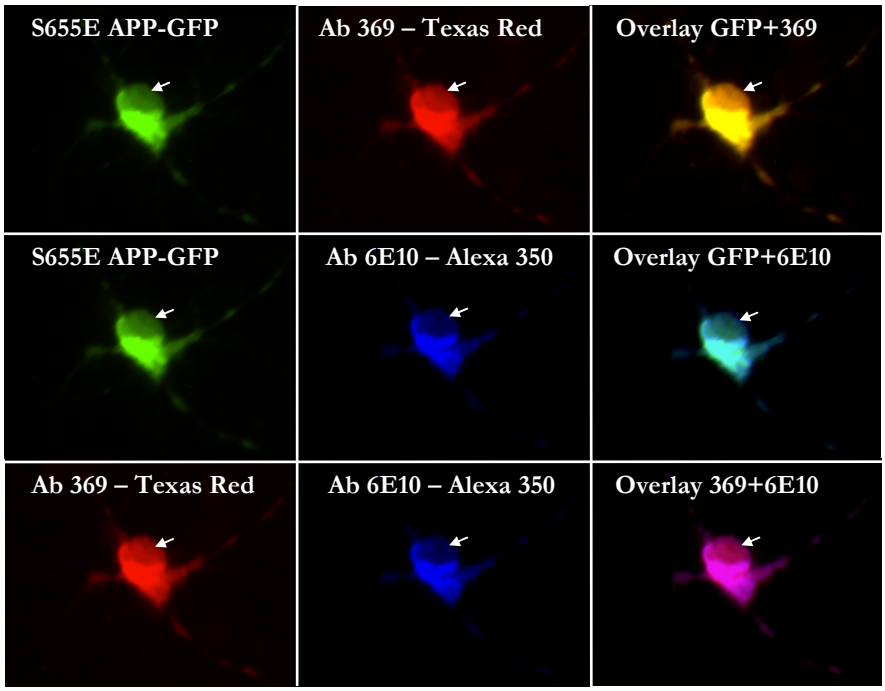

Figure V.5. Co-localization of neuronal somatic APP-GFP with APP C-terminal fragments. APP C-terminal fragments were detected with the anti-APP C-terminus 369 antibody, labelled with Texas Red-conjugated antibody, and the anti-APP Abeta region 6E10 antibody, labelled with the blue fluorescing Alexa 350-conjugated antibody. Arrows indicate the cell nucleus.

Figure V.5 shows that while the green (APP-GFP) and red (Ab 369, APP C-terminal fragments) nuclear fluorescences could be readily visible, the blue (Ab 6E10, APP Abeta region) fluorescence was apparently absent from the nucleus. A good correlation can be observed between GFP nuclear fluorescence and APP C-terminus red fluorescence (Fig. V.5, Overlay APP-GFP + Ab 369, arrow), that is less evident between the nuclear staining of the 369 and 6E10 antibodies (Fig. V.5, overlay Ab 369 + Ab 6E10, arrow). As observed in Chapter II, the 369 antibody recognizes full-length APP, both α- and βCTFs, and the AICD fragment. The 6E10 antibody recognizes full-length APP, the βCTF and Abeta fragments, but not the αCTFs and AICDs. Hence, the nuclear green fluorescence previously scored (Fig. V.4) seems to be due to the presence of AICDs or αCTFs APP-GFP-derived fragments, and not full-length APP-GFP, APP βCTFs fragments, or GFP alone.

V. 4. 4 – S655 PHOSPHORYLATION STATE-DEPENDENT GAP-43 NEURONAL EXPRESSION

The putative effects of the S655 phosphomutants neuronal expression on the levels of some proteins of interest are focus of current analysis. APP has been shown to possess synaptotrophic effects, and transgenic mice with neuronal APP overexpression were observed to present increased number of synaptophysin immunoreactive presynaptic terminals and increased expression of the growth-associated marker GAP-43 (Mucke et al., 1994). Here we present an Immunoblot analysis, performed in the neuronal lysates of Fig. V.2, where the effects of the expression of the different APP-GFP species on the protein levels of GAP-43 were evaluated (Fig. V.6).

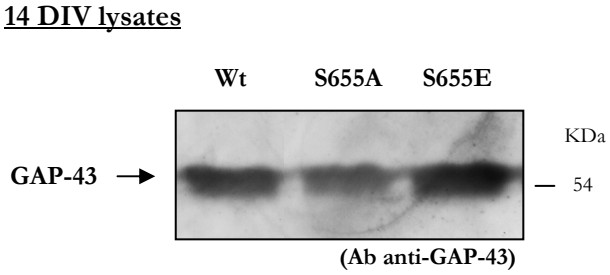

Figure V.6. APP S655 phosphorylation state-dependent GAP-43 expression in 14 DIV neuronal cells. Immunoblot analysis of GAP-43 expression in APP-GFP expressing 14 DIV neuronal lysates.

The relative levels of protein expression of the axonal GAP-43 protein were calculated by densitometry and found to be ~0.9 for the S655A and ~1.5 for the S655E phosphomutants (taken Wt O.D. data as 1). More striking differences in the GAP-43 levels arise when the neuronal APP-GFP expression levels (Fig. V.2) are taken into account: ~0.7 for S655A and ~1.7 for S655E. Hence, in comparison with the Wt species, the S655A neuronal expression had a down-regulation effect on GAP-43, while the expression of S655E in mature 14 DIV neurons seems to up-regulate the levels of this pre-synaptic and growth-cone enriched protein.

V. 5 – CONCLUSIONS

The S655 phosphomutant APP-GFP fusion constructs were used to determine putative regulatory functions of S655 phosphorylation in APP neuronal targeting. The major observations from these studies were:

1. The APP S655 phosphorylation-state is involved in the APP traffic in neuritic processes. This regulatory role seems to be dependent on the level of neuronal maturation.

2. In mature neurons, the S655A APP-GFP protein had a neuritic targeting that was slightly decreased or equal to the Wt protein. Conversely, the S655E protein, mimicking an APP S655 constitutive phosphorylated state, presented an increased neuritic targeting. Indeed, this phosphomutant was found present at higher amounts in neuritic portions and terminals more distal to the cell body.

3. S655 phosphorylation or dephosphorylation does not impair APP targeting to axonal or dendritic domains, with the S655 phosphomutants being found distributed through all neuronal domains. In fact, S655 phosphorylation appears to increase both axonal and dendritic APP transport.

4. In parallel with its higher length of distal transport, the S655E protein was present in a higher number of axonal and dendritic growth cones, labile zones at the tips of the neuritic terminals, related with neuritic outgrowth and signal transduction.

5. In agreement with the previous COS-7 cells results, the nuclear targeting of APP-GFP-derived AICD-GFP (or αCTF) was found increased for the S655E protein. In fact, there was a higher number of cells with nuclear S655E GFP fluorescence and, especially, these presented a higher nuclear GFP intensity.

6. APP S655 phosphorylation appears to have an important neuronal physiological role, not only in targeting, but also in signal transduction, as demonstrated by the alterations on the neuronal GAP-43 protein levels.

CHAPTER VI

DISCUSSION

CHAPTER VI – DISCUSSION

VI. 1 – OVERVIEW

AD is multifactorial in its aetiology and the complex cause-consequence mechanisms are still not completely understood. In the last few years the cellular mechanisms by which cellular APP is regulated have started to be unravelled. Related research has characterized APP binding proteins, identified some of the domains involved in these interactions, as well as the physiological relevance of these complexes. APP is a transmembranar protein processed via the secretory and endocytic pathways (see Chapter I) and, as part of its population is cleaved during its subcellular translocation, regulation of APP trafficking is thus of singular importance. APP proteolytic cleavages may be regulated by temporal APP substrate/enzyme co-distribution, and by substrate and enzyme activation. A possible scenario would involve APP substrate targeting to specific subcellular microdomains in order to perform a specific cellular function, for example activation of gene expression. Several factors have been described to regulate APP trafficking and proteolysis, among them protein phosphorylation. Moreover, APP phosphorylation and APP protein-protein interactions are found to be intimately related (Ando et al., 2001; Scheinfeld et al., 2002; Taru et al., 2004), with APP phosphorylation now emerging as a regulatory mechanism of APP binding to other proteins. Interestingly, in AD patients not only an impairment in the cellular phosphorylation system balance was detected, but alterations of the APP phosphorylation state were also found (Lee et al., 2003a). Additionally, Abeta phosphorylated at its serine residue 26 was reported in AD brains and this phosphorylation putatively implicated in Abeta toxicity (Milton, 2005). Nonetheless, little is known regarding the role of APP phosphoresidues, and even less regarding its ^{653}YTSI^{656} domain. In order to determine the consequence of APP S655 site specific phosphorylation in the dynamic process of APP targeting and processing, APP S655 phosphomutants and APP-GFP fusion constructs were engineered and used together with cellular biology, epifluorescence microscopy and proteomic techniques. The results obtained in the separate experiments discussed in the previous chapters are now object of an integrative analysis.

VI. 1. 1 – S655 PHOSPHORYLATION-DEPENDENT APP SORTING

ER exit. As a secretory protein, APP is synthesized in the ER, where it suffers its first maturation process, and it translocates to the cis-Golgi. The ER to Golgi translocation of the S655E mutant appeared to be slightly delayed relative to the other two APP-GFP species (Fig.s II.8, C and II.9, C). In parallel, the rate of disappearance of its immature form was slightly slower (Fig. III.1 B.I), with S655E having a half-life of 3 h, while the Wt and S655A have half-lives of 2.5-2.7 h. Different maturation rates are dismissed, as they were found to be identical for the three APP-GFP species. Immature APP was previously observed not to be phosphorylated at S655 (Suzuki et al., 1992; Oishi et al, 1997), and newly-synthesized and immature APP S655E passes the ER, a site where usually APP is not phosphorylated at S655. Hence, it is expected that immature S655E behaves slightly different from the other two immature APP-GFP species, which are much more alike in their behaviour.

TGN/Golgi sorting. In the assays monitoring APP trafficking (Fig.s II.8 and II.9), the S655A mutant exhibited slower packaging into post-TGN vesicles, which was further supported by the traffic assays at 20 ºC (Fig. III.5). In addition, part of its Golgi population remained at that organelle even after 5:00 h of monitoring (Fig.s II.8 and II.9), indicating a partial block in S655A Golgi exit. The S655E mutant presented an apparently normal TGN/Golgi exit (Fig.s II.8, II.9) and appeared to be preferentially targeted for post-TGN vesicle packaging (Fig. III.5). Figure VI.1 shows the percentage of GFP-positive Golgi for the three species, allowing for a better comparison of Golgi exit patterns. The high S655A Golgi percentages decrease little with time, suggesting Golgi retention for this mutant (Fig. VI.1). The number of cells with GFP-positive Golgi oscillated similarly for the Wt and the S655E species, especially between 1:30 and 3:00 h (Fig. VI.1). From 3.00 h on these patterns diverge significantly, and these will be discussed later.

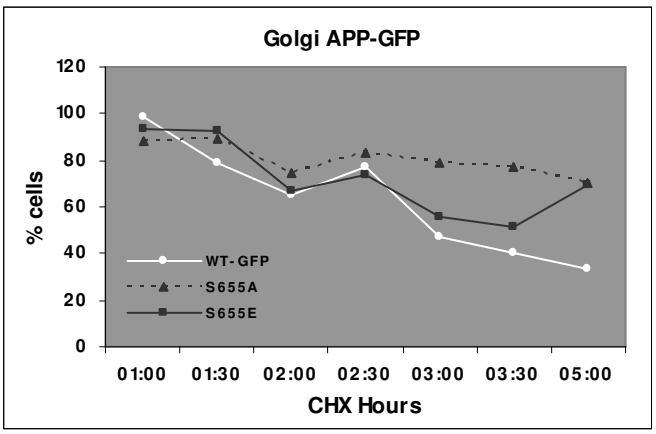

Figure VI.1. Time course analysis of APP-GFP-positive Golgi cell percentages (data derived from Fig. II.8).

Cell surface endocytosis. The differences observed in increased GFP fluorescence and increased APP retention for the S655A mutant at the plasma membrane, suggested that S655A was less endocytosed (Fig.s II.8, II.9, and II.15). The APP-GFP/transferrin co-localization assay (Fig. II.13) also indicated a decreased S655A incorporation into endocytic vesicles. Further support was obtained from the antibody uptake assays, either from visual analysis of the differential cell surface APP turnovers (Fig. II.15), or by directly scoring the number of APP-GFP-positive vesicles that resulted from surface APP being internalized (Fig. II.16). In summary, this significant novel finding shows that the S655 phosphorylation state is important in APP endocytosis, and is consistent with the APP ^{653}YTSI^{656} sequence being a consensus signal for internalization. In addition, Lai et al. (1995) had reported that the presence of the APP ^{653}YTSI^{656} sequence at the cytoplasmic domain of the transferrin receptor (TR) induces its partial internalization (~50% of Wt TR). The S655E mutant, however, also exhibited a slightly higher surface APP-GFP staining (Fig.s II.8 and II.9). Nonetheless, its slightly higher rate of membranar endocytosis and turnover (Fig. II.15) strongly suggests that this is not a resting population. Thus, the higher PM staining for both mutants seems to have different origins, which include higher rate of traffic between the TGN and the PM for S655E, and a lower rate of PM internalization for S655A. In conclusion, S655 phosphorylation seems to promote APP cell surface internalization by increasing APP endocytosis. Nonetheless, we can not exclude the possibility that the rates of cell surface APP recycling (back to the PM) may also be altered for the phosphomutants.

PM-to-TGN retrograde transport. Detailed analysis of Figure VI.1 reveals that although similar to the Wt, the S655E Golgi fluorescence pattern suffers more pronounced variations with time. These could reflect a higher income of APP-GFP to the Golgi, coming from the PM-to-TGN retrograde route at, e.g., 2:00-2:30 and 3.00-5:00 h of CHX exposure. This S655E APP Golgi population appears to be full-length, given the high Golgi co-localization of S655E APP-GFP with the APP N-terminal antibody 22C11 at 5:00 h (Fig. II.10). Further analysis using the antibody uptake assay confirmed that S655 phosphorylation also plays a role in APP sorting at endosomes. Co-localization of S655E-containing endocytic vesicles with the TGN/Golgi was faster and apparently higher (Fig. II.14). Indeed, retrograde transport of endocytosed APP to the TGN was found to be enhanced for S655E and impaired for the S655A mutant. Phosphorylation of the APP at S655 appears to function as a signal for endocytosed APP retrieval to the trans-Golgi network. This stimulation of the PM-to-TGN retrograde transport is most likely to be the cause of the cyclic point increases in

S655E Golgi fluorescence (Fig. VI.1 and Fig. II.8: 1:30, 3:30 and 5:00 h). The decreased S655A retrograde transport from the PM-to-TGN, along with its impaired Golgi exit, may explain the more constant pattern of S655A Golgi fluorescence with time (Fig. VI.1).

Lysosomal delivery. Further results indicated the three APP-GFP proteins also varied in their post-endocytic fate in terms of lysosomal delivery. A fraction of re-internalized APP is known to be targeted to lysosomes for complete degradation. For example, Haass et al. (1992a) observed that re-internalized APP partially co-distributes with Cathepsin D at lysosomes, using epifluorescence microscopy or lysosomal purification approaches. In agreement with this, APP-GFP fluorescence was also observed to partially co-localize with the lysosomal protein Cathepsin D. In COS-1 cells, a role for the APP ^{653}YTSI^{656} sequence in targeting to a cellular degradation pathway had already been described (Lai et al, 1995). In line with these findings, our results implicate S655 phosphorylation in APP lysosomal delivery. A higher targeting, almost double, of S655A APP-containing vesicles towards lysosomes was observed (Fig. II.17). In contrast, S655E was slightly less targeted to lysosomes. Furthermore, the half-lives and patterns of mature APP-GFP cellular catabolism support the existence of a S655 phosphorylation-dependent APP lysosomal targeting. First, the mature S655E form has a doubled half-life (5.56 ± 0.41 h) compared to mature Wt (2.46 ± 0.16 h) or mature S655A (2.12 ± 0.08 h) APP-GFP. Furthermore, mature Wt APP-GFP has a pattern of cellular catabolism that is initially similar to S655E, but approaches the S655A pattern in the later time points (Fig. III.1). This strongly suggests that there is a S655 phospho-dephospho event, only possible to occur for the Wt species, that affects the APP degradation rate. In addition, there was no direct correspondence between the S655E lower turnover rate and decreased sAPP production, or between the initially higher S655A turnover rate and enhanced sAPP production (Fig. III.3). In fact, at earlier time points, sAPP from S655A origin was the lowest (Fig. III.3). A higher targeting of this mutant to cellular degradation could also be denoted from its higher decreased cellular levels upon severe protein synthesis inhibition (Fig. III.2). Conversely, under these latter conditions, the S655E APP-GFP cellular and sAPP medium levels were less affected. Hence, part of the APP cellular catabolism is under the control of the S655 phosphorylation state, with phosphorylation rescuing APP from degradation.

Further support for a role of S655 phosphorylation in APP lysosomal targeting and degradation comes from comparison of the APP-GFP catabolism with previously reported work on APP lysosomal degradation. Interestingly, the pattern of mature S655E APP-GFP catabolism has close similarities with the pattern of mature APP catabolism upon inhibition of

lysosomal activity (Caporaso et al., 1992a). These authors observed that chloroquine-induced inhibition of lysosomal activity rendered no effect on immature APP processing but led to an enhancement of the mature APP half-life. Their time course analysis of endogenous mature APP (time of chase up to 8 h), and the results of CHX time course of mature Wt and S655E APP-GFP (adapted from Fig. III.1 B.II) are compared (Fig. VI.2).

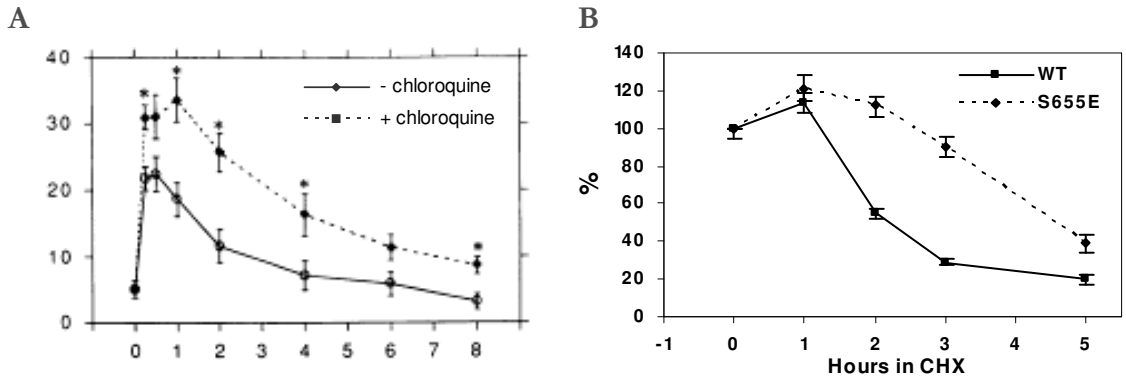

Figure VI.2. Comparison between the effects of lysosomal inhibition and S655 phosphorylation in APP mature levels. A: 8:00 h chase of endogenous radiolabelled APP mature levels in the presence (+) or absence (-) of chloroquine, a lysosomal activity inhibitor (Caporaso et al., 1992a); and **B:** 5:00 h time course of Wt and S655E APP-GFP mature levels in the presence of CHX .

Indeed, similarities can be draw between the metabolic degradation patterns of endogenous mature APP in the presence of the lysosomal inhibitor chloroquine (Fig. VI.2A), and of the mature S655E APP-GFP proteins (Fig. VI.2B). For example, chloroquine induced a significant effect on the mature APP turnover mature, with APP levels roughly duplicating in the presence of this drug. In the results presented here, the S655E APP-GFP mutant also exhibited a doubled half-life, relatively to the Wt or S655A species.

The YTSI Sorting signal and the Regulatory role of S655 Phosphorylation. A detailed search of the literature for traffic sorting motifs similar to the ^{653}YTSI^{656} domain provides further support for a S655 phosphorylation role in APP traffic sorting. For example, the YXXI motif present in the cytoplasmic terminus of lysosome membrane-associated glycoproteins (LAMPs), was found to be both necessary and sufficient for the targeting of these proteins or chimeric proteins to lysosomes (Williams and Fukuda, 1990; Rohrer et al., 1996). This motif also functions as a signal for protein sorting at several cellular sorting stations, and the surrounding amino acid sequence may also play an important role. At the TGN level, the presence of a glycine residue immediately upstream (GYQTI) targets proteins like LAMP-1 and Lgp120 from the TGN to lysosomal delivery through endosomes (Williams

and Fukuda, 1990; Harter and Mellman, 1992; Guarnieri et al., 1993; Honing and Hunziker, 1995). In addition, a small part of LAMP-1 and Lgp120 populations are, also due to the presence of the YXXI motif, sorted from the TGN to the PM. In the case of APP, the ^{653}YTSI^{656} is preceded by a glutamine (Q) residue, and so it is most probable that it is mainly sorted to the cell surface. At the PM, the YXXI motif is also responsible for the rapid internalization of proteins into clathrin-coated pits (Lai et al., 1995; Rohrer et al., 1996). For APP, there are two signals for PM endocytosis: the YNPTY and the YTSI motifs. Alone, these two motifs were similarly efficient (~50% of Wt TR) in the process of internalization of the transferrin receptor, together they appear to function in synergy (~80% of Wt TR) (Lai et al., 1995). A further step of sorting occurs at the early endosomes, to sort proteins to the late endosomes (and subsequently to lysosomes) or to recycle back to the plasma membrane in what is considered the default mechanism (Mayor et al., 1993). While proteins with an YTRF cytoplasmic motif, such as the TR receptor protein, are mainly early endosome residents (Mayor et al., 1993), the YXXI motif is responsible for protein sorting to late endosomes (Honing and Hunziker, 1995; Rohrer et al., 1996). Further protein sorting occurs to lysosomes or to the TGN/Golgi retrograde transport route, and in some cases such as for the cation-dependent mannose 6-phosphate receptor (CD-MPR), these are two competing routes (Rohrer et al., 1995). While sorting to lysosomes occurs at the late endosomes (Rohrer et al., 1995), sorting to TGN/Golgi may occur at the early/sorting endosome (Mallard et al, 1998; Mallard et al., 2002; Saint-Pol et al., 2004) or at the late endosome (Rohrer et al., 1995; Nair et al., 2003). In both sorting decisions the YXXI/L/V motifs may function as targeting signals. For example, the YQTI LAMP-1 motif targets the protein for lysosomal targeting (Rohrer et al., 1996), and the YQRL TGN38 motif regulates this protein's PM-to-TGN recycling (Reaves et al., 1993). Both of these are "four charged/polar residues Tyr-based motifs", but the latter has a higher charge due to the presence of the Arg residue (YQRL) instead of the Thr one (YQTI) at the third aa position. Interestingly, S655 phosphorylation at the APP ^{653}YTSI^{656} motif results in a similar effect of polar-to-charge substitution at the third aa position. Of note is that BACE-1 phosphorylation at a cytoplasmic serine residue, belonging to a sorting motif different to the YXXI one, targets the protein to TGN retrograde traffic and rescues it from lysosomal delivery (Walter et al., 2001; Wahle et al., 2005). It is possible that APP S655 phosphorylation, as BACE-1 S498 phosphorylation, enhances specific protein-protein binding, resulting in a higher PM-to-TGN retrograde transport, but further work has to be performed in this respect.

From the analysis of the APP-GFP trafficking and catabolism results, we conclude that the APP ^{653}YTSI^{656} domain must be involved in the targeting of APP at several sorting stations, and that S655 phosphorylation has an important regulatory role. At the TGN and cell surface, S655 phosphorylation seems to lead to higher transport efficiencies, as for example, a preference in S655 APP to be vesicle-incorporated. Upon internalization, two scenarios are possible depending where APP sorting towards the TGN occurs. If it occurs at the early/sorting endosomes, S655 dephosphorylation would be decisive for APP late endosomes delivery (S655A), and the phosphorylated form (S655E) directed for TGN recycling. If this sorting decision occurs at late endosomes, phospho S655 APP would be rescued from lysosomal degradation and targeted to be TGN delivered. It is of note that these targeting signals are not omnipotent, with proteins being preferentially but not exclusively target to one of these sorting pathways (Rohrer et al., 1996; Walter et al., 2001).

VI. 1. 2 – CONSEQUENCES OF S655 PHOSPHORYLATION-DEPENDENT SORTING ON THE APP PROTEOLYTIC PROCESSING

The different subcellular targeting of the APP-GFP phosphomutants in COS-7 cells had important effects on the rate of APP-GFP cleavage by α- and β-secretases. Indeed, APP proteolytic cleavages seem not to be directly dependent on the APP S655-phosphorylation state, but as the latter influences APP subcellular targeting, it has consequences on APP availability for subsequent cleavages. In addition, the results obtained also support the findings of the phosphomutants differential subcellular targeting.

α-secretase processing. S655 phosphorylation was found to increase APP processing by the α-secretase pathway. In fact, the S655E mutant presented a slightly faster rate and a higher fold-increase in αsAPP secretion (3.36 ± 0.14, Fig. III.3). Relatively to the Wt species, the S655A mutant had a slower rate of αsAPP secretion, although presenting a similar final fold-increase. The fact that the three APP-GFP species present similar basal levels of sAPP production and secretion (sections III.4.2 and III.4.3), may be explained by their subcellular distribution. The traffic assays (Fig.s II.8, II.9, and III.5) confirm that the S655E mutant has a higher and faster incorporation into post-TGN vesicles, while the opposite seems to occur for the S655A mutant. Nonetheless, the final net result must be similar for the two S665 phosphomutants in terms of availability to be cleaved by α-secretase: higher APP-GFP population at the main sites of α-secretase cleavage (TGN and PM), either dynamic (for

the S655E mutant) or resting (for the S655A mutant). Indeed, it seems that although not being preferentially targeted for TGN secretion, the higher retention time of the S655A mutant at the Golgi permits its cleavage by TGN α-secretases, as suggested by the sAPP assays at 20 ºC (Fig. III.5). Nonetheless, this S655A cleavage to sAPP or this latter subsequent secretion seem to occur slower than for the S655E mutant (Fig. III.3). Finally, considering the similar basal sAPP levels for the three APP-GFP species, the differences observed in the final levels of αsAPP production under CHX exposure must be related to the different mature APP-GFP half-lives. This is also indicated by the lower recovery of both S655A APP-GFP and sAPP levels after a period of severe protein synthesis inhibition (Fig. III.2).

β-secretase processing. Further characterization on the APP S655-phosphorylation state-dependent processing also revealed marginal differences on the S655 phosphomutants cleavage to Abeta. Although the S655A mutant had a higher percentage of cells with fluorescent Golgi with time (Fig.s II.8 and 9), the lower 22C11 Golgi staining at 5:00 h suggested that this pool had contributions from cleaved APP molecules lacking the N-terminal epitope (Fig. II.10). As the S655A α-secretase cleavage was not found to be increased, its rate of β-secretase cleavage was addressed, and the S655A-derived Abeta levels were observed to be slightly increased. Work from Hung and Selkoe (1994) on APP basal and regulated cleavage by secretases, suggested that the APP S655A mutant is more cleaved to Abeta. Under the presence of CHX, the cleavage of S655A by β- and γ-secretases to yield total Abeta was found to be increased by ~30% (Graph III.7, A.IV), although this increased was smaller (~10%) in the absence of CHX. In contrast but physiologically consistent, the S655E-derived Abeta production decreased by ~10% both in the presence or absence of CHX (Fig. III.7, A.IV and B.IV). The two reported main subcellular locations of Abeta production are the TGN and the endosomes, subcellular organelles enriched in β-secretase and γ-secretase. Although both S655 phosphomutants result in intense fluorescence of these subcellular compartments, the S655A has a higher time of residence at the Golgi, and this may be necessary and sufficient to be cleaved by the β-secretase at slightly higher rates. In addition, some competition between the S655 phosphorylation-dependent sorting/α-secretase and the β-secretase cleavage may exist. One hypothesis involves the preference of TGN phospho S655 APP to be vesicle incorporated and α-secretase cleaved, while dephospho S655 APP would have delayed vesicle incorporation and could be more available for β-secretase cleavage.

VI. 1. 3 – S655 PHOSPHORYLATION IN AICD NUCLEAR TARGETING

In agreement with previous direct visualizations of AICD nuclear targeting (Kinoshita et al., 2002; Muresan and Muresan, 2004, von Rotz et al., 2004), APP-GFP C-terminal fragments were also observed at the cells nuclei. These fragments most likely correspond to the expected AICD (although the αCTFs were not ruled out), as observed using Immunocytochemistry assays (Fig. II.11). Indeed, the APP-GFP-derived nuclear fluorescence co-localized and correlated with the staining of the anti-APP C-terminal antibody, but not with the staining of antibodies directed against the APP N-terminus or Abeta region. In addition to a S655 phosphorylation role in APP subcellular targeting and proteolytic processing, we could also observe alterations in the fate of the generated AICD peptides. Time-course analysis of the AICD-GFP nuclear localization led to the observation that S655E-derived AICD-GFP had slightly increased nuclear targeting kinetics, when compared with the Wt (Fig. II.8 and II.9). The S655A AICD-GFP, although initially having similar nuclear fluorescence percentages as the S655E mutant, failed to be highly nuclear targeted in the later time points, as observed to occur for the Wt and S655E species. In addition, the S655E AICD-GFP nuclear intensity was also overall higher than for Wt, and the S655A AICD-GFP nuclear fluorescence was overall less intense. Of note is that nuclear fluorescence intensity seems to reflect AICD-GFP abundance and provides a good visual correlation between the amounts of nuclear AICD and GFP intensity (Fig. II.12). These results are in agreement with the above mentioned higher processing of S655E APP by the α-secretase and consequently higher amounts of AICD generation. Hence, S655-phosphorylation may lead to a higher AICD generation through the α-secretase pathway, and to a higher AICD nuclear targeting. Taken together, these two facts support the hypothesis of APP as a RIP signalling molecule, and this is further discussed below.

VI. 1. 4 – SCHEMATIC REPRESENTATION OF S655 PHOSPHORYLATION-DEPENDENT APP CELLULAR PROCESSING

A schematic summary of the results obtained for the cellular fate of S655 phosphomutants in COS-7 cells, is presented in Figure VI.3, A. These schemes represents the main subcellular compartments for both the S655A and S655E mutants, and the observed alterations in terms of their cellular traffic sorting, proteolytic processing, and targeting of the generated AICD fragment. A synthesis of the main consequences of APP S655 phosphorylation in its cellular fate is presented in Figure VI.3., B.

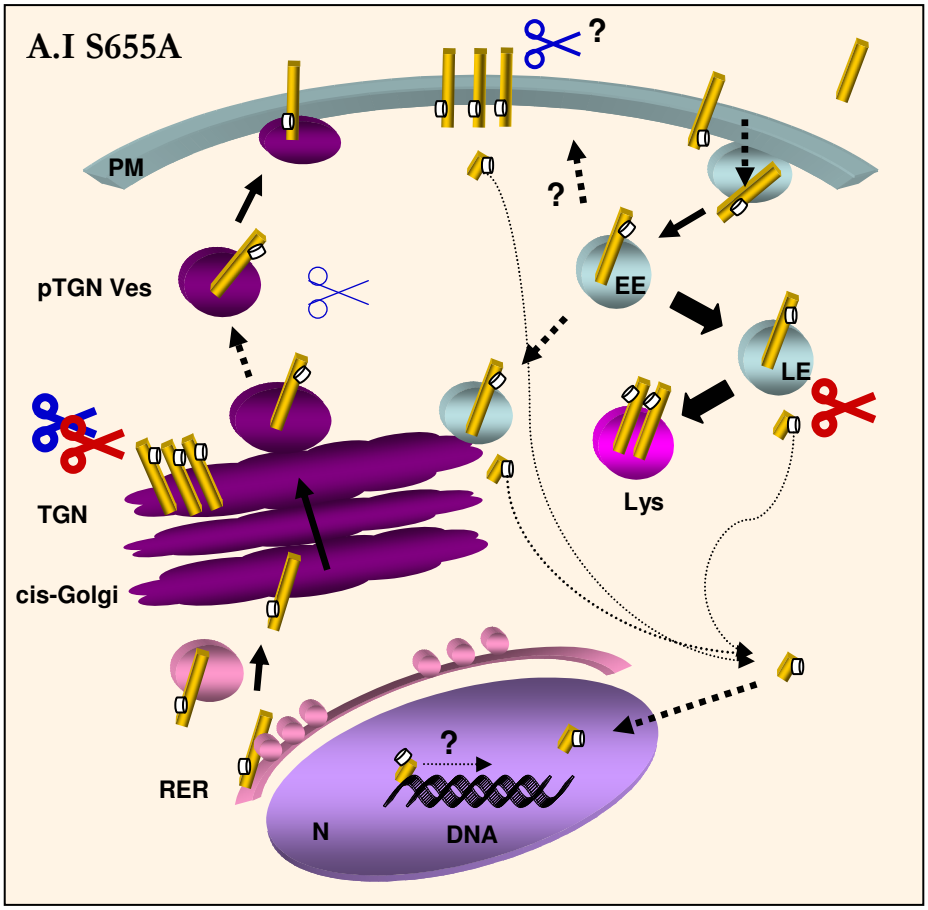
A.I S655A
PM
pTGN Ves
EE
LE
Lys
TGN
cis-Golgi
RER
N
DNA
?
APP:
S655A
S655E
sAPP:
AICD:
S655A
S655E

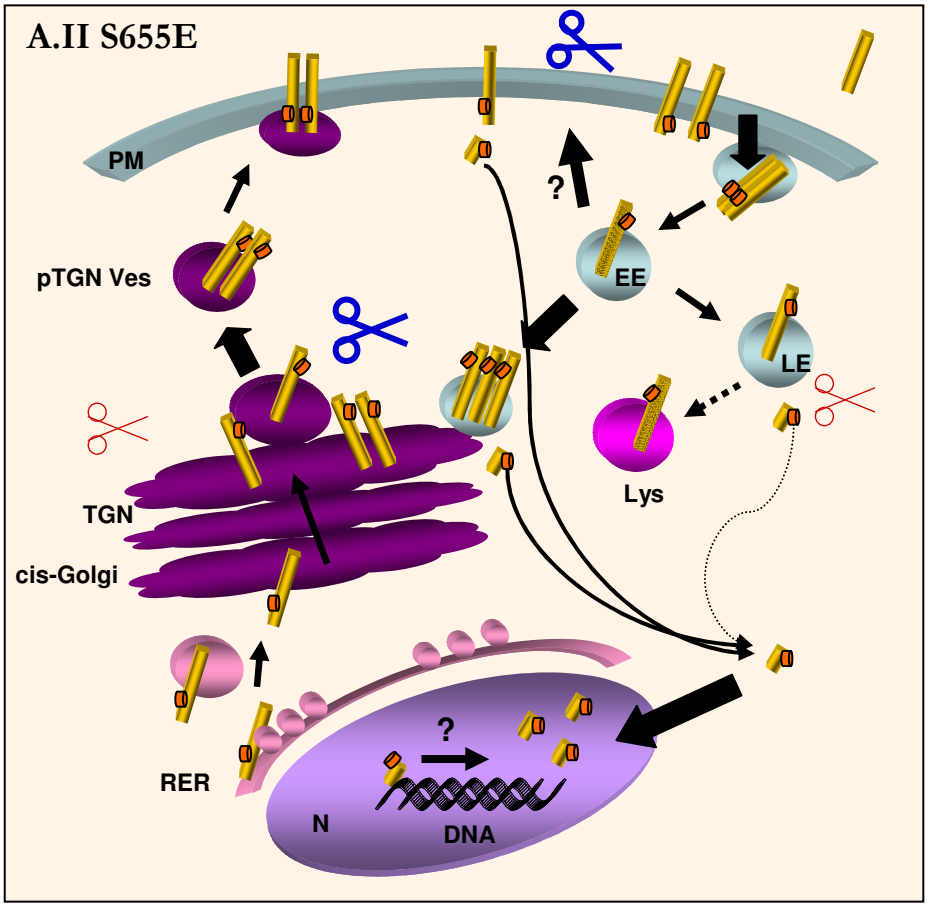
A.II S655E
PM
pTGN Ves
EE
LE
Lys
TGN
cis-Golgi
RER
N
DNA
?
Secretases:
α
β
Traffic &
Processing:
Decreased
Enhanced

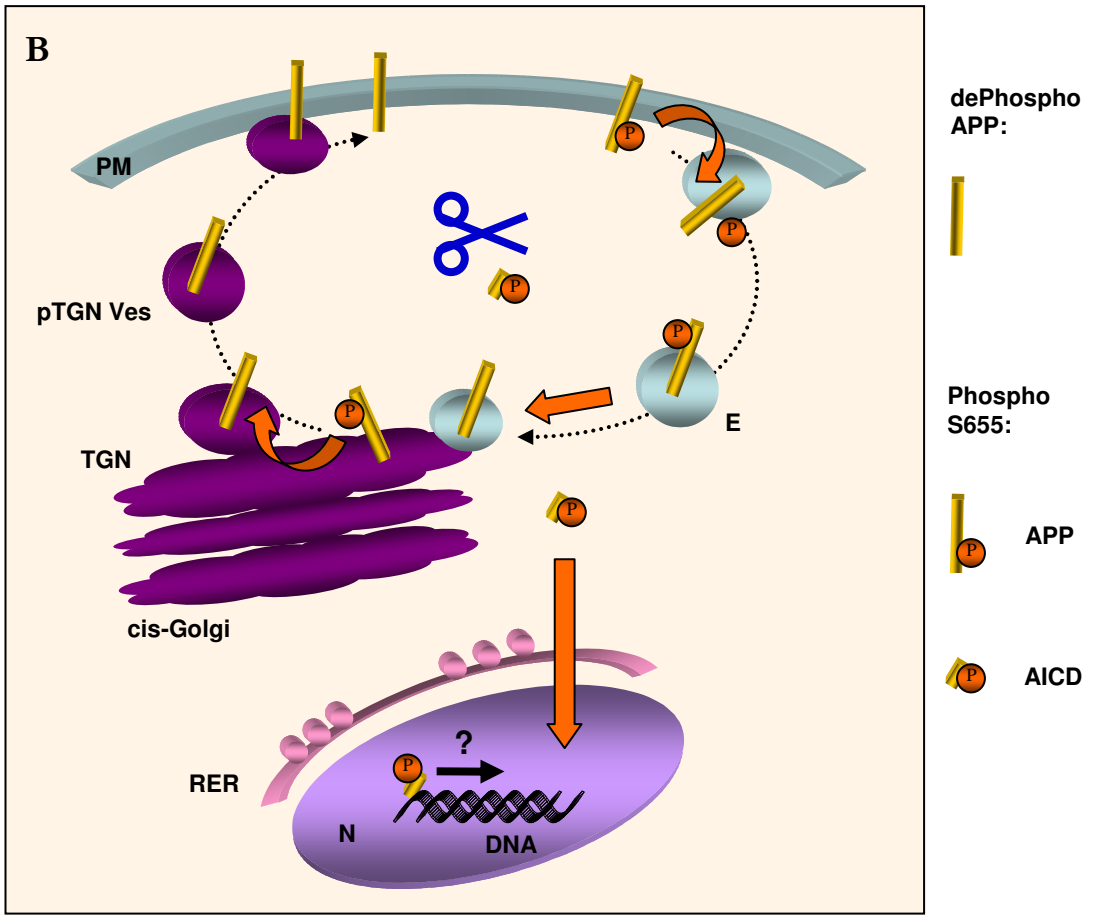

Figure VI.3. Schematic representation of S655 phosphorylated state-dependent APP cellular traffic and proteolytic processing in COS-7 cells. A: Summary of APP S655 phosphomutants (**A.I:** S655A; **A.II:** S655E) subcellular traffic and processing. **B:** S655 phosphorylation induces APP to circulate in a close circuit where it is mainly cleaved by the α-secretase. The generated AICD is nuclear targeted, where it may function as a gene transactivator. Orange arrows indicate direction of S655-induced APP/AICD traffic. **RER,** rough endoplasmic reticulum; **TGN,** trans-Golgi network; **pTGNV,** post-TGN vesicle (secretory vesicle); **PM,** plasma membrane; **EE,** early endosome; **LE,** late endosome; **Lys,** lysosome; **N,** nucleus. **E,** endosome. **Note:** in this scheme the early endosome was arbitrary taken as the sorting station where sorting and targeting of proteins to the retrograde TGN transport occurs.

Taken together, the results point to S655 phosphorylation as a cellular mechanism for activating the APP molecule to be preferentially cleaved through the α-secretase pathway and to generate its derived physiological active fragments: αsAPP and AICD. This is accomplished by decreasing mature APP degradation and targeting it to the subcellular compartments where α-secretase cleaves APP. Specifically, S655 phosphorylation "traps" APP, trafficking it between the trans-Golgi network and the plasma membrane. The generated AICD is, in addition, highly targeted to the cell nucleus, where it may form protein complexes with gene promoting activity.

VI. 1. 5 – S655 PHOSPHORYLATION-DEPENDENT APP NEURONAL TARGETING

In primary neurons of rat cortical origin, the APP S655 phosphorylation-state also influenced APP subcellular targeting. The S655E APP-GFP protein was observed to be targeted to more distal neuritic terminals than the other two APP-GFP species, in an apparent neuronal maturity-dependent manner (Fig. V.I). In turn, the S655A APP-GFP protein had a neuritic targeting that was slightly decreased and more resembling the Wt protein. The S655 phosphorylation state appeared not to influence the polarized intraneuronal APP targeting in terms of sorting into the axonal and somatodendritic domains (Fig. V.3, MAP-2 co-localization assays) but time-lapse experiments will be necessary to analyse this issue in more detail. In fact, it is possible that the S655E mutant is initially more targeted to the axon and subsequently endocytosed, and retrogradely transported back to the soma and dendritic compartments. The initial observations of S655E higher cell surface endocytosis and higher retrograde PM-to-TGN targeting in COS-7 cells support this hypothesis. As neuronal APP retrograde transport may occur via secondary endosomes, it is possible that the observed lower S655E lysosomal targeting in COS-7 cells may have a parallel in neurons. In a speculative hypothesis, S655E APP proteins arriving at the soma via retrograde axonal transport may be rescued from lysosomal delivery and degradation, being delivered instead to the dendrites. The net result of these hypotheses would still be the observed increase in both axonal and dendritic S655E APP-GFP transport. Interestingly from a signal transduction perspective, was the observation that the S655E protein was present in a higher number of axonal and dendritic growth cones. Axonal growth cones are specialized transduction systems involved in neuritic outgrowth and motility, which guide the elongating axon towards appropriate synaptic targets in response to extracellular signals or intrinsic cues. Two major proteins found in axonal growth cones are the APP-binding protein $G_0\alpha$ and its binding protein GAP-43 (Strittmatter et al., 1990; Strittmatter and Fishman, 1991), whose expression is up-regulated by APP (Mucke et al., 1994). The APP His^{657}-Lys^{676} hydrophobic pocket is necessary for APP-$G_0\alpha$ binding, and S655 phosphorylation may potentially regulate protein binding at this downstream region (see Chapter I). The finding that APP increases GAP-43 levels in a S655 phosphorylation state-dependent manner (Fig. V.6) suggests a role for S655 phosphorylation in neuronal APP RIP signalling, especially at neuritic growth cones. Further results supporting this hypothesis concern the observed higher targeting of nuclear S655E C-terminal fragments (Fig.s V.4 and V.5). This is in agreement with the previously observed higher nuclear targeting of S655E C-terminal fragments in COS-7 cells (Fig. II.8 and II.9).

VI. 2 – S655 PHOSPHORYLATION IN APP RIP SIGNALLING

Recent finding that APP has a physiological role as a nuclear gene transactivator have brought even more complexity to the putative APP functions and its mode of action. Only recently some of the physiological functions of AICD are being unravelled. AICD-containing nuclear complexes were observed to promote expression of genes such as *app* itself, *gsk-3β, tip60*, *bace* (Kim et al., 2003; von Rotz et al., 2004), *neprelysin* (Pardossi-Piquard et al., 2005), *kai1* (Baek et al., 2002; von Rotz et al., 2004; Telese et al., 2005). The first four seem to implicate AICD in an auto-positive feedback mechanism by the β-secretase (BACE) pathway, as GSK-3β was observed to phosphorylate APP at T668 (Aplin et al., 1996), apparently targeting APP to the β-secretase pathway. Tip60 is a nuclear histone acetylase involved in DNA binding and gene expression activation, which forms transactivation complexes with AICD and other proteins (Cao and Sudhof, 2001; von Rotz et al., 2004; Telese et al., 2005). The fifth gene (*neprelysin*) codes for an enzyme (Neprelysin, NEP), known to be involved in Abeta degradation. The sixth gene codes for KAI1, a tetraspanin protein involved in cell proliferation as a metastasis suppressor (reviewed in Jackson et al., 2005), and indicates a mechanism by which full-length APP may auto-regulate part of its functions (Qiu et al., 1995). Additionally, AICD was found to be involved in cellular Ca^{2+} signalling, and a mechanism of action was postulated involving transactivation of genes with *kai1* promoter elements, such as the gene coding for an ER Ca^{2+} ATPase (Leissring et al., 2002). This may also present a mechanism of APP involvement in cellular Ca^{2+}-dependent processes such as cellular differentiation, neurite outgrowth, and synaptic plasticity. Promoting APP expression may ultimately function to restore the cellular APP pool, but the fact that AICD up-regulates both BACE and NEP expression (with simultaneous enhancement of NEP activity) is intriguing. In fact, it seems that the generation of more AICD without possible pathogenic Abeta side-effects, would be more easily accomplished by up-regulation of *app* and *adamX* (X = 9, 10 or 17) genes. Nonetheless, AICD was not observed to induce *adam10* expression (von Rotz et al., 2004). Also intriguing is the finding that transfected AICD C59 inhibits, in a dose-dependent manner, the retinoic-acid (RA)-induced gene transactivation (Gao and Pimplikar, 2001). Retinoic acid is known to increase APP and BACE expressions (König et al., 1990; Lahiri and Nall, 1995; Beckman and Iverfeldt, 1997; Satoh and Kuroda, 2000), and recently it was observed to also induce *adam10* expression. APP/AICD and RA have some opposing effects in cells growth and differentiation, and APP/AICD antagonize RA-mediated responses

(Yoshikawa et al., 1992; Honda et al., 1998; Goodman and Pardee, 2003; Ono et al., 2004). Therefore, *app* expression and/or APP RIP signalling seem to set an end-point in RA-induced response. Hence, AICD signalling seems far more complex than expected, and may involve antagonistic effects (gene transcription inhibition or activation) under different physiological scenarios.

VI. 2. 1 – S655 PHOSPHORYLATION TRIGGERS APP RIP SIGNALLING

Kume et al. (2004) have shown that elevated β-secretase levels induce an increase in βCTF and Abeta generation, but led to a reduction of αCTF and AICD C50 generation. Furthermore, elevated α-secretase levels induced an increase of AICD C50. The generation of AICD C50 by epsilon-cleavage seems therefore to depend on αCTF, from which it seems to be more efficiently generated. This observation of gamma- and epsilon-cleavages being differentially regulated, is supported by findings of uncorrelated Abeta and AICD generation that will be discussed later (section VI.4). All these observations suggest that AICD C50 is mainly generated via the α-secretase pathway, as already expected from its much higher rate of APP cleavage. In addition, the α-secretase-triggered AICD generation was observed to be of central importance for APP nuclear signalling. Khvotchev and Sudhof (2004) have demonstrated that in COS, HEK 293, and PC12 cells, APP is cleaved at a high extent by the α-secretase at TGN and/or secretory vesicles. Disruption of the Golgi apparatus led to a severe inhibition of APP cleavage by the α-secretase, while inhibition of cellular exocytosis (but not of TGN and post-TGN vesicle release) did not inhibited APP cleavage although it did inhibit sAPP and Abeta secretions. Significantly, the authors observed that inhibition of APP processing by the α-secretase led to a severe down-regulation of AICD-induced transactivation, while sole inhibition of APP exocytosis did not render such an effect. Hence, the major route of physiological active AICD generation involves the APP α-secretase cleavage, which in COS-7 cells appears to occur to a higher extent at TGN and/or secretory vesicles. Our work supports the hypothesis that the main physiologically active AICD arrives from APP that is initially cleaved by the α-secretase, and that S655 phosphorylation regulates APP targeting to this pathway. As observed for the S655E mutant, S655 phosphorylation appears to mark the protein as a functional molecule and to lead to it's α-secretase cleavage and consequent AICD generation. Of note is that it is still unknown if the AICD generated from α- and β-secretase cleavages possess the same transactivation roles. In fact, although

being virtually identical, they may form different protein complexes due to being generated in different subcellular compartments, and thus induce different downstream effects. For example, phospho T668 APP is preferentially cleaved by the β-secretase and simultaneously interacts more loosely with one of the major AICD-binding protein (Fe65), which participates in most of the known AICD signalling complexes.

Protein phosphorylation is a well known strategy employed by the cells to regulate gene transactivation, including activation of latent transcription factors to perform their nuclear function. This may be accomplished by direct activation of the signalling protein (e.g. the signal transducers and activators of transcription - STAT - factors), or by inactivating its constitutive inhibitors (e.g for the transcription factor NF-κB; Rawson, 2002). In the APP RIP signalling context, "direct activation of the signalling molecule" may involve proteolytic activation of its precursor (APP) and/or of AICD itself. The first mechanism seems to occur after APP S655 phosphorylation and additionally, phospho S655 AICD appears to be in an activated "signalling mode", as it is highly targeted to the cells nuclei. One of the possible mechanisms involved in S655-induced AICD nuclear targeting is AICD stabilization. After being released from membranes to the cytoplasm, AICD is known to be rapidly degraded (Cupers et al., 2001; Kimberly et al., 2001), partially by the insulin degrading enzyme (Edbauer et al., 2002; Farris et al., 2003). AICD stabilization and nuclear targeting may be accomplished through AICD complex formation with specific proteins. In fact, AICD phosphorylation state-dependent formation of protein complexes seems the most attractive mechanism of modulating AICD effects on target genes.

VI. 3 – PUTATIVE MOLECULAR BASIS OF S655 PHOSPHORYLATION ACTION

Phosphorylation of APP at its C-terminus is believed to regulate binding of APP to other cellular proteins that participate and mediate APP cellular processing and function. Ando et al (2001) showed that the phosphorylation state of T668 regulates APP interactions at the ^{682}YENPTY^{687} motif. XL11 and mDab1 bind APP regardless of the phosphorylation state of APP T668, while Fe65 interaction with the APP recognition motif is weaker upon T668 phosphorylation. In addition, phosphorylation at this residue is associated with a preference for APP to be cleaved in the β-secretase pathway (Lee et al., 2003a; Muresan and Muresan, 2005). Nonetheless, it is still a matter of controversy if T668 phosphorylation results in higher

or decreased AICD nuclear targeting and transactivation (Zheng et al., 2003; Muresan and Muresan, 2004; Kimberly et al., 2005).

The targeting of APP to the α-secretase pathway by APP direct phosphorylation had not yet been observed. Our results implicate APP S655 phosphorylation in this targeting and strongly suggest its involvement in AICD nuclear signalling. The mechanisms by which S655 phosphorylation acts most probably include regulation of APP binding to specific proteins. For example, S655 phosphorylation may induce alterations in the APP affinity for specific APP binding proteins with roles as coat proteins or carrier microtubule-associated proteins, resulting in enhanced APP targeting to post-TGN, endocytic or specific neuronal vesicles. For example, BACE-1 S498 phosphorylation enhances its binding, through the S498-containing sorting motif, to the adaptor protein GGA (Shiba et al., 2004). This protein is involved in TGN anterograde transport and GGA-BACE-1 binding was later shown to be responsible for the phosphorylation-dependent BACE-1 retrograde transport (Wahle et al., 2005). A similar mechanism, involving a serine residue immediately upstream a sorting motif, occurs for the cation-independent MRP protein (Kato et al., 2002). APP S655 phosphorylation may therefore in this way accelerate specific vesicle traffic stages, such as APP cargo packaging, vesicle release, or vesicle targeting. Strong support for a regulatory role of S655 phosphorylation in APP binding comes from the reported effects of S655 phosphorylation on the APP molecule backbone. As indicated in Chapter I, characterization of APP phospho S655 molecules by multidimensional NMR spectroscopy points to S655 phosphorylation-induced structural changes in the ^{653}YTSI^{656} domain and in the downstream hydrophobic pocket (Ramelot and Nicholson, 2001). These alterations were also of higher range than T654 phosphorylation, with this latter only affecting the conformation of the ^{653}YTSI^{656} domain (Ramelot and Nicholson, 2001). The proteins that interact with these domains/sequences are the best candidates to bind APP in a S655 phosphorylation-dependent manner. These candidates include: APPBP2 (or PAT1), the alpha subunit of the G_0 protein, the Hsc73 (or Hsc70) chaperone, and an N-terminal acetyl-transferase protein (hARD1). This latter has not been well characterized and the only phenotype observed as a consequence of its binding to APP was a decreased Abeta generation, in an acetyl-transferase activity-dependent manner (Asaumi et al., 2005). The APP recognition sequence for the SET protein binding is still elusive, although it is thought to be at or near the ^{653}YTSI^{656} domain (Madeira et al., 2005). This protein appears to be involved in a Fe65/AICD/Tip60/SET protein complex, and to participate in AICD-mediated *kai1* gene transcription (Telese et al., 2005).

APPBP2 ("PAT1"). APPBP2 is a microtubule-interacting protein whose interaction with APP/AICD YXXI motif requires the Y653 integrity (Zheng et al., 1998). This binding leads to enhanced sAPP secretion into the medium (Zheng et al., 1998) and AICD nuclear targeting (Gao and Pimplikar, 2001). It is thought to increase sAPP secretion by increasing APP traffic to the secretory pathway. This protein has in its sequence four tandem repeats (TPR) conserved in all species of kinesin light chains (KLC). As the latter, APPBP2 binds to microtubules in an ATP-dependent manner (Zheng et al., 1998), and thus it may function as a motor protein, tracking vesicles along microtubules. Interestingly, APPBP2 is localized to the Golgi area, the cytoplasm and the nucleus, and it has been implicated in the neuronal anterograde transport and nuclear export of a herpes virus protein (Benboudjema et al., 2003). Hence, we postulate that APP phosphorylation at S655 enhances APP binding to APPBP2, thus leading to APP higher and faster vesicle trafficking.

The APP-APPBP2 binding may also be maintained after APP γ-secretase cleavage and play a role in APP nuclear targeting and nuclear function (Gao and Pimplikar, 2001). Co-transfection of MDCK cells with APPBP2 and AICD C59 or C57 lead to a higher AICD nuclear localization that was dependent on the presence of the APPBP2 nuclear localization signals (Gao and Pimplikar, 2001). This seems to implicate APPBP2-AICD binding in AICD stabilization and nuclear targeting, but a possible direct role for the APPBP2-AICD complex in transcription regulation is now emerging. Overexpression of APP or CTFs was reported to antagonize the RA-mediated responses, along with interfering with RA-induced mouse P19 stem cell differentiation. Furthermore, AICD was found to be a dose-dependent inhibitor of the retinoid pathway (see Gao and Pimplikar, 2001). As RA and AICD both promote *app* expression, the AICD may also have nuclear functions that are a part of an inhibitory mechanism of RA-mediated responses. In this transcription repression, the AICD may use APPBP2 DNA-binding motifs and its NR cyclin binding motif, which is commonly present in transcription corregulators. For instance, this NR cyclin motif is known to mediate the interaction of transactivators with their nuclear hormone receptors, such as the retinoid acid receptor (RAR). Interestingly, APPBP2 was found to form complexes with and to inhibit the action of the androgen receptor (Zhang et al., 2004), and of a strong inducer of the retinoid pathway, termed R3, that interferes with RAR function (Richards et al., 2003). Of note is that the sole co-expression of APPBP2 and AICD does not reverse the AICD-induced inhibition of the RA pathway (Gao and Pimplikar, 2001). AICD may also further inhibit its AICD-APPBP2 complex formation, as AICD C59 was reported to induce APPBP2 nuclear export along with its cytoplasmic proteasomal degradation (Gao and Pimplikar, 2001).

$G_0\alpha$. Beyond its known role in cell signalling as a subunit of G-proteins, $G_0\alpha$ was found to play a regulatory role in the process of cell secretion, including vesicle exocytosis (Lang et al., 1995). Interestingly, $G_0\alpha$ was observed to be present in cellular microdomains specialized in sorting, both secretory or endocytic in nature (Qian et al., 2003). In particular $G_0\alpha$ was detected in neuronal regulated vesicles: large dense core and small synaptic vesicles (Ahnert-Hilger et al., 1994). This G_0 subunit was also observed at the membrane of immature and mature vesicle granules of endocrine cells, and after a rapid carbachol-stimulus a part of this $G_0\alpha$ pool redistributes itself to the cytosol. As carbachol and other cholinergic-receptors agonists function as αsAPP inducers (Qiu et al., 2003), and carbachol enhances the secretion of APP-containing regulated vesicles (Efthimiopoulos et al., 1996), carbachol may function through $G_0\alpha$ traffic-regulation. $G_0\alpha$ has GTPase activity and Nishimoto and colleagues have demonstrated that an Ile^{656}-Lys^{676} hydrophobic pocket-containing APP sequence binds $G_0\alpha$ in a GTPγS-inhibitable manner (Nishimoto et al., 1993). Interestingly, the two types of molecules, along with cargo proteins, that are necessary for vesicle formation are: a small GTPase molecule and a coat protein, the latter necessary for cargo-recognition and destinations targeting. GTPases functions in traffic through coat-proteins activation and target, and in the vesicle uncoating for vesicle fusion with the acceptor membrane. $G_0\alpha$ GTPase activity and interaction with APP C-terminus ("cargo recognition") suggests that $G_0\alpha$ may function as an APP coat-protein in APP traffic. In total neuronal membranes and in CSEM, APP binding to an antibody against APP ectodomain (22C11) led to the reduction of the high-affinity G_0 GTPase activity. This inhibition was specific for $G_0\alpha$ and is reproduced by the addition of APP CTFs (Brouillet et al., 1999). Speculatively, S655 phosphorylation may direct APP to bind $G_0\alpha$, and in this way promote specific APP sorting at subcellular sorting stations and/or enhance APP packaging into specialized vesicles. This is important in neurons, with $G_0\alpha$ being potentially involved in APP neuritic traffic and signal transduction. In speculative terms, S655 phosphorylation may result in a more functional APP-mediated signalling at neuritic growth cones, by e.g. leading to more stable APP-$G_0\alpha$-GAP43 complexes and in that way stabilizing the neuronal GAP-43 pool. Furthermore, APP-$G_0\alpha$ binding may also be involved in AICD signalling after APP RIP cleavage, as evidences suggest that $G_0\alpha$ GTPase activity functions after γ-secretase cleavage of CTFs at the ε-site (AICD formation), and that AICD-$G_0\alpha$ may be involved in the AICD signalling (Yamatsuji et al., 1996; reviewed in Neve et al., 2001).

Hsc73. Hsc73 (or Hsc70), a nucleocytoplasmic chaperone with functions in protein traffic and protein degradation, was found to bind APP at the APP C-terminal sequence Q652-S675 (Kouchi et al., 1999). This sequence includes both the ^{653}YTSI^{656} and the hydrophobic pocket domains. Hsc73 is constitutively expressed in cells and is highly abundant in brain (Mathur et al., 1994). It may target proteins to proteasomal degradation, as a constituent of the 20S proteasome (Schmidt et al., 1997), or to lysosomal degradation (Agarraberes et al., 1997). Nonetheless, the proteasome has only been associated with immature and not mature APP degradation (Hare, 2001; Chen et al., 2005), and Hsc73 directs cytosolic but not membranar proteins to specific lysosomes and under stress conditions. As AICD degradation seems not to be dependent on lysosomal or proteasomal activity (Fadeeva et al., 2003), this will not be further discussed. Other important cellular processes in which Hsc73 is involved include cellular endocytosis, where it functions as an uncoating ATPase that selectively removes clathrin from brain coated vesicles (Honing et al., 1994; Buxbaum and Woodman, 1994), and nuclear protein import (Shi and Thomas, 1992), as is the case of nuclear hormone receptors (Hache et al., 1999; Krebs et al., 1999). Hence, Hsc73 binding to APP may be involved in its cell surface endocytosis and a putative Hsc73-AICD interaction may be involved in AICD nuclear inport. Thus, S655 phosphorylation may regulate APP RIP signalling by increasing APP endocytosis and/or AICD nuclear targeting through induction of APP/AICD binding to this cytosolic chaperone.

Figure VI.4 presents putative S655 phosphorylation-dependent binding of APP C-terminus to proteins with which it may form signalling complexes physiologically relevant in the APP cellular fate and RIP signalling contexts.

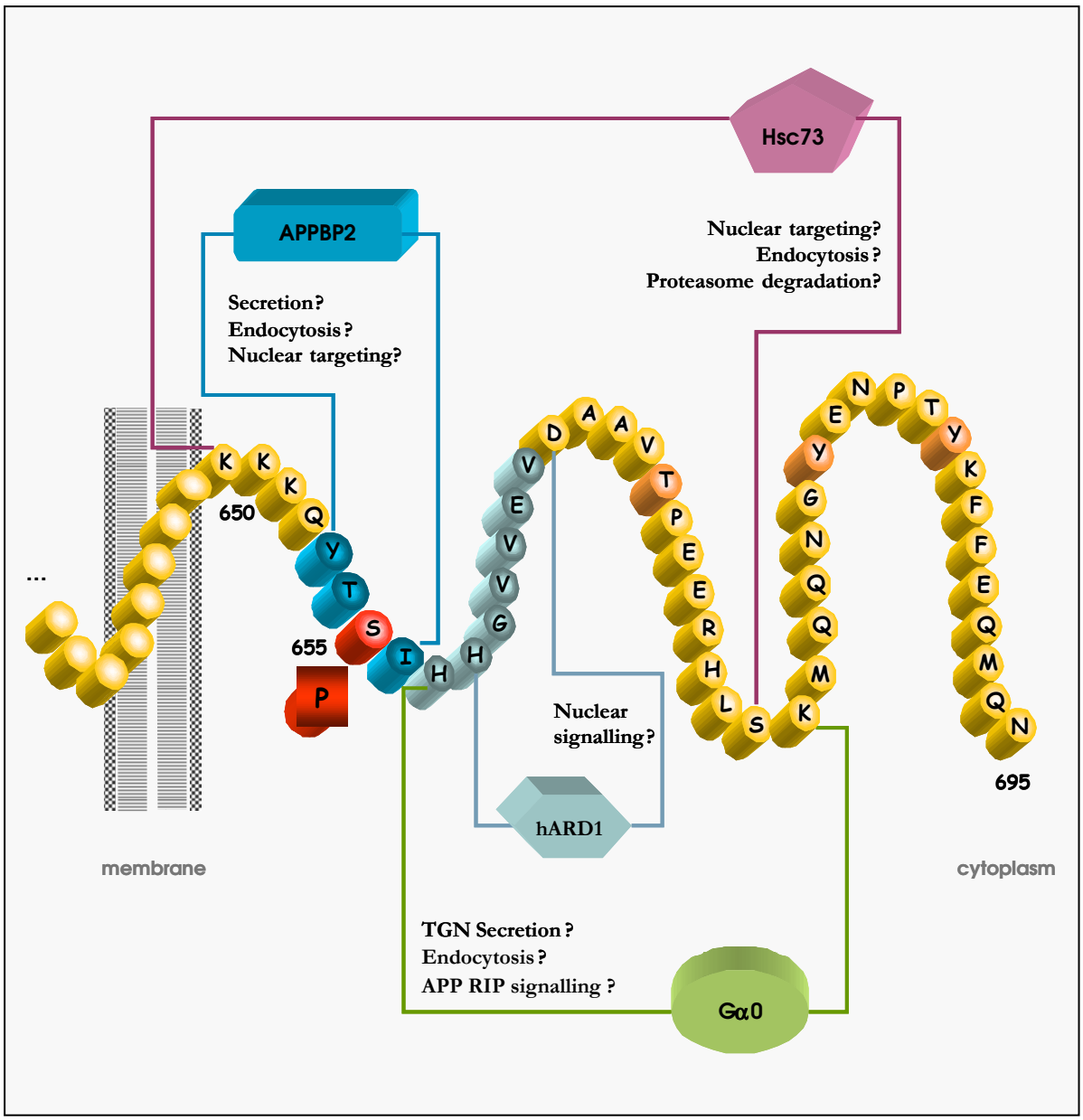

Figure VI.4. Schematic representation of putative S655 phosphorylated state-dependent APP interactions with proteins known to bind APP at its ^{653}YTSI^{656} domain, at the Ile^{656}-Val^{663} hydrophobic pocket, or at APP C-terminus sequence that includes both motifs.

VI. 4 – S655 PHOSPHORYLATION IN AD PATHOPHYSIOLOGY AND THERAPY

The importance of AD therapy can be outlined by the high number of reviews on this matter (200) just for the year 2005, and the over 200 different compounds that are at various stages of development for AD treatment. One of the main goals in AD therapy is to lower brain amyloid burden, with this being expected to be accomplished by 1) inhibition of Abeta production, 2) removal of amyloid plaques, and/or 3) inhibition of potential amyloidotrophic factors. Altogether, a minimum of six classes of compounds already exist, all of which are approved for clinical use and are either already being tested or ready for phase III clinical trials for the treatment of AD. These include: cholinesterase inhibitors, blockers of the NMDA receptor, antioxidants or blockers of oxidative deamination, anti-inflammatory agents, neurotrophic factors, and antiamyloid agents (including immunization, inhibition of the interaction between Abeta and its pathological chaperones, and cholesterol-lowering therapy) (reviewed in Schmitt et al., 2004). A GABA(B) antagonist is also being developed to be used in AD treatment (Ebert and Svendensen, 2005; Bullock, 2005). Nonetheless, no effective cure is yet available, and some of the trials in humans revealed to be disappointing. This is the case of Abeta immunization, for which the cognitive benefits of active immunization were difficult to show, and side effects were evident (high ventricular volumetry, acute autoimmune meningoencephalities, microhemorrhages within the brain vasculature) (Gandy and Heppner, 2005; Wisniewski and Frangione, 2005). The use of hormone replacement therapy has also generated controversy, as it leads to downstream effects in humans that include both decreased and increased dementia risk, with the latter being prevalent (Almeida and Flicker, 2005; Baum, 2005). Hence, adequate treatment strategies are still being actively pursued. A major field in new target molecules for anti-AD drugs concerns the finding of anti β- and γ-secretase inhibitors for lowering Abeta production (Thompson et al., 2005; Churcher and Beher, 2005). However, this is a challenging route, as γ-secretase is a promiscuous enzyme that is also responsible for intramembranous cleavage of a growing list of transmembrane proteins, which includes Notch (reviewed in Pollack and Lewis, 2005). In addition, γ-secretase is also needed for the APP RIP signalling process. BACE, on the other hand, seems to have fewer substrates, but care is needed as low levels of Abeta may possess normal cellular functions, such as neurite outgrowth. Hence, such β- and γ-secretase blocks over chronic periods of time may be deleterious, due to interference in other cell signalling pathways. Furthermore, the Abeta peptide is probably not the only causative agent of AD. AD patients of the Swedish

FAD type possess an abnormally low ratio of APP processing via the α-secretase pathway relative to the Abeta-generating one (Citron et al., 1992; Felsenstein et al., 1994). Transgenic mice with defective APP α-secretase processing show a severe phenotype of premature death, behavioural abnormalities, hippocampal and cortical neurodegeneration, and apoptosis (reviewed in Bayer et al., 2001). Recently, double-transgenic mouse studies have shown that increased activity of ADAM 10 can prevent plaque formation (Postina et al., 2004). These findings stress the importance of altered non-amyloidogenic cleavage in the disease process. Furthermore, several drugs with brain protective effects and that lower Abeta production, such as NSAIDs, statins and flavonoids, were recently found to channel APP to non-amyloidogenic processing (reviewed in Tang, 2005). Anti-AChE drugs, which increase acetylcholine brain levels, also lead to an increase in the αsAPP processing through m1 receptors. The benefit of neurotrophic factors in dementia has been highlighted (for example, Levy et al., 2005), and αsAPP is one such factor. Besides having synaptogenic properties, this APP fragment counteracts Abeta toxicity and glutamate-induced excitotoxicity and dendrite outgrowth inhibition, through modulation of cGMP and intracellular calcium levels (reviewed in Mattson, 2004). Inhibition of Abeta overproduction and stimulation of APP α-secretase processing are therefore part of the rationale strategies when AD prevention or progression reversion are considered. Another factor that may be contributing for AD development is impaired APP trafficking, which is also tightly interconnected with APP proteolytic processing (see Chapter V). For example, a major FAD gene (Barinaga, 1995) encodes a protein homologous to the *C. elegans* Spe4, a protein that plays a role in membrane sorting (L´Hernault and Arduengo, 1992). Furthermore, Abeta peptides may inhibit cellular secretion pathways, and thus impair APP trafficking. This may be accomplished through Abeta interaction with PKC, with this interaction provoking a decrease in the levels of activated cellular PKCα and PKCε and to decrease their translocation (Lee et al., 2003b). Hence, the high Abeta levels observed in AD patients may lead to altered protein traffic. Many authors now defend APP missorting and impaired APP secretory traffic as possible mechanisms contributing to some forms of AD. A more complete understanding of the normal physiological functions of APP and Abeta, and of the molecules that control APP trafficking and processing events, is therefore necessary if we are aiming to prevent AD and not only alleviate the disease symptoms.

The characteristics of APP as a signalling molecule and the involvement of APP RIP in AD onset and/or development are also the focus of interest in a large area of research.

Recent reports on AD, FAD mutations and APP RIP signalling dissociate the APP γ-secretase cleavages at the γ- and ε-sites, and thus the generation of Abeta and AICD. Several FAD mutations lead to Abeta enhanced production, but not all FAD mutations affect AICD C50 generation (Hecimovic et al., 2004). Furthermore, these authors observed that changes in total AICD C50 levels do not correlate with either an increase or a decrease of any Abeta species. This was also shown through pharmacological studies, using a compound (NSAIDs) that is being tested for lowering Abeta. This compound was able to decrease the Abeta levels without affecting the γ-secretase generation of AICD C50, AICD-Fe65 complex formation, or AICD-induced transcription (Weggen et al., 2003). Hence, a possible correlation between APP signalling and Abeta levels has still not been observed but, and as previously observed in section VI.2, APP RIP signalling may potentially alter Abeta production. In addition, the normal signalling mechanisms of AICD fragments may be are altered in an AD background. In many AD forms, especially the late-onset sporadic cases, defective degradation of Abeta and/or decreased APP α-secretase processing may be central to the disease process (Iwata et al., 2001; Leissring et al., 2003). Altered APP α-secretase processing potentially leads to down-regulated AICD production and function (Zheng et al., 2003; Khvotchev and Sudhof, 2004; Kume et al., 2004; Kimberly et al., 2005). Bergman et al. (2003) have also shown that FAD-carrying αCTF fragments are equally able to generate AICD C50 with signalling properties. Other possible contribution of APP C-terminal fragments in the AD disease is as cellular apoptotic inductors (reviewed in Neve et al., 2001). APP C-terminal fragments with or without the Abeta sequence were observed to be equally cytotoxic in differentiated PC12 cells and cortical neurons (Lee et al, 2000), directly implicating the AICD fragment as the active fragment. In this line, altered signalling properties of protein complexes formed by APP C-terminal fragments and $G_0\alpha$, may also be involved in AD. Some evidences indicate that $G_0\alpha$-APP/AICD altered binding leads to DNA fragmentation (reviewed in Neve et al., 2001). In fact, the APP London FAD mutation V642I causes neuronal DNA fragmentation in an APP-$G_0\alpha$ binding-dependent manner. This DNA fragmentation was prevented either by deletion of the APP hydrophobic pocket, by using a $G_0\alpha$ -inhibitor, or by expressing a $G_0\alpha$ dominant-negative mutant (Yamatsuji et al., 1996). Interestingly, this FAD mutation occurs in the APP sequence between the two AICD-generating γ-secretase cleavages, near the γ-secretase ε-site (L645), and inhibition of γ-secretase activity prevented DNA-fragmentation (Yamatsuji et al., 1996). Thus, a V642I AICD-$G_0\alpha$ protein complex appears to be the active complex involved

in the observed DNA fragmentation, and deregulated AICD-$G_0\alpha$-downstream signalling may be occurring (Giambarella et al., 1997). Hence, the mechanisms controlling APP RIP signalling are of growing interest as they may be involved in AD pathogenesis, and APP S655 phosphorylation may play an important role, as for example in regulating APP- $G_0\alpha$ binding.

S655 Phosphorylation in AD Pathophysiology and Therapy. From a therapeutic perspective, it appears desirable to aim for a situation where APP could still perform its nuclear signalling, but where Abeta levels would not be enhanced and APP traffic would not be inhibited. Our findings suggest that APP S655 phosphorylation may be suitable for all these purposes, with the benefit of being a post-translation modification that may be transiently modulated. In speculative terms, favouring the cerebral production of the neuroprotective αsAPP through S655 phosphorylation looks appealing, as it could also potentially maintain the Abeta levels low. S655 phosphorylation seems to "activate" the APP molecule to be targeted to subcellular sites of α-secretase processing. In addition, the S655A mutant is less efficiently sorted from the TGN, with consequences for increased cleavage by β-secretase. This slightly higher Abeta production, may have long-term effects on cells homeostasis. The observed higher S655E APP neuritic traffic has potential implications in its cleavage to the neurotrophic αsAPP (Parvathy et al., 1999), a hypothesis further supported by its higher nuclear targeting. Further work is therefore needed in clarifying the mechanisms of S655 phosphorylation action, and care must also be taken in developing treatment strategies. For example, although PKC is thought to induce APP S655 phosphorylation, long-term use of PKC drug activators was observed to decrease APP traffic, and to induce higher APP concentration at a cellular location where β-secretase is present. In fact, under these conditions, the Abeta levels were observed to be significantly increased (da Cruz e Silva et al., in preparation). Hence, long term use of PKC activators in AD therapy may potentially have an adverse effect and increase the Abeta burden. Additionally, adverse effects may occur resulting from the phosphorylation of other undetermined proteins. The development of therapeutic drugs targeting APP S655 phosphorylation may involve instead protein phosphatases or their binding proteins, which can provide tissue specificity (da Cruz e Silva et al., 2003 and 2004a).

VI. 5 – FINAL REMARKS

These APP phosphoresidue mutant studies represent a comprehensive analysis of APP trafficking and processing from a phosphorylation-dependent perspective and under a signal transduction AD therapeutic perspective. Analysis of the S655 phosphomutants trafficking reveals a role of S655 APP phosphorylation in the regulation of APP_{695} intracellular traffic between the TGN and the plasma membrane (COS-7 cells), and in the neuronal targeting of APP to functional neuritic terminals. These alterations in the APP molecule subcellular trafficking had consequences in its RIP processing. In COS-7 cells, mimicking constitutive S655 phosphorylation lead to an enhancement of the protein's half-life and to its increased α-secretase cleavage. The final objective of this APP activation and targeting to the α-secretase cleavage pathway strengthens the role of APP as a signalling molecule, as it leads to an enhancement in AICD nuclear targeting. A higher nuclear targeting of S655E APP C-terminal fragments was also observed in neurons. APP direct phosphorylation at its S655 residue may play important roles in regulating cerebral APP functions and neuronal signalling, an hypothesis supported by the higher expression of the growth associated protein 43 in S655E overexpressing cells.

The results here described help to unravel the key points of S655 phosphorylation-dependent non-pathogenic processing of APP, and to elucidate how pathological phosphorylation conditions maybe affecting cellular APP and amyloidogenic Abeta production. It is also worthwhile reinforcing that neuropathology has been associated with altered protein phosphorylation. Further characterization of S655 phosphorylation-dependent APP protein interactions and downstream effects will hopefully shed new light into these matters. Therefore, future research will focus on detailed characterization of key control points regulated by S655 phosphorylation, and in the identification of the underlying signal transduction cascades. The identity of target genes whose transcription may be regulated by S655 phosphorylation will also be addressed. Finally, the putative contributions of these interactions and downstream signalling to the AD pathogenesis will continue to be analysed.

ABBREVIATIONS

α	Anti- (applied for antibodies only)
aa	Amino Acid
Ab	Antibody
AD	Alzheimer's Disease
ADAM	A Desintegrin And Metalloproteinase
AICD/AID	APP Intracellular Domain
ANOVA	One way Analysis of Variance
AP	Amyloid Plaque (same as senile plaque)
APLP1/2	APP-Like Protein 1/2
APP	Alzheimer's Amyloid Precursor Protein
APPBP2	APP Binding Protein 2 (also named PAT1)
APP-GFP	APP_{695}-GFP fusion constructs or proteins
ApoE	Apolipoprotein E
ATP	Adenosine Triphosphate
BACE	β-site APP Cleaving Enzyme
BCA	Bicinchoninic Acid
BCIP	5-Bromo-4-Chloro-3-Indolyl Phosphate
BSA	Bovine Serum Albumin
CAM	Cell Adhesion Molecule
CCD	Charge Coupled Device Cameras
Cdc5	Cyclin-dependent protein kinase 5
Cdc2	Cyclin-dependent protein kinase 2
CD-MPR	Cation-Dependent Mannose 6-Phosphate Receptor
cDNA	Complementary DNA
CDK	Ciclin-Dependent Kinase
CSF	Cerebral Spinal Fluid
cGMP	Cyclic Guanosine Monophosphate
CHX	Cicloheximide
CNS	Central Nervous System
CSEM	Cholesterol and Sphingoglycolipid-Enriched Microdomains

(α/β)CTF	APP Carboxy-Terminal Fragment of α/β-secretase processing origin
DAG	Diacylglycerol
DMEM	Dulbecco's Modified Eagle's Medium
DNA	Deoxyribonucleic Acid
E. coli	Escherichia coli
ECL	Enhanced Chemiluminescence
EDTA	Ethylenodiaminoetetraacaetic Acid
EE	Early Endosome
EGFP	Enhanced Green Fluorescent Protein
ERK	Extracellular signal-Regulated Kinase
ER	Endoplasmic Reticulum
FAD	Familial Alzheimer's Disease
FBS	Fetal Bovine Serum
FDG-PET	Fluorodeoxyglucose - PET
Fig	Figure
g	Gravitational acceleration
G	Glicine amino acid residue
G_0	Heterotrimeric (α, β, and γ subunits) G_0 protein
G-cyclase	Guanylate cyclase
GFP	Green Fluorescent Protein
GGA	Golgi-localizing, γ-adaptin ear homology domain, ARF-interacting
GMP	Guanosine Monophosphate
GSK	Glycogen Synthase Kinase
GTP	Guanosine Triphosphate
HEPES	4-(2-HydroxyEthyl)-1-PiperazineEthane Sulfonic acid
h	Hour
I/Ile	Isoleucine amino acid residue
IgGs	Immunoglobulins G
Imm	Immature
Kai1	"Kang ai" (Chinese for anticancer) protein 1
KLC	Kinesin Light Chain
KPI	Kunitz-type serine Proteinase Inhibitor
LAMP	Lysosome Membrane-Associated Glycoproteins

LB	Luria Broth media
LE	Late Endosome
LTD	Long-Term Depression
LTP	Long-term Potentiation
mAb	Monoclonal Antibody
MAP-2	Microtubule Associated Protein 2
MAPK	Mitogen-activated protein kinase
Mat	Mature
MDCK	Madine-Darby Canine Kidney
min	Minute
MM	Molecular DNA length Markers
MOCK	Control cells subjected to equal procedures as tested cells
MPR	Mannose 6-Phosphate Receptor
mRNA	Messenger Ribonucleic Acid
NBT	Nitro Blue Tetrazolium
NEP	Neprelysin
NFT	Neurofibrillary Tangles
NICD	Notch Intracellular Domain
NMDA	N-Methly-D-Aspartate
NMR	Nuclear Magnetic Resonance spectroscopy
NSAIDs	Non Steroidal Anti-Inflammatory Drugs
NT	Non-Transfected
O.D.	Optical Density
p *aa*	Phospho *amino acid*
PAGE	PolyAcrylamide Gel Electrophoresis
PBS	Phosphate Buffer Saline (Modified Dulbecco's)
PCR	Polymerase Chain Reaction
PDBu	Phorbol Dibutyrate
PE	Phorbol Ester
pEGFP	EGFP-encoding mammalian expression plasmid vector
PET	Positron Emission Tomography (scans)
PhC	Phase Contrast
PHF	Paired Helical Filaments

PKC	Protein Kinase C
PKG	cGMP-dependent Protein Kinase
PLA2	Phospholipase A2
PLC	Phospholipase C
PM	Plasma Membrane
PMA	Phorbol 12-Myristate 13-Acetate
PS1/PS2	Presenilin 1 and 2
PP1/2	Protein Phosphatase type 1/2
Q/Gln	Glutamine amino acid residue
RA	Retinoic Acid
RAR	Retinoic Acid Receptor
RIP	Regulated Intramembranar Proteolysis
Rpm	Rotations per minute
RT-PCR	Reverse Transcriptase-Polymerase Chain Reaction
RT	Room Temperature
S/SerXXX	Serine amino acid residue at position XXX
(α/β)sAPP	Secreted APP of α/β-secretase processing origin
SAM	Substrate Adhesion Molecule
SDS	Sodium Dodecyl Sulfate
sec	Second
SEM	Standard Error of the Mean
STAT	Signal Transducers and Activators of Transcription
S655A	APP Serine 655 mutated to alanine
S655E	APP Serine 655 mutated to glutamate
T/ThrXXX	Threonine amino acid residue at position XXX
TACE	Tumor Necrosis Factor-α Converting Enzime
TBS	Tris Buffered Saline
TBS-T	TBS supplemented with Tween detergent
TEMED	N,N,N',N'-Tetramethylethylenediamine
TGN	Trans-Golgi Network
Tip60	Tat interactive protein, 60 kDa
TPR	Tandem Protein Repeats
TR	Transferrin Receptor

Tris-HCl	Tris (hydroxymethyl)-aminoethane Chloride
UV	Ultraviolet Light
Vs.	Versus
WR	Working Reagent
Wt	Wild-type
Y/Tyr	Tyrosine amino acid residue

REFERENCES

Abraham, C.R., Chen, C.-D., Weinmester, G., Neve, R.L. and Oh, S-Y. (2005). APP interacts with Notch receptors. 7th International Conference AD/PD, Sorrento, Italy. (OR)-61.

Agarraberes, F.A., Terlecky, S.R. and Dice, J.F. (1997). An intralysosomal hsp70 is required for a selective pathway of lysosomal protein degradation. *J. Cell Biol.* **137**: 825-34.

Ahlgren, S., Li, G.L. and Olsson, Y. (1996). Accumulation of beta-amyloid precursor protein and ubiquitin in axons after spinal cord trauma in humans: immunohistochemical observations on autopsy material. *Acta Neuropathol.* **92**: 49-55.

Ahnert-Hilger, G., Schafer, T., Spicher, K., Grund, C., Schultz, G. and Wiedenmann, B. (1994). Detection of G-protein heterotrimers on large dense core and small synaptic vesicles of neuroendocrine and neuronal cells. *Eur. J. Cell Biol.* **65**: 26-38.

Allinquant, B., Moya, K.L., Bouillot, C. and Prochiantz, A. (1994). Amyloid precursor protein in cortical neurons: coexistence of two pools differentially distributed in axons and dendrites and association with cytoskeleton. *J. Neurosci.* **14**: 6842-54.

Allsop, D., Landon, M. and Kidd, M. (1983). The isolation and amino acid composition of senile plaque core protein. *Brain Res.* **259**: 348-52.

Allsop, D. (2000). "Introduction to Alzheimer's Disease". *In.* Hooper, N.M. and Walker, J.M. *Eds* Alzheimer's disease: Methods and Protocols. Leeds, U.K: Humana Press, 1-22.

Almeida, O.P. and Flicker, L. (2005). Association between hormone replacement therapy and dementia: is it time to forget? *Int. Psychogeriatr.* **7**: 155-64. Review.

Alvarez, R., Alvarez, V., Lahoz, C.H., Martinez, C., Pena, J., Sanchez, J.M., Guisasola, L.M., Salas-Puig, J., Moris, G., Vidal, J.A., Ribacoba, R., Menes, B.B., Uria, D. and Coto, E. (1999). Angiotensin converting enzyme and endothelial nitric oxide synthase DNA polymorphisms and late onset Alzheimer's disease. *J. Neurol. Neurosurg. Psychiatr.* **67**: 733-36.

Alzheimer, A. (1907). Uber eine eigenartige Erkankung der Hirnrinde. *Allg. Zschr. F Psychiatr.-Gerichtl. Mediz.* **64**: 146-48.

Alzheimer, A. (1911). Über eigenartige Krankheitsfälle des späteren Alters. *Zbl. ges. Neurol. Psych.*. **4**: 356–85.

Amaducci, L., Falcini, M. and Lippi, A. (1992). Descriptive epidemiology and risk factors for Alzheimer's disease. *Acta Neurol. Scand. Suppl.* **139**: 21-25. Review.

Amaratunga, A. and Fine, R.E. (1995). Generation of amyloidogenic C-terminal fragments during rapid axonal transport in vivo of beta-amyloid precursor protein in the optic nerve. *J. Biol. Chem.* **270**: 17268-72.

Anders, A., Gilbert, S., Garten, W., Postina, R. and Fahrenholz, F. (2001). Regulation of the alpha-secretase ADAM10 by its prodomain and proprotein convertases. *FASEB J.* **15**: 1837-39.

Andersen, O.M., Reiche, J., Schmidt, V., Breiderhoff, T., Jansen, P., Wu, X., Bales, K.R., Cappai, R., Masters, C., Mufson, E.F., Paul, S.M., Gliemann, J., Nykjaer, A. and Willnow, T.E. (2005). SorLa/LR11, a neuronal sorting receptor that regulates processing of the Amyloid Precursor Protein. 7th International Conference AD/PD, Sorrento, Italy. (OR)-61.

Ando, K., Oishi, M., Takeda, S., Iijima, K., Isohara, T., Nairn, A.C., Kirino, Y., Greengard, P. and Suzuki, T. (1999). Role of phosphorylation of Alzheimer's amyloid precursor protein during neuronal differentiation. *J. Neurosci.* **19**: 4421-27.

Ando, K., Iijima, K.I., Elliott, J.I., Kirino, Y. and Suzuki, T. (2001). Phosphorylation-dependent regulation of the interaction of amyloid precursor protein with Fe65 affects the production of beta-amyloid. *J. Biol. Chem.* **276**: 40353-61.

Annaert, W. and De Strooper, B. (1999). Presenilins: molecular switches between proteolysis and signal transduction. *Trends Neurosci.* **22: 4**39-43. Review.

Aplin, A. E., Gibb, G.M., Jacobsen, J.S., Gallo, J.M. and Anderton, B.H. (1996). In vitro phosphorylation of the cytoplasmic domain of the amyloid precursor protein by glycogen synthase kinase-3beta. *J. Neurochem.* **67**: 699-707.

Asaumi, M., Iijima, K., Sumioka, A., Iijima-Ando, K., Kirino, Y., Nakaya, T. and Suzuki, T. (2005). Interaction of N-terminal acetyltransferase with the cytoplasmic domain of beta-amyloid precursor protein and its effect on Abeta secretion. *J. Biochem.* **137**: 147-55.

Atwood, C.S., Obrenovich, M.E., Liu, T., Chan, H., Perry, G., Smith, M.A. and Martins, R.N. (2003). Amyloid-beta: a chameleon walking in two worlds: a review of the trophic and toxic properties of amyloid-beta. *Brain Res. Brain Res. Rev.* **43**: 1-16. Review.

Baek, S.H., Ohgi, K.A., Rose, D.W., Koo, E.H., Glass, C.K. and Rosenfeld, M.G. (2002). Exchange of N-CoR corepressor and Tip60 coactivator complexes links gene expression by NF-kappaB and beta-amyloid precursor protein. *Cell* **110**: 55-67.

Bagshaw, R.D., Pasternak, S.H., Mahuran, D.J. and Callahan, J.W. (2003). Nicastrin is a resident lysosomal membrane protein. *Biochem. Biophys. Res. Commun.* **300**: 615-18.

Barger, S.W., Fiscus, R.R., Ruth, P., Hofmann, F. and Mattson, M.P. (1995). Role of cyclic GMP in the regulation of neuronal calcium and survival by secreted forms of beta-amyloid precursor. *J. Neurochem.* **64**: 2087-96.

Barinaga, M. (1995). New Alzheimer's gene found. *Science* **268**: 1845-46.

Baum, LW. (2005). Sex, hormones, and Alzheimer's disease. *J. Gerontol. A. Biol. Sci. Med. Sci.* **60**: 736-43. Review.

Bayer, T.A., Cappai, R., Masters, C.L., Beyreuther, K. and Multhaup, G. (1999). It all sticks together: the APP related family of proteins and Alzheimer's disease. *Mol. Psychiatry* **4**: 524-28.

Bayer, T.A., Wirths, O., Majtenyi, K., Hartmann, T., Multhaup, G., Beyreuther, K. and Czech, C. (2001). Key factors in Alzheimer's disease: beta-amyloid precursor protein processing, metabolism and intraneuronal transport. *Brain Pathol.* **11**: 1-11. Review.

Beckman, M. and Iverfeldt, K. (1997). Increased gene expression of beta-amyloid precursor protein and its homologues APLP1 and APLP2 in human neuroblastoma cells in response to retinoic acid. *Neurosci. Lett.* **221**: 73-76.

Beher, D., Hesse, L., Masters, C.L. and Multhaup, G. (1993). Regulation of amyloid protein precursor (APP) binding to collagen and mapping of the binding sites on APP and collagen type I. *J. Biol. Chem.* **271**: 1613-20.

Benboudjema, L., Mulvey, M., Gao, Y., Pimplikar, S.W. and Mohr, I. (2003). Association of the herpes simplex virus type 1 Us11 gene product with the cellular kinesin light-chain-related protein PAT1 results in the redistribution of both polypeptides. *J. Virol.* **77**: 9192-203.

Benmerah, A., Lamaze, C., Begue, B., Schmid, S.L., Dautry-Varsat, A. and Cerf-Bensussan, N. (1998). AP-2/Eps15 interaction is required for receptor-mediated endocytosis. *J. Cell Biol.* **140**: 1055-62.

Bennecib, M., Gong, C.X., Grundke-Iqbal, I. and Iqbal, K. (2000). Role of protein phosphatase-2A and -1 in the regulation of GSK-3, cdk5 and cdc2 and the phosphorylation of tau in rat forebrain. *FEBS Lett.* **485**: 87-93.

Bennett, B.D., Denis, P., Haniu, M., Teplow, D.B., Kahn, S., Louis, J.-C., Citron, M. and Vassar, R. (2000). A furin-like convertase mediates propeptide cleavage of BACE, the Alzheimer's beta -secretase. *J. Biol. Chem.* **275**: 37712-17.

Berezovska, O., Jack, C., Deng, A., Gastineau, N., Rebeck, G.W. and Hyman, B.T. (2001). Notch1 and amyloid precursor protein are competitive substrates for presenilin1-dependent gamma-secretase cleavage. *J. Biol. Chem.* **276**: 30018-23.

Bergman, A., Religa, D., Karlstrom, H., Laudon, H., Winblad, B., Lannfelt, L., Lundkvist, J. and Naslund, J. (2003). APP intracellular domain formation and unaltered signaling in the presence of familial Alzheimer's disease mutations. *Exp. Cell Res.* **287**: 1-9.

Black, R.A., Rauch, C.T., Kozlosky, C.J., Peschon, J.J., Slack, J.L., Wolfson, M.F., Castner, B.J., Stocking, K.L., Reddy, P., Srinivasan, S., Nelson, N., Boiani, N., Schooley, K.A., Gerhart, M., Davis, R., Fitzner, J.N., Johnson, R.S., Paxton, R.J., March, C.J. and Cerretti, D.P. (1997). A metalloproteinase disintegrin that releases tumour-necrosis factor-alpha from cells. *Nature* **385**: 729-33.

Borchelt, D.R., Thinakaran, G., Eckman, C.B., Lee, M.K., Davenport, F., Ratovitsky, T., Prada, C.M., Kim, G., Seekins, S., Yager, D., Slunt, H.H., Wang, R., Seeger, M., Levey, A.I., Gandy, S.E., Copeland, N.G., Jenkins, N.A., Price, D.L., Younkin, S.G. and Sisodia, S.S. (1996). Familial Alzheimer's disease-linked presenilin 1 variants elevate Abeta1-42/1-40 ratio in vitro and in vivo. *Neuron* **17**: 1005-13.

Borg, J.P., Ooi, J., Levy, E. and Margolis, B. (1996). The phosphotyrosine interaction domains of X11 and FE65 bind to distinct sites on the YENPTY motif of amyloid precursor protein. *Mol. Cell Biol.* **16**: 6229-41.

Bothwell, M. and Giniger, E. (2000). Alzheimer's disease: neurodevelopment converges with neurodegeneration. *Cell* **102**: 271-73. Review.

Bourgoin, S.G., Harbour, D. and Poubelle, P.E. (1996). Role of protein kinase C alpha, Arf and cytoplasmic calcium transients in phospholipase D activation by sodium fluoride in osteoblast-like cells. *J. Bone Miner. Res.* **11: 1**655-65.

Brakch, N., Allemandou, F., Cavadas, C., Grouzmann, E. and Brunner, H.R. (2002). Dibasic cleavage site is required for sorting to the regulated secretory pathway for both pro- and neuropeptide Y. *J. Neurochem.* **81**: 1166-75.

Brandt, R., Hundelt, M. and Shahani, N. (2005). Tau alteration and neuronal degeneration in tauopathies: mechanisms and models. *Biochim. Biophys. Acta* **1739:** 331-54. Review.

Breen, K.C., Bruce, M. and Anderton, B.H. (1991). Beta amyloid precursor protein mediates neuronal cell-cell and cell-surface adhesion. *J. Neurosci. Res.* **28**: 90-100.

Bressler, S.L., Gray, M.D., Sopher, B.L., Hu, Q., Hearn, M.G., Pham, D.G, Dinulos, M.B., Fukuchi, K., Sisodia, S.S., Miller, M.A., Disteche, C.M. and Martin, G.M. (1996). cDNA cloning and chromosome mapping of the human Fe65 gene: interaction of the conserved cytoplasmic domains of the human beta-amyloid precursor protein and its homologues with the mouse Fe65 protein. *Hum. Mol. Genet.* **5**: 1589-98.

Brion, C., Miller, S.G. and Moore, H.P. (1992). Regulated and constitutive secretion. Differential effects of protein synthesis arrest on transport of glycosaminoglycan chains to the two secretory pathways. *J. Biol. Chem.* **267**: 1477-83.

Brou, C., Logeat, F., Gupta, N., Bessia, C., LeBail, O., Doedens, J.R., Cumano, A., Roux, P., Black, R.A. and Israel, A. (2000). A novel proteolytic cleavage involved in Notch signaling: the role of the disintegrin-metalloprotease TACE. *Mol. Cell Biol.* **5**: 207–16.

Brouillet, E., Trembleau, A., Galanaud, D., Volovitch, M., Bouillot, C., Valenza, C., Prochiantz, A. and Allinquant, B. (1999). The amyloid precursor protein interacts with Go heterotrimeric protein within a cell compartment specialized in signal transduction. *J. Neurosci.* **19**: 1717-27.

Bullido, M.J., Munoz-Fernandez, M.A., Recuero, M., Fresno, M. and Valdivieso, F. (1996). Alzheimer's amyloid precursor protein is expressed on the surface of hematopoietic cells upon activation. *Biochim. Biophys. Acta* **1313**: 54-62.

Bullock, R. (2005). SGS-742 Novartis. *Curr. Opin. Investig. Drugs.* **6**: 108-13. Review.

Burdick, D., Soreghan, B., Kwon, M., Kosmoski, J., Knauer, M., Henschen, A., Yates, J., Cotman, C. and Glabe, C. (1992). Assembly and aggregation properties of synthetic Alzheimer's A4/beta amyloid peptide analogs. *J. Biol. Chem.* **267**: 546-54.

Busciglio, J., Gabuzda, D.H., Matsudaira, P. and Yankner, B.A. (1993). Generation of beta-amyloid in the secretory pathway in neuronal and nonneuronal cells. *Proc. Natl. Acad. Sci. USA* **90**: 2092-96.

Bush, A.I., Multhaup, G., Moir, R.D., Williamson, T.G., Small, D.H., Rumble, B., Pollwein, P., Beyreuther, K. and Masters, C.L. (1993). A novel zinc(II) binding site modulates the function of the beta A4 amyloid protein precursor of Alzheimer's disease. *J. Biol. Chem.* **268**: 16109-12.

Bush, A.I., Pettingell, W.H. Jr., Paradis, M.D. and Tanzi, R.E. (1994). The amyloid beta-protein precursor and its mammalian homologues. Evidence for a zinc-modulated heparin-binding superfamily. *J. Biol. Chem.* **269**: 26618-21.

Buxbaum, E. and Woodman, P.G. (1994). Selective action of uncoating ATPase towards clathrin-coated vesicles from brain. *J. Cell Sci.* **108**: 1295-306.

Buxbaum, J.D. and Greengard, P. (1996). Regulation of APP processing by intra- and intercellular signals. *Ann.. N. Y. Acad.. Sci.* **17:** 327-31. Review.

Buxbaum, J.D., Gandy, S.E., Cicchetti, P., Ehrlich, M.E., Czernik, A.J., Fracasso, R.P., Ramabhadran, T.V., Unterbeck, A.J. and Greengard, P. (1990). Processing of Alzheimer beta/A4 amyloid precursor protein: modulation by agents that regulate protein phosphorylation. *Proc. Natl. Acad. Sci. USA* **87**: 6003-06.

Buxbaum, J.D., Ruefli, A.A., Parker, C.A., Cypess, A.M. and Greengard, P. (1994). Calcium regulates processing of the Alzheimer amyloid protein precursor in a protein kinase C-independent manner. *Proc. Natl. Acad. Sci. USA* **91**: 4489-93.

Buxbaum, J.D., Thinakaran, G., Koliatsos, V., O'Callahan, J., Slunt, H.H., Price, D.L. and Sisodia, S.S. (1998). Alzheimer amyloid protein precursor in the rat hippocampus: transport and processing through the perforant path. *J. Neurosci.* **18**: 9629-37.

Caceres, A., Banker, G.A. and Binder, L., (1986). Immunocytochemical localization of tubulin and microtubule-associated protein 2 during the development of hippocampal neurons in culture. *J. Neurosci.* **6:** 714-22.

Cai, D., Leem, J.Y., Greenfield, J.P., Wang, P., Kim, B.S., Wang, R., Lopes, K.O., Kim, S.H., Zheng, H., Greengard, P., Sisodia, S.S., Thinakaran, G. and Xu, H. (2003). Presenilin-1 regulates intracellular trafficking and cell surface delivery of beta-amyloid precursor protein. *J. Biol. Chem.* **278**: 3446-54.

Cai, D., Zhong, M., Wang, R., Netzer, W.J., Shields, D., Zheng, H., Sisodia, S.S., Foster, D.A., Gorelick, F.S., Xu, H. and Greengard, P. (2006). Phospholipase D1 corrects impaired betaAPP trafficking and neurite outgrowth in familial Alzheimer's disease-linked presenilin-1 mutant neurons. *Proc. Natl. Acad. Sci. USA* **103**: 1936-1940.

Cai, H., Wang, Y., McCarthy, D., Wen, H., Borchelt, D.R., Price, D.L. and Wong, P.C. (2001). BACE1 is the major beta-secretase for generation of Abeta peptides by neurons. *Nat. Neurosci.* **4**: 233-34.

Cai, X.D., Golde, T.E. and Younkin, S.G. (1993). Release of excess amyloid beta protein from a mutant amyloid beta protein precursor. *Science* **259**: 514-16.

Cao, X. and Sudhof, T.C. (2001). A transcriptionally [correction of transcriptively] active complex of APP with Fe65 and histone acetyltransferase Tip60. *Science* **293**: 115-20. Erratum in: *Science* 2001 **293**: 1436.

Cao, X. and Sudhof, T.C. (2004). Dissection of amyloid-beta precursor protein-dependent transcriptional transactivation. *J. Biol. Chem.* **279**: 24601-11.

Capell, A., Grunberg, J., Pesold, B., Diehlmann, A., Citron, M., Nixon, R., Beyreuther, K., Selkoe, D.J. and Haass, C. (1998). The proteolytic fragments of the Alzheimer's disease-associated presenilin-1 form heterodimers and occur as a 100-150-kDa molecular mass complex. *J. Biol. Chem.* **273**: 3205-11.

Capell, A., Steiner, H., Willem, M., Kaiser, H., Meyer, C., Walter, J., Lammich, S., Multhaup, G. and Haass, C. (2000). Maturation and pro-peptide cleavage of beta-secretase. *J. Biol. Chem.* **275**: 30849-54.

Capell, A., Beher, D., Prokop, S., Steiner, H., Kaether, C., Shearman, M.S. and Haass, C. (2005). Gamma-secretase complex assembly within the early secretory pathway. *J. Biol. Chem.* **280**: 6471-78.

Caporaso, G.L., Gandy, S.E., Buxbaum, J.D. and Greengard, P. (1992a). Chloroquine inhibits intracellular degradation but not secretion of Alzheimer beta/A4 amyloid precursor protein. *Proc. Natl. Acad. Sci. USA* **89**: 2252-56.

Caporaso, G.L., Gandy, S.E., Buxbaum, J.D., Ramabhadran, T.V. and Greengard, P. (1992b). Protein phosphorylation regulates secretion of Alzheimer beta/A4 amyloid precursor protein. *Proc. Natl. Acad. Sci. USA* **89**: 3055-59.

Caporaso, G.L., Takei, K., Gandy, S.E., Matteoli, M., Mundigl, O., Greengard, P. and De Camilli, P. (1994). Morphologic and biochemical analysis of the intracellular trafficking of the Alzheimer beta/A4 amyloid precursor protein. *J Neurosci.* **14: 3**122-38.

Caputi, A., Barindelli, S., Pastorino, L., Cimino, M., Buxbaum, J.D., Cattabeni, F. and Di Luca, M. (1997). Increased secretion of the amino-terminal fragment of amyloid precursor protein in brains of rats with a constitutive up-regulation of protein kinase C. *J. Neurochem.* **68**: 2523-9.

Cedazo-Minguez, A., Bonecchi, L., Winblad, B., Post, C., Wong, E.H., Cowburn, R.F. and Benatti, L. (1999). Nicergoline stimulates protein kinase C mediated alpha-secretase processing of the amyloid precursor protein in cultured human neuroblastoma SH-SY5Y cells. *Neurochem. Int.* **35**: 307-15.

Chan, S.L., Furukawa, K. and Mattson, M.P. (2002). Presenilins and APP in neuritic and synaptic plasticity: implications for the pathogenesis of Alzheimer's disease. *Neuromolecular Med.* **2**: 167-96. Review.

Chapman, J., Wang, N., Treves, T.A., Korczyn, A.D. and Bornstein, N.M. (1998). ACE, MTHFR, factor V Leiden and ApoE polymorphisms in patients with vascular and Alzheimer's dementia. *Stroke* **29**: 1401-4.

Chartier-Harlin, M.C., Crawford, F., Houlden, H., Warren, A., Hughes, D., Fidani, L., Goate, A., Rossor, M., Roques, P., Hardy, J., et al. (1991). Early-onset Alzheimer's disease caused by mutations at codon 717 of the beta-amyloid precursor protein gene. *Nature* **353**: 844-46.

Checler, F. (1995). Processing of the beta-amyloid precursor protein and its regulation in Alzheimer's disease. *J. Neurochem.* **65**: 1431-44.

Checler, F., Cisse, M.A., Sunyach, C., Lefranc-Jullien, S. and Vincent, B. (2005). Physiological processing of cellular prion and beta-amyloid precursor proteins enzymes and regulation. 7th International Conference AD/PD, Sorrento, Italy. (IL)-4.

Chen, F., Yang, D.S., Petanceska, S., Yang, A., Tandon, A., Yu, G., Rozmahel, R., Ghiso, J., Nishimura, M., Zhang, D.M., Kawarai, T., Levesque, G., Mills, J., Levesque, L., Song, Y.Q., Rogaeva, E., Westaway, D., Mount, H., Gandy, S., St George-Hyslop, P. and Fraser, P.E. (2000). Carboxyl-terminal fragments of Alzheimer beta-amyloid precursor protein accumulate in restricted and unpredicted intracellular compartments in presenilin 1-deficient cells. *J. Biol. Chem.* **275**: 36794-802.

Chen, Q., Liu, J.B., Horak, K.M., Zheng, H., Kumarapeli, A.R., Li, J., Li, F., Gerdes, A.M., Wawrousek, E.F. and Wang, X. (2005). Intrasarcoplasmic amyloidosis impairs proteolytic function of proteasomes in cardiomyocytes by compromising substrate uptake. *Circ. Res.* **97**: 1018-26.

Chen, W.J., Goldstein, J.L. and Brown, M.S. (1990). NPXY, a sequence often found in cytoplasmic tails, is required for coated pit-mediated internalization of the low density lipoprotein receptor. *J. Biol. Chem.* **265**: 3116-23.

Churcher, I. and Beher, D. (2005). Gamma-secretase as a therapeutic target for the treatment of Alzheimer's disease. *Curr. Pharm. Des.* **11**: 3363-82. Review.

Citron, M., Oltersdorf, T., Haass, C., McConlogue, L., Hung, A.Y., Seubert, P., Vigo-Pelfrey, C., Lieberburg, I. and Selkoe, D.J. (1992). Mutation of the beta-amyloid precursor protein in familial Alzheimer's disease increases beta-protein production. *Nature* **360**: 672-74.

Clark, M.J., Gagnon, J., Williams, A.F. and Barclay, A.N. (1985). MRC OX-2 antigen: a lymphoid/neuronal membrane glycoprotein with a structure like a single immunoglobulin light chain. *EMBO J.* **4**: 113-18.

Clements, A., Walsh, D.M., Williams, C.H. and Allsop, D. (1993). Effects of the mutations Glu22 to Gln and Ala21 to Gly on the aggregation of a synthetic fragment of the Alzheimer's amyloid beta/A4 peptide. *Neurosci. Lett.* **161**: 17-20.

Cole, G., Dobkins, K.R., Hansen, L.A., Terry, R.D. and Saitoh, T. (1988). Decreased levels of protein kinase C in Alzheimer brain. *Brain Res.* **452**: 165-74.

Conlon, R.A., Reaume, A.G. and Rossant, J. (1995). Notch1 is required for the coordinate segmentation of somites. *Development* **121**: 1533-45.

Cook, D.G., Forman, M.S., Sung, J.C., Leight, S., Kolson, D.L., Iwatsubo, T., Lee, V.M. and Doms, R.W. (1997). Alzheimer's A beta(1-42) is generated in the endoplasmic reticulum/intermediate compartment of NT2N cells. *Nat. Med.* **3**: 1021-23.

Cottrell, B.A., Galvan, V., Banwait, S., Gorostiza, O., Lombardo, C.R., Williams, T., Schilling, B., Peel, A., Gibson, B., Koo, E.H., Link, C.D. and Bredesen, D.E. (2005). A pilot proteomic study of amyloid precursor interactors in Alzheimer's disease. *Ann. Neurol.* **58**: 277-89.

Coulson, E.J., Barrett, G.L., Storey, E., Bartlett, P.F., Beyreuther, K. and Masters, C.L. (1997). Down-regulation of the amyloid protein precursor of Alzheimer's disease by antisense oligonucleotides reduces neuronal adhesion to specific substrata. *Brain Res.* **770**: 72-80.

Coulson, E.J., Padiga, K., Beyreuther, K. and Masters, C.L. (2000). What the evolution of the amyloid protein precursor supergene family tells us about its function. *Neurochem. Int.* **36**: 175-84.

Crimson, M.L. and Eggert, A.E. (1999). 'Alzheimer's disease'. *In*: DiPiro, J.T., Talbert, R.L., Yee, G.C., Matzke, G.R., Wells, B.G. and Posey, L.M.. *Eds.* Pathophysiology: a pharmacotherapy approach, 4th edn. New York: Appleton & Lange, 1077.

Cruts, M., Backhovens, H., Wang, S.Y., Van Gassen, G., Theuns, J., De Jonghe, C.D., Wehnert, A., De Voecht, J., De Winter, G., Cras, P., et al. (1995). Molecular genetic analysis of familial early-onset Alzheimer's disease linked to chromosome 14q24.3. *Hum. Mol. Genet.* **4**: 2363-71.

Culvenor, J.G., Friedhuber, A., Fuller, S.J., Beyreuther, K. and Masters, C.L. (1995). Expression of the amyloid precursor protein of Alzheimer's disease on the surface of transfected HeLa cells. *Exp. Cell Res.* **220**: 474-81.

Cupers, P., Orlans, I., Craessaerts, K., Annaert, W. and De Strooper B. (2001). The amyloid precursor protein (APP)-cytoplasmic fragment generated by gamma-secretase is rapidly degraded but distributes partially in a nuclear fraction of neurones in culture. *J. Neurochem.* **78: 1**168-78.

Cupers, P., Bentahir, M., Craessaerts, K., Orlans, I., Vanderstichele, H., Saftig, P., De Strooper, B. and Annaert, W. (2005). The discrepancy between presenilin subcellular localization and gamma-secretase processing of amyloid precursor protein. *J. Cell Biol.* **154**: 731-40.

Czech, C., Tremp, G. and Pradier, L. (2000). Presenilins and Alzheimer's disease: biological functions and pathogenic mechanisms. *Prog. Neurobiol.* **60**: 363-84.

da Cruz e Silva, O.A.B., Iverfeldt, K., Oltersdorf, T., Sinha, S., Lieberburg, I., Ramabhadran, T.V., Suzuki, T., Sisodia, S.S., Gandy, S. and Greengard, P. (1993). Regulated cleavage of Alzheimer β-amyloid precursor protein in the absence of the cytoplasmic tail. *Neuroscience* **57**: 873–877.

da Cruz e Silva, E.F., da Cruz e Silva, O.A, Zaia, C.T. and Greengard, P. (1995a). Inhibition of protein phosphatase 1 stimulates secretion of Alzheimer amyloid precursor protein. *Mol. Med.* **5**: 535-41.

da Cruz e Silva, E.F., Fox, C.A., Ouimet, C.C., Gustafson, E., Watson, S.J. and Greengard, P. (1995b). Differential expression of protein phosphatase 1 isoforms in mammalian brain. *J. Neurosci.* **5**: 3375-89.

da Cruz e Silva, E.F. and da Cruz e Silva, O.A. (2003). Protein phosphorylation and APP metabolism. *Neurochem. Res.* **28**: 1553-61. Review.

da Cruz e Silva, O.A., Fardilha, M., Henriques, A.G., Rebelo, S., Vieira, S. and da Cruz e Silva, E.F. (2004a). Signal transduction therapeutics: relevance for Alzheimer's disease. *J. Mol. Neurosci.* **23**: 123-42. Review.

da Cruz e Silva, O.A.B, Vieira, S.I., Rebelo, S. and da Cruz e Silva, E.F. (2004b) A Model System to Study Intracellular Trafficking and Processing of the Alzheimer's Amyloid Precursor Protein. *Neurodegenerative. Dis.* **1**: 196-204.

Daigle, I. and Li, C. (1993). apl-1, a *Caenorhabditis elegans* gene enconding a protein related to the human beta-amyloid protein precursor. *Proc. Nat. Acad. Sci. USA* **90**: 12045-12049.

Dalby, B., Cates, S., Harris, A., Ohki, E.C., Tilkins, M.L., Price, P.J. and Ciccarone, V.V. (2004). Advanced transfection with Lipofectamine 2000 reagent: primary neurons, siRNA and high-throughput applications. *Methods* **33**: 95-103.

Demaerschalck, I., Delvaux, A. and Octave, J.N. (1993). Activation of protein kinase C increases the extracellular release of the transmembrane amyloid protein precursor of Alzheimer's disease. *Biochem. Biophys. Acta* **1181**: 214-8.

Desdouits, F., Buxbaum, J.D., Desdouits-Magnen, J., Nairn, A.C. and Greengard, P. (1996). Amyloid alpha peptide formation in cell-free preparations. Regulation by protein kinase C, calmodulin and calcineurin. *J. Biol. Chem.* **271**: 24670-4.

De Strooper, B., Van Leuven, F. and Van den Berghe, H. (1992). Alpha 2-macroglobulin and other proteinase inhibitors do not interfere with the secretion of amyloid precursor protein in mouse neuroblastoma cells. *FEBS Lett.* **308**: 50-53.

De Strooper, B., Umans, L., Van Leuven, F. and Van Den Berghe, H. (1993). Study of the synthesis and secretion of normal and artificial mutants of murine amyloid precursor protein (APP): cleavage of APP occurs in a late compartment of the default secretion pathway. *J. Cell Biol.* **121**: 295-04.

De Strooper, B., Saftig, P., Craessaerts, K., Vanderstichele, H., Guhde, G., Annaert, W., Von Figura, K. and Van Leuven, F. (1998). Deficiency of presenilin-1 inhibits the normal cleavage of amyloid precursor protein. *Nature* **391**: 387-90.

De Strooper, B., Annaert, W., Cupers, P., Saftig, P., Craessaerts, K., Mumm, J.S., Schroeter, E.H., Schrijvers, V., Wolfe, M.S., Ray, W.J., Goate, A. and Kopan, R. (1999). A presenilin-1-dependent gamma-secretase-like protease mediates release of Notch intracellular domain. *Nature* **398**: 518-22.

De Strooper, B. and Annaert, W. (2000). Proteolytic processing and cell biological functions of the amyloid precursor protein. *J. Cell. Sci.* **113**: 1857-1870.

De Strooper, B. (2003). Aph-1, Pen-2 and Nicastrin with Presenilin generate an active gamma-Secretase complex. *Neuron* **38**: 9-12. Review.

Diaz-Rodriguez, E., Montero, J.C., Esparis-Ogando, A., Yuste, L. and Pandiella, A. (2002). Extracellular signal-regulated kinase phosphorylates tumor necrosis factor alpha-converting enzyme at threonine 735: a potential role in regulated shedding. *Mol. Biol. Cell* **13**: 2031-44.

Dickson, D.W. (1997). The pathogenesis of senile plaques. *J. Neuropathol. Exp. Neurol.* **56**: 321-39. Review.

Dodart, J.C., Mathis, C. and Ungerer, A. (2000). The beta-amyloid precursor protein and its derivatives: from biology to learning and memory processes. *Rev. Neurosci.* **11**: 75-93. Review.

Donoviel, D.B., Hadjantonakis, A.K., Ikeda, M., Zheng, H., Hyslop, P.S. and Bernstein, A. (1999). Mice lacking both presenilin genes exhibit early embryonic patterning defects. *Genes Dev.* **13**: 2801-10.

Dotti CG, Sullivan CA, Banker GA. (1988). The establishment of polarity by hippocampal neurons in culture. *J. Neurosci.* **8**: 1454-68.

Doyle, E., Bruce, M.T., Breen, K.C., Smith, D.C. anderton, B. and Regan, C.M. (1990). Intraventricular infusions of antibodies to amyloid-beta-protein precursor impair the acquisition of a passive avoidance response in the rat. *Neurosci. Lett.* **115**: 97-02.

Drewes, G., Ebneth, A. and Mandelkow, E.-M. (1998). MAPs, MARKs and microtubule dynamics. *Trends Biochem. Sci.* **23**: 307-11. Review.

Duff, K., Eckman, C., Zehr, C., Yu, X., Prada, C.M., Perez-tur, J., Hutton, M., Buee, L., Harigaya, Y., Yager, D., Morgan, D., Gordon, M.N., Holcomb, L., Refolo, L., Zenk, B., Hardy, J. and Younkin, S. (1996). Increased amyloid-beta42(43) in brains of mice expressing mutant presenilin 1. *Nature* **383**: 710-13.

Dumanchin, C., Czech, C., Campion, D., Cuif, M.H., Poyot, T., Martin, C., Charbonnier, F., Goud, B., Pradier, L. and Frebourg, T. (1999). Presenilins interact with Rab11, a small GTPase involved in the regulation of vesicular transport. *Hum. Mol. Genet.* **7:** 1263-69.

Dyrks, T., Monning, U., Beyreuther, K. and Turner, J. (1994). Amyloid precursor protein secretion and beta A4 amyloid generation are not mutually exclusive. *FEBS Lett.* **349**: 210-14.

Ebert, A.D. and Svendsen, C.N. (2005). A new tool in the battle against Alzheimer's disease and aging: ex vivo gene therapy. *Rejuvenation Res.* **8**: 131-34. Review.

Ebihara, T., Kawabata, I., Usui, S., Sobue, K. and Okabe, S. (2003). Synchronized Formation and Remodeling of Postsynaptic Densities: Long-Term Visualization of Hippocampal Neurons Expressing Postsynaptic Density Proteins Tagged with Green Fluorescent Protein. *J. Neurosci.* **23**: 2170 –81.

Ebinu, J.O. and Yankner, B.A. (2002). A RIP Tide in Neuronal Signal Transduction. *Neuron* **34**: 499-02.

Edbauer, D., Willem, M., Lammich, S., Steiner, H. and Haass, C. (2002). Insulin-degrading enzyme rapidly removes the beta-amyloid precursor protein intracellular domain (AICD). *J. Biol. Chem.* **277**: 13389-93.

Efthimiopoulos, S., Vassilacopoulou, D., Ripellino, J.A., Tezapsidis, N. and Robakis, N.K. (1996). Cholinergic agonists stimulate secretion of soluble full-length amyloid precursor protein in neuroendocrine cells. *Proc. Natl. Acad. Sci. USA* **93**: 8046-50.

Eikelenboom, P., Zhan, S.S., van Gool, W.A. and Allsop, D. (1994). Inflammatory mechanisms in Alzheimer's disease. *Trends Pharmacol. Sci.* **15**: 447-50. Review.

El Khoury, J., Hickman, S.E., Thomas, C.A., Cao, L., Silverstein, S.C. and Loike, J.D. (1996). Scavenger receptor-mediated adhesion of microglia to beta-amyloid fibrils. *Nature* **382**: 716-19.

Ellinger, I., Klapper, H., Courtoy, P.J., Vaerman, J.P. and Fuchs, R. (2002). Different temperature sensitivity of endosomes involved in transport to lysosomes and transcytosis in rat hepatocytes: analysis by free-flow electrophoresis. *Electrophoresis* **23**: 2117-29.

Emilien, G., Beyreuther, K., Masters, C.L. and Maloteaux, J.M. (2000). Prospects for pharmacological intervention in Alzheimer's disease. *Arch. Neurol.* **57**: 454-59.

Ermak, G., Morgan, T.E. and Davies, K.J. (2001). Chronic overexpression of the calcineurin inhibitory gene DSCR1 (Adapt78) is associated with Alzheimer's disease. *J. Biol. Chem.* **276**: 38787-94.

Esch, F.S., Keim, P.S., Beattie, E.C., Blacher, R.W., Culwell, A.R., Oltersdorf, T., McClure, D. and Ward, P.J. (1990). Cleavage of amyloid beta peptide during constitutive processing of its precursor. *Science* **248**: 1122-24.

Esler, W.P., Kimberly, W.T., Ostaszewski, B.L., Diehl, T.S., Moore, C.L., Tsai, J.Y., Rahmati, T., Xia, W., Selkoe, D.J. and Wolfe, M.S. (2000). Transition-state analogue inhibitors of gamma-secretase bind directly to presenilin-1. *Nat. Cell Biol.* **2**: 428-34.

Esler, W.P. and Wolfe, M.S. (2001). A portrait of Alzheimer secretases - new features and familiar faces. *Science* **293**: 1449-54. Review.

Etcheberrigaray, R., Tan, M., Dewachter, I., Kuiperi, C., Van der Auwera, I., Wera, S., Qiao, L., Bank, B., Nelson, T.J., Kozikowski, A.P., Van Leuven, F., Alkon, D.L. (2004). Therapeutic effects of PKC activators in Alzheimer's disease transgenic mice. *Proc. Natl. Acad. Sci. USA* **101**: 11141-46.

Fadeeva, J.V., Walsh, D.M., LaVoie, M.J., Das, C., Wolfe, M.S., Wasco, W. and Selkoe, D.J. (2003). Progression and nuclear translocation of the intracellular C-terminal domain of the APP family of proteins. *Soc. Neurosci. Abst. 33* Prog. Number 295.3.

Fan, H., Turck, C.W. and Derynck, R. (2003). Characterization of growth factor-induced serine phosphorylation of tumor necrosis factor-alpha converting enzyme and of an alternatively translated polypeptide. *J. Biol. Chem.* **278**: 18617-27.

Farooqui, A.A., Ong, W.Y. and Horrocks, L.A. (2004). Biochemical aspects of neurodegeneration in human brain: involvement of neural membrane phospholipids and phospholipases A2. *Neurochem. Res.* **29**: 1961-77. Review.

Farris, W., Mansourian, S., Chang, Y., Lindsley, L., Eckman, E.A., Frosch, M.P., Eckman, C.B., Tanzi, R.E., Selkoe, D.J. and Guenette, S. (2003). Insulin-degrading enzyme regulates the levels of insulin, amyloid beta-protein and the beta-amyloid precursor protein intracellular domain in vivo. *Proc. Natl. Acad. Sci. USA* **100:** 4162-67.

Farzan, M., Schnitzler, C.E., Vasilieva, N., Leung, D. and Choe, H. (2000). BACE2, a beta -secretase homolog, cleaves at the beta site and within the amyloid-beta region of the amyloid-beta precursor protein. *Proc. Natl. Acad. Sci. USA* **97**: 9712-17.

Fassa, A., Parisiadou, L., Mehta, P. and Efthimiopoulos, S. (2005). Notch 1 interacts with the Amyloid Precursor Protein in a Numb-independent manner. 7th International Conference AD/PD, Sorrento, Italy. (OR)-61.

Felsenstein, K.M., Ingalls, K.M., Hunihan, L.W. and Roberts, S.B. (1994). Reversal of the Swedish familial Alzheimer's disease mutant phenotype in cultured cells treated with phorbol 12,13-dibutyrate. *Neurosci. Lett.* **174**: 173-6.

Ferreira, A., Cáceres, A. and Kosik, K.S. (1993). Intraneuronal compartments of the amyloid precursor protein. *J. Neurosci.* **13**: 3112-23.

Fiore, F., Zambrano, N., Minopoli, G., Donini, V., Duilio, A. and Russo, T. (1995). The regions of the Fe65 protein homologous to the phosphotyrosine interaction/phosphotyrosine binding domain of Shc bind the intracellular domain of the Alzheimer's amyloid precursor protein. *J. Biol. Chem.* **270**: 30853-56.

First, M.B. (1994). *DSM-IV: Diagnostic and Statistical Manual of Mental Disorders*, 4th edn. Washinton, DC: American Psychiatric Association, 139-42.

Flood, J.F., Morley, J.E. and Roberts, E. (1991). Amnestic effects in mice of four synthetic peptides homologous to amyloid beta protein from patients with Alzheimer disease. *Proc. Natl. Acad. Sci. USA* **88**: 3363-66.

Folin M., Baiguera S., Guidolin D., Di Liddo R., Grandi C., De Carlo E., Nussdorfer G.G. and Parnigotto P.P. (2006). Apolipoprotein-E modulates the cytotoxic effect of beta-amyloid on rat brain endothelium in an isoform-dependent specific manner. *Int. J. Mol. Med.* **17**: 821-26.

Forloni, G. (1996). Neurotoxicity of beta-amyloid and prion peptides. *Curr. Opin. Neurol.* **9**: 492–00.

Fossgreen, A., Bruckner, B., Czech, C., Masters, C.L., Beyreuther, K. and Paro, R. (1998). Transgenic Drosophila expressing human amyloid precursor protein show gamma-secretase activity and a blistered-wing phenotype. *Proc. Natl. Acad. Sci. USA* **95**: 13703-08.

Francis, R., McGrath, G., Zhang, J., Ruddy, D.A., Sym, M., Apfeld, J., Nicoll, M., Maxwell, M., Hai, B., Ellis, M.C., Parks, A.L., Xu, W., Li, J., Gurney, M., Myers, R.L., Himes, C.S., Hiebsch, R., Ruble, C., Nye, J.S. and Curtis, D. (2002). aph-1 and pen-2 are required for Notch pathway signaling, gamma-secretase cleavage of betaAPP and presenilin protein accumulation. *Dev. Cell* **3**: 85-97.

Friedman, L.M., Matsuda, Y. and Lazarovici, P. (1997). The microbial alkaloid toxin staurosporine blocks the phorbol ester-induced increase in beta-amyloid precursor protein in PC12 cells. *Nat. Toxins* **5**: 173-79.

Fukumoto, H., Cheung, B.S., Hyman, B.T. and Irizarry, M.C. (2002). Beta-secretase protein and activity are increased in the neocortex in Alzheimer disease. *Arch. Neurol.* **59**: 1381-89.

Furukawa, K., Barger, S.W., Blalock, E.M. and Mattson, M.P. (1996a). Activation of K+ channels and suppression of neuronal activity by secreted beta-amyloid-precursor protein. *Nature* **379**: 74-78.

Furukawa, K., Sopher, B.L., Rydel, R.E., Begley, J.G., Pham, D.G., Martin, G.M., Fox, M. and Mattson, M.P. (1996b). Increased activity-regulating and neuroprotective efficacy of alpha-secretase-derived secreted amyloid precursor protein conferred by a C-terminal heparin-binding domain. *J Neurochem.* **67**: 1882-96.

Furukawa, K. and Mattson, M.P. (1998). Secreted amyloid precursor protein alpha selectively suppresses N-methyl-D-aspartate currents in hippocampal neurons: involvement of cyclic GMP. *Neuroscience* **83**: 429-38.

Gabuzda, D., Busciglio, J. and Yankner, B.A. (1993). Inhibition of beta-amyloid production by activation of protein kinase C. *J. Neurochem.* **61**: 2326-29.

Gandy, S. and Heppner, F.L. (2005). Alzheimer's amyloid immunotherapy: quo vadis? *Lancet. Neurol.* **4**: 452-53. Review.

Gandy, S., Czernik, A.J. and Greengard, P. (1988). Phosphorylation of Alzheimer disease amyloid precursor peptide by protein kinase C and Ca2+/calmodulin-dependent protein kinase II. *Proc. Natl. Acad. Sci. USA* **85**: 6218-21.

Gandy, S. and Greengard, P. (1994). Regulated cleavage of the Alzheimer amyloid precursor protein: molecular and cellular basis. *Biochimie.* **76**: 300-03. Review.

Gao, Y. and Pimplikar, S.W. (2001). The gamma -secretase-cleaved C-terminal fragment of amyloid precursor protein mediates signaling to the nucleus. *Proc. Natl. Acad. Sci. USA* **98**: 14979-84.

Genoux, D., Haditsch, U., Knobloch, M., Michalon, A., Storm, D. and Mansuy, I.M. (2002). Protein phosphatase 1 is a molecular constraint on learning and memory. *Nature* **418**: 970-75.

Gervais, F.G., Xu, D., Robertson, G.S., Vaillancourt, J.P., Zhu, Y., Huang, J., LeBlanc, A., Smith, D., Rigby, M., Shearman, M.S., Clarke, E.E., Zheng, H., Van Der Ploeg, L.H., Ruffolo, S.C., Thornberry, N.A., Xanthoudakis, S., Zamboni, R.J., Roy, S. and Nicholson, D.W. (1999). Involvement of caspases in proteolytic cleavage of Alzheimer's amyloid-beta precursor protein and amyloidogenic Abeta peptide formation. *Cell* **97**: 395-406.

Geula, C., Wu, C.K., Saroff, D., Lorenzo, A., Yuan, M and Yankner BA. (1998). Aging renders the brain vulnerable to amyloid beta-protein neurotoxicity. *Nat. Med.* **4**: 827-31.

Ghiso, J., Rostagno, A., Gardella, J.E., Liem, L., Gorevic, P.D. and Frangione, B. (1992). A 109-amino-acid C-terminal fragment of Alzheimer's-disease amyloid precursor protein contains a sequence, -RHDS-, that promotes cell adhesion. *Biochem. J.* **288**: 1053-59.

Giambarella, U., Yamatsuji, T., Okamoto, T., Matsui, T., Ikezu, T., Murayama, Y., Levine, M.A., Katz, A., Gautam, N. and Nishimoto, I. (1997). G protein betagamma complex-mediated apoptosis by familial Alzheimer's disease mutant of APP. *EMBO J.* **16**: 4897-07.

Gillespie, S.L., Golde, T.E. and Younkin, S.G. (1992). Secretory processing of the Alzheimer amyloid beta/A4 protein precursor is increased by protein phosphorylation. *Biochem. Biophys. Res. Commun* **187**: 1285-90.

Goate, A., Chartier-Harlin, M.C., Mullan, M., Brown, J., Crawford, F., Fidani, L., Giuffra, L., Haynes, A., Irving, N., James, L., et al. (1991). Segregation of a missense mutation in the amyloid precursor protein gene with familial Alzheimer's disease. *Nature* **349**: 704-06.

Goedert, M., Jakes, R., Spillantini, M.G., Hasegawa, M., Smith, M.J. and Crowther, R.A. (1996). Assembly of microtubule-associated protein tau into Alzheimer-like filaments induced by sulphated glycosaminoglycans. *Nature* **383**: 550-53.

Golde, T.E., Estus, S., Usiak, M., Younkin, L.H. and Younkin, S.G. (1990). Expression of beta amyloid protein precursor mRNAs: recognition of a novel alternatively spliced form and quantitation in Alzheimer's disease using PCR. *Neuron* **4**: 253-67.

Goldstein, L.S. (2001). Kinesin molecular motors: transport pathways, receptors and human disease. *Proc. Natl. Acad. Sci. USA* **98**: 6999-03. Review.

Gong, C.X., Singh, T.J., Grundke-Iqbal, I. and Iqbal, K. (1993). Phosphoprotein phosphatase activities in Alzheimer disease brain. *J. Neurochem.* **61**: 921-27.

Goodman, A.B. and Pardee, A.B. (2003). Evidence for defective retinoid transport and function in late onset Alzheimer's disease. *Proc. Natl. Acad. Sci. USA* **100**: 2901-05. Review.

Goodman, Y. and Mattson, M.P. (1994). Secreted forms of beta-amyloid precursor protein protect hippocampal neurons against amyloid beta-peptide-induced oxidative injury. *Exp. Neurol.* **128**: 1-12.

Goslin, K. and Banker, G. (1989). Experimental observations on the development of polarity by hippocampal neurons in culture. *J. Cell Biol.* **108:** 1507-16.

Gotting, C., Kuhn, J., Brinkmann, T. and Kleesiek, K. (1998). Xylosylation of alternatively spliced isoforms of Alzheimer APP by xylosyltransferase. *J. Protein Chem.* **17**: 295-02.

Gouras, G.K., Tsai, J., Naslund, J., Vincent, B., Edgar, M., Checler, F., Greenfield, J.P., Haroutunian, V., Buxbaum, J.D., Xu, H., Greengard, P. and Relkin, N.R. (2000). Intraneuronal Aβ 42 accumulation in human brain. *Am. J. Pathol.* **156**: 15-20.

Gowing, E., Roher, A.E., Woods, A.S., Cotter, R.J., Chaney, M., Little, S.P. and Ball, M.J. (1994). Chemical characterization of Abeta 17-42 peptide, a component of diffuse amyloid deposits of Alzheimer disease. *J. Biol. Chem.* **269**: 10987-90.

Gray, C.W. and Patel, A.J. (1993a). Induction of beta-amyloid precursor protein isoform mRNAs by bFGF in astrocytes. *Neuroreport* **4**: 811-14.

Gray, C.W. and Patel, A.J. (1993b). Regulation of beta-amyloid precursor protein isoform mRNAs by transforming growth factor-beta 1 and interleukin-1 beta in astrocytes. *Brain Res. Mol. Brain Res.* **19**: 251-56.

Greenberg, S.M., Koo, E.H., Selkoe, D.J., Qiu, W.Q. and Kosik, K.S. (1994). Secreted beta-amyloid precursor protein stimulates mitogen-activated protein kinase and enhances tau phosphorylation. *Proc. Natl. Acad. Sci. USA* **91**: 7104-08.

Greenberg, S.M., Qiu, W.Q., Selkoe, D.J., Ben-Itzhak, A. and Kosik, K.S. (1995). Amino-terminal region of the beta-amyloid precursor protein activates mitogen-activated protein kinase. *Neurosci. Lett.* **198**: 52-56.

Greenfield, J.P., Tsai, J., Gouras, G.K., Hai, B., Thinakaran, G., Checler, F., Sisodia, S.S., Greengard, P. and Xu, H. (1999). Endoplasmic reticulum and trans-Golgi network generate distinct populations of Alzheimer beta-amyloid peptides. *Proc. Natl. Acad. Sci. USA* **96**: 742-47.

Guarnieri, F.G., Arterburn, L.M., Penno, M.B., Cha, Y. and August, J.T. (1993). The motif Tyr-X-X-hydrophobic residue mediates lysosomal membrane targeting of lysosome-associated membrane protein 1. *J. Biol. Chem.* **268**: 1941-46.

Guenette, S.Y., Chen, J., Jondro, P.D. and Tanzi, R.E. (1996). Association of a novel human FE65-like protein with the cytoplasmic domain of the beta-amyloid precursor protein. *Proc. Natl. Acad. Sci. USA* **93**: 10832-37.

Guenette, S.Y. (2002). A role for APP in motility and transcription? *Trends Pharmacol. Sci.* **23**: 203-05; discussion 205-06.

Gunawardena, S. and Goldstein, L.S. (2001). Disruption of axonal transport and neuronal viability by amyloid precursor protein mutations in Drosophila. *Neuron* **32**: 389-01.

Guo, Z., Cupples, L.A., Kurz, A., Auerbach, S.H., Volicer, L., Chui, H., Green, R.C., Sadovnick, A.D., Duara, R., DeCarli, C., Johnson, K., Go, R.C., Growdon, J.H., Haines, J.L., Kukull, W.A. and Farrer, L.A. (2000). Head injury and the risk of AD in the MIRAGE study. *Neurology* **54**: 59-66.

Haass, C., Koo, E.H., Mellon, A., Hung, A.Y. and Selkoe, D.J. (1992a). Targeting of cell-surface beta-amyloid precursor protein to lysosomes: alternative processing into amyloid-bearing fragments. *Nature* **357**: 500-03.

Haass, C., Schlossmacher, M.G., Hung, A.Y., Vigo-Pelfrey, C., Mellon, A., Ostaszewski, B.L., Lieberburg, I., Koo, E.H., Schenk, D., Teplow, D.B., et al. (1992b). Amyloid beta-peptide is produced by cultured cells during normal metabolism. *Nature* **359**: 322-25.

Haass, C., Hung, A.Y., Schlossmacher, M.G., Teplow, D.B. and Selkoe, D.J. (1993). beta-Amyloid peptide and a 3-kDa fragment are derived by distinct cellular mechanisms. *J. Biol. Chem.* **268**: 3021-24.

Haass, C., Koo, E.H., Capell, A., Teplow, D.B. and Selkoe, D.J. (1995). Polarized sorting of beta-amyloid precursor protein and its proteolytic products in MDCK cells is regulated by two independent signals. *J. Cell Biol.* **128**: 537-47.

Haass, C. and Steiner, H. (2002). Alzheimer disease gamma-secretase: a complex story of GxGD-type presenilin proteases. *Trends Cell Biol.* **12**: 556-62. Review.

Hache, R.J., Tse, R., Reich, T., Savory, J.G. and Lefebvre, Y.A. (1999). Nucleocytoplasmic trafficking of steroid-free glucocorticoid receptor. *J. Biol. Chem.* **274**: 1432-39.

Haniu, M., Denis, P., Young, Y., Mendiaz, E.A., Fuller, J., Hui, J.O., Bennett, B.D., Kahn, S., Ross, S., Burgess, T., Katta, V., Rogers, G., Vassar, R. and Citron, M. (2000). Characterization of Alzheimer's beta -secretase protein BACE. A pepsin family member with unusual properties. *J. Biol. Chem.* **275**: 21099-06.

Hardy, J. and Allsop, D. (1991). Amyloid deposition as the central event in the aetiology of Alzheimer's disease. *Trends Pharmacol. Sci.* **12**: 383-88.

Hardy, J. and Selkoe, D.J. (2002). The Amyloid Hypothesis of Alzheimer´s Disease: Progress and Problems on the Road to Therapeutics. *Science* **297:** 353-56.

Hare, J.F. (2001). Protease inhibitors divert amyloid precursor protein to the secretory pathway. *Biochem. Biophys. Res. Commun.* **281:** 1298–03.

Harper, J.D., Lieber, C.M. and Lansbury, P.T. Jr. (1997). Atomic force microscopic imaging of seeded fibril formation and fibril branching by the Alzheimer's disease amyloid-beta protein. *Chem. Biol.* **4**: 951-59.

Harter, C. and Mellman, I. (1992). Transport of the lysosomal membrane glycoprotein lgp120 (lgp-A) to lysosomes does not require appearance on the plasma membrane. *J. Cell Biol.* **117**: 311-25.

Hartmann, T., Bieger, S.C., Bruhl, B., Tienari, P.J., Ida, N., Allsop, D., Roberts, G.W., Masters, C.L., Dotti, C.G., Unsicker, K. and Beyreuther, K. (1997). Distinct sites of intracellular production for Alzheimer's disease A beta40/42 amyloid peptides. *Nat. Med.* **3**: 1016-20.

Hartmann, D., de Strooper, B., Serneels, L., Craessaerts, K., Herreman, A., Annaert, W., Umans, L., Lubke, T., Lena Illert, A., von Figura, K. and Saftig, P. (2002). The disintegrin/metalloprotease ADAM 10 is essential for Notch signalling but not for alpha-secretase activity in fibroblasts. *Hum. Mol. Genet.* **11**: 2615–24.

Hata, R., Masumura, M., Akatsu, H., Li, F., Fujita, H., Nagai, Y., Yamamoto, T., Okada, H., Kosaka, K., Sakanaka, M. and Sawada, T. (2001). Up-regulation of calcineurin Abeta mRNA in the Alzheimer's disease brain: assessment by cDNA microarray. *Biochem. Biophys. Res. Commun* **284**: 310-16.

Heber, S., Herms, J., Gajic, V., Hainfellner, J., Aguzzi, A., Rulicke, T., von Kretzschmar, H., von Koch, C., Sisodia, S., Tremml, P., Lipp, H.P., Wolfer, D.P. and Muller, U. (2000). Mice with combined gene knock-outs reveal essential and partially redundant functions of amyloid precursor protein family members. *J. Neurosci.* **20:** 7951-63.

Hecimovic, S., Wang, J., Dolios, G., Martinez, M., Wang, R. and Goate, A.M. (2004). Mutations in APP have independent effects on Abeta and CTFgamma generation. *Neurobiol. Dis.* **17**: 205-18.

Herreman, A., Hartmann, D., Annaert, W., Saftig, P., Craessaerts, K., Serneels, L., Umans, L., Schrijvers, V., Checler, F., Vanderstichele, H., Baekelandt, V., Dressel, R., Cupers, P., Huylebroeck, D., Zwijsen, A., Van

Leuven, F. and De Strooper, B. (1999). Presenilin 2 deficiency causes a mild pulmonary phenotype and no changes in amyloid precursor protein processing but enhances the embryonic lethal phenotype of presenilin 1 deficiency. *Proc. Natl. Acad. Sci. USA* **96**: 11872-77.

Hesse, L., Beher, D., Masters, C.L. and Multhaup, G. (1994). The beta A4 amyloid precursor protein binding to copper. *FEBS Lett.* **349**: 109-16.

Higgins, L.S., Holtzman, D.M., Rabin, J., Mobley, W.C. and Cordell B. (1994). Transgenic mouse brain histopathology resembles early Alzheimer's disease. *Ann. Neurol.* **35**: 598-07.

Hill, A.A., Edwards, D.H. and Murphey, R.K. (1994). The effect of neuronal growth on synaptic integration. *J. Comput. Neurosci.* **1:** 239-54.

Hill, K., Li, Y., Bennett, M., McKay, M., Zhu, X., Shern, J., Torre, E., Lah, J.J., Levey, A.I. and Kahn, R.A. (2003). Munc18 interacting proteins: ADP-ribosylation factor-dependent coat proteins that regulate the traffic of beta-Alzheimer's precursor protein. *J. Biol. Chem.* **278**: 36032-40.

Hirokawa, N. (1998). Kinesin and dynein superfamily proteins and the mechanism of organelle transport. *Science* **279**: 519-26. Review.

Ho, A. and Sudhof, T.C. (2004). Binding of F-spondin to amyloid-beta precursor protein: a candidate amyloid-beta precursor protein ligand that modulates amyloid-beta precursor protein cleavage. *Proc. Natl. Acad. Sci. USA* **101:** 2548-53.

Holzer, M., Bruckner, M.K., Beck, M., Bigl, V. and Arendt, T. (2000). Modulation of APP processing and secretion by okadaic acid in primary guinea pig neurons. *J. Neural. Transm.* **107**: 451-61.

Homayouni, R., Rice, D.S., Sheldon, M. and Curran, T. (1999). Disabled-1 binds to the cytoplasmic domain of amyloid precursor-like protein 1. *J. Neurosci.* **19**: 7507-15.

Honda, S, Itoh, F., Yoshimoto, M., Hinoda, Y. and Imai, K. (1998). Changes in morphology of neuroblastoma cells treated with all-trans retinoic acid combined with transfer of the C-terminal region of the amyloid precursor protein. *J. Clin. Lab. Anal.* **12**: 172-78.

Honing, S. and Hunziker, W. (1995). Cytoplasmic determinants involved in direct lysosomal sorting, endocytosis and basolateral targeting of rat lgp120 (lamp-I) in MDCK cells. *J. Cell Biol.* **128**: 321-32.

Honing, S., Kreimer, G., Robenek, H. and Jockusch, B.M. (1994). Receptor-mediated endocytosis is sensitive to antibodies against the uncoating ATPase (hsc70). *J. Cell Sci.* **107**: 1185-96.

Hooper, N.M. and Turner, A.J. (2002). The search for alpha-secretase and its potential as a therapeutic approach to Alzheimer s disease. *Curr. Med. Chem.* **9**: 1107-19. Review.

Howlett, D.R., Jennings, K.H., Lee, D.C., Clark, M.S., Brown, F., Wetzel, R., Wood, S.J., Camilleri, P. and Roberts, G.W. (1995). Aggregation state and neurotoxic properties of Alzheimer beta-amyloid peptide. *Neurodegeneration* **4**: 23–32.

Hoy, M., Berggren, P.O. and Gromada, J. (2003). Involvement of protein kinase C-epsilon in inositol hexakisphosphate-induced exocytosis in mouse pancreatic beta-cells. *J. Biol. Chem.* **278**: 35168-71.

Huber, G., Martin, J.R., Loffler, J. and Moreau, J.L. (1993). Involvement of amyloid precursor protein in memory formation in the rat: an indirect antibody approach. *Brain Res.* **603**: 348-52.

Hung, A.Y., Koo, E.H., Haass, C. and Selkoe, D.J. (1992). Increased expression of beta-amyloid precursor protein during neuronal differentiation is not accompanied by secretory cleavage. *Proc. Natl. Acad. Sci. USA* **89**: 9439-43.

Hung, A.Y., Haass, C., Nitsch, R.M., Qiu,, W.Q., Citron, M., Wurtman, R.J., Growdon, J.H. and Selkoe, D.J. (1993). Activation of protein kinase C inhibits cellular production of the amyloid-β-protein. *J. Biol. Chem.* **268**: 22959–62.

Hung, A.Y. and Selkoe, D.J. (1994). Selective ectodomain phosphorylation and regulated cleavage of β-amyloid precursor protein. *EMBO J.* **13**: 534-42.

Huse, J.T., Pijak, D.S., Leslie, G.J., Lee, V.M. and Doms, R.W. (2000). Maturation and endosomal targeting of beta-site amyloid precursor protein-cleaving enzyme. The Alzheimer's disease beta-secretase. *J. Biol. Chem.* **275**: 33729-37.

Hussain, I., Christie, G., Schneider, K., Moore, S. and Dingwall, C. (2001). Prodomain processing of Asp1 (BACE2) is autocatalytic. *J. Biol. Chem.* **276**: 23322-28.

Hutton, M., Busfield, F., Wragg, M., Crook, R., Perez-Tur, J., Clark, R.F., Prihar, G., Talbot, C., Phillips, H., Wright, K., Baker, M., Lendon, C., Duff, K., Martinez, A., Houlden, H., Nichols, A., Karran, E., Roberts,

G., Roques, P., Rossor, M., Venter, J.C., Adams, M.D., Cline, R.T., Phillips, C.A., Goate, A., et al. (1996). Complete analysis of the presenilin 1 gene in early onset Alzheimer's disease. *Neuroreport* **7**: 801-05.

Ichikawa, M., Muramoto, K., Kobayashi, K., Kawahara, M. and Kuroda, Y. (1993). Formation and maturation of synapses in primary cultures of rat cerebral cortical cells: an electron microscopic study. *Neurosci Res.* **16:** 95-03.

Iijima, K. ando, K., Takeda, S., Satoh, Y., Seki, T., Itohara, S., Greengard, P., Kirino, Y., Nairn, A.C. and Suzuki, T. (2000). Neuron-specific phosphorylation of Alzheimer's beta-amyloid precursor protein by cyclin-dependent kinase 5. *J. Neurochem.* **75**: 1085-91.

Iizuka, T., Shoji, M., Harigaya, Y., Kawarabayashi, T., Watanabe, M., Kanai, M. and Hirai, S. (1995). Amyloid beta-protein ending at Thr43 is a minor component of some diffuse plaques in the Alzheimer's disease brain, but is not found in cerebrovascular amyloid. *Brain Res.* **702**: 275-78.

Ikezu, T., Trapp, B.D., Song, K.S., Schlegel, A., Lisanti, M.P. and Okamoto, T. (1998). Caveolae, plasma membrane microdomains for alpha-secretase-mediated processing of the amyloid precursor protein. *J. Biol. Chem.* **273**: 10485-95.

Ikin, A.F., Annaert, W.G., Takei, K., Reinhard, P.C., Greengard, P. and Buxbaum, J.D. (1996). Alzheimer amyloid protein precursor is localized in nerve terminal preparations to Rab5-containing vesicular organelles distinct from those implicated in the synaptic vesicle pathway. *J. Biol. Chem.* **271:** 31783-86.

Inomata, H., Nakamura, Y., Hayakawa, A., Takata, H., Suzuki, T., Miyazawa, K. and Kitamura, N. (2003). A scaffold protein JIP-1b enhances amyloid precursor protein phosphorylation by JNK and its association with kinesin light chain 1. *J. Biol. Chem.* **278:** 22946-55.

Ishida, A., Shimazaki, K., Terashima, T. and Kawai, N. (1994). An electrophysiological and immunohistochemical study of the hippocampus of the reeler mutant mouse. *Brain Res.* **662:** 60-68.

Ishida, A., Furukawa, K., Keller, J.N. and Mattson, M.P. (1997). Secreted form of beta-amyloid precursor protein shifts the frequency dependency for induction of LTD and enhances LTP in hippocampal slices. *Neuroreport* **8:** 2133-37.

Ishiguro, M., Ohsawa, I., Takamura, C., Morimoto, T. and Kohsaka, S. (1998). Secreted form of beta-amyloid precursor protein activates protein kinase C and phospholipase Cgamma1 in cultured embryonic rat neocortical cells. *Brain Res. Mol. Brain Res.* **53**: 24-32.

Isohara, T., Horiuchi, A., Watanabe, T., Ando, K., Czernik, A.J., Uno, I., Greengard, P., Nairn, A.C. and Suzuki, T. (1999). Phosphorylation of the cytoplasmic domain of Alzheimer's beta-amyloid precursor protein at Ser655 by a novel protein kinase. *Biochem. Biophys. Res. Commun* **258**: 300-05.

Iversen, L., Mortishire, R.J., Pollack, S.J. and Shearman, M.S. (1995). The toxicity in vitro of β-amyloid protein. *Biochem. J.* **311**: 1-16.

Iwata, N., Tsubuki, S., Takaki, Y., Shirotani, K., Lu, B., Gerard, N.P., Gerard, C., Hama, E., Lee, H.J. and Saido, T.C. (2001). Metabolic regulation of brain Abeta by neprilysin. *Science* **292**: 1550-52.

Iwatsubo, T., Odaka, A., Susuki, N., Mizusawa, H., Nukina, H. and Ihara, Y. (1994). Visualization of Aβ 42(43) and Aβ 40 in senile plaques with end-specific Aβ monoclonals: evidence that an initially deposited species is Aβ 42(43). *Neuron* **13**: 45-53.

Iwatsubo, T., Mann, D.M., Odaka, A., Susuki, N. and Ihara, Y. (1995). Amyloid β-protein (Aβ) deposition: Aβ42(43) precedes Aβ40 in Down's syndrome. *Ann. Neurol.* **37**: 294-99.

Izumi, Y., Hirata, M., Hasuwa, H., Iwamoto, R., Umata, T., Miyado, K., Tamai, Y., Kurisaki, T., Sehara-Fujisawa, A., Ohno, S. and Mekada, E. (1998). A metalloprotease-disintegrin, MDC9/meltrin-gamma/ADAM9 and PKCdelta are involved in TPA-induced ectodomain shedding of membrane-anchored heparin-binding EGF-like growth factor. *EMBO J.* **17**: 7260-72.

Jackson, P., Marreiros, A. and Russell, P.J. (2005). KAI1 tetraspanin and metastasis suppressor. *Int. J. Biochem. Cell Biol.* **37**: 530-34. Review.

Jarrett, J.T. and Lansbury, P.T. Jr. (1992). Amyloid fibril formation requires a chemically discriminating nucleation event: studies of an amyloidogenic sequence from the bacterial protein OsmB. *Biochemistry* **31**: 12345-52.

Jarrett, J.T., Berger, E.P. and Lansbury, P.T. Jr. (1993). The carboxy terminus of the beta amyloid protein is critical for the seeding of amyloid formation: implications for the pathogenesis of Alzheimer's disease. *Biochemistry* **32**: 4693-97.

Jin, L.W., Ninomiya, H., Roch, J.M., Schubert, D., Masliah, E., Otero, D.A. and Saitoh, T. (1994). Peptides containing the RERMS sequence of amyloid beta/A4 protein precursor bind cell surface and promote neurite extension. *J. Neurosci.* **14**: 5461-70.

Jolly-Tornetta, C. and Wolf, B.A. (2000). Protein kinase C regulation of intracellular and cell surface amyloid precursor protein (APP) cleavage in CHO695 cells. *Biochemistry* **39:** 15282-90.

Kaether, C., Skehel, P. and Dotti, C.G. (2000). Axonal membrane proteins are transported in distinct carriers: a two-color video microscopy study in cultured hippocampal neurons. *Mol. Biol. Cell* **11**: 1213-24.

Kaether, C. and Haass, C. (2004). A lipid boundary separates APP and secretases and limits amyloid beta-peptide generation. *J. Cell Biol.* **167**: 809-12. Review.

Kaether, C., Schmitt, S., Willem, M. and Haass, C. (2006). Amyloid precursor protein and notch intracellular domains are generated after transport of their precursors to the cell surface. *Traffic* **7**: 408-15.

Kaltschmidt, B., Uherek, M., Volk, B., Baeuerle, P.A. and Kaltschmidt, C. (1997). Transcription factor NF-kappaB is activated in primary neurons by amyloid beta peptides and in neurons surrounding early plaques from patients with Alzheimer disease. *Proc. Natl. Acad. Sci. USA* **94**: 2642-47.

Kamal, A., Stokin, G.B., Yang, Z., Xia, C.H. and Goldstein, L.S. (2000). Axonal transport of amyloid precursor protein is mediated by direct binding to the kinesin light chain subunit of kinesin-I. *Neuron* **28**: 449-59.

Kamal, A., Almenar-Queralt, A., LeBlanc, J.F., Roberts, E.A. and Goldstein, L.S. (2001). Kinesin-mediated axonal transport of a membrane compartment containing beta-secretase and presenilin-1 requires APP. *Nature* **414**: 643-48.

Kametani, F., Usami, M., Tanaka, K., Kume, H. and Mori, H. (2004). Mutant presenilin (A260V) affects Rab8 in PC12D cell. *Neurochem. Int.* **44:** 313-20.

Kang, J., Lemaire, H.G., Unterbeck, A., Salbaum, J.M., Masters, C.L., Grzeschik, K.H., Multhaup, G., Beyreuther, K. and Muller-Hill, B. (1987). The precursor of Alzheimer's disease amyloid A4 protein resembles a cell-surface receptor. *Nature* **325**:733-36.

Kang, J. and Müller-Hill, B. (1990). Differential splicing of Alzheimer's disease amyloid A4 precursor RNA in rat tissues: PreA4(695) mRNA is predominantly produced in rat and human brain. *Biochem. Biophys. Res. Commun* **166**: 1192-00.

Kato, Y., Misra, S., Puertollano, R., Hurley, J.H. and Bonifacino, J.S. (2002). Phosphoregulation of sorting signal-VHS domain interactions by a direct electrostatic mechanism. *Nat. Struct. Biol.* **9:** 532-36.

Khvotchev, M. and Sudhof, T.C. (2004). Proteolytic processing of amyloid-beta precursor protein by secretases does not require cell surface transport. *J. Biol. Chem.* **279**: 47101-08.

Kibbey, M.C., Jucker, M., Weeks, B.S., Neve, R.L., Van Nostrand, W.E. and Kleinman, H.K. (1993). beta-Amyloid precursor protein binds to the neurite-promoting IKVAV site of laminin. *Proc. Natl. Acad. Sci. USA* **90**: 10150-53.

Kidd, M. (1964). Alzheimer's disease: an electron microscopical study. *Brain* **87**: 307-20.

Kim, E.M., Kim, H.S., Park, C.H., Kim, S. and Suh, Y.H. (2003). C-terminal fragments of amyloid precursor protein exert neurotoxicity by inducing glycogen synthase kinase-3beta expression. *Soc. Neurosci. Abst. 33*, Prog. Number 523.24.

Kim, S.H. and Sisodia, S.S. (2005). A sequence within the first transmembrane domain of PEN-2 is critical for PEN-2-mediated endoproteolysis of presenilin 1. *J. Biol. Chem.* **280**: 1992-01.

Kimberly, W.T., Zheng, J.B., Guenette, S.Y. and Selkoe, D.J. (2001). The intracellular domain of the beta-amyloid precursor protein is stabilized by Fe65 and translocates to the nucleus in a notch-like manner. *J. Biol. Chem.* **276**: 40288-92.

Kimberly, W.T., LaVoie, M.J., Ostaszewski, B.L., Ye, W., Wolfe, M.S. and Selkoe, D.J. (2003). Gamma-secretase is a membrane protein complex comprised of presenilin, nicastrin, Aph-1 and Pen-2. *Proc. Natl. Acad. Sci. USA* **100**: 6382-87.

Kimberly, W.T., Zheng, J.B., Town, T., Flavell, R.A. and Selkoe, D.J. (2005). Physiological regulation of the beta-amyloid precursor protein signaling domain by c-Jun N-terminal kinase JNK3 during neuronal differentiation. *J. Neurosci.* **25**: 5533-43.

Kinoshita, A., Whelan, C.M., Smith, C.J., Berezovska, O. and Hyman, B.T. (2002). Direct visualization of the gamma secretase-generated carboxyl-terminal domain of the amyloid precursor protein: association with Fe65 and translocation to the nucleus. *J. Neurochem.* **82**: 839-47.

Kinouchi, T., Sorimachi, H., Maruyama, K., Mizuno, K., Ohno, S., Ishiura, S. and Suzuki, K. (1995). Conventional protein kinase C (PKC)-alpha and novel PKC epsilon, but not -delta, increase the secretion of an N-terminal fragment of Alzheimer's disease amyloid precursor protein from PKC cDNA transfected 3Y1 fibroblasts. *FEBS Lett.* **364**: 203-06.

Kirazov, L., Loffler, T., Schliebs, R. and Bigl, V. (1997). Glutamate-stimulated secretion of amyloid precursor protein from cortical rat brain slices. *Neurochem. Int.* **30**: 557-63.

Kitaguchi, N., Takahashi, Y., Tokushima, Y., Shiojiri, S. and Ito, H. (1988). Novel precursor of Alzheimer's disease amyloid protein shows protease inhibitory activity. *Nature* **331**: 530-32.

Knauer, M.F., Orlando, R.A. and Glabe, C.G. (1996). Cell surface APP751 forms complexes with protease nexin 2 ligands and is internalized via the low density lipoprotein receptor-related protein (LRP). *Brain Res.* **740**: 6-14.

Koike, H., Tomioka, S., Sorimachi, H., Saido, T.C., Maruyama, K., Okuyama, A., Fujisawa-Sehara, A., Ohno, S., Suzuki, K. and Ishiura, S. (1999). Membrane-anchored metalloprotease MDC9 has an alpha-secretase activity responsible for processing the amyloid precursor protein. *Biochem. J.* **343**: 371-75.

Koizumi, S., Ishiguro, M., Ohsawa, I., Morimoto, T., Takamura, C., Inoue, K. and Kohsaka, S. (1998). The effect of a secreted form of beta-amyloid-precursor protein on intracellular Ca2+ increase in rat cultured hippocampal neurones. *Br. J. Pharmacol.* **123**: 1483-89.

König, G., Beyreuther, K., Masters, C.L., Schmitt, H.P. and Salbaum, J.M. (1989). PreA4 mRNA distribution in brain areas. *Prog. Clin. Biol. Res.* **317**: 1027-36.

König, G., Masters, C.L. and Beyreuther, K. (1990). Retinoic acid induced differentiated neuroblastoma cells show increased expression of the beta A4 amyloid gene of Alzheimer's disease and an altered splicing pattern. *FEBS Lett.* **269**: 305-10.

Koo, E.H. (1997). Phorbol esters affect multiple steps in beta-amyloid precursor protein trafficking and amyloid beta-protein production. *Mol. Med.* **3**: 204-11.

Koo, E.H. (2002). The beta-amyloid precursor protein (APP) and Alzheimer's disease: does the tail wag the dog? *Traffic* **3**: 763-70. Review.

Koo, E.H. and Squazzo, S.L. (1994). Evidence that production and release of amyloid beta-protein involves the endocytic pathway. *J. Biol. Chem.* **269**: 17386-89.

Koo, E.H., Sisodia, S.S., Archer, D.R., Martin, L.J., Weidemann, A., Beyreuther, K., Fischer, P., Masters, C.L. and Price, D.L. (1990). Precursor of amyloid protein in Alzheimer disease undergoes fast anterograde axonal transport. *Proc. Natl. Acad. Sci USA* **87**: 1561-65.

Koo, E.H., Squazzo, S.L., Selkoe, D.J. and Koo, C.H. (1996). Trafficking of cell-surface amyloid beta-protein precursor. I. Secretion, endocytosis and recycling as detected by labeled monoclonal antibody. *J. Cell Sci.* **109**: 991-98.

Kosik, K.S. (1993). Alzheimer's disease: a cell biological perspective. *Science* **256**: 780-83.

Kouchi, Z., Sorimachi, H., Suzuki, K. and Ishiura, S. (1999). Proteasome inhibitors induce the association of Alzheimer's amyloid precursor protein with Hsc73. *Biochem. Biophys. Res. Commun.* **254**: 804-10.

Kovacs, D.M., Wasco, W., Witherby, J., Felsenstein, K.M., Brunel, F., Roeder, R.G. and Tanzi, R.E. (1995). The upstream stimulatory factor functionally interacts with the Alzheimer amyloid beta-protein precursor gene. *Hum. Mol. Genet.* **4**: 1527-33.

Kowalska, A. (2004). Genetic basis of neurodegeneration in familial Alzheimer's disease. *Polish J. Pharmacol.*. **56**: 171-78. Review.

Krebs, C.J., Jarvis, E.D. and Pfaff, D.W. (1999). The 70-kDa heat shock cognate protein (Hsc73) gene is enhanced by ovarian hormones in the ventromedial hypothalamus. *Proc. Natl. Acad. Sci. USA.* **96**: 1686-91.

Kuentzel, S.L., Ali, S.M., Altman, R.A., Greenberg, B.D. and Raub, T.J. (1993). The Alzheimer beta-amyloid protein precursor/protease nexin-II is cleaved by secretase in a trans-Golgi secretory compartment in human neuroglioma cells. *Biochem. J.* **295**: 367-78.

Kuismanen, E. and Saraste, J. (1989). Low temperature-induced transport blocks as tools to manipulate membrane traffic. *Methods Cell Biol.* **32**: 257-74. Review.

Kume, H., Maruyama, K. and Kametani, F. (2004). Intracellular domain generation of amyloid precursor protein by epsilon-cleavage depends on C-terminal fragment by alpha-secretase cleavage. *Int. J. Mol. Med.* **13**: 121-25.

Kusiak, J.W., Lee, L.L. and Zhao, B. (2001). Expression of mutant amyloid precursor proteins decreases adhesion and delays differentiation of Hep-1 cells. *Brain Res.* **896**: 146-52.

L'Hernault, S.W. and Arduengo, P.M. (1992). Mutation of a putative sperm membrane protein in Caenorhabditis elegans prevents sperm differentiation but not its associated meiotic divisions. *J. Cell Biol.* **119**: 55-68.

Lahiri, D.K. and Nall, C. (1995). Promoter activity of the gene encoding the beta-amyloid precursor protein is up-regulated by growth factors, phorbol ester, retinoic acid and interleukin-1. *Brain Res. Mol. Brain Res.* **32**: 233-40.

Lai, A., Sisodia, S.S. and Trowbridge, I.S. (1995). Characterization of sorting signals in the beta-amyloid precursor protein cytoplasmic domain. *J. Biol. Chem.* **270**: 3565-73.

Lambert J.C., Mann D., Goumidi L., Harris J., Pasquier F., Frigard B., Cottel D., Lendon C., Iwatsubo T., Amouyel P. and Chartier-Harlin M.C. (2000). A FE65 polymorphism associated with risk of developing sporadic late-onset Alzheimer's disease but not with Abeta loading in brains. *Neurosci. Lett.* **293**: 29-32.

Lambert, M.P., Barlow, A.K., Chromy, B.A., Edwards, C., Freed, R., Liosatos, M., Morgan, T.E., Rozovsky, I., Trommer, B., Viola, K.L., Wals, P., Zhang, C., Finch, C.E., Krafft, G.A. and Klein, W.L. (1998). Diffusible, nonfibrillar ligands derived from Abeta 1-42 are potent central nervous system neurotoxins. *Proc. Natl. Acad. Sci. USA* **95**: 6448-53.

Lammich, S., Kojro, E., Postina, R., Gilbert. S., Pfeiffer, R., Jasionowski, M., Haass, C. and Fahrenholz, F. (1999). Constitutive and regulated alpha-secretase cleavage of Alzheimer's amyloid precursor protein by a disintegrin metalloprotease. *Proc. Natl. Acad. Sci. USA* **96**: 3922-27.

Lang, J., Nishimoto, I., Okamoto, T., Regazzi, R., Kiraly, C., Weller, U. and Wollheim, C.B. (1995). Direct control of exocytosis by receptor-mediated activation of the heterotrimeric GTPases Gi and G(o) or by the expression of their active G alpha subunits. *EMBO J.* **14**: 3635-44.

Lanni, C., Mazzucchelli, M., Porrello, E., Govoni, S. and Racchi, M. (2004). Differential involvement of protein kinase C alpha and epsilon in the regulated secretion of soluble amyloid precursor protein. *Eur. J. Biochem.* **271**: 3068-75.

Lau, K., Standen, C.L., Ackerley, S., McLoughlin, D.M. and Miller, C.C.J. (2003). X11α and a novel transcription factor, X11αBP1, signal to the nucleus to repress glycogen synthase kinase-3β promoter activity and regulate tau phosphorylation. *Soc. Neurosci. Abst.* Prog. Number 524.1.

LeBlanc, A.C., Chen, H.Y., Autilio-Gambetti, L. and Gambetti, P. (1991). Differential APP gene expression in rat cerebral cortex, meninges and primary astroglial, microglial and neuronal cultures. *FEBS Lett.* **292**: 171-78.

Lee, J.P., Chang, K.A., Kim, H.S., Kim, S.S., Jeong, S.J. and Suh, Y.H. (2000). APP carboxyl-terminal fragment without or with abeta domain equally induces cytotoxicity in differentiated PC12 cells and cortical neurons. *J. Neurosci. Res.* **60**: 565-70.

Lee, M.S., Kao, S.C., Lemere, C.A., Xia, W., Tseng, H.C., Zhou, Y., Neve, R., Ahlijanian, M.K. and Tsai, L.H. (2003a). APP processing is regulated by cytoplasmic phosphorylation. *J.Cell Biol.* **163**: 83-95.

Lee, W., Boo, J.H., Jung, M.W., Park, S.D., Kim, Y.H., Kim, S.U. and Mook-Jung I. (2003b) Amyloid beta peptide directly inhibits PKC activation. *Mol. Cell Neurosci.* **26**: 222-31.

Leem, J.Y., Vijayan, S., Han, P., Cai, D., Machura, M., Lopes, K.O., Veselits, M.L., Xu, H. and Thinakaran, G. (2002). Presenilin 1 is required for maturation and cell surface accumulation of nicastrin. *J. Biol. Chem.* **277**: 19236-40.

Lehel, C., Olah, Z., Jakab, G. and Anderson, W.B. (1995). Protein kinase C epsilon is localized to the Golgi via its zinc-finger domain and modulates Golgi function. *Proc. Natl. Acad. Sci. USA* **92**: 1406-10.

Lehtonen, J.Y., Holopainen, J.M. and Kinnunen, P.K. (1996). Activation of phospholipase A2 by amyloid beta-peptides in vitro. *Biochemistry* **35**: 9407-14.

Leissring, M.A., Murphy, M.P., Mead, T.R., Akbari, Y., Sugarman, M.C., Jannatipour, M., Anliker, B., Muller, U., Saftig, P., De Strooper, B., Wolfe, M.S., Golde, T.E. and LaFerla, F.M. (2002). A physiologic signaling role for the gamma -secretase-derived intracellular fragment of APP. *Proc. Natl. Acad. Sci. USA* **99**: 4697-02.

Leissring, M.A., Lu, A., Condron, M.M., Teplow, D.B., Stein, R.L., Farris, W. and Selkoe, D.J. (2003). Kinetics of amyloid beta-protein degradation determined by novel fluorescence- and fluorescence polarization-based assays. *J. Biol. Chem.* **278**: 37314-20.

Lemere, C.A., Lopera, F., Kosik, K.S., Lendon, C.L., Ossa, J., Saido, T.C., Yamaguchi, H., Ruiz, A., Martinez, A., Madrigal, L., Hincapie, L., Arango, J.C., Anthony, D.C., Koo, E.H., Goate, A.M., Selkoe, D.J. and Arango, J.C. (1996). The E280A presenilin 1 Alzheimer mutation produces increased Abeta 42 deposition and severe cerebellar pathology. *Nat. Med.* **2**: 1146-50.

Lesuisse, C. and Martin, L.J. (2002). Long-term culture of mouse cortical neurons as a model for neuronal development, aging, and death. *J. Neurobiol.* **51**: 9-23.

Leverenz, J.B. and Raskind, M.A. (1998). Early amyloid deposition in the medial temporal lobe of young Down syndrome patients: a regional quantitative analysis. *Experimental Neurol.* **150**: 296-04.

Levy, Y.S., Gilgun-Sherki, Y., Melamed, E. and Offen, D. (2005). Therapeutic potential of neurotrophic factors in neurodegenerative diseases. *BioDrugs.* **19**: 97-127. Review.

Lewczuk, P., Esselmann, H., Bibl, M., Paul, S., Svitek, J., Miertschischk, J., Meyrer, R., Smirnov, A., Maler, J.M., Klein, C., Otto, M., Bleich, S., Sperling, W., Kornhuber, J., Ruther, E. and Wiltfang, J. (2004). Electrophoretic separation of amyloid beta peptides in plasma. *Electrophoresis* **25**: 3336-43.

Lewis, J., Dickson, D.W., Li, W. L., Chisholm, L., Corral, A., Jones, G., Yen, S.H., Saham, N., Skipper, L., Yager, D., Eckman, C., Hardy, J., Hutton, M. and McGowan, E. (2001). Enhanced neurofibrillary degeneration in transgenic mice expressing mutant tau and APP. *Science* **293**: 1487-91.

Li, Y.M., Xu, M., Lai, M.T., Huang, Q., Castro, J.L., DiMuzio-Mower, J., Harrison, T., Lellis, C., Nadin, A., Neduvelil, J.G., Register, R.B., Sardana, M.K., Shearman, M.S., Smith, A.L., Shi, X.P., Yin, K.C., Shafer, J.A. and Gardell, S.J. (2000). Photoactivated gamma-secretase inhibitors directed to the active site covalently label presenilin 1. *Nature* **405**: 689-94.

Lichtenthaler, S.F., Schobel, S., Neumann, S. and Haass, C. (2005). A novel sorting nexin modifies the alpha- and beta-secretase cleavage of APP. 7th International Conference AD/PD, Sorrento, Italy. (OR)-102.

Loffler, J. and Huber, G. (1992). Beta-amyloid precursor protein isoforms in various rat brain regions and during brain development. *J. Neurochem.* **59**: 1316-24.

Lorenzo, A., Yuan, M., Zhang, Z., Paganetti, P.A., Sturchler-Pierrat, C., Staufenbiel, M., Mautino, J., Vigo, F.S., Sommer, B. and Yankner, B.A. (2000). Amyloid beta interacts with the amyloid precursor protein: a potential toxic mechanism in Alzheimer's disease. *Nat. Neurosci.* **3**: 460-64.

Lu, D.C., Rabizadeh, S., Chandra, S., Shayya, R.F., Ellerby, L.M., Ye, X., Salvesen, G.S., Koo, E.H. and Bredesen, D.E. (2000). A second cytotoxic proteolytic peptide derived from amyloid beta-protein precursor. *Nat. Med.* **6**: 397-04.

Luo, L., Tully, T. and White, K. (1992). Human amyloid precursor protein ameliorates behavioural deficit of flies deleted gene for App1 gene. *Neuron* **9**: 595-05.

Luo, Y., Sunderland, T. and Wolozin, B. (1996a). Physiologic levels of beta-amyloid activate phosphatidylinositol 3-kinase with the involvement of tyrosine phosphorylation. *J. Neurochem.* **67**: 978-87.

Luo, Y., Sunderland, T., Roth, G.S. and Wolozin, B. (1996b). Physiological levels of beta-amyloid peptide promote PC12 cell proliferation. *Neurosci. Lett.* **217**: 125-28.

Luo, Y., Bolon, B., Kahn, S., Bennett, B.D., Babu-Khan, S., Denis, P., Fan, W., Kha, H., Zhang, J., Gong, Y., Martin, L., Louis, J.C., Yan, Q., Richards, W.G., Citron, M. and Vassar, R. (2001). Mice deficient in BACE1, the Alzheimer's beta-secretase, have normal phenotype and abolished beta-amyloid generation. *Nat. Neurosci.* **4**: 231-32.

Lyckman, A.W., Confaloni, A.M., Thinakaran, G., Sisodia, S.S. and Moya, K.L. (1998). Post-translational processing and turnover kinetics of presynaptically targeted amyloid precursor superfamily proteins in the central nervous system. *J. Biol. Chem.* **273**: 11100-06.

Maasch, C., Wagner, S., Lindschau, C., Alexander, G., Buchner, K., Gollasch, M., Luft, F.C. and Haller, H. (2000). Protein kinase calpha targeting is regulated by temporal and spatial changes in intracellular free calcium concentration [Ca(2+)](i). *FASEB J.* **14**: 1653-63.

Madeira, A., Pommet, J.M., Prochiantz, A. and Allinquant B. (2005). SET protein (TAF1beta, I2PP2A) is involved in neuronal apoptosis induced by an amyloid precursor protein cytoplasmic subdomain. *FASEB J.* **19**: 1905-07.

Maiese, K. and Chong, Z.Z. (2004). Insights into oxidative stress and potential novel therapeutic targets for Alzheimer disease. *Restor. Neurol. Neurosci.* **22:** 87-04. Review.

Mallard, F., Antony, C., Tenza, D., Salamero, J., Goud, B. and Johannes, L. (1998). Direct pathway from early/recycling endosomes to the Golgi apparatus revealed through the study of shiga toxin B-fragment transport. *J. Cell Biol.* **143**: 973-90.

Mallard, F., Tang, B.L., Galli, T., Tenza, D., Saint-Pol, A., Yue, X., Antony, C., Hong, W., Goud, B. and Johannes, L. (2002). Early/recycling endosomes-to-TGN transport involves two SNARE complexes and a Rab6 isoform. *J. Cell Biol.* **156**: 653-64.

Marambaud, P., Chevallier, N., Barelli, H., Wilk, S. and Checler, F. (1997a). Proteasome contributes to the alpha-secretase pathway of amyloid precursor protein in human cells. *J. Neurochem.* **68**: 698-03.

Marambaud, P., Lopez-Perez, E., Wilk, S. and Checler, F. (1997b). Constitutive and protein kinase C-regulated secretory cleavage of Alzheimer's beta-amyloid precursor protein: different control of early and late events by the proteasome. *J. Neurochem.* **69**: 2500-05.

Marquez-Sterling, N.R., Lo, A.C., Sisodia, S.S. and Koo, E.H. (1997). Trafficking of cell-surface beta-amyloid precursor protein: evidence that a sorting intermediate participates in synaptic vesicle recycling. *J. Neurosci.* **17**: 140-51.

Masliah, E., Cole, G., Shimohama, S., Hansen, L., DeTeresa, R., Terry, R.D. and Saitoh, T. (1990) Differential involvement of protein kinase C isozymes in Alzheimer's disease. *J. Neurosci.* **10**: 2113-24.

Mathews, P.M., Jiang, Y., Schmidt, S.D., Grbovic, O.M., Mercken, M. and Nixon, R.A. (2002). Calpain activity regulates the cell surface distribution of amyloid precursor protein. Inhibition of clapains enhances endosomal generation of beta-cleaved C-terminal APP fragments. *J. Biol. Chem.* **277**: 36415-24.

Mathur, S.K., Sistonen, L., Brown, I.R., Murphy, S.P., Sarge, K.D. and Morimoto, R.I. (1994). Deficient induction of human hsp70 heat shock gene transcription in Y79 retinoblastoma cells despite activation of heat shock factor 1. *Proc. Natl. Acad. Sci. USA* **91**: 8695-99.

Matsuda, S., Yasukawa, T., Homma, Y., Ito, Y., Niikura, T., Hiraki, T., Hirai, S., Ohno, S., Kita, Y., Kawasumi, M., Kouyama, K., Yamamoto, T., Kyriakis, J.M. and Nishimoto, I. (2001). c-Jun N-terminal kinase (JNK)-interacting protein-1b/islet-brain-1 scaffolds Alzheimer's amyloid precursor protein with JNK. *J. Neurosci.* **21**: 6597-07.

Matsumoto, A., Itoh, K. and Matsumoto, R. (2000). A novel carboxypeptidase B that processes native beta-amyloid precursor protein is present in human hippocampus. *Eur. J. Neurosci.* **12**: 227-38.

Matsushima, H., Shimohama, S., Chachin, M., Taniguchi, T. and Kimura, J. (1996). Ca2+-dependent and Ca2+-independent protein kinase C changes in the brain of patients with Alzheimer's disease. *J. Neurochem.* **67**: 317-23.

Mattson, M.P. (1994). Secreted forms of beta-amyloid precursor protein modulate dendrite outgrowth and calcium responses to glutamate in cultured embryonic hippocampal neurons. *J. Neurobiol.* **25**: 439-50.

Mattson, M.P. (1997). Cellular actions of beta-amyloid precursor protein and its soluble and fibrillogenic derivatives. *Physiol. Rev.* **77**: 1081-32.

Mattson, M.P. (2004). Pathways towards and away from Alzheimer's disease. *Nature.* **430**: 631-39. Review.

Mattson, M.P., Cheng, B., Culwell, A.R., Esch, F.S., Lieberburg, I. and Rydel, R.E. (1993). Evidence for excitoprotective and intraneuronal calcium-regulating roles for secreted forms of the beta-amyloid precursor protein. *Neuron* **10**: 243-54.

Mayeux, R., Saunders, A.M., Shea, S., Mirra, S., Evans, D., Roses, A.D., Hyman, B.T., Crain, B., Tang. M,X. and Phelps, C.H. (1998). Utility of the apolipoprotein E genotype in the diagnosis of Alzheimer's disease. Alzheimer's Disease Centers Consortium in Apolipoprotein E and Alzheimer's Disease. *N. Engl. J. Med.* **338**: 506-11.

Mayor, S., Presley, J.F. and Maxfield, F.R. (1993). Sorting of membrane components from endosomes and subsequent recycling to the cell surface occurs by a bulk flow process. *J. Cell Biol.* **121**: 1257-69.

McLaughlin, M. and Breen, K.C. (1999). Protein kinase C activation potentiates the rapid secretion of the amyloid precursor protein from rat cortical synaptosomes. *J. Neurochem.* **72**: 273-81.

McLoughlin, D.M. and Miller, C.C. (1996). The intracellular cytoplasmic domain of the Alzheimer's disease amyloid precursor protein interacts with phosphotyrosine-binding domain proteins in the yeast two-hybrid system. *FEBS Lett.* **397**: 197-00.

Mehta, N.D., Refolo, L.M., Eckman, C., Sanders, S., Yager, D., Perez-Tur, J., Younkin, S., Duff, K., Hardy, J. and Hutton, M. (1998). Increased Abeta42(43) from cell lines expressing presenilin 1 mutations. *Ann. Neurol.* **43**: 256-58.

Merlos-Suarez, A., Fernandez-Larrea, J., Reddy, P., Baselga, J. and Arribas, J. (1998). Pro-tumor necrosis factor-alpha processing activity is tightly controlled by a component that does not affect notch processing. *J. Biol. Chem.* **273**: 24955-62.

Meziane, H., Dodart, J.C., Mathis, C., Little, S., Clemens, J., Paul, S.M. and Ungerer, A. (1998). Memory-enhancing effects of secreted forms of the beta-amyloid precursor protein in normal and amnestic mice. *Proc. Natl. Acad. Sci. USA* **95**: 12683-88.

Mileusnic, R., Lancashire, C.L., Johnston, A.N. and Rose, S.P. (2000). APP is required during an early phase of memory formation. *Eur. J. Neurosci.* **12**: 4487-95.

Mills, J. and Reiner, P.B. (1996). Phorbol esters but not the cholinergic agonists oxotremorine-M and carbachol increase release of the amyloid precursor protein in cultured rat cortical neurons. *J. Neurochem.* **67**: 1511-18.

Mills, J. and Reiner, P.B. (1999). Regulation of amyloid precursor protein cleavage. *J. Neurochem.* **72**: 443-60. Review.

Mills, J., Laurent Charest, D., Lam, F., Beyreuther, K., Ida, N., Pelech, S.L. and Reiner, P.B. (1997). Regulation of amyloid precursor protein catabolism involves the mitogen-activated protein kinase signal transduction pathway. *J. Neurosci.* **17**: 9415-22.

Milton, N.G. (2005). Phosphorylated amyloid-beta: the toxic intermediate in alzheimer's disease neurodegeneration. *Subcell. Biochem.* **38**: 381-02. Review.

Minopoli, G., de Candia, P., Bonetti, A., Faraonio, R., Zambrano, N. and Russo, T. (2001). The beta-amyloid precursor protein functions as a cytosolic anchoring site that prevents Fe65 nuclear translocation. *J. Biol. Chem.* **276**: 6545-50.

Moir, R.D., Lynch, T., Bush, A.I., Whyte, S., Henry, A., Portbury, S., Multhaup, G., Small, D.H., Tanzi, R.E., Beyreuther, K. and Masters, C.L. (1998). Relative increase in Alzheimer's disease of soluble forms of cerebral Abeta amyloid protein precursor containing the Kunitz protease inhibitory domain. *J. Biol. Chem.* **273**: 5013-19.

Moreira, P.I., Honda, K., Zhu, X., Nunomura, A., Casadesus, G., Smith, M.A. and Perry, G. (2006). Brain and brawn: parallels in oxidative strength. *Neurology* **66**: S97-01.

Mosconi, L., Tsui, W.H., De Santi, S., Li, J., Rusinek, H., Convit, A., Li, Y., Boppana, M. and de Leon, M.J. (2005). Reduced hippocampal metabolism in MCI and AD: automated FDG-PET image analysis. *Neurology* **64**: 1860-67.

Mucke, L., Masliah, E., Johnson, W.B., Ruppe, M.D., Alford, M., Rockenstein, E.M., Forss-Petter, S., Pietropaolo, M., Mallory, M. and Abraham, C.R. (1994). Synaptotrophic effects of human amyloid beta protein precursors in the cortex of transgenic mice. *Brain Res.* **666**: 151-67.

Mueller, H.T., Borg, J.P., Margolis, B. and Turner, R.S. (2000). Modulation of amyloid precursor protein metabolism by X11alpha /Mint-1. A deletion analysis of protein-protein interaction domains. *J. Biol. Chem.* **275**: 39302-06.

Mulkey, R.M., Endo, S., Shenolikar, S. and Malenka, R.C. (1994). Involvement of a calcineurin/inhibitor-1 phosphatase cascade in hippocampal long-term depression. *Nature* **369**: 486-88.

Muller, U., Cristina, N., Li, Z.W., Wolfer, D.P., Lipp, H.P., Rulicke, T., Brandner, S., Aguzzi, A. and Weissmann, C. (1994). Behavioral and anatomical deficits in mice homozygous for a modified beta-amyloid precursor protein gene. *Cell* **79**: 755-65.

Muller, U. and Kins, S. (2002). APP on the move. *Trends Mol Med.* **8**: 152-55.

Multhaup, G. (1994). Identification and regulation of the high affinity binding site of the Alzheimer's disease amyloid protein precursor (APP) to glycosaminoglycans. *Biochimie.* **76**: 304-11. Review.

Multhaup, G., Bush, A.I., Pollwein, P. and Masters, C.L. (1994). Interaction between the zinc (II) and the heparin binding site of the Alzheimer's disease beta A4 amyloid precursor protein (APP). *FEBS Lett.* **355**: 151-54.

Multhaup, G., Mechler, H. and Masters, C.L. (1995). Characterization of the high affinity heparin binding site of the Alzheimer's disease beta A4 amyloid precursor protein (APP) and its enhancement by zinc(II). *J. Mol. Recognit.* **8**: 247-57.

Multhaup, G., Schlicksupp, A., Hesse, L., Beher, D., Ruppert, T., Masters, C.L. and Beyreuther, K. (1996). The amyloid precursor protein of Alzheimer's disease in the reduction of copper(II) to copper(I) *Science* **271**: 1406-09.

Mumm, J.S., Schroeter, E.H., Saxena, M.T., Griesemer, A., Tian, X., Pan, D.J., Ray, W.J. and Kopan, R. (2000). A ligand-induced extracellular cleavage regulates gamma-secretase-like proteolytic activation of Notch1. *Mol. Cell* **5**: 197-06.

Muresan, Z. and Muresan, V. (2004). A phosphorylated, carboxy-terminal fragment of beta-amyloid precursor protein localizes to the splicing factor compartment. *Hum. Mol. Genet.* **13**: 475-88.

Muresan, Z. and Muresan, V. (2005). c-Jun NH2-terminal kinase-interacting protein-3 facilitates phosphorylation and controls localization of amyloid-beta precursor protein. *J. Neurosci.* **25**: 3741-51.

Murrell, J., Farlow, M., Ghetti, B. and Benson, M.D. (1991). A mutation in the amyloid precursor protein associated with hereditary Alzheimer's disease. *Science* **254**: 97-99.

Nair, P., Schaub, B.E. and Rohrer, J. (2003). Characterization of the endosomal sorting signal of the cation-dependent mannose 6-phosphate receptor. *J. Biol. Chem.* **278**: 24753-58.

Neve, R.L., Finch, E.A. and Dawes, L.R. (1988). Expression of the Alzheimer amyloid precursor gene transcripts in the human brain. *Neuron* **1**: 669-77.

Neve, R.L., McPhie, L. and Chen, Y. (2001). Alzheimer's disease: dysfunction of a signaling pathway mediated by the amyloid precursor protein?. *Biochem. Soc. Symp.* **67**: 37-50.

Neves, S.R., Ram, P.T. and Iyengar, R. (2002). G protein pathways. *Science* **296**: 1636-39. Review.

Nilsberth, C., Westlind-Danielsson, A., Eckman, C.B., Condron, M.M., Axelman, K., Forsell, C., Stenh, C., Luthman, J., Teplow, D.B., Younkin, S.G., Naslund, J. and Lannfelt, L. (2001). The 'Arctic' APP mutation (E693G) causes Alzheimer's disease by enhanced Abeta protofibril formation. *Nat. Neurosci.* **4**: 887-93.

Ninomiya, H., Roch, J.M., Sundsmo, M.P., Otero, D.A. and Saitoh, T. (1993). Amino acid sequence RERMS represents the active domain of amyloid beta/A4 protein precursor that promotes fibroblast growth. *J. Cell Biol.* **121**: 879-86.

Nishimoto, I., Okamoto, T., Matsuura, Y., Takahashi, S., Okamoto, T., Murayama, Y. and Ogata, E. (1993). Alzheimer amyloid protein precursor complexes with brain GTP-binding protein G(o) *Nature* **362**: 75-79.

Nishiyama, K., Trapp, B.D., Ikezu, T., Ransohoff, R.M., Tomita, T., Iwatsubo, T., Kanazawa, I., Hsiao, K.K., Lisanti, M.P. and Okamoto, T. (1999). Caveolin-3 upregulation activates beta-secretase-mediated cleavage of the amyloid precursor protein in Alzheimer's disease. *J. Neurosci.* **19**: 6538-48.

Nitsch, R.M., Slack, B.E., Farber, S.A., Schulz, J.G., Deng, M., Kim, C., Borghesani, P.R., Korver, W., Wurtman, R.J. and Growdon, J.H. (1994). Regulation of proteolytic processing of the amyloid beta-protein precursor of Alzheimer's disease in transfected cell lines and in brain slices. *J. Neural Transm. Suppl.* **44**: 21-27. Review.

Nitsch, R.M., Deng, A., Wurtman, R.J. and Growdon, J.H. (1997). Metabotropic glutamate receptor subtype mGluR1alpha stimulates the secretion of the amyloid beta-protein precursor ectodomain. *J. Neurochem.* **69**: 704-12.

Nordstedt, C., Caporaso, G.L., Thyberg, J., Gandy, S.E. and Greengard, P. (1993). Identification of the Alzheimer beta/A4 amyloid precursor protein in clathrin-coated vesicles purified from PC12 cells. *J. Biol. Chem.* **268**: 608-12.

Nunan, J. and Small, D.H. (2000). Regulation of APP cleavage by alpha-, beta- and gamma-secretases. *FEBS Lett.* **483**: 6-10. Review.

Ohgami, T., Kitamoto, T. and Tateishi, J. (1993). The rat central nervous system expresses Alzheimer's amyloid precursor protein APP695, but not APP677 (L-APP form). *J. Neurochem.* **61**: 1553-56.

Ohsawa, I., Takamura, C. and Kohsaka, S. (1997). The amino-terminal region of amyloid precursor protein is responsible for neurite outgrowth in rat neocortical explant culture. *Biochem. Biophys. Res. Commun* **236**: 59-65.

Ohsawa, I., Takamura, C. and Kohsaka, S. (2001). Fibulin-1 binds the amino-terminal head of beta-amyloid precursor protein and modulates its physiological function. *J. Neurochem.* **76**: 1411-20.

Oishi, M., Nairn, A.C., Czernik, A.J., Lim, G.S., Isohara, T., Gandy, S.E., Greengard, P. and Suzuki, T. (1997). The cytoplasmic domain of Alzheimer's amyloid precursor protein is phosphorylated at Thr654, Ser655 and Thr668 in adult rat brain and cultured cells. *Mol. Med.* **3**: 111-23.

Okado, H. and Okamoto, H. (1992). A *Xenopus* homologue of the human beta-amyloid precursor protein: developmental regulation of its gene expression. *Biochem. Biophys. Res. Commun* **189**: 1561-68.

Okamoto, T., Takeda, S., Murayama, Y., Ogata, E. and Nishimoto, I. (1995). Ligand-dependent G protein coupling function of amyloid transmembrane precursor. *J. Biol. Chem.* **270**: 4205-08.

Oltersdorf, T., Ward, P.J., Henriksson, T., Beattie, E.C., Neve, R., Lieberburg, I. and Fritz, L.C. (1990). The Alzheimer amyloid precursor protein. Identification of a stable intermediate in the biosynthetic/ degradative pathway. *J. Biol. Chem.* **265**: 4492-97.

Ono, K., Yoshiike, Y., Takashima, A., Hasegawa, K., Naiki, H. and Yamada, M. (2004). Vitamin A exhibits potent antiamyloidogenic and fibril-destabilizing effects in vitro. *Exp. Neurol.* **189**: 380-92.

Pahlsson, P. and Spitalnik, S.L. (1996). The role of glycosylation in synthesis and secretion of beta-amyloid precursor protein by Chinese hamster ovary cells. *Arch. Biochem. Biophys.* **331**: 177-86.

Panegyres, P.K., Zafiris-Toufexis, K. and Kakulas, B.A. (2000). Amyloid precursor protein gene isoforms in Alzheimer's disease and other neurodegenerative disorders. *J. Neurol. Sci.* **173**: 81-92.

Pangalos, M.N., Shioi, J., Efthimiopoulos, S., Wu, A. and Robakis, N.K. (1996). Characterization of appican, the chondroitin sulfate proteoglycan form of the Alzheimer amyloid precursor protein. *Neurodegeneration* **5**: 445-51. Review.

Parat, M.O. and Fox, P.L. (2001). Palmitoylation of caveolin-1 in endothelial cells is post-translational but irreversible. *J. Biol. Chem.* **276**: 15776-82.

Pardossi-Piquard, R., Petit, A., Kawarai, T., Sunyach, C., Alves da Costa, C., Vincent, B., Ring, S., D'Adamio, L., Shen, J., Muller, U., St George Hyslop, P. and Checler F. (2005). Presenilin-dependent transcriptional control of the Abeta-degrading enzyme neprilysin by intracellular domains of betaAPP and APLP. *Neuron* **46**: 541-54.

Parvathy, S., Hussain, I., Karran, E.H., Turner, A.J. and Hooper, N.M. (1999). Cleavage of Alzheimer's amyloid precursor protein by alpha-secretase occurs at the surface of neuronal cells. *Biochemistry* **38**: 9728-34.

Pascale, A., Fortino, I., Govoni, S., Trabucchi, M., Wetsel, W.C. and Battaini, F. (1996). Differential isoform-specific regulation of calcium-independent protein kinase C in rat cerebral cortex. *Neurosci. Lett.* **214**: 99-02.

Pasternak, S.H., Bagshaw, R.D., Guiral, M., Zhang, S., Ackerley, C.A., Pak, B.J., Callahan, J.W. and Mahuran, D.J. (2003). Presenilin-1, nicastrin, amyloid precursor protein and gamma-secretase activity are co-localized in the lysosomal membrane. *J. Biol. Chem.* **278**: 26687-94.

Pellegrini, L., Passer, B.J., Tabaton, M., Ganjei, J.K. and D'Adamio, L. (1999). Alternative, non-secretase processing of Alzheimer's beta-amyloid precursor protein during apoptosis by caspase-6 and -8. *J. Biol. Chem.* **274**: 21011-16.

Peraus, G.C., Masters, C.L. and Beyreuther, K. (1997). Late compartments of amyloid precursor protein transport in SY5Y cells are involved in beta-amyloid secretion. *J. Neurosci.* **17**: 7714-24.

Perez, R.G., Soriano, S., Hayes, J.D., Ostaszewski, B., Xia, W., Selkoe, D.J., Chen, X., Stokin, G.B. and Koo, E.H. (1999). Mutagenesis identifies new signals for beta-amyloid precursor protein endocytosis, turnover and the generation of secreted fragments, including Abeta42. *J. Biol. Chem.* **274**: 18851-56.

Phinney, A.L., Deller, T., Stalder, M., Calhoun, M.E., Frotscher, M., Sommer, B., Staufenbiel, M. and Jucker, M. (1999). Cerebral amyloid induces aberrant axonal sprouting and ectopic terminal formation in amyloid precursor protein transgenic mice. *J. Neurosci.* **19**: 8552-59.

Piccini, A., Ciotti, M.T., Vitolo, O.V., Calissano, P., Tabaton, M. and Galli, C. (2000). Endogenous APP derivatives oppositely modulate apoptosis through an autocrine loop. *Neuroreport* **11**: 1375-79.

Pigino, G., Morfini, G., Pelsman, A., Mattson, M.P., Brady, S.T. and Busciglio, J. (2003). Alzheimer's presenilin 1 mutations impair kinesin-based axonal transport. *J. Neurosci.* **23**: 4499-08.

Pinnix, I., Musunuru, U., Tun, H., Sridharan, A., Golde, T., Eckman, C., Ziani-Cherif, C., Onstead, L. and Sambamurti, K. (2001). A novel gamma -secretase assay based on detection of the putative C-terminal fragment-gamma of amyloid beta protein precursor. *J. Biol. Chem.* **276**: 481-87.

Pollack, S.J. and Lewis, H. (2005). Secretase inhibitors for Alzheimer's disease: challenges of a promiscuous protease. *Curr. Opin. Investig. Drugs.* **6**: 35-47. Review.

Ponte, P., Gonzalez-DeWhitt, P., Schilling, J., Miller, J., Hsu, D., Greenberg, B., Davis, K., Wallace, W., Lieberburg, I. and Fuller, F. (1988). A new A4 amyloid mRNA contains a domain homologous to serine proteinase inhibitors. *Nature* **331**: 525-27.

Ponting, C.P., Hutton, M., Nyborg, A., Baker, M., Jansen, K. and Golde, T.E. (2002). Identification of a novel family of presenilin homologues. *Hum. Mol. Genet.* **11**: 1037-44.

Poorkaj, P., Bird, T.D., Wijsman, E., Nemens, E., Garruto, R.M., Anderson, L., Andreadis, A., Wiederholt, W.C., Raskind, M. and Schellenberg, G.D. (1998). Tau is a candidate gene for chromosome 17 frontotemporal dementia. *Ann. Neurol.* **43**: 815-25.

Post, G.R. and Brown, J.H. (1996). G protein-coupled receptors and signaling pathways regulating growth responses. *FASEB J.* **10**: 741-49. Review.

Postina, R., Schroeder, A., Dewachter, I., Bohl, J., Schmitt, U., Kojro, E., Prinzen, C., Endres, K., Hiemke, C., Blessing, M., Flamez, P., Dequenne, A., Godaux, E., van Leuven, F. and Fahrenholz, F. (2004). A disintegrin-metalloproteinase prevents amyloid plaque formation and hippocampal defects in an Alzheimer disease mouse model. *J. Clin. Invest.* **113**: 1456-64.

Pradier, L., Carpentier, N., Delalonde, L., Clavel, N., Bock, M.D., Buee, L., Mercken, L., Tocque, B. and Czech, C. (1999). Mapping the APP/presenilin (PS) binding domains: the hydrophilic N-terminus of PS2 is sufficient for interaction with APP and can displace APP/PS1 interaction. *Neurobiol. Dis.* **6**: 43-55.

Prange, O. and Murphy, T.H. (2001). Modular transport of postsynaptic density-95 clusters and association with stable spine precursors during early development of cortical neurons. *J. Neurosci.* **21**: 9325-33.

Praprotnik, D., Smith, M.A., Richey, P.L., Vinters, H.V. and Perry, G. (1996). Filament heterogeneity within the dystrophic neurites of senile plaques suggests blockage of fast axonal transport in Alzheimer's disease. *Acta Neuropathol.* **91**: 226-35.

Press, B., Feng, Y., Hoflack, B. and Wandinger-Ness, A. (1998). Mutant Rab7 Causes the Accumulation of Cathepsin D and Cation-independent Mannose 6-Phosphate Receptor in an Early Endocytic Compartment. *J. Cell Biol.* **140**: 1075-89.

Qian, L., Yang, T., Chen, H., Xie, J., Zeng, H., Warren, D.W., MacVeigh, M., Meneray, M.A., Hamm-Alvarez, S.F. and Mircheff, A.K. (2003). Heterotrimeric GTP-binding proteins in the lacrimal acinar cell endomembrane system. *Exp. Eye Res.* **74**: 7-22.

Qiu, W.Q., Ferreira, A., Miller, C., Koo, E.H. and Selkoe, D.J. (1995). Cell-surface β-amyloid precursor protein stimulates neurite outgrowth of hippocampal neurons in an isoform-dependent manner. *J. Neurosci.* **15**: 2157-67.

Qiu Y, Wu XJ, Chen HZ. (2003). Simultaneous changes in secretory amyloid precursor protein and beta-amyloid peptide release from rat hippocampus by activation of muscarinic receptors. *Neurosci. Lett.* **352**: 41-44.

Ramelot, T.A. and Nicholson, L.K. (2001). Phosphorylation-induced structural changes in the amyloid precursor protein cytoplasmic tail detected by NMR. *J. Mol. Biol.* **307**: 871-84.

Ramelot, T.A., Gentile, L.N. and Nicholson, L.K. (2000). Transient structure of the amyloid precursor protein cytoplasmic tail indicates preordering of structure for binding to cytosolic factors. *Biochemistry* **39**: 2714-25.

Rassoulzadegan, M., Yang, Y. and Cuzin, F. (1998). APLP2, a member of the Alzheimer precursor protein family, is required for correct genomic segregation in dividing mouse cells. *EMBO J.* **17**: 4647-56.

Rawson, R.B. (2002). Regulated intramembrane proteolysis: from the endoplasmic reticulum to the nucleus. *Essays Biochem.* **38**: 155-68. Review.

Reaves, B., Horn, M. and Banting, G. (1993). TGN38/41 recycles between the cell surface and the TGN: brefeldin A affects its rate of return to the TGN. *Mol. Biol. Cell.* **4**: 93-05.

Riddell, D.R., Christie, G., Hussain, I. and Dingwall, C. (2001). Compartmentalization of beta-secretase (Asp2) into low-buoyant density, noncaveolar lipid rafts. *Curr. Biol.* **11**: 1288-93.

Richard, F. and Amouyel, P. (2001). Genetic susceptibility factors for Alzheimer's disease. *Eur. J. Pharmacol.* **412**: 1-12.

Richards, B., Karpilow, J., Dunn, C., Peterson, I., Maxfield, A., Zharkikh, L., Abedi, M., Hurlburt, A., Hardman, J., Hsu, F., Li, W., Rebentisch, M., Sandrock, R., Sandrock, T., Kamb, A. and Teng, D.H. (2003). Genetic selection for modulators of a retinoic-acid-responsive reporter in human cells. *Genetics* **163**: 1047-60.

Robakis, N.K., Vassilacopoulou, D., Efthimiopoulos, S., Sambamurti, K., Refolo, L.M. and Shioi, J. (1993). Cellular processing and proteoglycan nature of amyloid precursor proteins. *Ann. N. Y. Acad. Sci.* **695**: 132-38.

Roberds, S.L. anderson, J., Basi, G., Bienkowski, M.J., Branstetter, D.G., Chen, K.S., Freedman, S.B., Frigon, N.L., Games, D., Hu, K., Johnson-Wood, K., Kappenman, K.E., Kawabe, T.T., Kola, I., Kuehn, R., Lee, M., Liu, W., Motter, R., Nichols, N.F., Power, M., Robertson, D.W., Schenk, D., Schoor, M., Shopp, G.M., Shuck, M.E., Sinha, S., Svensson, K.A., Tatsuno, G., Tintrup, H., Wijsman, J., Wright, S. and McConlogue, L. (2001). BACE knockout mice are healthy despite lacking the primary beta-secretase activity in brain: implications for Alzheimer's disease therapeutics. *Hum. Mol. Genet.* **10**: 1317-24.

Roberts, S.B., Ripellino, J.A., Ingalls, K.M., Robakis, N.K. and Felsenstein, K.M. (1994). Non-amyloidogenic cleavage of the beta-amyloid precursor protein by an integral membrane metalloendopeptidase. *J. Biol. Chem.* **269**: 3111-16.

Rockenstein, E.M., McConlogue, L., Tan, H., Power, M., Masliah, E. and Mucke, L. (1995). Levels and alternative splicing of amyloid beta protein precursor (APP) transcripts in brains of APP transgenic mice and humans with Alzheimer's disease. *J. Biol. Chem.* **270**: 28257-67.

Rodriguez Martin, T., Callela, A., Silva, S., Munna, E., Modena, P. and Chiesa, R. (2000). ApoE and polymorphism of presenilin 1 and α1-anti-chymotrypsin in Alzheimer and vascular dementia. *Dementia Geriat. Cognit. Dis.* **11**: 239-44.

Rogers, J. (1998). Candle and Darkness: *Current Research in Alzheimer's Disease.* Chicago. Bonus Books Inc., 131-33.

Roghani, M., Becherer, J.D., Moss, M.L., Atherton, R.E., Erdjument-Bromage, H., Arribas, J., Blackburn, R.K., Weskamp, G., Tempst, P. and Blobel, C.P. (1999). Metalloprotease-disintegrin MDC9: intracellular maturation and catalytic activity. *J. Biol. Chem.* **274**: 3531-40.

Rohan de Silva, H.A., Jen, A., Wickenden, C., Jen, L.S., Wilkinson, S.L. and Patel, A.J. (1997). Cell-specific expression of beta-amyloid precursor protein isoform mRNAs and proteins in neurons and astrocytes. *Brain Res. Mol. Brain Res.* **47**: 147-56.

Roher, A.E., Chaney, M.O., Kuo, Y.M., Webster, S.D., Stine, W.B., Haverkamp, L.J., Woods, A.S., Cotter, R.J., Tuohy, J.M., Krafft, G.A. and Bonnell, B.S. (1996). Emmerling MR. Morphology and toxicity of Abeta-(1-42) dimer derived from neuritic and vascular amyloid deposits of Alzheimer's disease. *J. Biol. Chem.* **271**: 20631-35.

Rohrer, J., Schweizer, A., Johnson, K.F. and Kornfeld, S. (1995). A determinant in the cytoplasmic tail of the cation-dependent mannose 6-phosphate receptor prevents trafficking to lysosomes. *J. Cell Biol.* **130**: 1297-06.

Rohrer, J., Schweizer, A., Russell, D. and Kornfeld, S. (1996). The targeting of Lamp1 to lysosomes is dependent on the spacing of its cytoplasmic tail tyrosine sorting motif relative to the membrane. *J. Cell Biol.* **132**: 565-76.

Roncarati, R., Sestan, N., Scheinfeld, M.H., Berechid, B.E., Lopez, P.A., Meucci, O., McGlade, J.C., Rakic, P. and D'Adamio, L. (2002). The gamma-secretase-generated intracellular domain of beta-amyloid precursor protein binds Numb and inhibits Notch signaling. *Proc. Natl. Acad. Sci. USA* **99**: 7102-07.

Rondeau, V., Commenges, D., Jacqmin-Gadda, H. and Dartigues, J.F. (2000). Relation between aluminum concentrations in drinking water and Alzheimer's disease: An eight year follow-up study. *Am. J. Epidemiology* **152**: 59-66.

Rooke, J., Pan, D., Xu, T. and Rubin, G.M. (1996). KUZ, a conserved metalloprotease-disintegrin protein with two roles in Drosophila neurogenesis. *Science* **273**: 1227-31.

Rosen, D.R., Martin-Morris, L., Luo, L.Q. and White, K. (1989). A Drosophila gene encoding a protein resembling the human beta-amyloid protein precursor. *Proc. Natl. Acad. Sci. USA* **86**: 2478-82.

Rossner, S., Beck, M., Stahl, T., Mendla, K., Schliebs, R. and Bigl, V. (2001a). Constitutive overactivation of protein kinase C in guinea pig brain increases alpha-secretory APP processing without decreasing beta-amyloid generation. *Eur. J. Neurosci.* **12**: 3191-00.

Rossner, S., Mendla, K., Schliebs, R. and Bigl, V. (2001b) Protein kinase Calpha and beta1 isoforms are regulators of alpha-secretory proteolytic processing of amyloid precursor protein in vivo. *Eur. J. Neurosci.* **13**: 1644-48.

Rouot, B., Brabet, P., Homburger, V., Toutant, M. and Bockaert, J. (1987). Go, a major brain GTP binding protein in search of a function: purification, immunological and biochemical characteristics. *Biochimie.* **69**: 339-49. Review.

Russo, C., Salis, S., Dolcini, V., Venezia, V., Song, X.H., Teller, J.K. and Schettini, G. (2001). Amino-terminal modification and tyrosine phosphorylation of [corrected] carboxy-terminal fragments of the amyloid precursor protein in Alzheimer's disease and Down's syndrome brain. *Neurobiol. Dis.* **8**: 173-80.

Sabatini, D.D., Adesnik, M., Ivanov, I.E. and Simon, J.P. (1996). Mechanism of formation of post Golgi vesicles from TGN membranes: Arf-dependent coat assembly and PKC-regulated vesicle scission. *Biocell* **20: 2**87-00. Review.

Sabo, S.L., Ikin, A.F., Buxbaum, J.D. and Greengard, P. (2001). The Alzheimer amyloid precursor protein (APP) and FE65, an APP-binding protein, regulate cell movement. *J. Cell Biol.* **153**: 1403-14.

Sabo, S.L., Ikin, A.F., Buxbaum, J.D. and Greengard, P. (2003). The amyloid precursor protein and its regulatory protein, FE65, in growth cones and synapses in vitro and in vivo. *J. Neurosci.* **23**: 5407-15.

Saint-Pol, A., Yelamos, B., Amessou, M., Mills, I.G., Dugast, M., Tenza, D., Schu, P., Antony, C., McMahon, H.T., Lamaze, C. and Johannes, L. (2004). Clathrin adaptor epsinR is required for retrograde sorting on early endosomal membranes. *Dev. Cell* **6**: 525-38.

Sambamurti, K., Shioi, J. Anderson, J.P., Pappolla, M.A. and Robakis, N.K**.** (1992). Evidence for intracellular cleavage of the Alzheimer's amyloid precursor in PC12 cells. *J. Neurosci. Res.* **33**: 319-29.

Sandbrink, R., Masters, C.L. and Beyreuther, K. (1994a). Beta A4-amyloid protein precursor mRNA isoforms without exon 15 are ubiquitously expressed in rat tissues including brain, but not in neurons. *J. Biol. Chem.* **269**: 1510-17.

Sandbrink, R., Masters, C.L. and Beyreuther, K. (1994b). APP gene family: unique age-associated changes in splicing of Alzheimer's betaA4-amyloid protein precursor. *Neurobiol. Dis.* **1**: 13-24.

Sandbrink, R., Masters, C.L. and Beyreuther, K. (1996a). APP gene family. Alternative splicing generates functionally related isoforms. *Ann. N. Y. Acad. Sci.* **777**: 281-87.

Sandbrink, R., Hartmann, T., Masters, C.L. and Beyreuther, K. (1996b). Genes contributing to Alzheimer's disease. *Mol. Psychiatry* **1**: 27-40. Review.

Saura, C.A., Tomita, T., Davenport, F., Harris, C.L., Iwatsubo, T. and Thinakaran, G. (1999). Evidence that intramolecular associations between presenilin domains are obligatory for endoproteolytic processing. *J. Biol. Chem.* **274**: 13818-23.

Sastre, M., Turner, R.S. and Levy, E. (1998). X11 interaction with beta-amyloid precursor protein modulates its cellular stabilization and reduces amyloid beta-protein secretion. *J. Biol. Chem.* **273**: 22351-57.

Sastre, M., Steiner, H., Fuchs, K., Capell, A., Multhaup, G., Condron, M.M., Teplow, D.B. and Haass, C. (2001). Presenilin-dependent gamma-secretase processing of beta-amyloid precursor protein at a site corresponding to the S3 cleavage of Notch. *EMBO Rep.* **2:** 835-41.

Satoh, J., Kuroda, Y. (2000). Amyloid precursor protein beta-secretase (BACE) mRNA expression in human neural cell lines following induction of neuronal differentiation and exposure to cytokines and growth factors. *Neuropathology* **20**: 289-96.

Satpute-Krishnan, P., DeGiorgis, J.A. and Bearer, E.L. (2003). Fast anterograde transport of herpes simplex virus: role for the amyloid precursor protein of Alzheimer's disease. *Aging Cell.* **2:** 305-18.

Schellenberg, G.,D., (1995). Progress in Alzheimer's disease genetics. *Curr. Opin. Neurol.* **8**: 262-67.

Scheinfeld, M.H., Roncarati, R., Vito, P., Lopez, P.A., Abdallah, M. and D'Adamio, L. (2002). Jun NH2-terminal kinase (JNK) interacting protein 1 (JIP1) binds the cytoplasmic domain of the Alzheimer's beta-amyloid precursor protein (APP). *J. Biol. Chem.* **277**: 3767-75.

Scheper, W., Zwart, R. and Baas, F. (2004). Rab6 membrane association is dependent of Presenilin 1 and cellular phosphorylation events. *Brain. Res. Mol. Brain Res.* **122**: 17-23.

Scheuner, D., Eckman, C., Jensen, M., Song, X., Citron, M., Suzuki, N., Bird, T.D., Hardy, J., Hutton, M., Kukull, W., Larson, E., Levy-Lahad, E., Viitanen, M., Peskind, E., Poorkaj, P., Schellenberg, G., Tanzi, R., Wasco, W., Lannfelt, L., Selkoe, D. and Younkin, S. (1996). Secreted amyloid beta-protein similar to that in the senile plaques of Alzheimer's disease is increased in vivo by the presenilin 1 and 2 and APP mutations linked to familial Alzheimer's disease. *Nat. Med.* **2**: 864-70.

Schlondorff, J., Becherer, J.D. and Blobel, C.P. (2000). Intracellular maturation and localization of the tumour necrosis factor alpha convertase (TACE). *Biochem. J.* **347**: 131-38.

Schmitt, B., Bernhardt, T., Moeller, H.J., Heuser, I. and Frolich, L. (2004). Combination therapy in Alzheimer's disease: a review of current evidence. *CNS Drugs.* **18**: 827-44. Review.

Schroeter, E.H., Kisslinger, J.A. and Kopan, R. (1998). Notch-1 signalling requires ligand-induced proteolytic release of intracellular domain. *Nature* **393**: 382-86.

Schubert, W., Prior, R., Weidemann, A., Dircksen, H., Multhaup, G., Masters, C.L. and Beyreuther, K. (1991). Localization of Alzheimer beta A4 amyloid precursor protein at central and peripheral synaptic sites. *Brain Res.* **563**: 184-94.

Schubert, D. and Behl, C. (1993). The expression of amyloid beta protein precursor protects nerve cells from beta-amyloid and glutamate toxicity and alters their interaction with the extracellular matrix. *Brain Res.* **629**: 275-82.

Schmidt, M., Schmidtke, G. and Kloetzel, P.M. (1997). Structure and structure formation of the 20S proteasome. *Mol. Biol. Rep.* **24**: 103-12. Review.

Seiffert, D., Bradley, J.D., Rominger, C., M., Rominger, D.H., Yang, F., Meredith, J.E.Jr., Wang, Q., Roach, A.H., Thompson, L.A., Spitz, S.M., Higaki, J.N., Prakash, S.R., Combs, A.P., Copeland, R.A., Arneric, S.P., Hartig, P.R., Robertson, D.W., Cordell, B., Stern, A.M., Olson, R.E. and Zaczek, R. (2000). Presenilin-1 and -2 are molecular targets for gamma-secretase inhibitors. *J. Biol. Chem.* **275**: 34086-91.

Selkoe, D.J., Podlisny, M.B., Joachim, C.L., Vickers, E.A., Lee, G., Fritz, L.C. and Oltersdorf, T. (1988). Beta-amyloid precursor protein of Alzheimer disease occurs as 110- to 135-kilodalton membrane-associated proteins in neural and nonneural tissues. *Proc. Natl. Acad. Sci. U S A* **85**: 7341-45.

Selkoe, D.J. (1994). Normal and abnormal biology of the beta-amyloid precursor protein. *Ann. Rev. Neurosci.* **17**: 489-17.

Selkoe, D.J., Yamazaki, T., Citron, M., Podlisny, M.B., Koo, E.H., Teplow, D.B. and Haass, C. (1996). The role of APP processing and trafficking pathways in the formation of amyloid beta-protein. *Ann. N. Y. Acad. Sci.* **777**: 57-64. Review.

Selkoe, D.J. (2001). Alzheimer's disease results from the cerebral accumulation and cytotoxicity of amyloid β-protein. *Journal of Alzheimer's Disease* **3**: 75-80.

Selkoe, D. and Kopan, R. (2003). Notch and Presenilin: regulated intramembrane proteolysis links development and degeneration. *Annu. Rev. Neurosci.* **26:** 565-97. Review.

Seubert, P., Vigo-Pelfrey, C., Esch, F., Lee, M., Dovey, H., Davis, D., Sinha, S., Schlossmacher, M., Whaley, J., Swindlehurst, C., et al. (1992). Isolation and quantification of soluble Alzheimer's beta-peptide from biological fluids. *Nature* **359**: 325-27.

Seubert, P., Oltersdorf, T., Lee, M.G., Barbour, R., Blomquist, C., Davis, D.L., Bryant, K., Fritz, L.C., Galasko, D., Thal, L.J., et al. (1993). Secretion of beta-amyloid precursor protein cleaved at the amino terminus of the beta-amyloid peptide. *Nature* **361**: 260-63.

Sherrington, R., Rogaev, E.I., Liang, Y., Rogaeva, E.A., Levesque, G., Ikeda, M., Chi, H., Lin, C., Li, G., Holman, K., et al. (1995). Cloning of a gene bearing missense mutations in early-onset familial Alzheimer's disease. *Nature* **375**: 754-60.

Shi, Y. and Thomas, J.O. (1992). The transport of proteins into the nucleus requires the 70-kilodalton heat shock protein or its cytosolic cognate. *Mol. Cell Biol.* **12**: 2186-92.

Shiba, T., Kametaka, S., Kawasaki, M., Shibata, M., Waguri, S., Uchiyama, Y. and Wakatsuki, S. (2004). Insights into the phosphoregulation of beta-secretase sorting signal by the VHS domain of GGA1. *Traffic* **5**: 437-48.

Shimohama, S., Narita, M., Matsushima, H., Kimura, J., Kameyama, M., Hagiwara, M., Hidaka, H. and Taniguchi, T. (1993). Assessment of protein kinase C isozymes by two-site enzyme immunoassay in human brains and changes in Alzheimer's disease. *Neurology* **43**: 1407-13.

Shoji, M., Golde, T.E., Ghiso, J., Cheung, T.T., Estus, S., Shaffer, L.M., Cai, X.D., McKay, D.M., Tintner, R., Frangione, B., et al. (1992). Production of the Alzheimer amyloid beta protein by normal proteolytic processing. *Science* **258**: 126-29.

Silverman, M.A., Kaech, S., Jareb, M., Burack, M.A., Vogt, L., Sonderegger, P. and Banker, G. (2001). Sorting and directed transport of membrane proteins during development of hippocampal neurons in culture. *PNAS* **98:** 7051-57.

Simon, J.P., Ivanov, I.E., Adesnik, M. and Sabatini, D.D. (1996). The production of post-Golgi vesicles requires a protein kinase C-like molecule, but not its phosphorylating activity. *J. Cell Biol.* **135**: 355-70.

Simons, M., Ikonen, E., Tienari, P.J., Cid-Arregui, A., Monning, U., Beyreuther, K. and Dotti, C.G. (1995). Intracellular routing of human amyloid protein precursor: axonal delivery followed by transport to the dendrites. *J. Neurosci. Res.* **41**: 121-28.

Simons, M., de Strooper, B., Multhaup, G., Tienari, P.J., Dotti, C.G. and Beyreuther, K. (1996). Amyloidogenic processing of the human amyloid precursor protein in primary cultures of rat hippocampal neurons. *J. Neurosci.* **16**: 899-08.

Singer, W.D., Brown, H.A., Jiang, X. and Sternweis, P.C. (1996). Regulation of phospholipase D by protein kinase C is synergistic with ADP-ribosylation factor and independent of protein kinase activity. *J. Biol. Chem.* **271:** 4504-10.

Sisodia, S.S. (1992). Alzheimer's disease: perspectives for the new millennium. *J. Clin. Invest.* **104**: 1169-70. Review.

Sisodia, S.S. (2000). An Accomplice for γ-Secretase Brought into Focus. *Science* **289**: 2296-97.

Sisodia, S.S. (2002). Biomedicine. A cargo receptor mystery APParently solved? *Science* **295**: 805-07.

Sisodia, S.S. and Price, D.L. (1995). Role of the beta-amyloid protein in Alzheimer's disease. *FASEB J.* **9**: 366-70. Review.

Sisodia, S.S., Annaert, W., Kim, S.H. and De Strooper, B. (2001). Gamma-secretase: never more enigmatic. *Trends Neurosci.* **24**: S2-6. Review.

Skovronsky, D.M., Moore, D.B., Milla, M.E., Doms, R.W. and Lee, V.M. (2000). Protein kinase C-dependent alpha-secretase competes with beta-secretase for cleavage of amyloid-beta precursor protein in the trans-golgi network. *J. Biol. Chem.* **275**: 2568-75.

Slack, B.E., Nitsch, R.M., Livneh, E., Kunz, G.M. Jr, Breu, J., Eldar, H. and Wurtman, R.J. (1993). Regulation by phorbol esters of amyloid precursor protein release from Swiss 3T3 fibroblasts overexpressing protein kinase C alpha. *J. Biol. Chem.* **268**: 21097-01.

Slack, B.E., Ma, L.K. and Seah, C.C. (2001). Constitutive shedding of the amyloid precursor protein ectodomain is up-regulated by tumour necrosis factor-alpha converting enzyme. *Biochem. J.* **357**: 787-94.

Small, D.H., Nurcombe, V., Reed, G., Clarris, H., Moir, R., Beyreuther, K. and Masters, C.L. (1994). A heparin-binding domain in the amyloid protein precursor of Alzheimer's disease is involved in the regulation of neurite outgrowth. *J. Neurosci.* **14**: 2117-27.

Small, D.H., Williamson, T., Reed, G., Clarris, H., Beyreuther, K., Masters, C.L. and Nurcombe, V. (1996). The role of heparan sulfate proteoglycans in the pathogenesis of Alzheimer's disease. *Ann N Y Acad Sci.* **777**: 316-21. Review.

Small, D.H. and McLean, C.A. (1999). Alzheimer's disease and the amyloid β protein: what is the role of Amyloid? *J. Neurochem.* **73**: 443-49.

Smith, C.U.M. (1996). *Elements of Molecular Neurobiology*, 2nd edn. Chichester: John Wiley & Sons, 460-70.

Smith, R.P., Higuchi, D.A. and Broze, G.J. Jr. (1990). Platelet coagulation factor XIa-inhibitor, a form of Alzheimer amyloid precursor protein. *Science* **248**: 1126-28.

Soba, P., Eggert, S., Wagner, K., Zentgraf, H., Siehl, K., Kreger, S., Lower, A., Langer, A., Merdes, G., Paro, R., Masters, C.L., Muller, U., Kins, S. and Beyreuther, K. (2005). Homo- and heterodimerization of APP family members promotes intercellular adhesion. *EMBO J.* **24**: 3624-34.

Soh, J.W., Lee, Y.S. and Weinstein, I.B. (2003). Effects of regulatory domains of specific isoforms of protein kinase C on growth control and apoptosis in MCF-7 breast cancer cells. *J. Exp. Ther. Oncol.* **3**: 115-26.

Song, J.C., Rangachari, P.K. and Matthews, J.B. (2002). Opposing effects of PKCalpha and PKCepsilon on basolateral membrane dynamics in intestinal epithelia. *Am. J. Physiol. Cell Physiol.* **283**: C1548-56.

Soriano, S., Lu, D.C., Chandra, S., Pietrzik, C.U. and Koo, E.H. (2001). The amyloidogenic pathway of amyloid precursor protein (APP) is independent of its cleavage by caspases. *J. Biol. Chem.* **276**: 29045-50.

Spiegel, A.M. (1987). Signal transduction by guanine nucleotide binding proteins. *Mol. Cell Endocrinol.* **49**: 1-16. Review.

Spillantini, M.G., Murrell, J.R., Goedert, M., Farlow, M.R., Klug, A. and Ghetti, B. (1998). Mutation in the tau gene in familial multiple system tauopathy with presenile dementia. *Proc. Natl. Acad. Sci. USA* **95**: 7737-41.

Sprecher, C.A., Grant, F.J., Grimm, G., PJ, O.H., Norris, F., Norris, K. and Foster, D.C. (1993). Molecular cloning of cDNA for a human amyloid precursor protein homolog: evidence for a multigene family. *Biochemistry* **32**: 4481-86.

St. George-Hyslop, P.H. (1999). Molecular genetics of Alzheimer disease. *Semin. Neurol.* **19**: 371-83. Review.

Stalder, M., Phinney, A., Probst, A., Sommer, B., Staufenbiel, M. and Jucker, M. (1999). Association of microglia with amyloid plaques in brains of APP23 transgenic mice. *Am. J. Pathol.* **154**: 1673-84.

Stamer, K., Vogel, R., Thies, E., Mandelkow, E. and Mandelkow, E.M. (2002). Tau blocks traffic of organelles, neurofilaments and APP vesicles in neurons and enhances oxidative stress. *J. Cell Biol.* **156**: 1051-63.

Standen, C.L., Brownlees, J., Grierson, A.J., Kesavapany, S., Lau, K.-F., McLoughlin, D.M. and Miller, C.C.J. (2001). Phosphorylation of thr668 in the cytoplasmic domain of the Alzheimer's disease amyloid precursor protein by stress-activated protein kinase 1b (Jun N-terminal kinase-3). *J. Neurochem.* **76**: 316-20.

Steiner, H., Winkler, E., Edbauer, D., Prokop, S., Basset, G., Yamasaki, A., Kostka, M. and Haass, C. (2002). PEN-2 is an integral component of the gamma-secretase complex required for coordinated expression of presenilin and nicastrin. *J. Biol. Chem.* **277**: 39062-65.

Storey, E., Katz, M., Brickman, Y., Beyreuther, K. and Masters, C.L. (1999). Amyloid precursor protein of Alzheimer's disease: evidence for a stable, full-length, trans-membrane pool in primary neuronal cultures. *Eur. J. Neurosci.* **11**: 1779-88.

Strittmatter, S.M. and Fishman, M.C. (1991). The neuronal growth cone as a specialized transduction system. *Bioessays* **13**: 127-34. Review.

Strittmatter, S.M., Valenzuela, D., Kennedy, T.E., Neer, E.J. and Fishman, M.C. (1990). G0 is a major growth cone protein subject to regulation by GAP-43. *Nature* **344**: 836-41.

Struhl, G. and Adachi, A. (2000). Requirements for presenilin-dependent cleavage of notch and other transmembrane proteins. *Mol. Cell* **6**: 625-36.

Suzuki, T., Nairn, A.C., Gandy, S.E. and Greengard, P. (1992). Phosphorylation of Alzheimer amyloid precursor protein by protein kinase C. *Neuroscience* **48**: 755–61.

Suzuki, T., Oishi, M., Marshak, D.R., Czernik, A.J., Nairn, A.C. and Greengard, P. (1994). Cell cycle-dependent regulation of the phosphorylation and metabolism of the Alzheimer amyloid precursor protein. *EMBO J.* **13**: 1114-22.

Suzuki, T. ando, K., Isohara, T., Oishi, M., Lim, G.S., Satoh, Y., Wasco, W., Tanzi, R.E., Nairn, A.C., Greengard, P., Gandy, S.E. and Kirino, Y. (1997). Phosphorylation of Alzheimer beta-amyloid precursor-like proteins. *Biochemistry* **36**: 4643-49.

Sykes, C.M., Marks, D.F. and McKinley, J.M. (2001). Alzheimer disease and associated disorders: project funding opportunities within the European community. *Alzheimer Dis. Assoc. Disord.* **15**: 102-05.

Tagawa, K., Yazaki, M., Kinouchi, T., Maruyama, K., Sorimachi, H., Tsuchiya, T., Suzuki, K. and Ishiura, S. (1993). Amyloid precursor protein is found in lysosomes. *Gerontology* **39** S**1**: 24-29.

Tanaka, S., Shiojiri, S., Takahashi, Y., Kitaguchi, N., Ito, H., Kameyama, M., Kimura, J., Nakamura, S. and Ueda, K. (1989). Tissue-specific expression of three types of beta-protein precursor mRNA: enhancement of protease inhibitor-harboring types in Alzheimer's disease brain. *Biochem. Biophys. Res. Commun.* **165**: 1406-14.

Tang, B.L. (2005). Alzheimer's disease: channeling APP to non-amyloidogenic processing. *Biochem. Biophys. Res. Commun.* **331**: 375-78. Review.

Tanimukai, S., Hasegawa, H., Nakai, M., Yagi, K., Hirai, M., Saito, N., Taniguchi, T., Terashima, A., Yasuda, M., Kawamata, T. and Tanaka, C. (2002). Nanomolar amyloid beta protein activates a specific PKC isoform mediating phosphorylation of MARCKS in Neuro2A cells. *Neuroreport* **13**: 549-53.

Tanzi, R.E., Gusella, J.F., Watkins, P.C., Bruns, G.A., St George-Hyslop, P., Van Keuren, M.L., Patterson, D., Pagan, S., Kurnit, D.M. and Neve, R.L. (1987). Amyloid beta protein gene: cDNA, mRNA distribution and genetic linkage near the Alzheimer locus. *Science* **235**: 880-84.

Tanzi, R.E., McClatchey, A.I., Lamperti, E.D., Villa-Komaroff, L., Gusella, J.F. and Neve, R.L. (1988). Protease inhibitor domain encoded by an amyloid protein precursor mRNA associated with Alzheimer's disease. *Nature* **331**: 528-30.

Tanzi, R.E., Wenniger, J.J. and Hyman, B.T. (1993). Cellular specificity and regional distribution of amyloid beta protein precursor alternative transcripts are unaltered in Alzheimer hippocampal formation. *Brain Res. Mol. Brain Res.* **18**: 246-52.

Tarr, P.E., Contursi, C., Roncarati, R., Noviello, C., Ghersi, E., Scheinfeld, M.H., Zambrano, N., Russo, T. and D'Adamio, L. (2002). Evidence for a role of the nerve growth factor receptor TrkA in tyrosine phosphorylation and processing of beta-APP. *Biochem. Biophys. Res. Commun.* **295**: 324-29.

Taru, H., Yoshikawa, K. and Suzuki, T. (2004). Suppression of the caspase cleavage of beta-amyloid precursor protein by its cytoplasmic phosphorylation. *FEBS Lett.* **567**: 248-52.

Telese, F., Bruni, P., Donizetti, A., Gianni, D., D'Ambrosio, C., Scaloni, A., Zambrano, N., Rosenfeld, M.G. and Russo, T. (2005). Transcription regulation by the adaptor protein Fe65 and the nucleosome assembly factor SET. *EMBO Rep.* **6**: 77-82.

Terry, R.D., Gonatas, H.K. and Weiss, M. (1964). Ultrastructural studies in Alzheimer's presenile dementia. *Am. J. Pathol.* **44**: 269-97.

Thompson, L.A., Bronson, J.J. and Zusi, F.C. (2005). Progress in the discovery of BACE inhibitors. *Curr. Pharm. Des.* **11**: 3383-04. Review.

Tian, Q. and Wang, J. (2002). Role of serine/threonine protein phosphatase in Alzheimer's disease. *Neurosignals.* **11**: 262-69. Review.

Tienari, P.J., De Strooper, B., Ikonen, E., Ida, N., Simons, M., Masters, C.L., Dotti, C.G. and Beyreuther, K. (1996a). Neuronal sorting and processing of amyloid precursor protein: implications for Alzheimer's disease. *Cold Spring Harb. Symp. Quant. Biol.* **61**: 575-85.

Tienari, P.J., De Strooper, B., Ikonen, E., Simons, M., Weidemann, A., Czech, C., Hartmann, T., Ida, N., Multhaup, G., Masters, C.L., Van Leuven, F., Beyreuther, K. and Dotti, C.G. (1996b). The beta-amyloid domain is essential for axonal sorting of amyloid precursor protein. *EMBO J.* **15**: 5218-29.

Thinakaran, G., Slunt, H.H. and Sisodia, S.S. (1995). Novel regulation of chondroitin sulfate glycosaminoglycan modification of amyloid precursor protein and its homologue, APLP2. *J. Biol. Chem.* **270**: 16522-25.

Thinakaran, G., Borchelt, D.R., Lee, M.K., Slunt, H.H., Spitzer, L., Kim, G., Ratovitsky, T., Davenport, F., Nordstedt, C., Seeger, M., Hardy, J., Levey, A.I., Gandy, S.E., Jenkins, N.A., Copeland, N.G., Price, D.L. and Sisodia, S.S. (1996). Endoproteolysis of presenilin 1 and accumulation of processed derivatives in vivo. *Neuron* **17**: 181-90.

Tomimoto, H., Akiguchi, I., Wakita, H., Nakamura, S. and Kimura, J. (1995). Ultrastructural localization of amyloid protein precursor in the normal and postischemic gerbil brain. *Brain Res.* **672**: 187-95.

Tomita, S., Kirino, Y. and Suzuki, T. (1998). Cleavage of Alzheimer's amyloid precursor protein (APP) by secretases occurs after O-glycosylation of APP in the protein secretory pathway. Identification of intracellular compartments in which APP cleavage occurs without using toxic agents that interfere with protein metabolism. *J. Biol. Chem.* **273**: 6277-84.

Torroja, L., Chu, H., Kotovsky, I. and White, K. (1999a). Neuronal overexpression of APPL, the Drosophila homologue of the amyloid precursor protein (APP), disrupts axonal transport. *Curr. Biol.* **9:** 489-92.

Torroja, L., Packard, M., Gorczyca, M., White, K. and Budnik, V. (1999b). The Drosophila beta-amyloid precursor protein homolog promotes synapse differentiation at the neuromuscular junction. *J. Neurosci.* **19**: 7793-03.

Tousseyn, T., Serneels, L., Thathiah, A., jorissen, E., Reiss, K., Nyabi, O., Maes, E., Snellinx, A., Blobel, C., Weskamp, G., Annaert, W., Sciot, R., Saftig, P., De Strooper, B. and Hartmann, D. (2005). Sequential ectodomain shedding and intramembrane proteolysis of ADAM10 results in a soluble alpha-secretase and abeta degrading enzyme and the nuclear translocation of the ADAM10 intracellular domain. 7th International Conference AD/PD, Sorrento, Italy. (OR)-102.

Trejo, J., Massamiri, T., Deng, T., Dewji, N.N., Bayney, R.M. and Brown, J.H. (1994). A direct role for protein kinase C and the transcription factor Jun/AP-1 in the regulation of the Alzheimer's beta-amyloid precursor protein gene. *J. Biol. Chem.* **269**: 21682-90.

Turner, P.R., O'Connor, K., Tate, W.P. and Abraham, W.C. (2003). Roles of amyloid precursor protein and its fragments in regulating neural activity, plasticity and memory. *Prog. Neurobiol.* **70**: 1-32. Review.

Uberall, F., Kampfer, S., Doppler, W. and Grunicke, H.H. (1994). Activation of c-fos expression by transforming Ha-ras in HC11 mouse mammary epithelial cells is PKC-dependent and mediated by the serum response element. *Cell Signal.* **6**: 285-97.

Ueda, K., Cole, G., Sundsmo, M., Katzman, R. and Saitoh, T. (1989). Decreased adhesiveness of Alzheimer's disease fibroblasts: is amyloid beta-protein precursor involved? *Ann. Neurol.* **25**: 246-51.

Van Nostrand, W.E. and Cunningham, D.D. (1987). Purification of protease nexin II from human fibroblasts. *J. Biol. Chem.* **262**: 8508-14.

Vassar, R., Bennett, B.D., Babu-Khan, S., Kahn, S., Mendiaz, E.A., Denis, P., Teplow, D.B., Ross, S., Amarante, P., Loeloff, R., Luo, Y., Fisher, S., Fuller, J., Edenson, S., Lile, J., Jarosinski, M.A., Biere, A.L., Curran, E., Burgess, T., Louis, J.C., Collins, F., Treanor, J., Rogers, G. and Citron, M. (1999). Beta-secretase cleavage of Alzheimer's amyloid precursor protein by the transmembrane aspartic protease BACE. *Science* **286**: 735-41.

Vassar, R. (2004). BACE1: the beta-secretase enzyme in Alzheimer's disease. *J. Mol. Neurosci.* **23**: 105-14. Review.

Vijayan, S., El-Akkad, E., Grundke-Iqbal, I. and Iqbal, K. (2001). A pool of beta-tubulin is hyperphosphorylated at serine residues in Alzheimer disease brain. *FEBS Lett.* **509**: 375-81.

von Koch, C.S., Zheng, H., Chen, H., Trumbauer, M., Thinakaran, G., van der Ploeg, L.H., Price, D.L. and Sisodia, S.S. (1997). Generation of APLP2 KO mice and early postnatal lethality in APLP2/APP double KO mice. *Neurobiol. Aging* **18**: 661-69.

von Rotz, R.C., Kohli, B.M., Bosset, J., Meier, M., Suzuki, T., Nitsch, R.M., Konietzko, U. (2004). The APP intracellular domain forms nuclear multiprotein complexes and regulates the transcription of its own precursor. *J. Cell Sci.* **117**: 4435-48.

Waddell, S. (2003). Protein phosphatase 1 and memory: practice makes PP1 imperfect? *Trends Neurosci.* **26**: 117-19. Review.

Wagey, R.T. and Krieger, C. (1998). Abnormalities of protein kinases in neurodegenerative diseases. *Prog. Drug Res.* **51**: 133-83. Review.

Wagner, S.L., Siegel, R.S., Vedvick, T.S., Raschke, W.C. and van Nostrand, W.E. (1992). High level expression, purification, and characterization of the Kunitz-type protease inhibitor domain of protease nexin-2/amyloid beta-protein precursor. *Biochem. Biophys. Res.* **186**: 1138-45.

Wahle, T., Prager, K., Raffler, N., Haass, C., Famulok, M. and Walter, J. (2005). GGA proteins regulate retrograde transport of BACE1 from endosomes to the trans-Golgi network. *Mol. Cell Neurosci.* **29**: 453-61.

Walter, J., Capell, A., Grunberg, J., Pesold, B., Schindzielorz, A., Prior, R., Podlisny, M.B., Fraser, P., Hyslop, P.S., Selkoe, D.J. and Haass, C. (1996). The Alzheimer's disease-associated presenilins are differentially phosphorylated proteins located predominantly within the endoplasmic reticulum. *Mol. Med.* **2**: 673-91.

Walter, J., Capell, A., Hung, A.Y., Langen, H., Schnolzer, M., Thinakaran, G., Sisodia, S.S., Selkoe, D.J. and Haass, C. (1997). Ectodomain phosphorylation of beta-amyloid precursor protein at two distinct cellular locations. *J. Biol. Chem.* **272**: 1896-03.

Walter, J., Grunberg, J., Schindzielorz, A. and Haass, C. (1998). Proteolytic fragments of the Alzheimer's disease associated presenilins-1 and -2 are phosphorylated in vivo by distinct cellular mechanisms. *Biochemistry* **37:** 5961-67.

Walter, J., Schindzielorz, A., Grunberg, J. and Haass, C. (1999). Phosphorylation of presenilin-2 regulates its cleavage by caspases and retards progression of apoptosis. *Proc. Natl. Acad. Sci. USA* **96:** 1391-96.

Walter, J., Schindzielorz, A., Hartung, B. and Haass, C. (2000). Phosphorylation of the beta-amyloid precursor protein at the cell surface by ectocasein kinases 1 and 2. *J. Biol. Chem.* **275**: 23523-29.

Walter, J., Fluhrer, R., Hartung, B., Willem, M., Kaether, C., Capell, A., Lammich, S., Multhaup, G. and Haass, C. (2001). Phosphorylation regulates intracellular trafficking of beta-secretase. *J. Biol. Chem.* **276**: 14634-41.

Wang, H.Y., Pisano, M.R. and Friedman, E. (1994). Attenuated protein kinase C activity and translocation in Alzheimer's disease brain. *Neurobiol. Aging* **15**: 293-98.

Wasco, W., Gurubhagavatula, S., Paradis, M.D., Romano, D.M., Sisodia, S.S., Hyman, B.T., Neve, R.L. and Tanzi, R.E. (1993). Isolation and characterization of APLP2 encoding a homologue of the Alzheimer's associated amyloid beta protein precursor. *Nat. Genet.* **5**: 95-00.

Watanabe, T., Sukegawa, J., Sukegawa, I., Tomita, S., Iijima, K., Oguchi, S., Suzuki, T., Nairn, A.C. and Greengard, P. (1999). A 127-kDa protein (UV-DDB) binds to the cytoplasmic domain of the Alzheimer's amyloid precursor protein. *J. Neurochem.* **72**: 549-56.

Weggen, S., Eriksen, J.L., Sagi, S.A., Pietrzik, C.U., Golde, T.E. and Koo, E.H. (2003). Abeta42-lowering nonsteroidal anti-inflammatory drugs preserve intramembrane cleavage of the amyloid precursor protein (APP) and ErbB-4 receptor and signaling through the APP intracellular domain. *J. Biol. Chem.* **278**: 30748-54.

Weidemann, A., Konig, G., Bunke, D., Fischer, P., Salbaum, J.M., Masters, C.L. and Beyreuther, K. (1989). Identification, biogenesis and localization of precursors of Alzheimer's disease A4 amyloid protein. *Cell* **57**: 115-26.

Weidemann, A., Paliga, K., Durrwang, U., Czech, C., Evin, G., Masters, C.L. and Beyreuther, K. (1997). Formation of stable complexes between two Alzheimer's disease gene products: presenilin-2 and beta-amyloid precursor protein. *Nat. Med.* **3**: 328-32.

Weidemann, A., Paliga, K., Durrwang, U., Reinhard, F.B., Schuckert, O., Evin, G. and Masters, C.L. (1999). Proteolytic processing of the Alzheimer's disease amyloid precursor protein within its cytoplasmic domain by caspase-like proteases. *J. Biol. Chem.* **274**: 5823-29.

Wera, S. and Hemmings, B.A. (1995). Serine/threonine protein phosphatases. *Biochem. J.* **311**: 17-29. Review.

Williams, B.R. (2001). "Geriatric dementias". *In:* Koda Kimble, M.A. and Young, L.Y. *Eds.* Applied therapeutics: the clinical use of drugs, 7th edn. Lippincott: Williams & Wilkins, 98.1-98.9.

Williams, M.A. and Fukuda, M. (1990). Accumulation of membrane glycoproteins in lysosomes requires a tyrosine residue at a particular position in the cytoplasmic tail. *J. Cell Biol.* **111**: 955-66.

Williamson, T.G., Mok, S.S., Henry, A., Cappai, R., Lander, A.D., Nurcombe, V., Beyreuther, K., Masters, C.L. and Small, D.H. (1996). Secreted glypican binds to the amyloid precursor protein of Alzheimer's disease (APP) and inhibits APP-induced neurite outgrowth. *J Biol Chem.* **271**: 31215-21.

Wilson, C.A., Doms, R.W., Zheng, H. and Lee, V.M. (2002). Presenilins are not required for A beta 42 production in the early secretory pathway. *Nat. Neurosci.* **5**: 849-55.

Wisniewski, T. and Frangione, B. (2005). Immunological and anti-chaperone therapeutic approaches for Alzheimer disease. *Brain Pathol.* **15**: 72-77. Review.

Wisniewski, T., Ghiso, J. and Frangione, B. (1991). Peptides homologous to the amyloid protein of Alzheimer's disease containing a glutamine for glutamic acid substitution have accelerated amyloid fibril formation. *Biochem. Biophys. Res. Commun.* **179**: 1247-54.

Wolfe, M.S. (2001). gamma-Secretase inhibitors as molecular probes of presenilin function. *J. Mol. Neurosci.* **17**: 199-04. Review.

Wolfe, M.S. and Haass, C. (2001). The Role of presenilins in gamma-secretase activity. *J. Biol. Chem.* **276**: 5413-16. Review.

Wolozin, B., Kellman, W., Ruosseau, P., Celesia, G.G. and Siegel, G. (2000). Decreased prevalence of Alzheimer's disease associated with 3-hydroxy-3-methyglutaryl coenzyme A reductase inhibitors. *Arch Neurol.* **57**: 1439-43.

Yamatsuji, T., Matsui, T., Okamoto, T., Komatsuzaki, K., Takeda, S., Fukumoto, H., Iwatsubo, T., Suzuki, N., Asami-Odaka, A., Ireland, S., Kinane, T.B., Giambarella, U. and Nishimoto, I. (1996). G protein-mediated neuronal DNA fragmentation induced by familial Alzheimer's disease-associated mutants of APP. *Science.* **272**: 1349-52.

Yamazaki, T., Selkoe, D.J. and Koo, E.H. (1995). Trafficking of cell surface beta-amyloid precursor protein: retrograde and transcytotic transport in cultured neurons. *J. Cell Biol.* **129**: 431-42.

Yamazaki, T., Koo, E.H. and Selkoe, D.J. (1996). Trafficking of cell-surface amyloid beta-protein precursor. II. Endocytosis, recycling and lysosomal targeting detected by immunolocalization. *J Cell Sci.* **109**: 999-08.

Yan, R., Bienkowski, M.J., Shuck, M.E., Miao, H., Tory, M.C., Pauley, A.M., Brashier, J.R., Stratman, N.C., Mathews, W.R., Buhl, A.E., Carter, D.B., Tomasselli, A.G., Parodi, L.A., Heinrikson, R.L. and Gurney, M.E. (1999a). Membrane-anchored aspartyl protease with Alzheimer's disease beta-secretase activity. *Nature.* **402**: 533-37.

Yan, Z., Hsieh-Wilson, L., Feng, J., Tomizawa, K., Allen, P.B., Fienberg, A.A., Nairn, A.C. and Greengard, P. (1999b). Protein phosphatase 1 modulation of neostriatal AMPA channels: regulation by DARPP-32 and spinophilin. *Nat. Neurosci.* **2**: 13-17.

Yan, R., Munzner, J.B., Shuck, M.E. and Bienkowski, M.J. (2001). BACE2 functions as an alternative alpha-secretase in cells. *J Biol Chem.* **276**: 34019-27.

Yang, Y., Turner, R.S. and Gaut, J.R. (1998). The chaperone BiP/GRP78 binds to amyloid precursor protein and decreases Abeta40 and Abeta42 secretion. *J. Biol. Chem.* **273**: 25552-55.

Yeon, S.W., Jung, M.W., Ha, M.J., Kim, S.U., Huh, K., Savage, M.J., Masliah, E. and Mook-Jung, I. (2001). Blockade of PKC epsilon activation attenuates phorbol ester-induced increase of alpha-secretase-derived secreted form of amyloid precursor protein, *Biochem. Biophys. Res. Commun.* **280:** 782-87.

Yoon, S.Y., Choi, J.E., Yoon, J.H., Huh, J.W. and Kim, D.H. (2006). BACE inhibitor reduces APP-beta-C-terminal fragment accumulation in axonal swellings of okadaic acid-induced neurodegeneration. *Neurobiol Dis.* **22:** 435-44.

Yoshikawa, K., Aizawa, T. and Hayashi, Y. (1992). Degeneration in vitro of post-mitotic neurons overexpressing the Alzheimer amyloid protein precursor. *Nature.* **359**: 64-67.

Younkin, S.G. (1998). The role of Abeta 42 in Alzheimer's disease. *J. Physiol. Paris.* **92**: 289-92. Review.

Yu, G., Nishimura, M., Arawaka, S., Levitan, D., Zhang, L., Tandon, A., Song, Y.Q., Rogaeva, E., Chen, F., Kawarai, T., Supala, A., Levesque, L., Yu, H., Yang, D.S., Holmes, E., Milman, P., Liang, Y., Zhang, D.M., Xu, D.H., Sato, C., Rogaev, E., Smith, M., Janus, C., Zhang, Y., Aebersold, R., Farrer, L.S., Sorbi, S., Bruni, A., Fraser, P. and St George-Hyslop, P. (2000). Nicastrin modulates presenilin-mediated notch/glp-1 signal transduction and betaAPP processing. *Nature.* **407**: 48-54.

Xia, W. (2001). Amyloid metabolism and secretases in Alzheimer's disease. *Curr. Neurol. Neurosci. Rep.* **1**: 422-27. Review.

Xia, W., Zhang, J., Perez, R., Koo, E.H. and Selkoe, D.J. (1997). Interaction between amyloid precursor protein and presenilins in mammalian cells: implications for the pathogenesis of Alzheimer disease. *Proc. Natl. Acad. Sci. U. S. A.* **94**: 8208-13.

Xia, W., Zhang, J., Ostaszewski, B.L., Kimberly, W.T., Seubert, P., Koo, E.H., Shen, J. and Selkoe, D.J. (1998). Presenilin 1 regulates the processing of beta-amyloid precursor protein C-terminal fragments and the generation of amyloid beta-protein in endoplasmic reticulum and Golgi. *Biochemistry.* **37**: 16465-71.

Xu, H., Greengard, P. and Gandy, S. (1995). Regulated formation of Golgi secretory vesicles containing Alzheimer beta-amyloid precursor protein. *J. Biol. Chem.* **270**: 23243-45.

Xu, H., Sweeney, D., Wang, R., Thinakaran, G., Lo, A.C., Sisodia, S.S., Greengard, P. and Gandy, S. (1997). Generation of Alzheimer beta-amyloid protein in the trans-Golgi network in the apparent absence of vesicle formation. *Proc. Natl. Acad. Sci. USA* **94**: 3748-52.

Xu, M., Lai, M.T., Huang, Q., DiMuzio-Mower, J., Castro, J.L., Harrison, T., Nadin, A., Neduvelil, J.G., Shearman, M.S., Shafer, J.A., Gardell, S.J. and Li, Y.M. (2002). Gamma-Secretase: characterization and implication for Alzheimer disease therapy. *Neurobiol. Aging.* **23**: 1023-30.

Zambrano, N., Bruni, P., Minopoli, G., Mosca, R., Molino, D., Russo, C., Schettini, G., Sudol, M. and Russo, T. (2001). The beta-amyloid precursor protein APP is tyrosine-phosphorylated in cells expressing a constitutively active form of the Abl protoncogene. *J. Biol. Chem.* **276**: 19787-92.

Zambrano, N., Gianni, D., Bruni, P., Passaro, F., Telese, F. and Russo, T. (2004). Fe65 is not involved in the platelet-derived growth factor-induced processing of Alzheimer's amyloid precursor protein, which activates its caspase-directed cleavage. *J. Biol. Chem.* **279**: 16161-69.

Zhang, C., Lambert, M.P., Bunch, C., Barber, K., Wade, W.S., Krafft, G.A. and Klein, W.L. (1994). Focal adhesion kinase expressed by nerve cell lines shows increased tyrosine phosphorylation in response to Alzheimer's Abeta peptide. *J. Biol. Chem.* **269**: 25247-50.

Zhang, W., Espinoza, D., Hines, V., Innis, M., Mehta, P. and Miller, D.L. (1997). Characterization of beta-amyloid peptide precursor processing by the yeast Yap3 and Mkc7 proteases. *Biochi.m Biophys. Acta* **1359:** 110-22.

Zhang, Y., Yang, Y., Yeh, S. and Chang, C. (2004). ARA67/PAT1 functions as a repressor to suppress androgen receptor transactivation. *Mol. Cell Biol.* **24**: 1044-57.

Zhang, Z., Kolls, J.K., Oliver, P., Good, D., Schwarzenberger, P.O., Joshi, M.S., Ponthier, J.L. and Lancaster, J.R. Jr. (2000). Activation of tumor necrosis factor-alpha-converting enzyme-mediated ectodomain shedding by nitric oxide. *J. Biol. Chem.* **275**: 15839-44.

Zheng, B., Kimberly, W.T. and Selkoe, D.J. (2003). Temporal Regulation of the endogenous APP intracellular domain (AICD) in primary neurons. *Soc. Neurosci. Abst. 33,* Prog. Number 336.1.

Zheng, H., Jiang, M., Trumbauer, M.E., Hopkins, R., Sirinathsinghji, D.J., Stevens, K.A., Conner, M.W., Slunt, H.H., Sisodia, S.S., Chen, H.Y. and Van der Ploeg, L.H. (1996). Mice deficient for the amyloid precursor protein gene. *Ann. N. Y. Acad. Sci.* **777**: 421-26.

Zheng, P., Eastman, J., Vande Pol, S. and Pimplikar, S.W. (1998). PAT1, a microtubule-interacting protein, recognizes the basolateral sorting signal of amyloid precursor protein. *Proc. Natl. Acad. Sci. U.S.A.* **95**: 14745-50.

Zhu, G., Wang, D., Lin, Y.H., McMahon, T., Koo, E.H. and Messing, R.O. (2001). Protein kinase C epsilon suppresses Abeta production and promotes activation of alpha-secretase, *Biochem. Biophys. Res. Commun.* **285:** 997-1006.

Zhu, X., Smith, M.A., Perry, G. and Aliev, G. (2004). Mitochondrial failures in Alzheimer's disease. *Am. J. Alzheimers Dis. Other Demen.* **19:** 345-52. Review.

APPENDIX

APPENDIX I – SOLUTIONS

DNA Manipulation

➢ Solutions for bacterial cultures, transformation and DNA extraction:

- SOB (Fluka) 25.5 g/L

- SOC

- SOB	49 ml
- 1 M Glucose stock solution	1 ml

- Competent cells solutions

Solution I (1 L)**:**

- $MnCl_2.4H_2O$	9.9 g
- $CaCl_2.2H_2O$	1.5 g
- Glycerol	150 g
- KHAc	30 ml (1 M)

adjust pH to 5.8 with HAc, filter through a 0.2 μm filter and store at 4 ºC.

Solution II (1 L)**:**

- MOPS (0.5 M, pH 6.8)	20 ml
- RbCl	1.2 g
- $CaCl_2.2H_2O$	11 g
- Glycerol	150 g

filter through a 0.2 μm filter and store at 4 ºC.

- LB (Luria-Broth) medium (Sigma) 20 g/L

- LB agar plates

For a final volume of 1 L, to 950 ml of LB medium add 12 g of agar. Mix until the solutes have dissolved. Adjust the volume of the solution to 1 litre with LB medium and sterilize by autoclaving. When at cooling pour into bacterial culture plates (~ 20 ml/ 100 mm plate). After solidify store inverted at 4 ºC.

- 100 mg/ml Antibiotics stock solutions (Ampicilin or Kanamycin) (1000x)

Dissolve 1 g of the antibiotic in 10 ml of deionized H_2O. Mix until the solutes have dissolved, filter through a 0.2 μm filter, aliquot and store at -20 ºC.

- DNA extraction ('mini and maxi preps')

Solution I ('resuspension'):

- Glucose	50 mM
- Tris.Cl (pH 8.0)	25 mM
- EDTA (pH 8.0)	10 mM

Solution II ('alkaline lysis'):

- NaOH	0.2 N
- SDS	1%

Solution III ('neutralization'):

- 5 M Potassium acetate	3 M
- Glacial acetic acid	2 M

- 50X TAE solution (1 L)

- Tris base	242 g
- Glacial acetic acid	57.1 ml
- EDTA (pH 8.0)	100 ml

- TE buffer, pH 7.5

- Tris-HCl (pH 7.5)	10 mM
- EDTA (pH 8.0)	1 mM

- RNase stock solution 10 mg/ml

- 10 mM dNTPs solution (100 µl)

- dATP	10 µl
- dTTP	10 µl
- dCTP	10 µl
- dGTP	10 µl
- H_2O	60 µl

aliquot and keep at -20 ºC.

Cell Culture and Rat Cortex Samples

➢ Cells seeding, maintenance and experiments:

- DMEM medium (COS-7 cells)

For a final volume of 1 L, dissolve one pack of DMEM powder (with L-glutamine and 4500 mg glucose/L, Sigma Aldrich) in deionised H_2O and add:

- $NaHCO_3$ (Sigma-Aldrich) 3.7 g

adjust to pH 7.4. Sterilize by filtering through a 0.2 µm filter and store at 4 ºC.

- Complete DMEM (COS-7 cells)

For a final volume of 1 L, when preparing DMEM medium adjust to pH 7.4 and before sterilizing add:

- Fetal Bovine Serum (FBS) (Gibco BRL, Invitrogen) 100 ml (10% v/v)

Notes: FBS is heat-inactivated for 30 min at 45 ºC. For cells maintenance, prior to pH adjustment add 100 U/ml penicillin and 100 mg/ml streptomycin [10 ml Streptomycin/ Penicilin/ Amphotericin solution (Gibco BRL, Invitrogen)].

DMEM Components:	**(g/L)**
L-Arginine•HCl	0.084
L-Cystine•2HCl	0.0626
L-Glutamine	0.584
Glycine	0.03
L-Histidine•HCl• H2O	0.042
L-Isoleucine	0.105
L-Leucine	0.105
L-Lysine•HCl	0.146
L-Methionine	0.03
L-Phenylalanine	0.066
L-Serine	0.042
L-Threonine	0.095
L-Tryptophan	0.016
L-Tyrosine 2Na•2H2O	0.10379
L-Valine	0.094
Choline Chloride	0.004
Folic Acid	0.004
myo-Inositol	0.0072
Niacinamide	0.004
D-Pantothenic Acid hemicalcium	0.004
Pyridoxal•HCl	0.004
Riboflavin	0.0004
Thiamine•HCl	0.004
Calcium Chloride [Anhydrous]	0.2
Ferric Nitrate•9H2O	0.0001
Magnesium Sulfate [Anhydrous]	0.09767
Potassium Chloride	0.4
Sodium Chloride	6.4
Sodium Phosphate Monobasic [Anhydrous]	0.109
Glucose	4.5
Phenol Red•Na	0.0159

- PBS (1x)

For a final volume of 500 ml, dissolve one pack of BupH Modified Dulbecco's Phosphate Buffered Saline Pack (Pierce) in deionised H_2O. Final composition:

- Sodium Phosphate	8 mM
- Potassium Phosphate	2 mM
- NaCl	140 mM
- KCl	10 mM

Sterilize by filtering through a 0.2 μm filter and store at 4 ºC.

- Complete Neurobasal medium (primary neuronal cultures)

This serum-free medium (Neurobasal; Gibco, BRL) is supplemented with:

- B27 supplement (Gibco, BRL)	2%
- L-glutamine (Gibco, BRL)	0.5 mM
- Gentamicine (Gibco, BRL)	60 μg/ml
- Phenol Red (Sigma Aldrich, Portugal)	0.001%

adjust to pH 7.4. Sterilize by filtering through a 0.2 μm filter and store at 4 ºC.

- Hank's balanced salt solution (primary neuronal cultures)

This salt solution is prepared with deionised H_2O. Final composition:

- NaCl	137 mM
- KCl	5.36 mM
- KH_2PO_4	0.44 mM
- $Na_2HPO_42H_2O$	0.34 mM
- $NaHCO_3$	4.16 mM
- Glucose	5 mM
- Sodium pyruvate	1 mM
- HEPES	10 mM

adjust to pH 7.4. Sterilize by filtering through a 0.2 μm filter and store at 4 ºC.

➢ Cells fixation and Imunocytochemistry:

- 1 mg/ml Poly-L-ornithine solution (10x) (COS-7 cells)

To a final volume of 100 ml, dissolve in deionised H_2O 100 mg of poly-L-ornithine (Sigma-Aldrich, Portugal).

- 10 mg/ml Poly-D-lysine stock (100x) (neuronal cells)

To a final volume of 10 ml, dissolve in deionised H_2O 100 mg of poly-D-lysine (Sigma-Aldrich).

- Borate buffer (neuronal cells)

To a final volume of 1 L, dissolve in deionised H_2O 9.28 g of boric acid (Sigma-Aldrich). Adjust to pH 8.2, sterilize by filtering through a 0.2 μm filter, and store at 4 ºC.

- Poly-D-lysine solution (neuronal cells)

To a final volume of 100 ml, dilute 1 ml of the 10 mg/ml poly-D-lysine stock solution in borate buffer.

- 4% Paraformaldehyde Fixative solution

To a final volume of 100 ml, to 25 ml deionised H_2O add 4 g of paraformaldehyde. Dissolve by heating the mixture at 58 ºC while stirring. Add 1-2 drops of 1 M NaOH to clarify the solution and filter (0.2 μm). Add 50 ml of 2X PBS and adjust the volume to 100 ml with deionised H_2O.

➢ Rat Cortex Lysates:

- 0.32 M sucrose and 10 mM HEPES solution (rat cortex lysates)

For a final volume of 1 L, dissolve in deionised H_2O:

- Sucrose	109.54 g

- HEPES 2.60 g

adjust to pH 7.4. Sterilize by filtering through a 0.2 μm filter and store at 4 ºC.

Proteins Manipulation

➢ SDS-PAGE:

- LGB (Lower gel buffer) (4x) (1 L)

- Tris 181.65 g
- SDS 4 g

Shake until the solutes have dissolved. Adjust the pH to 8.9 with HCl and adjust the volume to 1 L with deionised H_2O.

- UGB (Upper gel buffer) (5x)

Per litre, to 900 ml of deionised H_2O add 75.7 g of Tris base. Shake until the solute has dissolved. Adjust the pH to 6.8 with HCl and adjust the volume to 1 L with deionised H_2O.

- 30% Acrylamide / 0.8% Bisacrylamide solution

Per 100 ml, to 70 ml of deionised H_2O add:

- Acrylamide 29.2 g
- Bisacrylamide 0.8 g

Shake until the solutes have dissolved. Adjust the volume to 100 ml with deionised H_2O. Filter through a 0.2 μm filter and store at 4 ºC.

- 10% APS (ammonium persulfate)

In 10 ml of deionised H_2O dissolve 1 g of APS. Note: prepare fresh before use.

- 10% SDS (sodium dodecilsulfate)

In 10 ml of deionised H_2O dissolve 1 g of SDS.

- Loading (sample) gel buffer (4x) (10 ml)

- 1M Tris solution (pH 6.8) 2.5 ml (250 mM)
- SDS 0.8 g (8%)
- Glicerol 4 ml (40%)
- β-Mercaptoetanol 2 ml (2%)
- Bromofenol blue 1 mg (0.01%)

Adjust the volume to 10 ml with deionised H_2O. Store in darkness at RT.

- 1 M Tris (pH 6.8) solution

For a final volume of 250 ml, dissolve 30.3 g of Tris base in 150 ml of deionised H_2O, adjust pH to 6.8, and adjust final volume to 250 ml.

- Running buffer (10x) (1 L)

- Tris	30.3 g (250 mM)
- Glycine	144.2 g (2.5 M)
- SDS	10 g (1%)

Dissolve in deionised H_2O, adjust pH to 8.3, and adjust volume to 1 litre.

15 cm gels:

- Resolving (lower) gel solution (60 ml)	**7.5%**	**12%**	**6.5%**
- H_2O	29.25 ml	20.7 ml	31.25 ml
- 30% Acryl/0.8% Bisacryl solution	15.0 ml	24.0 ml	13.0 ml
- LGB (4x)	15.0 ml	15.0 ml	15.0 ml
- 10% APS	300 µl	300 µl	300 µl
- TEMED	30 µl	30 µl	30 µl

- Stacking (upper) gel solution (20 ml)	**3.5%**
- H_2O	13.2 ml
- 30% Acryl/0.8% Bisacryl solution	2.4 ml
- UGB (5x)	4.0 ml
- 10% SDS	200 µl
- 10% APS	200 µl
- TEMED	20 µl

➢ Immunoblotting solutions:

- Electrotransfer buffer (1x)

Per litre, to 700 ml of deionised H_2O add:

- Tris	3.03 g (25 mM)
- Glycine	14.41 g (192 mM)

Mix until solutes dissolution. Adjust the pH to 8.3 with HCl and adjust the volume to 800 ml with deionised H_2O. Just prior to use add 200 ml of methanol (20%).

- TBS (Tris Buffered Saline) (10x)

Per litre, to 700 ml of deionised H_2O add

- Tris	12.11 g (10 mM)
- NaCl	87.66 g (150 mM)

Adjust the pH to 8.0 with HCl and adjust the volume to 1 L with deionised H_2O.

- TBS-T (Tris Buffered Saline + Tween) (10x)

For a final volume of 1 L, to 700 ml of deionised H_2O add

- Tris	12.11 g (10 mM)
- NaCl	87.66 g (150 mM)
- Tween 20	5 ml (0.05%)

Adjust the pH to 8.0 with HCl and adjust the volume to 1 L with deionised H_2O.

- Blocking solution (100 ml)

- TBS-T stock solution (10x)	10 ml
- non-fat milk (dry powder)	5 g

Dissolve in deionised H_2O and adjust volume to 100 ml.

- Antibody solution (25 ml)

- TBS-T stock solution (10x)	2.5 ml
- non-fat milk (dry powder)	0.75 g

Dissolve in deionised H_2O and adjust volume to 25 ml. Add antibody, mix gently without vortex, and store at -20 ºC.

- Alkaline Phosphatase (AP) Reaction Solution (1 L)

- Tris-HCl (pH 9.5)	12.11 g (100 mM)
- NaCl	5.85 g (100 mM)
- $MgCl_2$	1.02 g (5 mM)

Dissolve Tris base in deionised H_2O and adjust solution to pH 9.5 with HCl. Dissolve the other solutes and adjust volume to 1 L.

- AP Stop Solution (1 L)

- Tris-HCl (pH 9.5)	2.42 g (20 mM)
- EDTA	1.86 g (5 mM)

Dissolve Tris in deionised H_2O and adjust with HCl to pH 9.5. Add EDTA after and adjust volume to 1000 ml.

- Membranes Stripping Solution (500 ml)

- Tris-Cl (pH 6.7)	3.76 g (62.5 mM)
- SDS	10 g (2%)
- β-mercaptoethanol	3.5 ml (100 mM)

Dissolve Tris and SDS in deionised H_2O and adjust with HCl to pH 6.7. Add the mercaptoethanol and adjust volume to 500 ml.

APPENDIX II – KITS AND METHODS

DNA Manipulation

➢ PCR (polymerase chain reaction) for mutant and wt APP cDNAs amplification:

PCR was performed using Pfu DNA polymerase (Promega), and the amplification reactions were set up according to the manufacturer instructions. The standard amplification reactions were performed in 0.2 ml microtubes as follows (Table A.1):

Table A.1. Reagents mixtures used in APP isoform 695 cDNAs PCR amplification. Total volume: 50 µl

Tube	Template 0.1 ng	Template 1.0 ng	Negative Control 1 (w/primers, w/o template	Negative Control 2 (w/o primers, w/ template)
10x Pfu buffer	5 µl	5 µl	5 µl	5 µl
dNTPs (10 mM)	1.5 µl	1.5 µl	1.5 µl	1.5 µl
Primer NAPN	1.5 µl (10 pmol)	1.5 µl (10 pmol)	1.5 µl (10 pmol)	-
Primer S1	1.5 µl (10 pmol)	1.5 µl (10 pmol)	1.5 µl (10 pmol)	-
APP cDNA (template)	1 µl	10 µl	-	1 µl Wt APP cDNA
Pfu polymerase	1 µl	1 µl	1 µl	1 µl
H_2O	38.5 µl	29.5 µl	39.5 µl	41.5 µl

- PCR amplification program

1 min 94 ºC	1x	(Denaturation)
30 sec 94 ºC 30 sec 67 ºC 1 min 72 ºC	5x	(Denaturation, Annealing, Polymerization)
30 sec 94 ºC 3 min 72 ºC	25x	(Denaturation, Polymerization)
7 min 72 ºC	1x	(Polymerization; "Extension" step)

The annealing temperature depends on the primers melting temperatures (Tm) and it should usually be =(Tm – 8) ºC. For some reactions it was necessary to undergo further amplification cycles: more 20 cycles (30 sec 94 ºC, 3 min 72 ºC) followed by another extension step of 1x 7 min 72 ºC. Amplification was confirmed by resolving a PCR reaction aliquot (10 µl) in a 1.2% agarose gel electrophoresis.

➢ PCR cDNA products digestion with restriction enzymes:

The amplified APP cDNA fragments were sequentially digested with the restriction endonucleases *Nru* I and *Age* I to allow further insertion into the EGFP-N1 plasmid. APP cDNAs were inserted between the *Sma* I and *Age* I sites of the pEGFP-N1 vector, upstream of the enhanced green fluorescent protein (EGFP) cassette and in the correct open reading frame. For a typical DNA digestion, the following components were added to the following concentrations:

- 100 μg/ml cDNA
- 1X reaction buffer (specific for each restriction enzyme)
- 1U restriction enzyme /μg cDNA

The mixture was incubated at the appropriate temperature for a few hours (or overnight if convenient). When sequential digestions with different enzymes were carried out the DNA was purified between the two reactions (see below). Table A.2 presents the restriction enzymes and specific mixtures used in the APP-GFP translational fusions production and previous confirmation before sequencing. Prior to sequencing, the plasmid DNA extracted from transformants and the EGFP-N1 vector (for control), were sequentially digested with *Xba* I, *Eco*R I, and *Pst* I.

Table A.2. Mixtures used in APP_{695} and EGFP vector cDNAs digestion with restriction enxymes. Restriction enzymes: *Nru* I and *Age* I (NEB); *Sma* I, *Xba* I and *Eco*R I (Fermentas).

Objective:	**APP subcloning into the EGFP vector**				**Confirmation of APP-GFP fusion**		
Restriction Enzyme / Mixture Components	***Nru* I** (APP cDNAs, PCR products)	***Age* I** (APP cDNAs, PCR products)	***Sma* I** (N1 vector)	***Age* I** (N1 vector)	***Xba* I** (putative APP-GFP clones)	***EcoR* I** (putative APP-GFP clones, after *Xba* I confirmation)	***Pst* I** (putative APP-GFP clones, after *Xba* I confirmation)
Buffer 10x	10 μl	5 μl	10 μl	10 μl	1 μl	1 μl	1 μl
Enzyme	2 μl	1 μl	3.5 μl	3.5 μl	1 μl	1 μl	1 μl
DNA	40 μl of PCR product	Pellet of purified cDNA pre-cuted with *Nru*I	20 μl (± 12 μg) of gel extracted N1 vector	Pellet of purified cDNA pre-cuted with *Sma*I	3 μl of the clone miniprep	3 μl of the clone miniprep	3 μl of the clone miniprep
H_2O	48 μl	44 μl	66.5 μl	86.5 μl	5 μl	5 μl	5 μl
Final Volume	100 μl	50 μl	100 μl	100 μl	10 μl	10 μl	10 μl
Temperature	37 ºC	25 ºC	30 ºC	25 ºC	37 ºC	37 ºC	37 ºC
Reaction Time	4 h	Overnight	4 h	Overnight	2 h	4 h	4 h

➢ DNA purification:

- Method 1: QIAquick PCR Purification Kit Protocol (QIAgen # 28706)

This kit was used to purify DNA fragments from PCR and other enzymatic reactions. It allowed purification from primers, nucleotides, DNA polymerases and salts by using QIAquick spin columns in a microfuge tube. The manufacturer's protocol was used as follows: 5 volumes of buffer PB were added to 1 volume of the reaction to be purified, and mixed. The QIAquick spin column was placed in a provided 2 ml collection tube and the sample was applied to the column and centrifuged for 1 min at 14,000 rpm to allow for DNA binding. The first flow-through was discarded and the column washed with 0.75 ml of buffer PE and centrifuged for 1 min at 14,000 rpm. The second flow-through was discarded, the column placed back in the same tube and centrifuged again to remove traces of washing buffer. The column was finally placed in a clean microtube, 50 µl of H_2O were added and let to stand for 1 min. To elute the DNA, the column was centrifuged for 1 min at 14,000 rpm.

- Method 2: DNA precipitation with ethanol

This method was used to concentrate nucleic acids as well as to purify them (e.g. for cell culture transfection). Approximately 1/10 volume of 3 M sodium acetate (pH 5.2) was added to the DNA solution to adjust the salt concentration, followed by 2 volumes of ice-cold ethanol. The solution was mixed thoroughly and stored at –20 ºC for 30 min to allow the DNA precipitate to form. DNA was recovered by centrifugation at 4 ºC for 15 min at 14,000 rpm. The supernatant was carefully removed without disturbing the pellet. The microtube was half filled with ice-cold 70% ethanol and re-centrifuged using the same conditions as above for 5 min. The supernatant was again removed and the pellet allowed to dry before being resuspended in sterile water.

➢ Electrophoretic analysis of DNA:

An electrophoresis apparatus was prepared and the electrophoresis tank was filled with enough 1X TAE to cover the agarose gel. The appropriate amount of agarose (to a final percentage of 0.8 – 1.2%) was transferred to an Erlenmeyer with 50 ml 1X TAE, and this slurry was heated until agarose dissolution and allowed to cool to 60 ºC before adding ethidium bromide to a final concentration of 0.5 µg/ml. The agarose solution was poured into the tray and a comb was positioned on it. After the gel was completely set, the comb was carefully removed and the gel mounted in the tank. DNA samples were mixed with the 6X DNA loading buffer (DNA LB) (0.25% bromophenol blue/30% glycerol in water) and the mixture was loaded into the slots of the submerged gel. Marker DNA (λ-Hind III fragments or Invitrogen 1 Kb ladder) of known size was also loaded into the gel. The lid of the gel tank was closed and the electrical leads were attached so that the DNA migrated towards the anode. The gel was run at 100 V, and finally examined by UV light and photographed, or analysed on a Molecular Imager (Biorad).

- DNA Gel Extraction kit (QIAgen)

For the EGFP-N1 cDNA extraction, 0.8% gels were set as described above with some differences. 10 µl of non-cutted and 90 µl of *Sma* I/*Age* I cutted EGFP-N1 vector cDNA were loaded and resolved. The DNA standard and 10 µl lanes were UV exposed and the migration distance of the digested cDNA band registered. The 90 µl band was finally

extracted from the gel (without being exposed to UV light) with a clean spatula. The destination microtube was weighted, before and after receiving the extracted band, to calculate the cDNA weight. EGFP-N1 cDNA was further purified by using the QIAquick Gel Extraction Kit protocol. Briefly, 3 volumes of Buffer QG were added to 1 volume of gel (100 mg ~100 µl). This mixture was incubated at 50 ºC for 10 min (or until the gel slice was completely dissolved), while inverting the microtube every when. After the gel slice complete dissolution, pH was confirmed to be ≤ 7.5, and 1 gel volume of isopropanol was added to the sample and mixed. This sample was applied to a QIAquick spin column, previously placed in a 2 ml collection tube, and the tube centrifuged at 10,000 x *g* or 1 min. The flow-through was discarded, 0.5 ml of Buffer QG were applied to the column and a further 1 min centrifugation was performed. 0.75 ml of Buffer PE were used to wash the column by two sequential centrifugations at 10,000 x *g*, and the flow-through discarded. The column was placed in a clean 1.5 ml tube and the DNA eluted with 50 µl of deionised H_20 after 1 min standing in the column and a last 1 min centrifugation.

➢ Ligation of cohesive termini and blunt ended DNA

Digested fragments (*Sma* I/*Age* I EGFP-N1 plasmid and the Nru I/*Age* I APP-GFP cDNA fragment to be inserted) were separated by gel electrophoresis and purified. 0.1 µg of vector DNA were transferred to a microtube with an equimolar amount (or more) of insert DNA. Ligations were performed using the bacteriophage T4 DNA ligase (Promega), in a total volume mixture of 20 µl, and were carried out for 4 h at room temperature or overnight at 16 ºC. Additional control reactions were also set up (Table A.3).

Table A.3 – APP/GFP bacteriophage T4 DNA Ligations.

	Ligations		**Ligations Controls**		
Tube	**1** (2 µl of *Nru* I/*Age* I PCR product)	**2** (6 µl of *Nru* I/*Age* I PCR product)	**Control 1** (w/o cDNA)	**Control 2** (non-cutted EGFP vector)	**Control 3** (cutted EGFP vector)
10x T4 ligase buffer	2 µl	2 µl	2 µl	2 µl	2 µl
EGFP vector cDNA	3.5 µl (100 ng)	3.5 µl (100 ng)	-	1 µl (1 ng)	3.5 µl (100 ng)
APP PCR products	2.5 µl (± 20 ng)	6.0 µl (± 50 ng)	-	-	-
T4 DNA ligase	1.0 µl	1.0 µl	1.0 µl	1.0 µl	1.0 µl
H_2O	13.5 µl	11 µl	17 µl	16 µl	14.5 µl

➢ Bacteria Transformation:

- Preparation of competent cells

A single colony of *E. coli* XL1-Blue was incubated overnight in 10 ml SOB medium at 37 ºC. 1 ml of this overnight culture was used to incubate 50 ml SOB until OD_{550}= 0.3. This culture was incubated on ice for 15 min and centrifuged at 4,000 rpm (4 ºC) for 5 min. The supernatant was discarded and 15 ml of Solution I were added. After allowing standing on ice for 15 min, cells were centrifuged at 4,000 rpm (5 min, 4 ºC) and 3 ml of Solution II were added to the pellet. Cells were immediately divided in 0.1 ml aliquots and stored at -80 ºC.

- Bacteria transformation with plasmid DNA

Competent cells (50 µl) were thawed on ice and 2 or 5 µl of each ligation product (0.1 - 50 ng of DNA) were added to the cells with gentle swirling. The microtubes were incubated on ice for 20 min and heat shocked at 42 ºC for 60 sec. Further incubation on ice for 2 min was performed, and 0.9 ml of SOC medium was added. The tubes were incubated at 37 ºC for 1 hour with shaking at 225 rpm. 1/10 and 9/10 of this cells solution were plated on the appropriate antibiotic (100 µg/ml kanamycin) agar medium plates (pre-heated) and incubated at 37 ºC for ~16 h until colonies appeared. Control transformations were also performed in parallel, which always included a negative control transformation without DNA and a positive control transformation with 0.1 ng of the control plasmid.

➢ Amplification and isolation of plasmid DNA from bacteria:

- Alkaline lysis mini-prep

This method was used to screen the bacterial plates for transformant colonies. A single positive (transformant) bacterial colony was transferred to a tube containing 5 ml of LB plus antibiotic medium and incubated overnight at 37 ºC with vigorous shaking. After overnight culture growth, 1 ml of the 5 ml culture was centrifuged at 14,000 rpm and 4 ºC for 1 min. The medium was removed by aspiration and the bacterial pellet ressuspended in 100 µl of ice-cold solution I ('ressuspension' solution) by vigorous vortexing. Afterwards, 200 µl of Solution II was added ('alkaline lysis'), and the content of the tube mixed by inverting it several times. The microtube was placed on ice, 150 µl of ice-cold solution III ('neutralization' solution) was added and the tube gently vortexed. After standing on ice for 5 min, a 10 min centrifuge at 14,000 x *g* and 4 ºC was performed, and the supernatant transferred to a clean microtube. The DNA was precipitated with 2 volumes of ethanol at RT and this mixture was allowed to stand for 10 min at RT. After this period, the microtube was centrifuged at 14,000 x *g* and 4 ºC for 5 min. The supernatant was completely removed and the pellet washed with 70% ethanol and allowed to air-dry for 10 min. Purified DNA was dissolved in 20 µl H_2O containing DNAse-free pancreatic RNAse (20 µg/ml) and stored at -20 ºC.

- Mega-prep (Promega)

The Promega kit Wizard™ Plus Megapreps DNA purification System # A7300 was used in this procedure. One litre of a single-transformant cell culture was pelleted by centrifugation at 1,500 x *g* for 20 min at RT. The cell pellet was resuspended in 30 ml of cell resuspension solution [50 mM Tris-HCl (pH 7.5)/10 mM EDTA/100 µg/ml RNAase A] by manually disrupting the pellet with a pipette. Afterwards, 30 ml of cell lyses solution (0.2 M

NaOH/ 1% SDS) were added to the cells and the solution mixed gently by tube inversion until it became clear and viscous. 30 ml of neutralization solution [1.32 M potassium acetate (pH 4.8)] were added and the tube immediately mixed by inversion. After centrifugation at 14,000 x *g* for 15 min at RT the clear supernatant was transferred by filtering it through gauze swabs into a new tube, and the supernatant volume was measured. At this stage 0.5 volumes of RT isopropanol were added and the solution mixed by inversion. This solution was centrifuged at 14,000 x *g* for 15 min at RT, the supernatant discarded and the pellet resuspended in 4 ml of TE buffer. 20 ml of Wizard ™ Megapreps DNA purification Resin were added to the DNA and mixed by swirl. A Wizard ™ Megacolumn was inserted into the vacuum manifold port and the DNA/resin mix was transferred onto the Megacolumn. Vacuum was applied to pull the mix into the Megacolumn. Two washes with 25 ml of column wash solution (80 mM potassium acetate/8.3 mM Tris-HCl/40 µM EDTA/55% ethanol) were performed and the resin was rinsed with 10 ml of 80% ethanol. The Megacolumn was inserted into a 50 ml screw cap tube and centrifuged at 2,500 rpm for 5 min using a swinging bucket rotor centrifuge. The Megacolumn was removed from the tube and placed in a clean tube, and 3 ml of pre-heated water (70 ºC) were added to the column. After 1 min standing, the DNA was eluted by centrifugation at 2,500 rpm for 5 min. The DNA was stored at –20 ºC, and a 400 µl DNA aliquot was purified by ethanol (and kept sterile) and its concentration and 260/280 nm purity ratio calculated by densitometry measurements at the indicated wavelengths.

➢ APP-GFP DNA sequencing

All the DNA samples to be sequenced followed the same protocol. In a microtube the following components were added:

- 1 ng dsDNA (column purified)
- 4 µl of Ready Reaction Mix*
- 15 pmol primer (1.5 µl of 10 pmol/µl)
- H_2O to a final volume of 20 µl

* Ready Reaction Mix is composed of: dye terminators, deoxynucleoside triphosphates, AmpliTaq DNA polymerase, FS, rTth pyrophosphatase, magnesium chloride and buffer (Applied Biosystems).

This reaction mixture was vortexed and spun down for a few seconds. PCR was then performed using the following conditions:

96 ºC 30 sec
42 ºC 15 sec
60 ºC 4 min
} 25 cycles

Afterwards, samples were purified by ethanol precipitation (as described above). Briefly, 2.0 µl of 3 M sodium acetate (pH 5.2) and 50 µl of 95% ethanol were added to the reaction microtube. The microtube was vortexed and incubated at RT for 15 min to precipitate the extension products. The microtube was then centrifuged at 14,000 rpm for 20 min at RT. After discarding the supernatant, 250 µl of 70% ethanol were added, the microtube was briefly vortexed and re-centrifuged for 5 min at 14,000 rpm at RT. The supernatant was again discarded and the pellet dried. After this procedure the samples were loaded in the ABIPRISM (Applied Biosystems) Automated DNA Sequencer.

Cell Culture and Rat Cortex Samples

➢ COS-7 cell culture maintenance:

COS-7 cells were grown in complete DMEM medium (DMEM medium supplemented with 10% FBS) to which 100 U/ml penicillin and 100 mg/ml streptomycin (Gibco BRL, Invitrogen) were added. Cells were plated in 100 mm diameter plates or 6-well plates (35 mm diameter), and grown in a humidified incubator at 37 ºC and 5% CO_2. Cells were subcultured whenever ~95% confluence was reached.

➢ Rat cortical primary cultures:

Rat cortical neurons were isolated from cortex of Wistar Hannover 18 days rat embryos whose mother was killed by rapid cervical dislocation. After cortex dissection, tissues were treated for 10 min at 37 ºC with a 0.45 mg/ml trypsin/0.18 mg/ml deoxyribonuclease solution in Ca^{2+}- and Mg^{2+}-free HBSS (Gibco, BRL), supplemented with BSA (Merck, VWR International). Cells were washed with HBSS supplemented with 10% FBS to stop trypsinization, centrifuged at 1,000 rpm for 3 min, and further washed and centrifuged with HBSS for serum withdraw. Cells pellet was ressuspended in complete Neurobasal medium, which is supplemented with 2% B27. Viability and cellular concentration were assessed by using the Trypan Blue excluding dye [0.4% Trypan Blue solution (Sigma)], and cells with (dead) or without (living) intracellular blue staining were counted in a hemocytometer chamber. Cellular viability was calculated and normally higher than 95%. These neuronal cells were plated at 9.0 x 10^4 cells/cm^2 on 100 μg/ml poly-D-lysine pre-coated glass coverslips that were placed in six-well plates. Cells were maintained in 2 ml of complete Neurobasal medium in a humidified incubator at 37 ºC and 5% CO_2. Three and seven days after plating, 500 μl of cultured medium was replaced with 750 μl of gentamicine-free complete Neurobasal medium.

➢ Rat cortex isolation:

Young (1-2 month old) adult male rats were sacrificed by cervical dislocation and decapitation. Cerebral cortex was rapidly dissected on ice-cold 0.32 M sucrose/10 mM HEPES (pH 7.4) solution and weighted. Boiling SDS was added to a final 1% SDS solution (at ~ 10% w/v solution), samples were homogenised with a Potter-Elvehjem type homogenizer and further boiled for 10 min.

➢ Cells cDNA Transfection with Lipofectamine 2000:

Lipofectamine 2000 (Invitrogen) is a cationic liposome formulation that functions by complexing with nucleic acid molecules, allowing them to overcome the electrostatic repulsion of the cell membrane and to be taken by the cell. The method of DNA delivery in culture cell lines and primary neurons is well described in Dalby et al. (2004), from where the following protocols were based:

- COS-7 cell line (Table A.4)

Cells were grown in complete DMEM until 85 - 95% confluence and at the transfection day the culture medium was replaced for complete medium (antibiotic/antymicotic-free). The appropriate amount of DNA for each plate/well was diluted in DMEM (serum- and antibiotic/antymicotic-free). The Lipofectamine 2000 reagent was diluted at the appropriated amount in the same medium, and the tubes were left to rest for 5 min. The DNA solution was added to the Lipofectamine solution drop by drop, and the solution was mixed by gentle bubbling with the pipette. In order to form the DNA-lipid complexes, the tube was left to rest at for 25 - 30 min RT, after what the complexes solution was directly added onto the cells medium, drop by drop and with gentle rocking of the plate. The cells were further incubated at 37 ºC/5% CO_2 for the indicated transfection time prior to cell collection or fixation.

Table A.4 – COS-7 cells transfection reagents

Culture Plates	Medium w/ serum (plate)	DNA (μg)	Lipofectamine 2000 (μl)	Medium w/o serum (per tube)
100 mm plate	15 ml	8	50	1500 μl
60 mm plate	5.0 ml	4	15	500 μl
35 mm 6-wells	2.0 ml	2	10	250 μl

- Primary Neuronal cultures

Replace the culture medium in each 35 mm well for 0.8 ml of fresh gentamicine-free complete Neurobasal medium. Per each 35 mm well to transfect, 8 μl of Lipofectamine 2000 were diluted in 100 μl of DMEM, and the microtube was left to rest at RT for 5 min. 2 μg of APP-GFP cDNA were also diluted in 100 μl of DMEM, and this solution was added drop by drop to the Lipofectamine solution. The final solution was mixed by gentle bubbling with the pipette, and left to rest for 25 - 30 min at RT in order to form the DNA-lipid complexes. This 200 μl DMEM complexes solution was directly added onto the cells medium, drop by drop and with gentle rocking of the plate. Neuronal cells were further incubated at 37 ºC/5% CO_2 for 5 h, after what medium was substituted by fresh complete neurobasal medium and left for 24 h prior to cell collection or fixation.

➢ Culture cells Fixation and Immunocytochemistry:

COS-7 and neuronal primary cells were grown in 1M HCL pre-treated glass coverslips pre-coated with 100 μg/ml poly-L-ornithine or poly-D-lysine, respectively. After the experimental procedures, cells were washed three times with 1 ml of the serum-free DMEM, after which 1 ml of a 1:1 DMEM/4% paraformaldehyde fixative solution was gently added and allowed to stand for 1-2 min. Subsequently, 1 ml of fixative solution was gently added for 25 minutes. Finally, cells were washed 3 times with PBS for 10 min, being ready for Immunocytochemistry procedures or to be directly mounted with 1 drop of anti-fading reagent (Fluoroguard, BioRad) on glass microscope slides for epifluorescence microscopy analysis. For Immunocytochemistry procedures, a permeabilization step with methanol was

taken (2 min at RT) and cells were immediately washed four times with PBS. Afterward, cells were incubated with primary antibody diluted in 3% BSA in PBS for 2-4 h at RT. The primary antibody was removed by washing the coverslips 3 times with PBS and a secondary antibody (also diluted in 3% BSA in PBS) was added for 2 h at RT. After washing three times with PBS the coverslips were mounted with one drop of the antifading reagent on a glass slide.

Proteins Manipulation

➢ Protein Assay kit (BCA, Pierce):

Samples total protein measurements were performed with Pierce's BCA protein assay kit, following the manufacturer's instructions. The method combines the reduction of Cu^{2+} to Cu^{+} by protein in an alkaline medium (the biuret reaction) with a sensitive colorimetric detection of the Cu^{+} cation using a reagent containing bicinchoninic acid (BCA). The purple-coloured reaction product of this assay is formed by the chelation of two molecules of BCA with one Cu^{+} ion. This water-soluble complex exhibits a strong absorbance at 562 nm that is linear with increasing protein concentration over a working range of 20 μg/ml to 2000 μg/ml.

- Working Reagent (W.R.)

The W.R. was prepared by mixing X ml of BCA reagent A with Y ml of BCA reagent B in the proportion of 50:1.

- Samples preparation

A microtube per sample was prepared to be assayed with 25 μl of each sample plus 25 μl of the solution in which the sample was collected (1% SDS).

- Standard curve

Microtubes with standard protein concentrations were prepared as described below (Table A.5).

Table A.5 – Standards used in the BCA protein assay method. BSA, Bovine serum albumin solution (2 mg/ml).

Standard	BSA (μl)	10% SDS (μl)	H_2O (μl)	Protein mass (μg)	W.R. (ml)
P_0	-	5	45	0	1
P_1	1	5	44	2	1
P_2	2	5	43	4	1
P_3	5	5	40	10	1
P_4	10	5	35	20	1
P_5	20	5	25	40	1
P_6	40	5	5	80	1

- Incubation and absorbance measurement

1 ml of W.R. was rapidly added to each microtube (standards and samples) and the microtubes were incubated at 37 ºC exactly for 30 min. Tubes cool to RT and immediately measure their absorbance at 562 nm.

- Samples concentration

A standard curve is prepared by plotting BSA standard absorbance vs. BSA concentration, and used to determine the total protein concentration of each sample.

➢ SDS-PAGE (for Western blotting):

SDS polyacrylamide gel electrophoresis (SDS-PAGE) separations were carried out using well established methods (Laemmli, 1970), where proteins are separated by their molecular weight and negative net charge due to SDS-amino acid binding. The gels percentage and size chosen depend on the molecular weight of the proteins to be separated in the gel. Gels were prepared by mixing several components (Appendix I). The resolving gel solution was immediately and carefully pipetted down the spacer into the gel sandwich, leaving free space for the stacking gel. Water was carefully added to cover the top of the gel and the gel was allowed to polymerize for 1 h. Stacking gel solution was prepared according to Appendix I. The water was poured out and the stacking gel was added to the gel sandwich; a comb was inserted and the gel allowed to polymerize for 1 h. In parallel, samples were prepared by adding to the protein sample solution ¼ volume of 4X LB (Loading Buffer). Samples microtubes were boiled and spinned down, the combs removed and the gels wells filled with Tris-Glycine running buffer. The samples were carefully loaded into the wells, and electrophoretically separated using a 90 mA electric current. Molecular weight markers (Kaleidoscope Prestained Standards or Prestained SDS-PAGE Standards – Broad Range, Bio Rad) were also loaded and resolved side-by-side with the samples.

➢ Proteins Electrotransfer:

Through the Western Blotting technique, proteins that were electrophoretically separated by SDS-PAGE can be transferred to membranes (nitrocellulose membranes, for instance), while keeping their positions. 3MM blotter papers and a nitrocellulose membrane were used to build up the transfer sandwich. The gel was removed from the electrophoresis device and the stacking gel discarded. A transfer sandwich was assembled under transfer buffer, in the following order: sponge, 3MM blotter paper, gel, nitrocellulose membrane, 3MM paper, sponge. The cassette was placed in the transfer device, previously filled with transfer buffer, oriented so that the negatively charged proteins migrate towards the anode. Electrotransfer was allowed to proceed for 18 h at 200 mA, after what the membrane was allowed to dry on a clean paper.

➢ Immunoblot analysis:

After proteins electrotransfer, the nitrocellulose membranes could be used immediately, and membranes were initially soaped in 1X TBS for 10 min. Blocking of possible non-specific binding sites of the primary antibody was performed by immersing the membrane in 5% (w/v) non-fat dry milk in 1X TBST solution for 1 - 4 h. Further incubation

with primary antibody was carried out for the specified times, ranging from 2 h to overnight incubation at 4 ºC with agitation. After three washes with 1X TBS-T, of 10 min each, the membrane was further incubated with the appropriate secondary antibody for 2 h with agitation. All primary and secondary antibodies used were diluted in 1X TBS-T/non-fat dry milk (3% w/v) at the dilutions specified in Chapters II, IV and V (Table II.1, IV.1 and V.1). Membranes were additional washed three times with 1X TBST, before being submitted to one of the following detection methods:

- Colorimetric detection (NBT/BCIP, Pierce)

Each 15 cm membrane was developed by adding to it a solution of 66 µl NBT and 33 µl BCIP in 10 ml Alkaline Phosphatase reaction buffer. When a coloured signal was achieved, the developing reaction was stopped by adding 20 ml of AP stop solution. Membrane was washed twice with deionised water and air dried at RT.

- Enhanced chemiluminescence detection (ECL and ECL+ Kits, Amersham Pharmacia)

ECL™ Western blotting from Amersham Pharmacia Biotech is a light emitting non-radioactive method for detection of immobilised specific antigens, conjugated directly or indirectly with horseradish peroxidase-labelled antibodies (Fig. A.II.1).

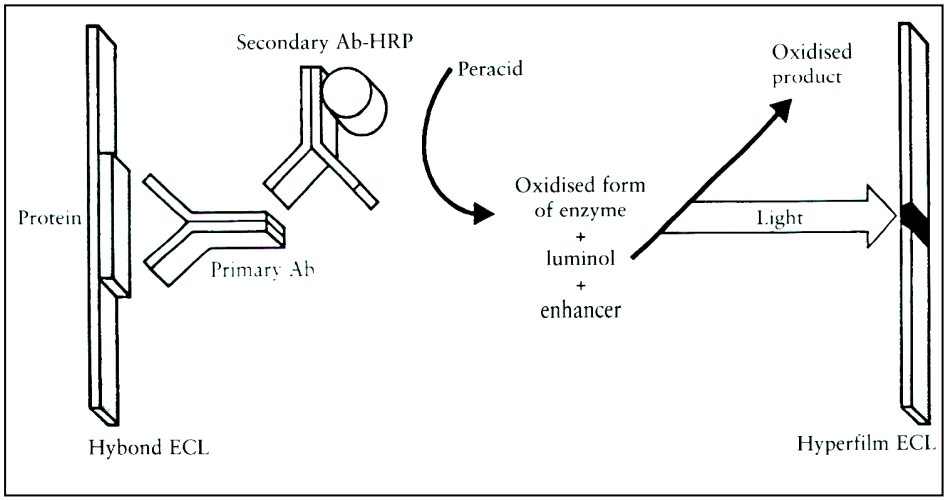

Figure A.II.1. The ECL analysis system detects the presence of an antibody labelled with horseradish peroxidase by catalysing the oxidation of luminol, leading to the emission of light, which can be detected by an autoradiography film (From the manufacturer datasheet).

The membrane was incubated for 1 min at RT with the ECL detection solution or for 5 min with the ECL+ detection solution. These solutions were prepared fresh following the manufacturer's instructions. ECL/ECL+ detection solution in excess was drained by touching the edge of the membrane against tissue paper and the membrane was gently wrapped in cling-film, eliminating all the air bubbles. In a dark room, an autoradiography film (XAR-5 film, Kodak, Sigma Aldich) was placed on the top of the membrane, inside a film cassette. The cassette was closed and the blot exposed for an appropriate period of time. The film was then removed and developed in a developing solution (Kodak, Sigma Aldrich), washed in water, and fixed in a fixing solution (Kodak, Sigma Aldrich).

APPENDIX III – SEQUENCES AND TECHNICAL DATA

➢ APP_{695} sequences (GenBank Acession NM_201414):

- cDNA sequence

```
   1 atgctgcccg gtttggcact gctcctgctg gccgcctgga cggctcgggc gctggaggta cccactgatg
  71 gtaatgctgg cctgctggct gaaccccaga ttgccatgtt ctgtggcaga ctgaacatgc acatgaatgt
 141 ccagaatggg aagtgggatt cagatccatc agggaccaaa acctgcattg ataccaagga aggcatcctg
 211 cagtattgcc aagaagtcta ccctgaactg cagatcacca atgtggtaga agccaaccaa ccagtgacca
 281 tccagaactg gtgcaagcgg ggccgcaagc agtgcaagac ccatccccac tttgtgattc cctaccgctg
 351 cttagttggt gagtttgtaa gtgatgccct tctcgttcct gacaagtgca aattcttaca ccaggagagg
 421 atggatgttt gcgaaactca tcttcactgg cacaccgtcg ccaaagagac atgcagtgag aagagtacca
 491 acttgcatga ctacggcatg ttgctgccct gcggaattga caagttccga ggggtagagt ttgtgtgttg
 561 cccactggct gaagaaagtg acaatgtgga ttctgctgat gcggaggagg atgactcgga tgtctggtgg
 631 ggcggagcag acacagacta tgcagatggg agtgaagaca aagtagtaga agtagcagag gaggaagaag
 701 tggctgaggt ggaagaagaa gaagccgatg atgacgagga cgatgaggat ggtgatgagg tagaggaaga
 771 ggctgaggaa ccctacgaag aagccacaga gagaaccacc agcattgcca ccaccaccac caccaccaca
 841 gagtctgtgg aagaggtggt tcgagaggtg tgctctgaac aagccgagac ggggccgtgc cgagcaatga
 911 tctcccgctg gtactttgat gtgactgaag ggaagtgtgc cccattcttt tacggcggat gtggcggcaa
 981 ccggaacaac tttgacacag aagagtactg catggccgtg tgtggcagcg ccatgtccca aagtttactc
1051 aagactaccc aggaacctct tgcccgagat cctgttaaac ttcctacaac agcagccagt acccctgatg
1121 ccgttgacaa gtatctcgag acacctgggg atgagaatga acatgcccat ttccagaaag ccaaagagag
1191 gcttgaggcc aagcaccgag agagaatgtc ccaggtcatg agagaatggg aagaggcaga acgtcaagca
1261 aagaacttgc ctaaagctga taagaaggca gttatccagc atttccagga gaaagtggaa tctttggaac
1331 aggaagcagc caacgagaga cagcagctgg tggagacaca catggccaga gtggaagcca tgctcaatga
1401 ccgccgccgc ctggccctgg agaactacat caccgctctg caggctgttc ctcctcggcc tcgtcacgtg
1471 ttcaatatgc taaagaagta tgtccgcgca gaacagaagg acagacagca caccctaaag catttcgagc
1541 atgtgcgcat ggtggatccc aagaaagccg ctcagatccg gtcccaggtt atgacacacc tccgtgtgat
1611 ttatgagcgc atgaatcagt ctctctccct gctctacaac gtgcctgcag tggccgagga gattcaggat
1681 gaagttgatg agctgcttca gaaagagcaa aactattcag atgacgtctt ggccaacatg attagtgaac
1751 caaggatcag ttacggaaac gatgctctca tgccatcttt gaccgaaacg aaaaccaccg tggagctcct
1821 tcccgtgaat ggagagttca gcctggacga tctccagccg tggcattctt ttggggctga ctctgtgcca
1891 gccaacacag aaaacgaagt tgagcctgtt gatgcccgcc ctgctgccga ccgaggactg accactcgac
1961 caggttctgg gttgacaaat atcaagacgg aggagatctc tgaagtgaag atggatgcag aattccgaca
2031 tgactcagga tatgaagttc atcatcaaaa attggtgttc tttgcagaag atgtgggttc aaacaaaggt
2101 gcaatcattg gactcatggt gggcggtgtt gtcatagcga cagtgatcgt catcaccttg gtgatgctga
2171 agaagaaaca gtacacatcc attcatcatg gtgtggtgga ggttgacgcc gctgtcaccc cagaggagcg
2241 ccacctgtcc aagatgcagc agaacggcta cgaaaatcca acctacaagt tctttgagca gatgcagaac
2311 tag
```

- Amino acid sequence

M L P G L A L L L L A A W T A R A L E V P T D G N A G L L A E P Q I A M F C G R L N M H M N V Q N G K W
D S D P S G T K T C I D T K E G I L Q Y C Q E V Y P E L Q I T N V V E A N Q P V T I Q N W C K R G R K Q C K
T H P H F V I P Y R C L V G E F V S D A L L V P D K C K F L H Q E R M D V C E T H L H W H T V A K E T C S E
K S T N L H D Y G M L L P C G I D K F R G V E F V C C P L A E E S D N V D S A D A E E D D S D V W W G G A
D T D Y A D G S E D K V V E V A E E E E V A E V E E E E A D D D E D D E D G D E V E E E A E E P Y E E A
T E R T T S A I T T T T T T T T E S V E E V V R V P T T A A S T P D A V D K Y L E T P G D E N E H A H F Q K A K
E R L E A K H R E R M S Q V M R E W E E A E R Q A K N L P K A D K K A V I Q H F Q E K V E S L E Q E A A
N E R Q Q L V E T H M A R V E A M L N D R R R L A L E N Y I T A L Q A V P P R P R H V F N M L K K Y V R A
E Q K D R Q H T L K H F E H V R M V D P K K A A Q I R S Q V M T H L R V I Y E R M N Q S L S L L Y N V P A
V A E E I Q D E V D E L L Q K E Q N Y S D D V L A N M I S E P R I S Y G N D A L M P S L T E T K T T V E L L
P V N G E F S L D D L Q P W H S F G A D S V P A N T E N E V E P V D A R P A A D R G L T T R P G S G L T N I
K T E E I S E V K M *D A E F R H D S G Y E V H H Q K L V F F A E D V G S N K G A I I G L M V G G V V I A* T
V I V I T L V M L **K K K Q** ^{653}**Y T S I**^{656} **H H G V V E V D A A V T P E E R H L S K M Q Q N G Y E N P T Y K F F E Q M Q N**

Legend:

Italic – Abeta sequence
Bold – Cytoplasmic sequence

➢ Oligonucleotides:

- Primers used for APP-GFP constructs engineering

NAPN (N-terminal APP primer with *NruI* consensus sequence). Length: 32 nts; Melting Temperature: 102 ºC.

5' – CTT AAG CTT CGC GAT GCT GCC CGG TTT GGC AC – 3'

S1 (C-terminal APP primer without STOP codon and with *AgeI* consensus sequence). Length: 38 nts; Melting Temperature: 114 ºC.

5' – ATG GTA CCG GTG GGT TCT GCA TCT GCT CAA AGA ACT TG – 3'

- Primers used for APP-GFP constructs sequencing

NAPN (above).

APP 500 (at the beginning of APP exon 5, nucleotide 478 - APP_{695} numbering). Length: 24 nts; Melting Temperature: 70 ºC.

5' – GAG AAG AGT ACC AAC TTG CAT GAC – 3'

APP 1100 (at the beginning of APP exon 9, nucleotide 866 - APP_{695} numbering). Length: 14 nts; Melting Temperature: 42 ºC.

5' – TCC TAC AAC AGC AG – 3'

APP 1500 (at the end of APP exon 11, nucleotide 1204 - APP_{695} numbering). Length: 14 nts; Melting Temperature: 44 ºC.

5' – ATC ACC GCT CTG CA – 3'

APP 1800 (at the beginning of APP exon 14, nucleotide 1507 - APP_{695} numbering). Length: 16 nts; Melting Temperature: 46 ºC.

5' – GCC AAC ATG ATT AGT G – 3'

APP 2000 (at the end of APP exon 16, nucleotide 1806 - APP_{695} numbering). Length: 22 nts; Melting Temperature: 60 ºC.

5' – TGA CTC AGG ATA TGA AGT TCA T – 3'

➢ pEGFP-N1 Plasmid:

- pEGFP-N1 (Clontech, BD Biosciences; GenBank Accession #U55762)

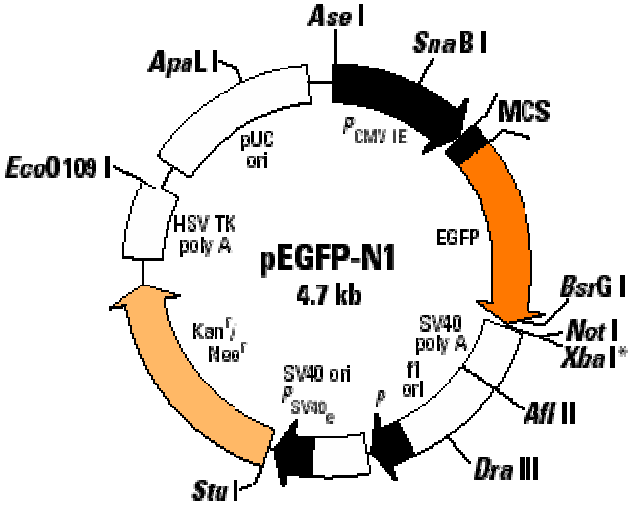

MCS:

Restriction Map and Multiple Cloning Site of pEGFP-N1. (Unique restriction sites are in color or bold.) The *Not* I site follows the EGFP stop codon. The *Xba* I site (*) is methylated in the DNA provided by CLONTECH. If you wish to digest the vector with this enzyme, you will need to transform the vector into a *dam*- host and make fresh DNA.

Description: pEGFP-N1 encodes a red-shifted variant of wild-type GFP (1-3) which has been optimized for brighter fluorescence and higher expression in mammalian cells. (Excitation maximum = 488 nm; emission maximum = 507 nm.) The MCS in pEGFP-N1 is between the immediate early promoter of CMV ($P_{CMV\ IE}$) and the EGFP coding sequences. Genes cloned into the MCS will be expressed as fusions to the N-terminus of EGFP if they are in the same reading frame as EGFP and there are no intervening stop codons. SV40 polyadenylation signals downstream of the EGFP gene direct proper processing of the 3' end of the EGFP mRNA. A bacterial promoter upstream of this cassette (P_{amp}) expresses kanamycin resistance in *E. coli*. The pEGFP-N1 backbone also provides a pUC19 origin of replication for propagation in *E. coli* and an f1 origin for single-stranded DNA production.

Use: Fusions to the N-terminus of EGFP retain the fluorescent properties of the native protein allowing the localization of the fusion protein *in vivo*. The target gene should be cloned into pEGFP-N1 so that it is in frame with the EGFP coding sequences, with no intervening in-frame stop codons. The inserted gene should include the initiating ATG codon. The recombinant EGFP vector can be transfected into mammalian cells using any standard transfection method. If required, stable transformants can be selected using G418 (7). pEGFP-N1 can also be used simply to express EGFP in a cell line of interest (e.g., as a transfection marker).

(From: http://www.bdbiosciences.com/clontech/techinfo/vectors/vectorsE/pEGFP-N1.shtml)

- Bacteria strain (plasmid DNA amplification)

E. coli XL1- blue:
*recA endA1 gyrA96 thi-1 hsd*R17 *supE44 relA1 lac[F' proAB lacZΔM15 Tn10(Tetr)]*

➢ Protein Markers of Subcellular Compartments:

- Monoclonal Antibody anti-Syntaxin 6 (BD Transduction Laboratories)

Syntaxin 6 is a 255 amino acid member of the Syntaxin family. It contains a C-terminal transmembrane domain and is located at the Golgi apparatus.

- Policlonal Antibody Anti-Calnexin (StressGen Biotechnologies)

Calnexin is a ~90 KDa unglycosylated molecular chaperone and a resident ER transmembrane protein.

➢ Fluorophores Excitation and Emission Spectra:

- EGFP-N1 (pEGFP encoded) (Clontech, BD Biosciences). Excitation and Emission Spectra for BD Living Colors™ Fluorescent Proteins:

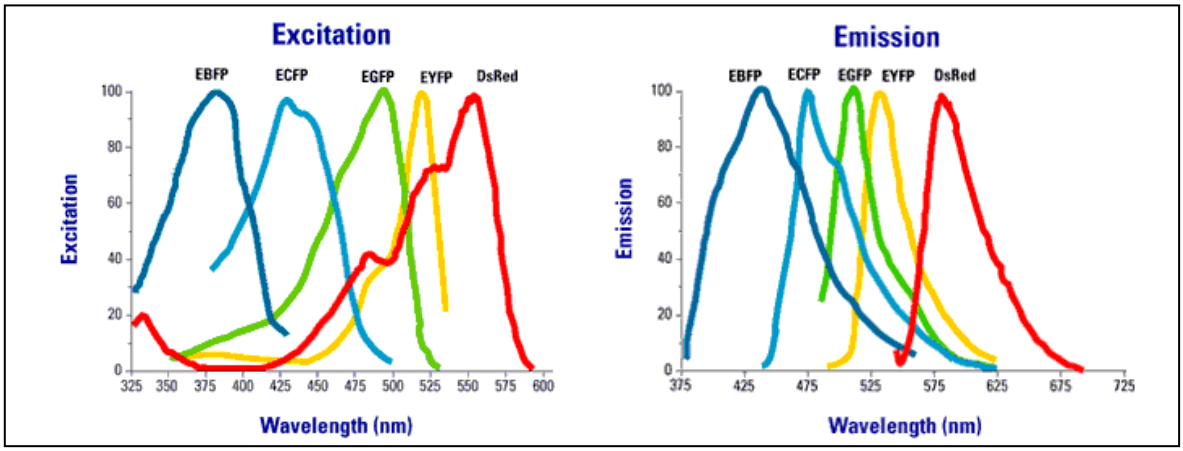

- Secondary Fluorescent Antibodies:

A. Fluorescein goat anti–mouse IgG antibody/pH 8.0 (Molecular Probes) (fluorescence absorption and emission spectra in pH 8.0 buffer)

B. Texas Red-X goat anti–mouse IgG antibody/pH 7.2 (Molecular Probes) (fluorescence excitation and emission spectra in pH 7.2 buffer)

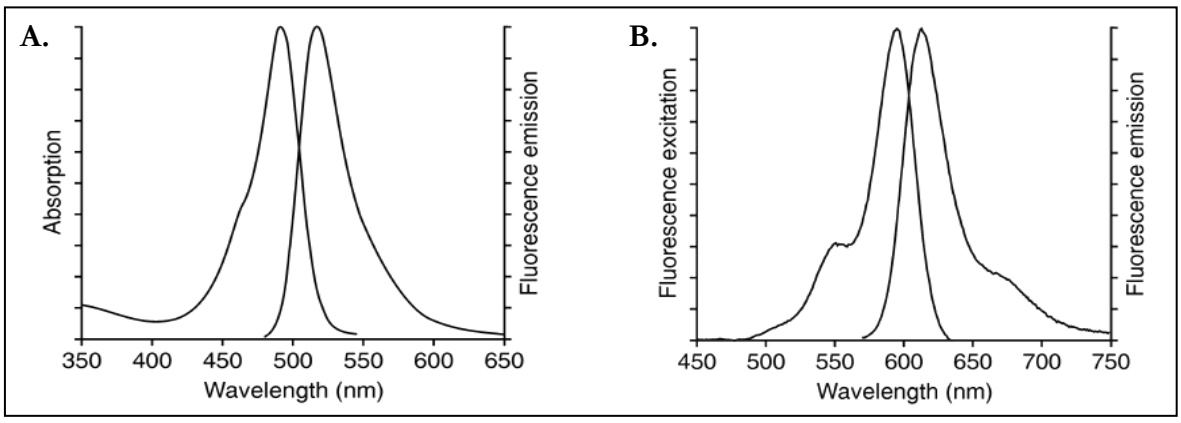

➢ **Epifluorescence Microscope filter cubes** (Chroma)**:**

Set ID: 41020
Fluorophore: EGFP. Narrow-band GFP for eliminating auto-fluorescence

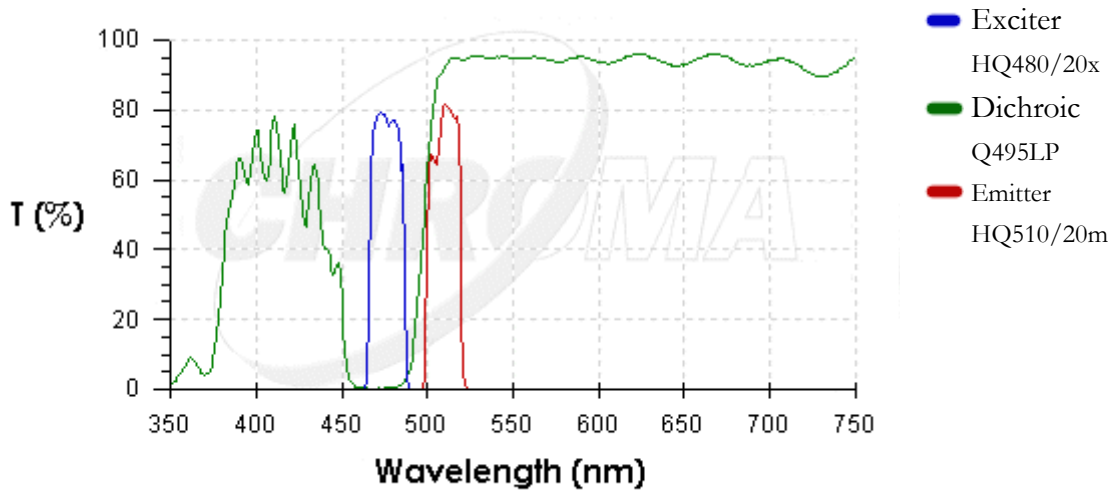

Set ID: 41004
Fluors: Texas Red. Other: Alexa 568™ Alexa 594™ Bodipy TR Calcium Crimson™ Cy3.5™ DsRed Rhodamine Mitotracker Red 580 Mitottracker Red Mitottracker Red 580 Rhodamine Red Tetramethylrhodamine Texas Red™ X-Rhodamine

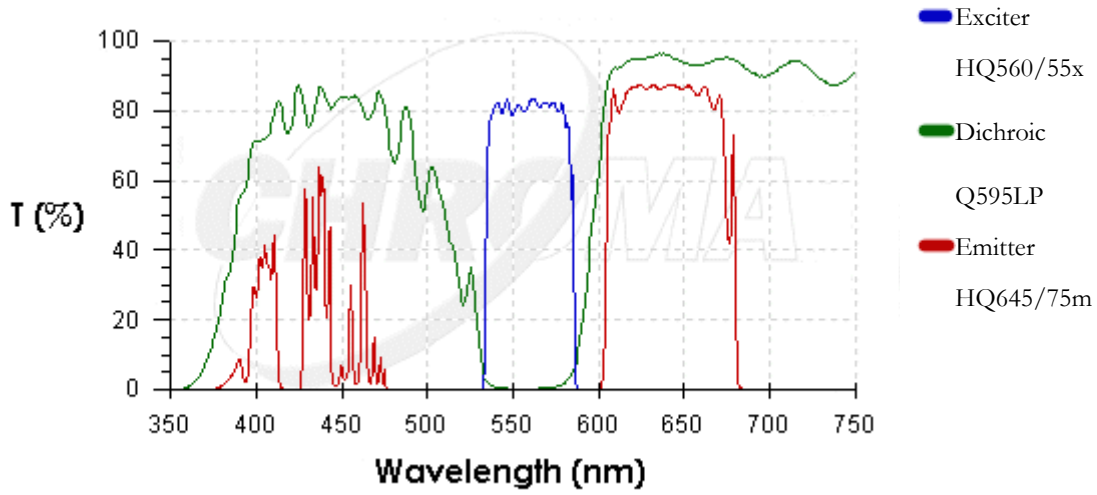

Do men quest the Line of Truth or the mere control of it?
and is it reasonable to draw parallels, when
tangency is, at minimum, uncertain?

(though, what a trilling path,
what a privilege,
as Truth is, by intangibleness,
such a necessary desire)